



**WYDZIAŁ BIOLOGII
i OCHRONY ŚRODOWISKA**
Uniwersytet Łódzki

Stacjonarne Studia Doktoranckie
Genetyki Molekularnej, Cytogenetyki
i Biofizyki Medycznej

Kinga Malinowska

Ocena właściwości prooksydacyjnych,
genotoksycznych i proapoptotycznych
nanocząstek polistyrenu w jednojądrzastych
komórkach krwi obwodowej człowieka

Determination of prooxidative, genotoxic and proapoptotic
properties of polystyrene nanoparticles in human peripheral blood
mononuclear cells

Praca doktorska

wykonana w Katedrze Biofizyki Skażeń Środowiska
Instytutu Biofizyki UŁ

Promotor:

➔ Prof. dr hab. Bożena Bukowska

Promotor pomocniczy:

➔ Dr Paulina Sicińska

➔ Łódź, 2023

PODZIĘKOWANIA

Chciałabym serdecznie podziękować
wszystkim osobom które przyczyniły się do
powstania mojej pracy doktorskiej
Przede wszystkim chciałabym wyrazić swoje
uznanie i wdzięczność mojej pani promotor
prof. dr hab. Bożenie Bukowskiej,
oraz pani promotor pomocniczej
dr Paulinie Sicińskiej
za cierpliwość, profesjonalizm oraz wskazówki,
który były dla mnie niezwykle pomocne w procesie
pisanie pracy.

Bardzo dziękuję również
wszystkim **pracownikom**
Katedry Biofizyki Skażeń Środowiska
którzy swoją wiedzą i doświadczeniem przyczynili
się do rozwoju mojej pracy doktorskiej.

Mojemu Partnerowi i Mamie,
oraz najbliższej rodzinie
za wspieranie mnie w trudnych momentach
i motywację do ciągłej pracy.

CZĘŚĆ BADAŃ WCHODZĄCYCH W SKŁAD ROZPRAWY DOKTORSKIEJ REALIZOWANA BYŁA W:

ramach dwuletniego grantu Preludium 20 nr 2021/41/N/NZ7/02049 (kod projektu: B2211000001190100) przyznanego przez Narodowe Centrum Nauki. Projekt zatytułowany jest: *„Nanocząstki polistyrenowe i ich właściwości epigenetyczne i genotoksyczne w ludzkich jednojądrzastych komórkach krwi obwodowej”*.



N A R O D O W E C E N T R U M N A U K I

SPIS TREŚCI

Spis publikacji wchodzących w zakres rozprawy doktorskiej	5
Streszczenie w języku polskim.....	6
Streszczenie w języku angielskim	8
Cel naukowy oraz omówienie wyników	10
Dorobek naukowy	26
Kopie publikacji wchodzących w zakres rozprawy doktorskiej	29
Oświadczenia współautorów prac	120

SPIS PUBLIKACJI WCHODZĄCYCH W ZAKRES ROZPRAWY DOKTORSKIEJ

1. **Kik (Malinowska) K.**, Bukowska B., Sicińska P. (2020). *Polystyrene nanoparticles: Sources, occurrence in the environment, distribution in tissues, accumulation and toxicity to various organisms*. Environmental Pollution 262; 114297. <https://doi.org/10.1016/j.envpol.2020.114297>.
Praca przeglądowa
Punkty MEiN: 100
Impact Factor: 8,041
2. **Kik (Malinowska) K.**, Bukowska B., Sicińska P. (2022). *Oxidative properties of polystyrene nanoparticles with different diameters in human peripheral blood mononuclear cells (in vitro study)*. International Journal of Molecular Sciences 22 (9); 4406. <https://doi.org/10.3390/ijms22094406>.
Praca oryginalna
Punkty MEiN: 140
Impact Factor: 6,208
3. **Malinowska K.**, Bukowska B., Piwoński I., Foksiński M., Kisielewska A., Zarakowska E., Gackowski D., Sicińska P. (2022). *Polystyrene nanoparticles – the mechanism of their genotoxicity in human peripheral blood mononuclear cells*. Nanotoxicology 16 (6-8), 791-811. <https://doi.org/10.1080/17435390.2022.2149360>
Praca oryginalna
Punkty MEiN: 140
Impact Factor: 5,881
4. **Malinowska K.**, Sicińska P., Michałowicz J., Bukowska B., *The effect of non-functionalized polystyrene nanoparticles of different diameters on apoptosis induction in human peripheral blood mononuclear cells*. Chemosphere 335, 139137; 1-13. <https://doi.org/10.1016/j.chemosphere.2023.139137>
Praca oryginalna
Punkty MEiN: 140
Impact Factor: 8,943

Sumaryczna wartość **impact factor** publikacji wchodzących w zakres rozprawy doktorskiej wynosi **29,073 (520 punktów MEiN)** (zgodnie z rokiem opublikowania).

STRESZCZENIE W JĘZYKU POLSKIM

Zanieczyszczenie tworzywami sztucznymi uznawane jest obecnie za globalny problem. Co roku do środowiska dostają się olbrzymie ilości odpadów plastikowych w wyniku niewłaściwej gospodarki odpadami i niewystarczający recykling, a także z uwagi na długi okres rozkładu tych tworzyw. W 2021 roku na świecie wytworzono 390,7 mln ton plastiku w tym 57,2 mln ton w Europie. Poważne zagrożenie ekotoksykologiczne dla organizmów stanowią cząstki powstałe z rozpadu dużych fragmentów plastiku tzw. mikrocząstki o średnicy < 5000 nm oraz nanocząstki o średnicy < 100 nm, których obecność stwierdzono w powietrzu, wodzie, glebie i żywności. Mikro i nanocząstki są szeroko stosowane w różnych gałęziach przemysłu m.in. farmaceutycznym, laboratoryjnym oraz kosmetycznym.

Jednym z najczęściej badanych tworzyw syntetycznych o strukturze nanometrycznej jest polistyren powstający w procesie polimeryzacji monomerów styrenu. Tworzywo to wykorzystywane jest do produkcji opakowań, sprzętu elektronicznego i AGD oraz stosowane do ocieplania budynków (styropian). Cząstki polistyrenu ze względu na małe rozmiary, mogą łatwo przedostawać się do organizmów żywych poprzez układ oddechowy, pokarmowy czy przez skórę i w konsekwencji przechodzić przez bariery biologiczne i kumulować się w tkankach.

Celem badań niniejszej pracy doktorskiej była ocena działania prooksydacyjnego, proapoptotycznego i genotoksycznego nanocząstek polistyrenu (PS-NP) o różnych średnicach (29 nm, 44 nm i 72 nm) w jednojądrzastych komórkach krwi obwodowej człowieka.

Na wstępie przeprowadzono badania właściwości fizyko-chemicznych nanocząstek polistyrenu w celu potwierdzenia zadeklarowanej przez producentów ich średnicy. Uzyskane zdjęcia oraz wyniki z wykorzystaniem mikroskopii sił atomowych (AFM) i skaningowej mikroskopii atomowej (SEM) były zgodne z parametrami podanymi przez producenta cząstek. Badania wykonane za pomocą techniki pomiaru wielkości cząstek (DLS) polistyrenu inkubowanych w wodzie także potwierdziły średnicę cząstek, którą deklarowali producenci, podczas gdy inkubacja badanych cząstek w pożywce RPMI znacząco zwiększała ich średnicę, nawet trzykrotnie w przypadku najmniejszych nanocząstek. Ponadto, dokonano oceny potencjału zeta, który zmieniał się wraz ze wzrostem średnicy cząstek.

Rozpoczynając badania biologiczne oceniono cytotoksyczność nanocząstek polistyrenu o różnych średnicach. Cząstki te spowodowały spadek żywotności i zmiany w aktywności metabolicznej jednojądrzastych komórek krwi obwodowej człowieka, ale w bardzo wysokich stężeniach powyżej 300 $\mu\text{g/ml}$.

Następnie dokonano oceny ich właściwości prooksydacyjnych. Dowiedziono, że nanocząstki polistyrenu indukują powstawanie reaktywnych form tlenu oraz wysoce reaktywnych form tlenu, w tym rodnika hydroksylowego. Z kolei analiza poziomu

peroksydacji lipidów i białek wykazała, że powodują one spadek fluorescencji tryptofanu w białkach oraz znaczny spadek fluorescencji kwasu *cis*-parynarowego.

W kolejnym etapie określono działanie genotoksyczne nanocząstek polistyrenu. Udowodniono, że badane nanocząstki o wszystkich analizowanych średnicach powodują powstawanie pęknięć jedno- i dwuniciowych w badanych komórkach krwi, oraz indukują pęknięcia dwuniciowe, ale tylko po narażeniu badanych komórek na mniejsze nanocząstki o średnicy 29 nm i 44 nm. Ponadto wykazano powstawanie zmodyfikowanych oksydacyjnie zasad purynowych i pirymidynowych po traktowaniu jednojądrzastych komórek krwi obwodowej nanocząstkami polistyrenu. Większy poziom uszkodzeń oksydacyjnych zaobserwowano po zastosowaniu w teście genotoksyczności glikozylazy formamido-pirymidyny (Fpg). Dowiedziono także, że wzrost utleniania pirymidyny (zastosowanie w analizie endonukleazy III) następował przy wyższych stężeniach nanocząstek w porównaniu z próbkami do których dodawano Fpg. Wzrost poziomu 8-hydroksy-2-deoksyguanozyny zaobserwowano tylko po ekspozycji jednojądrzastych komórek krwi na najmniejsze nanocząstki (29 nm). Powstałe uszkodzenia DNA spowodowane przez większe nanocząstki (44 nm i 72 nm) zostały całkowicie naprawione po 120 minutach, natomiast w przypadku mniejszych cząstek (29 nm) naprawa nie była w pełni skuteczna.

Trzeci etap badań dotyczył oceny właściwości proapoptotycznych badanych cząstek. Nanocząstki polistyrenu zwiększały liczbę komórek apoptotycznych, podwyższały poziom jonów wapnia w cytozolu komórek, zmniejszały wartość transbłonowego potencjału mitochondrialnego oraz zwiększały aktywność kaspazy 9 i 3. Ponadto najmniejsze nanocząstki o średnicy 29 nm spowodowały aktywację kaspazy 8.

W rozprawie posługiwano się licznymi metodami opartymi o cytofluorymetrię, fluorymetrię, spektrofotometrię, mikroskopię fluorescencyjną, mikroskopię sił atomowych, mikroskopię elektronową, elektroforezę i dwuwymiarową chromatografię cieczową.

Wykazano, że badane nanocząstki polistyrenu charakteryzowały się właściwościami cytotoksycznymi, prooksydacyjnymi, genotoksycznymi i proapoptotycznymi. Porównując działanie nanocząstek o różnych średnicach można stwierdzić, że najmniejsze nanocząstki (29 nm) wykazywały największą toksyczność względem badanych komórek. Powodowały one zmiany ww. parametrów już przy bardzo niskich stężeniach w porównaniu z cząstkami o większej średnicy, co może być związane z ich łatwiejszym wnikaniem do komórek ze względu na małe rozmiary i mniejszą wartość ujemnego potencjału zeta.

STRESZCZENIE W JĘZYKU ANGIELSKIM

Summary

Plastic pollution of the environment is now considered to be a global problem. Huge amounts of plastics waste enter the environment every year due to poor waste management and insufficient recycling as well as due to the long decomposition period of these plastics. In 2021, 390.7 million tons of plastic were produced worldwide, including 57.2 million tons in Europe. A serious ecotoxicological threat to organisms are particles formed from the breakdown of large pieces plastics so-called microparticles with diameters < 5000 nm and nanoparticles with diameters < 100 nm, which have been found in air, water, soil and food. Micro and nanoparticles are widely used in branches of industry, among others pharmaceutical, laboratory and cosmetics.

One of the most studied nanometer-structured synthetic plastics is polystyrene, which is formed by polymerization of styrene monomers. This plastic is used for packaging, production of electronics devices, household appliances, as well as to insulate buildings (styrofoam). Polystyrene particles, due to their small size, can easily enter living organisms through the respiratory, digestive or skin systems, and consequently pass through biological barriers and accumulate in tissues.

The aim of the research of this dissertation was to evaluate the pro-oxidant, pro-apoptotic and genotoxic effects of polystyrene nanoparticles (PS-NP) with different diameters (29 nm, 44 nm and 72 nm) in human peripheral blood mononuclear cells.

In this dissertation, the physico-chemical properties of polystyrene nanoparticles were tested to confirm the parameters of these particles declared by the manufacturers. The AFM and SEM images were consistent with the parameters stated in the labels of the purchased particles. Tests performed using the DLS technique of polystyrene nanoparticles incubated in water confirmed the particle diameter provided by the manufacturers, while incubation of the tested particles in RPMI medium significantly increased their diameter by up to three times for the smallest nanoparticles. In addition, the zeta potential was evaluated, which showed a significant change in the studied parameter depending on the particle size.

Starting with biological studies, the cytotoxicity of polystyrene nanoparticles of various diameters was evaluated. These particles caused a decrease in viability and changes in metabolic activity of human peripheral blood mononuclear cells (PBMCs), but only at very high concentrations of above 300 $\mu\text{g/mL}$.

Then, pro-oxidant properties of tested PS-NPs were evaluated. Polystyrene nanoparticles have been shown to induce the formation of reactive oxygen species (ROS) and highly reactive oxygen species, including hydroxyl radical. In turn, analysis of lipid and protein peroxidation showed, that PS-NPs caused a decrease in tryptophan fluorescence of proteins and induced a significant decrease in the fluorescence of cis-parinaric acid.

In the next phase, genotoxic effects of polystyrene nanoparticles were determined. PS-NPs of all analyzed diameters have been shown to induce single and double strand-breaks in studied cells, as well as caused double strand-breaks formation, but only after the exposure to smaller nanoparticles with diameters of 29 nm and 44 nm. In addition, it has been demonstrated the formation of oxidized purine and pyrimidine bases after treatment of peripheral blood mononuclear cells with tested polystyrene nanoparticles. Higher oxidative damage was observed when formamidopyrimidine glycosylase (Fpg) was used in the genotoxicity test. It was also proven that an increase in pyrimidine oxidation (the use of endonuclease III in the analysis) occurred at higher concentrations when compared to fpg-treated samples. An increase in 8-hydroxy-2-deoxyguanosine level was observed only after the exposure of tested cells to the smallest nanoparticles of 29 nm. The resulting DNA damage caused by larger nanoparticles of 44 nm and 72 nm was completely repaired after 120 min., while the repair of DNA lesions was not fully effective in the cells treated with the smallest particles of 29 nm.

The third step of this study was to assess proapoptotic properties of tested particles. Polystyrene nanoparticles increased the number of apoptotic cells, increased the level of cytosolic calcium ions, decreased transmembrane mitochondrial potential, and increased the activity of caspase-9 and caspase-3. In addition, the smallest nanoparticles of 29 nm in diameter, induced caspase-8 activation.

In this dissertation, number of methods was used based on cytofluorimetry, fluorimetry, spectrophotometry, fluorescence microscopy, atomic force microscopy, electron microscopy and two-dimensional liquid chromatography.

The tested NP-PSs are characterized by cytotoxic, pro-oxidative, genotoxic and pro-apoptotic properties. Comparing the effects of nanoparticles of different diameters, it can be concluded that the smallest nanoparticles of 29 nm are the most toxic to the tested cells. They caused changes in the above-mentioned parameters at lower concentrations compared to larger particles, which may be related to their easier penetration into cells due to their smaller size and lower value of negative zeta potential.

CEL NAUKOWY ORAZ OMÓWIENIE WYNIKÓW

WPROWADZENIE

Obecnie na całym świecie szczególną uwagę skupia się wokół mikro (MP) i nanoplastików (NP) w związku z rosnącym tempem ich emisji do środowiska naturalnego oraz zagrożeń wynikających z ich potencjalnego niekorzystnego oddziaływania na organizmy żywe. Mikroplastiki to drobiny tworzyw sztucznych o średnicy $< 5 \mu\text{m}$, które ulegają fragmentacji do nanoplastików o średnicy $< 0,1 \mu\text{m}$. Częstki są stosowane w wielu branżach m.in. farmaceutycznej, kosmetycznej czy laboratoryjnej (Dalela i wsp., 2015, Wang i wsp., 2018, Hernandez i wsp., 2017). Coraz większa ilość pojawiających się badań wskazuje na obecność omawianych cząstek w wodzie, glebie, powietrzu oraz żywności (Song i wsp., 2018, Zhang i wsp., 2018, Gasperi i wsp., 2018). Istotnym niekorzystnym faktem jest kumulowanie się cząstek plastiku w łańcuchu troficznym (Yee i wsp., 2021; Kik i wsp., 2020), co skutkuje ich obecnością w owocach morza (Hoogenboom, 2016) i ostatecznie przedostawaniem się do organizmów ludzi. Szereg badań wskazuje na fakt, że droga pokarmowa jest głównym sposobem przedostawania się cząstek do organizmów ludzi. Większość nanocząsteczek przedostających się do przewodu pokarmowego wchłania się przez barierę jelitową (Kreyling i wsp., 2017). Po przekroczeniu bariery jelitowej cząstki plastiku o wielkości $< 100 \text{ nm}$ mogą również przekraczać barierę krew-mózg (Wright i Kelly, 2017), a także barierę łożyskową (Graefmueller i wsp., 2015).

Inną drogą narażenia ludzi na cząsteczki nanoplastiku jest wdychanie powietrza. Wdychane nanocząsteczki mogą być eliminowane przez oczyszczanie śluzowo-rzęskowe, ale mogą również osadzać się w płucach lub być wchłaniane do układu krążenia (Geiser i Kreyling, 2010). Wdychane cząstki mikroplastiku mogą sprzyjać rozwojowi różnych chorób płuc poprzez indukowanie stanu zapalnego (Lu i wsp., 2022).

Kontakt dermalny został również uznany za jedną z dróg narażenia człowieka na cząstki nanoplastiku. Wykazano, że nanocząstki o średnicy mniejszej niż 40 nm dostają się do organizmu przez naskórek (Schneider i wsp., 2009).

Ostatnio Leslie i wsp. (2022) wykazali obecność plastiku we krwi 17 z 22 przebadanych osób. Co więcej, najnowsze badanie kohortowe 196 osób potwierdziło obecność cząstek nanoplastiku we krwi obwodowej wszystkich badanych osób (Salvia i wsp., 2023).

Wiadomo, że nanocząstki przenikają przez bariery biologiczne organizmów żywych i w konsekwencji kumulują się w tkankach (Al-Sid-Cheikh i wsp., 2018, Pitt i wsp., 2018). Udowodniono, że cząstki plastiku gromadzą się w jelitach i mogą zostać wydalone wraz z kałem (Lehner i wsp., 2017; Schwabl i wsp., 2019). Geiser i Kreyling (2010) wykazali, że nanocząstki plastiku wdychane do płuc mogą być dalej transportowane do układu

krwionośnego. Ponadto zaobserwowano, że mogą one przekraczać barierę łożyskową w wyniku dyfuzji pasywnej (Grafmüller i wsp., 2015). Wokół cząsteczek nanoplastiku może tworzyć się tzw. korona białkowa, która znacząco wpływa na ich właściwości takie jak: rozmiar, kształt, ładunek (Francia i wsp., 2019; Kihara i wsp., 2019). Występują dwa rodzaje korony białkowej „twarda” oraz „miękka”, które obejmują odpowiednio oddziaływanie nanocząstek z wewnętrzną i zewnętrzną warstwą białek (Kihara i wsp., 2020). Sugeruje się, że korona białkowa wpływa na transport nano- i mikroplastików do komórki. Badania Kihara i wsp., 2020 wykazały znaczące zmiany konformacyjne w białkach korony twardej wokół mniejszych nanocząstek o średnicy 20 nm w porównaniu do cząstek większych o średnicy 200 nm, co sugeruje że mniejsze nanocząstki plastiku mogą zakłócać procesy biochemiczne silniej niż większe cząstki.

Obecność cząstek plastiku w ludzkim ciele może powodować uszkodzenie komórek i prawdopodobnie wywoływać efekty immunologiczne (Rawle i wsp., 2022; Yin i wsp., 2023). Zauważono, że wdychanie cząstek stałych może powodować powstawanie chorób autoimmunologicznych takich jak: astma czy alergia poprzez mechanizmy translokacji cząstek, uwalnianie modulatorów immunologicznych, stres oksydacyjny oraz aktywację komórek odpornościowych, co w konsekwencji prowadzi do nadmiernej ekspozycji organizmu na antygeny i przeciwciała (Farhat i wsp., 2011). Niektóre wyniki badań *in vitro* sugerują, że nanocząstki polistyrenu mogą zmieniać funkcję układu odpornościowego (Rubio i wsp., 2020; Forte i wsp., 2016; Li i wsp., 2022).

Nie ma badań dotyczących toksycznego działania nanoplastików na ludzki układ krwionośny i jego komórki natomiast interakcje między komórkami krwi, w tym jednojądrzastymi komórkami krwi obwodowej i nanocząstkami polistyrenu obecnymi we krwi, mogą mieć istotne konsekwencje biologiczne. Ze względu na dużą liczbę jednojądrzastych komórek krwi obwodowej w układzie krążenia i ich zasadniczą rolę w układzie odpornościowym, są one często wykorzystywane jako komórki modelowe w badaniach oceniających toksyczność ksenobiotyków (Santovito i wsp., 2014; Sarma i wsp., 2022). Komórki te są istotnymi czynnikami odpowiedzi immunologicznej bowiem odpowiadają za eliminowanie komórek zakażonych wirusami oraz komórek nowotworowych, a także są odpowiedzialne za produkcję przeciwciał i regulację odpowiedzi immunologicznej (Larosa i Orange, 2008). Wykazano, że dysregulacja układu odpornościowego poprzez np. przyspieszoną śmierć jednojądrzastych komórek krwi obwodowej wiąże się z niekorzystnymi dla zdrowia zmianami w układzie odpornościowym i może skutkować osłabieniem odporności (Chu i wsp., 2021; Weinberg i wsp., 2004), co może w konsekwencji prowadzić do chorób autoimmunologicznych (cukrzyca typu 1, astma, alergie) i nowotworów (Hallit i Salameh, 2017; Ratomski i wsp., 2007).

Pomimo, powszechności występowania cząstek, w tym nanocząstek plastiku we krwi, a tym samym potencjalnego narażenia ludzi na ich wpływ, brak jest danych

toksykologicznych pozwalających na udzielenie odpowiedzi, czy plastikowe (polistyrenowe) nanocząstki są bezpieczne dla ludzi. Wydaje się zatem w pełni uzasadnione podjęcie badań dotyczących oceny wpływu nanocząstek polistyrenu w układzie *in vitro* na jednojądrzaste komórki krwi obwodowej człowieka w aspekcie ich działania prooksydacyjnego, genotoksycznego i proapoptotycznego.

CEL PRACY

Celem pracy doktorskiej było zbadanie mechanizmu działania niefunkcjonalizowanych nanocząstek polistyrenu o różnych średnicach (29, 44 i 72 nm) w jednojądrzastych komórkach krwi obwodowej człowieka poprzez określenie ich właściwości cytotoksycznych, prooksydacyjnych, genotoksycznych oraz proapoptotycznych.

MATERIAŁ BADAWCZY I METODY

Materiał badawczy

Materiał do badań stanowiły jednojądrzaste komórki krwi obwodowej wyizolowane z kożuszka leukocytarno-płytkowego zdrowych dawców. Krew pobierana była przez pracowników Regionalnego Centrum Krwiodawstwa i Krwiolecznictwa w Łodzi, a następnie poddawana diagnostyce laboratoryjnej. Katedra Biofizyki Skażeń Środowiska w której wykonano niniejszą pracę doktorską zakupuje krew do doświadczeń w oparciu o umowę z w/w Centrum, które posiada akredytację Ministra Zdrowia (nr BA/2/2004). Badania przedstawione w niniejszej pracy uzyskały również zgodę Komisji do spraw bioetyki badań naukowych UŁ No. 8/KBBN-UŁ/II/2019 (08/04/2019).

Badane związki

- niefunkcjonalizowane nanocząstki polistyrenu (ang. polystyrene nanoparticles – PS-NP) o średnicy 29, 44 i 72 nm zakupione w firmie Polysciences Europe GmbH

Przygotowanie prób

Do zawiesiny komórek (gęstość 1×10^6) dodawano przygotowany roztwór nanocząstek (o odpowiednich stężeniach wyjściowych) rozpuszczonych w PBS-ie, uzyskując końcowe stężenia plastiku w zakresie od 0,0001 do 1000 $\mu\text{g/ml}$. Do prób kontrolnych dodawano zamiast PS-NP bufor fosforanowy. Komórki kontrolne i z nanocząstkami inkubowano w pożywce RPMI przez 24 godziny w temp. 37 °C.

Metody

Charakterystyka fizyko-chemiczna nanocząstek

- ➔ Wykonanie zdjęć testowanych nanocząstek za wykorzystaniem mikroskopu sił atomowych (AFM) i skaningowego mikroskopu elektronowego (SEM).
- ➔ Ocena hydrodynamicznego rozmiaru nanocząstek polistyrenu za pomocą techniki dynamicznego rozpraszania światła (DLS) w środowisku wodnym oraz w pożywce RPMI.
- ➔ Ocena potencjału zeta nanocząstek w wodzie i pożywce RPMI.

Charakterystyka właściwości biologicznych nanocząstek

- ➔ Ocena żywotności komórek z wykorzystaniem znaczników fluorescencyjnych kalceiny-AM i jodku propidyny przy zastosowaniu cytometrii przepływowej (BD LSR II).
- ➔ Analiza aktywności metabolicznej za pomocą spektrofotometrycznej metody MTT opartej na redukcji soli tetrazolowej – bromek 3-(4,5-dimetylotiazol-2-yl)-2,5 difenylotetrazoliowy przez reduktazy komórkowe, głównie mitochondrialną dehydrogenazę bursztynianową.
- ➔ Ocena poziomu reaktywnych form tlenu (RFT) i wysoce reaktywnych form tlenu (w tym rodnika hydroksylowego) przy użyciu sond fluorescencyjnych: diocjanu 6-karboksy-2',7'-dichlorodihydroksyfluoresceiny (DCFH₂DA) oraz 3'-(p-hydroksyfenylo) fluoresceiny (HPF) z wykorzystaniem cytometru przepływowego (BD LSR II).
- ➔ Analiza poziomu peroksydacji lipidów przez pomiar fluorescencji kwasu cisparynarowego (maksima wzbudzenia/emisji: 320/432 nm) przy użyciu czytnika mikropłytek (CaryEclipse, Varian).
- ➔ Ocena utleniania białek poprzez pomiar fluorescencji tryptofanu (maksima wzbudzenia/emisji: 295/340 nm) przy użyciu czytnika mikropłytek (CaryEclipse, Varian).
- ➔ Analiza pojedynczych i podwójnych pęknięć DNA przy użyciu metody kometowej w wersji alkalicznej i mikroskopii fluorescencyjnej.
- ➔ Ocena poziomu uszkodzeń dwuniciowych DNA przy użyciu metody kometowej w wersji neutralnej i mikroskopii fluorescencyjnej.
- ➔ Oznaczenie oksydacyjnych uszkodzeń DNA przy użyciu enzymów restrykcyjnych tj. endonukleazy III (EndoIII) oraz glikozylazy formamidopirymidyny DNA (Fpg) z wykorzystaniem wersji alkalicznej testu kometowego i mikroskopii fluorescencyjnej.
- ➔ Ocena poziomu 8-hydroksy-2-deoksyguanozyny z zastosowaniem dwuwymiarowej chromatografii cieczowej.
- ➔ Ocena poziomu naprawy DNA z wykorzystaniem metody kometowej w wersji alkalicznej i mikroskopii fluoroscencyjnej.

- ➔ Analiza zmian w eksternalizacji fosfatydyloseryny (jako markera apoptozy) z wykorzystaniem znaczników fluorescencyjnych AneksynyV-FITC/jodku propidyny z użyciem cytometrii przepływowej (LSR II, Becton Dickinson).
- ➔ Analiza poziomu jonów wapnia w cytozolu z wykorzystaniem znacznika Fluo-3/AM, wykazującego, po związaniu z Ca^{2+} , silną zieloną fluorescencję. Wzbudzenie i emisja Fluo-3 następuje odpowiednio przy długości fali 490 nm/528 nm. Pomiar fluorescencji został przeprowadzony przy użyciu cytometru przepływowego (LSR II, Becton Dickinson).
- ➔ Ocena mitochondrialnego potencjału transbłonowego za pomocą znacznika fluorescencyjnego MitoTracker Red CMXRos (maksimum wzbudzenia/emisji – 490/515 nm). Fluorescencję zmierzono na czytniku mikropłytek (Cary Eclipse, Varian).
- ➔ Aktywność kaspaz 3 i 8 oparto na pomiarze fluorescencji 7-amino-4-metylokumaryny powstałej po hydrolizie substratów peptydowych odpowiednio Acetylo-Ile-GluThr-Asp-7-amino-4-metylokumaryny (Ac IETD-AMC) oraz acetylo-Asp-Glu-Val-Asp-7-amino-4-metylokumaryny (AcDEVD-AMC). Długość fali wzbudzenia dla AMC wynosiła 360 nm natomiast fali emisji 460 nm. Fluorescencję zmierzono na czytniku mikropłytek (Fluoroskan Ascent FL, Labsystem).
- ➔ Ocenę aktywności kaspazy 9 oparto na hydrolizie substratu Acetyl-Leu-Glu-His-Asp-p-nitroaniliny (Ac-LEHDpNA) do p-nitroaniliny (pNA), której absorbancję zmierzono przy długości fali wynoszącej 405 nm. Aktywność kaspazy 9 mierzono przy użyciu absorpcyjnego czytnika mikropłytek (BioTek ELx808, Bio-Tek).
- ➔ Poziom serynowo/treoninowej kinazy białkowej mTOR badano przy użyciu zestawu ELISA. Wartości absorbancji proporcjonalnej do ilości mTOR odczytano przy długości fali 405 nm za pomocą czytnika mikropłytek (BioTek, Synergy H1).

OMÓWIENIE WYNIKÓW

Cykl artykułów wchodzących w skład dysertacji otwiera publikacja przeglądowa pt. „*Polystyrene nanoparticles: occurrence in the environment, distribution in tissues, accumulation and toxicity to various organisms*”. W pracy tej skupiono się na omówieniu aktualnej literatury dotyczącej występowania mikro- i nanocząstek polistyrenu w środowisku, ich kumulacji w tkankach i toksyczności dla organizmów. W pierwszej kolejności dokonano charakterystyki cząstek plastiku, wymieniono najczęściej stosowane rodzaje plastików w tym polistyren oraz przedstawiono dane dotyczące światowego i europejskiego zużycia plastików. Następnie dokonano charakterystyki właściwości fizykochemicznych polistyrenu oraz wymieniono jego zastosowanie w różnych gałęziach przemysłu takich jak elektronika, kosmetologia, medycyna, budownictwo. W następnym etapie przedstawiono źródła mikro-

i nanocząstek polistyrenu w środowisku i ich akumulację w organizmach żywych. Na podstawie różnych doniesień literaturowych zilustrowano akumulację cząstek plastiku w łańcuchu pokarmowym. Z wielu opisanych badań wynika, że nano- i mikrocząstki znajdujące się w wodzie docierają do organizmów żywych na różnych poziomach łańcucha pokarmowego. Podkreślono, że nanocząstki po dostaniu się do organizmów mogą przenikać przez barierę krew-mózg, a tym samym mogą gromadzić się w mózgu. W kolejnym punkcie opisano tworzenie korony białkowej przez białka wiążące się z powierzchnią nanoplastików oraz mechanizm pobierania nanocząstek przez komórkę. Na końcu przedstawiono najnowsze publikacje dotyczące toksyczności nanoplastików zarówno w badaniach *in vivo* jak i *in vitro*.

Dokonano oceny właściwości fizyko-chemicznych nanocząstek polistyrenu i opublikowano je w drugiej pracy doświadczalnej pt. „*Polystyrene nanoparticles – the mechanism of their genotoxicity in human peripheral blood mononuclear cells*”. Wykonano zdjęcia nanocząstek za pomocą mikroskopu sił atomowych (AFM) i skaningowego mikroskopu elektronowego (SEM) oraz oceniono hydrodynamiczny rozmiar nanocząstek polistyrenu za pomocą techniki dynamicznego rozpraszania światła (DLS) w środowisku wodnym i pożywce RPMI. Badania średnicy nanocząstek w środowisku wodnym potwierdziły ich wielkość zgodną z deklaracją producenta. Natomiast w pożywce RPMI (zawierającej albuminę) stwierdzono większą średnicę nanocząstek (szczególnie w przypadku najmniejszych nanocząstek wykazano aż 3-krotnie większą średnicę), co prawdopodobnie było spowodowane powstaniem korony białkowej.

Ocena potencjału zeta w wodzie i w pożywce RPMI wykazała z kolei znaczną zmianę potencjału zeta w zależności od wielkości cząstek i zastosowanego środowiska chemicznego. W RPMI od -41 ± 3 mV (dla najmniejszych cząstek o wielkości 29 nm) do -56 ± 2 mV (dla największych cząstek o wielkości 71 nm). Natomiast bezwzględna wartość potencjału zeta w wodzie wynosiła od -40 ± 1 mV (dla najmniejszych cząstek o wielkości 29 nm) do -36 ± 1 mV (dla największych cząstek o średnicy 72 nm).

W pierwszej pracy doświadczalnej pt. „*Oxidative properties of polystyrene nanoparticles with different diameters in human peripheral blood mononuclear cells (in vitro study)*” oceniono żywotność jednojądrzastych komórek krwi obwodowej oraz parametry stresu oksydacyjnego indukowane przez nanocząstki polistyrenu o średnicy 29 nm, 44 nm i 72 nm. Analiza żywotności z zastosowaniem jodku propidyny i kalceiny-AM przeprowadzona była po 24-godzinnej inkubacji komórek z nanocząstkami i pozwoliła dobrać odpowiednie stężenia cząstek do wykonania dalszych badań. Statystycznie istotny spadek żywotności komórek obserwowano dla nanocząstek o średnicy 29 nm i 44 nm przy stężeniu 500 µg/ml, zaś dla największych nanocząstek o średnicy 72 nm odnotowano spadek badanego parametru wyłącznie przy stężeniu 1000 µg/ml.

Analizowane nanocząstki w niskich stężeniach (0,01 µg/ml/0,1 µg/ml) wykazywały zdolność generowania reaktywnych form tlenu oraz przy nieco wyższych stężeniach (1 µg/ml

i 10 µg/ml) indukowały powstawanie wysoce reaktywnych form tlenu (w tym rodnika hydroksylowego). Najintensywniejszy wzrost (od najniższych stężeń 0,01 µg/ml) poziomu RFT powodowały najmniejsze nanocząstki. Wzrostowi RFT towarzyszy uszkodzenie makromolekuł komórkowych. W związku z tym kolejnym etapem badań była ocena wpływu badanych nanocząstek polistyrenowych na indukcję uszkodzeń oksydacyjnych białek i lipidów. Stwierdzono, że badane cząstki wzmagają peroksydację lipidów oraz utlenianie białek, przy czym ponownie najsilniejsze zmiany w badanych parametrach wykazano w komórkach inkubowanych z najmniejszymi nanocząstkami.

Oznaczono również zmiany w liczbie komórek apoptotycznych. Wzrost odsetka komórek apoptotycznych wykazano przy niższych stężeniach nanocząstek o średnicy 29 nm od stężenia 1 µg/ml oraz od stężeń 10 µg/ml i 100 µg/ml odpowiednio dla nanocząstek o średnicy 44 nm i 72 nm. Przeprowadzono również badania dotyczące apoptotycznego mechanizmu działania nanocząstek. Uzyskane wyniki zawarte są w manuskrypcie gotowym do wysłania (3 praca doświadczalna).

Druga praca doświadczalna pt. „*Polystyrene nanoparticles – the mechanism of their genotoxicity in human peripheral blood mononuclear cells*” dotyczyła badań mających na celu wyjaśnienie mechanizmu genotoksycznego działania nanocząstek polistyrenowych o różnych średnicach w jednojądrzastych komórkach krwi obwodowej człowieka.

Wzrost poziomu reaktywnych form tlenu (obserwowany w pierwszej pracy oryginalnej) może przyczyniać się do uszkodzania białek i lipidów, ale także do oksydacyjnych zmian w strukturze DNA. Tym samym w kolejnym etapie badań dokonano oceny potencjału genotoksycznego badanych nanocząstek w jednojądrzastych komórkach krwi obwodowej człowieka. Stwierdzono, że badane cząstki po 24-godzinnej inkubacji spowodowały powstanie zarówno pojedynczych, jak i podwójnych pęknięć nici DNA. Największe uszkodzenia odnotowano pod wpływem najmniejszych nanocząstek o średnicy 29 nm, które były istotne statystycznie już od stężenia 0,01 µg/ml. Mniejsze zmiany odnotowano pod wpływem nanocząstek o średnicy 44 nm od stężenia 0,1 µg/ml, a najniższy poziom uszkodzeń stwierdzono w przypadku największych nanocząstek o średnicy 72 nm dopiero od stężenia 10 µg/ml. Wykazano także, że badane nanocząstki indukowały uszkodzenia dwuniciowe DNA, jednak tylko przy najwyższych stężeniach tj. 10 i 100 µg/ml odpowiednio dla nanocząstek o średnicy 29 nm i 44 nm.

Następnie oceniono oksydacyjne uszkodzenia puryn i pirymidyn w DNA jednojądrzastych komórek krwi obwodowej człowieka narażonych na działanie badanych nanocząstek. Nanocząstki polistyrenu spowodowały wzrost poziomu oksydacyjnie zmodyfikowanych pirymidyn, jednak tylko w wysokich stężeniach, tj. 10 µg/ml i 100 µg/ml odpowiednio dla cząstek o średnicy 29 nm oraz 44 nm i 72 nm. Stwierdzono również, że badane nanocząstki spowodowały silniejsze oksydacyjne uszkodzenia puryn niż pirymidyn w badanych komórkach krwi. Zmiany w ww. parametrach były istotne w stężeniach 1 µg/ml,

10 µg/ml i 100 µg/ml odpowiednio pod wpływem nanocząstek o średnicy 29 nm, 44 nm i 72 nm.

Zastosowano również dwuwymiarową chromatografię cieczową do analizy 8-hydroksy-2-deoksyguanozyny (8-oksodG), wykazując niewielki wzrost poziomu tej pochodnej od stężenia 0,1 mg/ml tylko pod wpływem nanocząstek o najmniejszym rozmiarze tj. średnicy 29 nm.

Wykazano również, że jednojądrzaste komórki krwi obwodowej człowieka efektywnie naprawiały w czasie 2 godzin uszkodzenia DNA spowodowane działaniem nanocząstek o średnicy 44 nm i 72 nm w stężeniu 100 µg/ml, jednak nie były w stanie całkowicie usunąć powstałych zmian pod wpływem najmniejszych cząstek w identycznym stężeniu.

Przeprowadzone badania wykazały, że analizowane nanocząstki spowodowały uszkodzenia struktury DNA prawdopodobnie pośrednio na skutek indukowanych przez nie RFT.

Należy nadmienić, iż powstawanie uszkodzeń jednoniciowych DNA stwierdzono pod wpływem ww. nanocząstek w stężeniach, które potencjalnie mogą być obecne w organizmie człowieka wskutek podwyższonego narażenia na te substancje.

Zaobserwowaliśmy, że PS-NP o najmniejszej średnicy i najniższej bezwzględnej wartości ujemnego potencjału zeta wykazywały najsilniejszą cytotoksyczność i genotoksyczność, co prawdopodobnie było związane z ich najłatwiejszym wnikaniem do badanych komórek. Istotną rolę w przenikaniu badanych nanocząstek do komórek odgrywa prawdopodobnie powstająca korona białkowa.

Uzyskana średnica zmierzona metodą DLS dla najmniejszych cząstek (29 nm) w pożywce RPMI zawierającej albuminę była trzykrotnie większa niż wartość zmierzona w wodzie i deklarowana przez producenta. Średnica największych cząstek 72 nm, zmierzona metodą DLS, była najbliższa tej uzyskanej w wodzie, a także zadeklarowanej przez producenta. Nasze obserwacje są zgodne z badaniami Gopinath i wsp. (2019), którzy wykazali, że nanocząstki z koroną białkową spowodowały większe efekty genotoksyczne i cytotoksyczne w ludzkich komórkach krwi niż nanocząstki nieopłaszczone.

Ostatnia praca doświadczalna pt. „*The effect of non-functionalized polystyrene nanoparticles of different diameters on the induction of apoptosis and mTOR level in human peripheral blood mononuclear cells*” dotyczy określenia proapoptotycznego mechanizmu działania nanocząstek polistyrenu w jednojądrzastych komórkach krwi obwodowej człowieka.

Zmiany w liczbie (odsetku) komórek apoptotycznych analizowano w pierwszej pracy doświadczalnej, natomiast w niniejszej (trzeciej) pracy zobrazowano zmiany apoptotyczne za pomocą podwójnego barwienia z jodkiem propidyny i Aneksyną-V skoniugowaną z izotiocyanianem fluoresceiny (FITC). Wykazano, że proces apoptozy był najsilniej wzmagany przez najmniejsze nanocząstki, które spowodowały (wyniki uzyskane w oparciu o przeprowadzoną analizę cytometryczną oceniającą poziom eksternalizacji

fosfatydyloseryny) istotny statystycznie wzrost odsetka komórek apoptotycznych od stężenia 1 $\mu\text{g/ml}$.

Następnie zbadano poziom jonów wapnia w cytozolu oraz poziom transbłonowego potencjału mitochondrialnego ($\Delta\Psi_m$) w jednojądrzastych komórkach krwi obwodowej człowieka inkubowanych przez 24 godziny z badanymi nanocząstkami w zakresie stężeń od 0,001 do 100 $\mu\text{g/ml}$. Statystycznie istotny wzrost poziomu jonów wapnia w cytozolu zaobserwowano w komórkach inkubowanych z nanocząstkami o średnicy 29 nm w stężeniach od 0,001 do 0,1 $\mu\text{g/ml}$, z nanocząstkami o średnicy 44 nm w stężeniach od 0,01 do 10 $\mu\text{g/ml}$ oraz z nanocząstkami o średnicy 72 nm w stężeniach od 0,1 i 10 $\mu\text{g/ml}$. Jon wapnia jest ważnym regulatorem apoptozy. Wzrost mitochondrialnego wychwytu Ca^{2+} skutkuje zmianą depolaryzacji mitochondriów, a następnie otwarciem porów przejściowych przepuszczalności (mPTP) w tym organellum, co prowadzi do apoptotycznej śmierci komórki. Jony wapnia mogą również aktywować kalpains, które rozszczepiają różne białka z rodziny BCL-2 (D'Orsi i wsp., 2012; Hajnóczy i wsp., 2003; Sukumaran i wsp., 2021). Uzyskane wyniki wykazały wzrost poziomu jonów wapnia w cytozolu przy stężeniach nanocząstek niższych niż te, które spowodowały zmiany w pozostałych parametrach apoptozy, co wskazuje, że proces ten poprzedzał całą kaskadę zmian apoptotycznych.

Zaobserwowano również statystycznie istotny spadek wartości potencjału transbłonowego mitochondriów w komórkach traktowanych wszystkimi testowanymi cząstkami. Nanocząstki o średnicy 29 nm spowodowały zmiany wartości $\Delta\Psi_m$ od stężenia 1 $\mu\text{g/ml}$, podczas gdy cząstki o większej średnicy indukowały zmiany tego parametru od stężenia 10 $\mu\text{g/ml}$. Według badań obniżenie wartości potencjału mitochondrialnego może występować w początkowym etapie apoptozy, ale może być także skutkiem tego procesu (Wacquier i wsp., 2020; Ly i wsp., 2003). Niewątpliwie jednak, zmiany potencjału mitochondrialnego są związane z zaburzeniami w przepuszczalności błony mitochondrialnej, co może skutkować inicjacją apoptozy poprzez uwolnienie z mitochondriów czynników proapoptotycznych.

Enzymami biorącymi udział w apoptozie są kaspazy 9, 8 i 3. Kaspaza 9 bierze aktywny udział w apoptotycznym szlaku wewnętrznym natomiast kaspaza 8 uczestniczy w szlaku zewnętrznym apoptozy. Oba enzymy aktywują kaspazę 3, będącą kaspazą efektorową. Proteaza ta reguluje funkcjonowanie licznych cząsteczek biologicznych i odpowiada za proces kontrolowanej śmierci komórki.

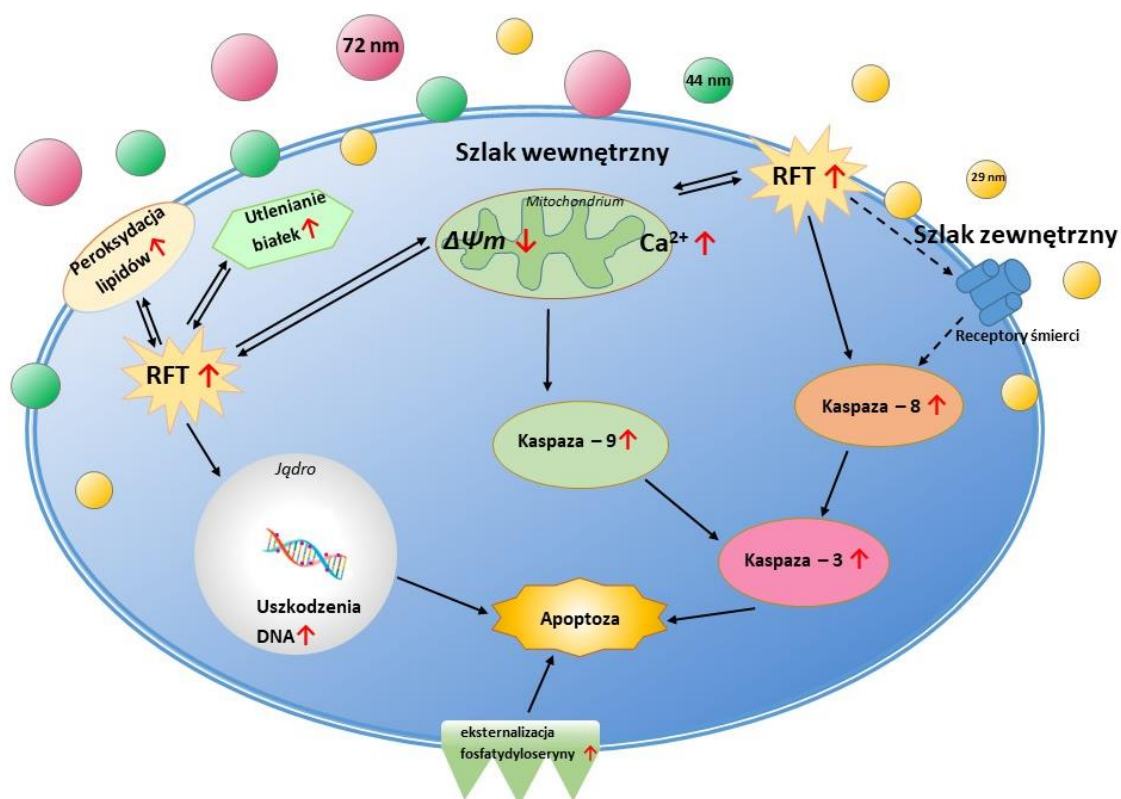
Zaobserwowano, że wyłącznie nanocząstki polistyrenu o średnicy 29 nm spowodowały statystycznie istotne zmiany w aktywności wszystkich testowanych kaspaz. Z kolei cząstki o średnicach 44 nm i 72 nm spowodowały zmiany w aktywności kaspazy 9 i kaspazy 3, natomiast nie aktywowały kaspazy 8.

W niniejszej pracy analizowano także poziom białka mTOR, będącego kinazą serynowo-treoninową zaangażowaną w regulację różnych procesów komórkowych, takich jak

metabolizm energii komórkowej, autofagia i apoptoza (Wang i wsp., 2022). Zaobserwowano statystycznie istotny wzrost poziomu mTOR po inkubacji jednojądrzastych komórek krwi obwodowej zbadanymi cząstkami o różnej wielkości. Nanocząstki polistyrenu o średnicy 29 nm spowodowały wzrost poziomu mTOR w zakresie stężeń od 0,1 do 1 µg/ml, natomiast nanocząstki o średnicy 44 nm podwyższały badany parametr w stężeniach 0,1 µg/ml i 10 µg/ml. Największe nanocząstki o średnicy 72 nm zwiększały poziom mTOR przy najwyższych stężeniach, tj.: 10 µg/ml i 100 µg/ml. Wzrost poziomu mTOR odnotowano przy stężeniach mniejszych niż te, które indukowały apoptozę, po czym odnotowano zmniejszenie aktywacji badanej kinazy pod wpływem nanocząstek w stężeniach porównywalnych do tych, przy których obserwowano apoptozę. Ostatecznie, przy najwyższych stężeniach nanocząstek (29 nm, stężenia 10 µg/ml i 100 µg/ml) poziom mTOR osiągnął wartość zbliżoną do kontroli.

Dotychczas opublikowane dane wskazują na fakt, że całkowity poziom ATP (Budd i wsp., 2000; Leist i wsp., 1997) pozostaje niezmienny we wczesnych stadiach apoptozy, a Lu i wsp., (2022) zasugerowali nawet, że warunkiem wstępnym apoptotycznej śmierci komórki jest wzrost poziomu ATP w cytozolu. W niniejszych badaniach nie odnotowano podwyższonego poziomu ATP, a jedynie spadek tego parametru po ekspozycji badanych komórek na najmniejsze nanocząstki o średnicy 29 nm w stężeniu 100 µg/mL i 200 µg/mL.

Podsumowując można stwierdzić, że testowane nanocząstki indukowały apoptozę poprzez eksternalizację fosfatydyloseryny w błonie komórkowej, zwiększając cytozolowy poziom Ca^{2+} , zmniejszając transbłonowy potencjał mitochondrialny, a także aktywując kaspazę 9 i kaspazę 3. Badane nanocząstki indukowały apoptozę poprzez zaangażowanie szlaku mitochondrialnego; tym niemniej najmniejsze nanocząstki o średnicy 29 nm aktywowały dodatkowo zewnętrzny szlak apoptotyczny. Podobnie, jak w przypadku wyników badań dotyczących oksydacyjnych uszkodzeń biomolekuł, największe efekty apoptotyczne odnotowano pod wpływem najmniejszych nanocząstek polistyrenu o średnicy 29 nm, w porównaniu z większymi nanocząstkami, szczególnie tymi o średnicy 72 nm. Zmiany apoptotyczne odnotowano pod wpływem nanocząstek w stężeniach, które najprawdopodobniej nie mogą być oznaczone we krwi ludzi narażonych środowiskowo na te substancje.



Schemat 1. Proponowany mechanizm działania nanocząstek w jednojądrzastych komórkach krwi obwodowej człowieka.

PODSUMOWANIE

- Badane nanocząstki indukowały stres oksydacyjny poprzez wzrost poziomu reaktywnych form tlenu, w tym wysoce reaktywnych form tlenu, oksydacyjne uszkodzenia lipidów i białek oraz zasad purynowych i pirymidynowych w DNA.

Parametry/Związek [μg/ml]	PS-NP 29 nm	PS-NP 44 nm	PS-NP 72 nm
Odsetek komórek żywych	500 ↓	500 ↓	1000 ↓
Aktywność metaboliczna	300 ↓	500 ↓	500 ↓
Poziom RFT	0,01 ↑	0,01 ↑	0,1 ↑
Poziom wysoce reaktywnych form tlenu	1 ↑	10 ↑	10 ↑
Poziom peroksydacji lipidów	0,1 ↑	1 ↑	1 ↑
Poziom utleniania białek	0,1 ↑	1 ↑	1 ↑

- Badane nanocząstki polistyrenu indukowały jedno- i dwuniciowe uszkodzenia DNA. Najmniejsze nanocząstki powodowały także powstawanie utlenionej pochodnej

8-hydroksy-2-deoksyguanozyny, a uszkodzenia DNA przez nie indukowane nie były naprawiane w pełni w czasie 2 h.

Parametry/Związek [μg/ml]	PS-NP 29 nm	PS-NP 44 nm	PS-NP 72 nm
Poziom uszkodzeń jedno- i dwuniciowych	0,01 ↑	0,1 ↑	10 ↑
Poziom uszkodzeń dwuniciowych	10 ↑	100 ↑	–
Poziom uszkodzeń zasad purynowych	1 ↑	10 ↑	100 ↑
Poziom uszkodzeń zasad pirymidynowych	10 ↑	100 ↑	100 ↑
Poziom 8-hydroksy-2-deoksyguanozyny	0,1 ↑	–	–
Całkowita naprawa DNA (120 minut)	Nie	Tak	Tak

- ➔ Wszystkie badane nanocząstki indukowały apoptozę poprzez szlak wewnętrzny, podwyższając poziom jonów wapnia w cytozolu komórek, obniżając potencjał mitochondrialny oraz aktywując kaspazę 9 i kaspazę 3. Najmniejsze nanocząstki polistyrenu aktywowały również kaspazę 8, co wskazuje na możliwość zaangażowania szlaku zewnętrznego przez te badane substancje.

Parametry/Związek [μg/ml]	PS-NP 29 nm	PS-NP 44 nm	PS-NP 72 nm
Odsetek komórek apoptotycznych	1 ↑	10 ↑	100 ↑
Poziom jonów wapnia w cytozolu	0,001 ↑	0,01 ↑	0,1 ↑
Poziom transblonowego potencjału mitochondrialnego ($\Delta\Psi_m$)	1 ↓	10 ↓	10 ↓
Aktywność kaspazy 8	1 ↑	–	–
Aktywność kaspazy 9	10 ↑	100 ↑	100 ↑
Aktywność kaspazy 3	10 ↑	10 ↑	10 ↑

- ➔ Nanocząstki polistyrenu podwyższały poziom mTOR w stężeniach mniejszych niż te, które indukowały apoptozę. Obserwowano także zmniejszenie poziomu mTOR przy stężeniach nanocząstek porównywalnych do tych, które wzmacniały proces apoptozy, aż do osiągnięcia poziomu kontrolnego.

WNIOSKI

- ➔ Niefunkcjonalizowane nanocząstki polistyrenu o średnicach 29 nm, 44 nm i 72 nm charakteryzują się zróżnicowanym potencjałem cytotoksycznym, oksydacyjnym, genotoksycznym oraz apoptotycznym w jednojądrzastych komórkach krwi obwodowej człowieka.
- ➔ Największe zmiany w analizowanych parametrach zaobserwowano pod wpływem nanocząstek o najmniejszej średnicy 29 nm, co może wiązać się z najniższą wartością bezwzględną ujemnego potencjału zeta tych cząstek i możliwością łatwiejszego wnikania do komórek.
- ➔ Zmiany w poziomie RFT oraz uszkodzeniach DNA odnotowano pod wpływem niskich stężeń PS-NP, które prawdopodobnie mogą być oznaczane w organizmie człowieka przy podwyższonym narażeniu na te nanocząstki.

LITERATURA UZUPEŁNIAJĄCA

1. Al-Sid-Cheikh M., Rowland J. S., Stevenson K., Rouleau C., Henry B.T., Thompson C.R. 2018. Uptake, Whole-Body Distribution, and Depuration of Nanoplastics by the Scallop *Pecten maximus* at Environmentally Realistic Concentrations. *Environmental Science Technology*, 52, 24, 14480-14486.
2. Budd S.L., Tenneti L., Lishnak T., Lipton S.A. 2000. Mitochondrial and extramitochondrial apoptotic signaling pathways in cerebrocortical neurons. *Proceedings of the National Academy of Sciences of the United States of America*, 97, 6161–6166.
3. Chu C.-M., Chiu L.-C., Yu C.-C., Chuang L.-P., Kao K.-C., Li L.-F., Wu H.-P. 2021. Increased Death of Peripheral Blood Mononuclear Cells after TLR4 Inhibition in Sepsis Is Not via TNF/TNF Receptor-Mediated Apoptotic Pathway. *Mediators of Inflammation* 2021, 1–9.
4. D’Orsi B., Bonner H., Tuffy L.P., Düssmann H., Woods I., Courtney M.J., Ward M.W., Prehn J.H.M. 2012. Calpains Are Downstream Effectors of bax -Dependent Excitotoxic Apoptosis *Journal Neurosciences*, 32, 1847–1858.
5. Dalela M., Shrivastav T.G., Kharbanda S., Singh H. 2015. pH-Sensitive Biocompatible Nanoparticles of Paclitaxel-Conjugated Poly(styrene- co -maleic acid) for Anticancer Drug Delivery in Solid Tumors of Syngeneic Mice. *ACS Applied Materials and Interfaces*, 7, 26530–26548.
6. Farhat S., C. Silva M. Orione L., Campos A., Sallum and A. Braga. 2011. Air Pollution in Autoimmune Rheumatic Diseases: A Review. *Autoimmunity Reviews* 11 (1): 14–21.
7. Forte M., Iachetta G., Tussellino M., Carotenuto R., Prisco M., De Falco M., Laforgia V., Valiante S. 2016. Polystyrene nanoparticles internalization in human gastric adenocarcinoma cells. *Toxicology in Vitro* 31, 126–136.

8. Francia V., Yang K., Deville S., Reker-Smit C., Nelissen I., Salvati A. 2019. Corona composition can affect the mechanism cells use to internalize nanoparticles. *ACS Nano*, 22; 13(10): 11107-11121.
9. Gasperi J., Wright S.L., Dris R., Collard F., Mandin C., Guerrouache M., Langlois V., Kelly F.J., Tassin B. 2018. Microplastics in air: Are we breathing it in? *Current Opinion in Environmental Science & Health* 1, 1–5.
10. Geiser M., Kreyling W.G. 2010. Deposition and biokinetics of inhaled nanoparticles. *Particle and Fibre Toxicology*, 7, 2.
11. Gopinath M.P., Saranya V., Vijayakumar S., Meera M.M., Ruprekha S., Kunal R., Pranay A., Thomas J., Mukherjee A., Chandrasekaran N. 2019. Assessment on interactive prospectives of nanoplastics with plasma proteins and the toxicological impacts of virgin, coronated and environmentally released-nanoplastics. *Scientific Reports*, 9, 8860.
12. Grafmueller S., Manser P., Diener L., Diener P.-A., Maeder-Althaus X., Maurizi L., Jochum W., Krug H.F., Buerki-Thurnherr T., von Mandach U., Wick P. 2015. Bidirectional Transfer Study of Polystyrene Nanoparticles across the Placental Barrier in an ex Vivo Human Placental Perfusion Model. *Environmental Health Perspectives* 123, 1280–1286.
13. Hajnóczky G., Davies E., Madesh M. 2003. Calcium signaling and apoptosis. *Biochemical and Biophysical Research Communications* 304, 445–454.
14. Hallit S., Salameh P. 2017. Exposure to toxics during pregnancy and childhood and asthma in children: A pilot study. *JEGH* 7, 147.
15. Hernandez M., L., Xu G.E., Larsson E.C.H., Tahara R., Maisuria B.V., Tufenkji N. 2019. Plastic teabags release billions on microplastics into tea. *Environmental Science Technology*, 53, 21, 12300-12310.
16. Hernandez M.L., Yousefi N., Tufenkji N. 2017. Are there nanoplastics in your personal care products *Environmental Science Technology Letters*, 4 (7): 280-285.
17. Hoogenboom L.A.P., Statement: Presence of microplastics and nanoplastics in food, with particular focus on seafood. *EFSA Journal* 1-30.
18. Kihara S., Ghosh S., McDougall R.D., Whitten E.A., Mata P.J., Koper I., McGillivray J.D. 2020. Structure of soft and hard protein corona around polystyrene nanoplastics- Particle size and protein types. *Biointerphases*, 11; 15(5): 051002.
19. Kihara S., Heijden van der J.N., Seal K.C., Mata P.J., Whitten E.A., Köper I., Duncan J McGillivray J.D. 2019. Soft and hard interactions between polystyrene nanoplastics and human serum albumin protein corona. *Bioconjugate Chemistry*, 17, 30(4): 1067-1076.
20. Kole J.P., Lohr J.A., Belleghem Van J.A.G.F., Ragas J.M. 2017. Wear and tear of tyres: A stealthy source of microplastics in the environment. *Environmental Research and Public Health*, 14(10), 1265.
21. Kreyling W.G., Holzwarth U., Haberl N., Kozempel J., Hirn, S., Wenk A., Schleh C., Schäffler M., Lipka J., Semmler-Behnke M., Gibson N. 2017. Quantitative biokinetics of titanium dioxide nanoparticles after intravenous injection in rats: Part 1. *Nanotoxicology* 11, 434–442.
22. Larosa F.D., Orange S.J. 2008. Lymphocytes. *Journal of Allergy and Clinical Immunology*, 121(2): S364-9.

23. Lehner R., Petri-Fink A., Rothen-Rutishauser B. 2017. Nanoplastic impact on human health- a 3D intestinal model to study the interaction with nanoplastic particles. Proceedings of the international conference on microplastic pollution in the Mediterranean Sea, 167-170.
24. Leist M., Single B., Castoldi A.F., Kühnle S., Nicotera P. 1997. Intracellular Adenosine Triphosphate (ATP) Concentration: A Switch in the Decision Between Apoptosis and Necrosis. *Journal of Experimental Medicine* 185, 1481–1486.
25. Leslie A. H., van Velzen M. J. M., Brandsma H. S., Vethaak D. A., Garcia-Vallejo J. J. and Lamoree M. H. 2022. Discovery and Quantification of Plastic Particle Pollution in Human Blood. *Environment International* 163: 107199.
26. Li Y., Xu M., Zhang Z., Halimu G., Li, Yongqiang Li, Yansheng Gu, W., Zhang B., Wang X. 2022. In vitro study on the toxicity of nanoplastics with different charges to murine splenic lymphocytes. *Journal of Hazardous Materials* 424, 127508.
27. Lu K., Zhan D., Fang Y., Li L., Chen G., Chen S., Wang L. 2022. Microplastics, potential threat to patients with lung diseases. *Frontiers in Toxicology*, 4, 958414.
28. Lu K., Zhan D., Fang Y., Li, L., Chen G., Chen S., Wang L. 2022. Microplastics, potential threat to patients with lung diseases. *Frontiers in Toxicology*, 4, 958414.
29. Ly J.D., Grubb D.R., Lawen A. 2003. The mitochondrial membrane potential ($\Delta\psi_m$) in apoptosis; an update. *Apoptosis* 8, 115–128.
30. Pitt A.J., Trevisan R., Massarsky A., Kozal S.J., Levin D.E., Giulio Di T.R. 2018. Maternal transfer of nanoplastic to offspring in zebrafish (*Danio rerio*): a case study with nanopolystyrene. *Science of the Total Environment*, 1(643) 324-334.
31. Ratomski K., Skotnicka B., Kasprzycka E., Żelazowska-Rutkowska B., Wysocka J., Anisimowicz S. 2007. Ocena odsetka limfocytów CD19+CD5+ w przerosłych migdałkach gardłowych u dzieci chorych na wysiękowe zapalenie ucha środkowego. *Otolaryngologia Polska* 61, 962–966.
32. Rawle D.J., Dumenil T., Tang B., Bishop C.R., Yan K., Le T.T., Suhrbier A. 2022. Microplastic consumption induces inflammatory signatures in the colon and prolongs a viral arthritis. *Science of The Total Environment* 809, 152212.
33. Rubio L., Barguilla I., Domenech J., Marcos R., Hernández A. 2020. Biological effects, including oxidative stress and genotoxic damage, of polystyrene nanoparticles in different human hematopoietic cell lines. *Journal of Hazardous Materials* 398, 122900.
34. Salvia R., Rico G.L., Bradford A.J., Ward D.M., Olszowy W.M., Martinez C., Madrid-Aris D.A., Grifols R.J., Ancochea A., Gomez-Munoz L., Vives-Pi M., Martinez-Caceres E., Fernandez A.M., Sorigue M., Petriz J. 2023. Fast-screening flow cytometry method for detecting nanoplastics in human peripheral blood. *MethodsX*. 6, 10, 102057.
35. Santovito A., Cervella P., Delpero M. 2014. Chromosomal damage in peripheral blood lymphocytes from nurses occupationally exposed to chemicals. *Human Experimental Toxicology*, 33, 897–903.
36. Sarma D.K., Dubey R., Samarth R.M., Shubham S., Chowdhury P., Kumawat M., Verma V., Tiwari R.R., Kumar M. 2022. The biological effects of polystyrene nanoplastics on human peripheral blood lymphocytes. *Nanomaterials* 12, 1632.
37. Schneider M., Stracke F., Hansen S., Schaefer U.F. 2009. Nanoparticles and their interactions with the dermal barrier. *Dermato-Endocrinology*, 1, 197–206.

38. Schwabl P., Koppel S., Konigshofer P., Bucsics T., Trauner M., Reiberger T., Liebmann B. 2019. Detection of various microplastics in human stool: a prospective case series. *Annals of International Medicine*, 1, 171(7): 453-457.
39. Song Y.K., Hong S.H., Eo S., Jang M., Han G.M., Isobe A., Shim W.J. 2018. Horizontal and Vertical Distribution of Microplastics in Korean Coastal Waters. *Environmental Science Technology*, 52, 12188–12197.
40. Sukumaran P., Nascimento Da Conceicao V., Sun Y., Ahamad N., Saraiva L.R., Selvaraj S., Singh B.B. 2021. Calcium Signaling Regulates Autophagy and Apoptosis. *Cells* 10, 2125.
41. Vogt A., Combadiere B., Hadam S., Stieler K.M., Lademann J., Schaefer H., Autran B., Sterry W., Blume-Peytavi U. 2006. Nanoparticles Enter Epidermal CD1a+ Cells after Transcutaneous Application on Human Skin. *Journal of Investigative Dermatology* 126, 1316–1322.
42. Wacquier B., Combettes L., Dupont G. 2020. Dual dynamics of mitochondrial permeability transition pore opening. *Scientific Reports*, 10, 3924.
43. Wang L., Xie X., Cao T., Bosset J., Bakker E. 2018. Surface-Doped Polystyrene Microsensors Containing Lipophilic Solvatochromic Dye Transducers. *Chemistry European Journal*, 24, 7921–7925.
44. Wang, X. 2022. In vitro study on the toxicity of nanoplastics with different charges to murine splenic lymphocytes. *Journal of Hazardous Materials* 424, 127508.
45. Weinberg A., Jesser R.D., Edelstein C.L., Bill J.R., Wohl D.A. 2004. Excess apoptosis of mononuclear cells contributes to the depressed cytomegalovirus-specific immunity in HIV-infected patients on HAART. *Virology* 330, 313–321.
46. Wright S.L., Kelly F.J. 2017. Plastic and Human Health: A Micro Issue? *Environmental Science Technology*, 51, 6634–6647.
47. Yee L-S. M., Hii W-L., Looi K. C., Lim M-W., Wong F-S., Kok Y-Y., Tan K-B., Wong Y-C., Leong O-C. 2021. Impact of Microplastics and Nanoplastics on Human Health *Nanomaterials (Basel)* 11(2):496.
48. Yin K., Wang D., Zhang Y., Lu H., Hou L., Guo T., Zhao H., Xing M. 2023. Polystyrene microplastics promote liver inflammation by inducing the formation of macrophages extracellular traps. *Journal of Hazardous Materials* 452, 131236.
49. Zhang G.S., Liu Y.F. 2018. The distribution of microplastics in soil aggregate fractions in southwestern China. *Science of The Total Environment* 642, 12–20.

DOROBK NAUKOWY

Artykuły wchodzące w skład rozprawy doktorskiej:

1. **Kik K.**, Bukowska B., Sicińska P. 2020. „*Polystyrene nanoparticles: Sources, occurrence in the environment, distribution in tissues, accumulation and toxicity to various organisms*” *Environmental Pollution*, 262: 114297 (IF: 8,041; pkt. MEiN 100).
2. **Kik K.**, Bukowska B., Krokosz A., Sicińska P. 2021 „*Oxidative Properties of Polystyrene Nanoparticles with Different Diameters in Human Peripheral Blood Mononuclear Cells (In Vitro Study)*” *International Journal of Molecular Sciences* 22(9), 4406 (IF: 6,208; pkt. MEiN= 140).
3. **Malinowska K.**, Bukowska B., Piwoński I., Foksiński M., Kisielewska A., Zarakowska E., Gackowski D., Sicińska P. 2022. „*Polystyrene nanoparticles: the mechanism of their genotoxicity in human peripheral blood mononuclear cells*” *Nanotoxicology*, 6(6-8):791-811 (IF: 5.881; pkt. MEiN= 140).
4. **Malinowska K.**, Sicińska P., Michałowicz J., Bukowska B., „*The effect of non-functionalized polystyrene nanoparticles of different diameters on the induction of apoptosis and mTOR level in human peripheral blood mononuclear cells*” *Chemosphere* 335, 139137; 1-13 (IF: 8,943; pkt. MEiN= 140).

Łączny *impact factor* powyższych prac jest równy **29,073 (520 punktów MEiN)**.

Inne artykuły z list JCR

1. Sicińska P., **Kik K.**, Bukowska B. 2020 *Human erythrocytes exposed to phthalates and their metabolites alter antioxidant enzyme activity and hemoglobin oxidation*. *International Journal of Molecular Science* 24; 21(12): 4480. (IF: 4,556; pkt. MEiN 140)

Łączny *impact factor* wszystkich prac jest równy **33,629 (680 punktów MEiN)** (zgodnie z rokiem opublikowania).

Rozdziały w monografiach

1. **Kik K.**, Bukowska B. 2019. *Plastik w środowisku. Co wiemy o jego szkodliwości?* Enterprise Europe Network, Nr 9(170), ISSN:2544-0675
2. **Kik K.** 2020. *Wpływ nanocząstek polistyrenu na komórki krwi*. Biomedycyna środowiska i zdrowie, Wydawnictwo ArchaeGraph, Kielce, s. 87-100, ISBN: 978-83-66709-16-4 (IF-; pkt. MEiN 20)

Doniesienia zjazdowe:

1. **Kik K.**, „Wpływ wybranych ftalanów i ich metabolitów na aktywność systemu antyoksydacyjnego w erytrocytach człowieka” IX Sesja Magistrantów i Doktorantów Łódzkiego Środowiska Chemików, Łódź 21 czerwca 2018 r. (sesja plakatowa)
2. **Kik K.**, Sicińska P., Bukowska B. „*The effect of polystyrene nanoparticles on living organisms*” 5th International Conference of Cell Biology, Kraków 10-12 maj 2019 r. (sesja plakatowa)
3. Sicińska P., **Kik K.**, Michałowicz J., Bukowska B. „*Changes in antioxidant enzymes activities and reactive oxygen species level in human erythrocytes exposed to selected phthalates*” XVII Conference of the Polish Biophysical Society, Olsztyn 24-27 maj 2019 r. (sesja plakatowa)
4. **Kik K.**, Sicińska P., Bukowska B. „*Ocena wpływu nanocząstek polistyrenu na jednojądrzaste komórki krwi obwodowej człowieka*” V Ogólnopolska Konferencja Doktorantów Nauk o Życiu, Łódź 30-31 maj 2019 r. (sesja plakatowa)
5. **Kik K.**, Sicińska P., Krokosz A., Bukowska B. „*The effect of polystyrene nanoparticles on oxidative stress induction in human peripheral blood mononuclear cells*”. 6th International Conference of cell biology, Kraków 06-08 listopad 2020 r. (sesja plakatowa)
6. **Kik K.**, Sicińska P., Madalski J., Bukowska B., „*Wpływ nanocząstek polistyrenu o różnej średnicy na system antyoksydacyjny w erytrocytach człowieka (in vitro)*” VI Ogólnopolska Konferencja Doktorantów Nauk o Życiu, Łódź 15-16 kwiecień 2021 r. (sesja plakatowa)
7. **Kik K.**, Sicińska P., Krokosz A., Bukowska B. „*The effect of polystyrene nanoparticles of different diameters on DNA damage in peripheral blood mononuclear cells*”. Intercollegiate Biotechnology Symposium „Symbiosis” Warszawa 21-23 maj 2021 r. (sesja plakatowa)
8. **Malinowska K.**, Sicińska P., Bukowska B. „*Polystyrene nanoparticles and their genotoxic properties in human peripheral blood mononuclear cells*” Maastricht (Holandia) 18-21 wrzesień 2022 r. (sesja plakatowa)

Popularyzowanie nauki

Prelekcje

1. **Kik K.** *Plastik w środowisku. Co wiemy o jego szkodliwości?* Ośrodek Enterprise Europe Network przy Fundacji Rozwoju Przedsiębiorczości, Łódź 12 wrzesień 2019 r. (prezentacja ustna)
2. **Kik K.** *Plastik w środowisku. Toksyczność nanocząstek polistyrenu*” Współczesne zagrożenia środowiska. Plastik i jego dodatki. Warsztaty dla szkół, Łódź 03 grudnia 2019 r. (prezentacja ustna)

Warsztaty:

1. Sicińska P., **Kik K.**, „*Biologia sądowa*”. Łódź, 02.2019 r. (warsztaty dla uczniów klas 2-gich III LO w Koninie).
2. Sekcja Ekohydrologii Studenckiego Koła Naukowego Biologów na Wydziale Biologii i Ochrony Środowiska UŁ prowadzący mgr Paweł Jarosiewicz „*Ekohydrologia- świat niezwyklej zależności pomiędzy wodą, a środowiskiem*” Festiwal Nauki Techniki i Sztuki, Łódź Manufaktura, 13.04-14.04.2019 r. (pokaz, konkurs, eksperymenty).
3. Włuka A., **Kik K.**, Mokra K. „*Tajemnica przystosowania miast do zmian klimatu*”, Noc Biologów, Łódź 10.01.2020 r. (warsztaty).
4. Udział w warsztatach pt. *Związki endokrynnie aktywne w środowisku*, realizowanych w ramach programu wieloletniego „poprawa bezpieczeństwa warunków pracy” etap IV (2017–2019) koordynator CIOP-PIB, Łódź, Instytut Medycyny Pracy im. Prof. J. Nofera, 17.10.2019 r.

**KOPIE PUBLIKACJI WCHODZĄCYCH W ZAKRES ROZPRAWY
DOKTORSKIEJ**



Polystyrene nanoparticles: Sources, occurrence in the environment, distribution in tissues, accumulation and toxicity to various organisms[☆]

Kinga Kik, Bożena Bukowska, Paulina Sicińska^{*}

University of Lodz, Faculty of Biology and Environmental Protection, Department of Biophysics of Environmental Pollution, Pomorska 141/143 Str., 90-236 Lodz, Poland

ARTICLE INFO

Article history:

Received 8 July 2019

Received in revised form

17 February 2020

Accepted 28 February 2020

Available online 2 March 2020

Keywords:

Polystyrene nanoparticles

Food chain

Protein corona

Degradation of plastic

Polystyrene toxicity

ABSTRACT

Civilization development is associated with the use of plastic. When plastic was introduced to the market, it was assumed that it was less toxic than glass. Recently, it is known that plastics are serious ecological problem they, do not degrade and remain in the environment for hundreds of years.

Plastic may be degraded into micro-particles < 5000 nm in diameter, and further into nanoparticles (NPs) < 100 nm in diameter. NPs have been detected in air, soil, water and sludge.

One of the most commonly used plastics is polystyrene (PS) - a product of polymerization of styrene monomers. It is used for the production of styrofoam and other products like toys, CDs and cup covers. *In vivo* and *in vitro* studies have suggested that polystyrene nanoparticles (PS-NPs) may penetrate organisms through several routes i.e. skin, respiratory and digestive tracts. They can be deposited in living organisms and accumulate further along the food chain. NPs are surrounded by "protein corona" that allows them penetrating cellular membranes and interacting with cellular structures. Depending on the cell type, NPs may be transported through pinocytosis, phagocytosis, or be transported passively. Currently there are no studies that would indicate a carcinogenic potential of PS-NPs. On the other hand, the PS monomer (styrene) was classified by the International Agency for Research on Cancer (IARC) as a potentially carcinogenic substance (carcinogenicity class B2).

Despite of the widespread use of plastics and the presence of plastic NPs of secondary or primary nature, there are no studies that would assess the effect of those substances on human organism. This study was aimed at the review of the literature data concerning the formation of PS-NPs in the environment, their accumulation along the food chain, and their potential adverse effects on organisms on living various organization levels.

© 2020 The Authors. Published by Elsevier Ltd. This is an open access article under the CC BY-NC-ND license (<http://creativecommons.org/licenses/by-nc-nd/4.0/>).

1. General characteristics of plastic, its micro- and nanoparticles

1.1. Types of plastic

Plastics are made mostly of synthetic organic polymers: polystyrene (PS), low-density polyethylene (LDPE), high-density polyethylene (HDPE), polypropylene (PP), polyvinyl chloride (PVC) and polyethylene terephthalate (PET). Plastics are thermoplastic, and therefore they can be formed in any shapes and repeatedly melted.

World production of plastic is constantly growing. In the 1950s around 1.7 million tons of plastics were produced, the amount has risen 200-fold to 299 million tons worldwide in 2013 and from the years 2015–2016 from 322 to 335 million tons a year (Plastics - The Facts, 2017) (Fig. 1). It has been estimated that amounts of produced plastics may increase significantly and even be doubled in the coming years (Hesler et al., 2019).

1.2. Synthesis and use of polystyrene

PS is an aromatic polymer formed as a result of polymerization of styrene monomers (Fig. 2). Styrene (vinylbenzene) is produced from ethylene and benzene. Massive production of PS is carried out by catalytic dehydrogenation of ethylbenzene that leads to

[☆] This paper has been recommended for acceptance by Maria Cristina Fossi.

^{*} Corresponding author.

E-mail address: paulina.sicinska@biol.uni.lodz.pl (P. Sicińska).

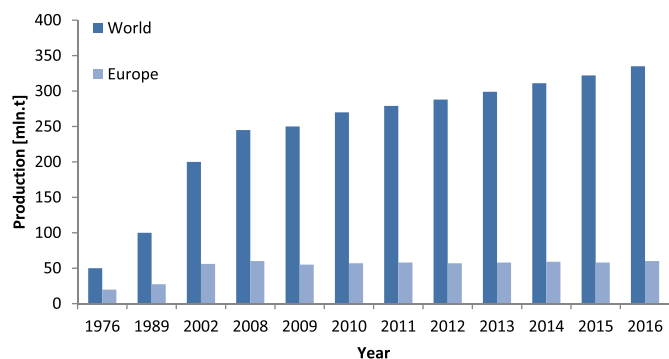


Fig. 1. Plastic production in 1976–2016 in Europe and in the World (based on work [Plastics-The Facts, 2017](#)).

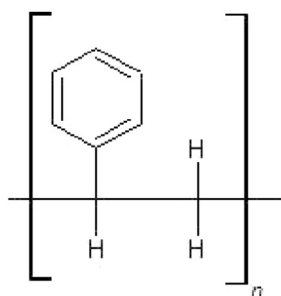


Fig. 2. Chemical structure of polystyrene.

formation of styrene monomers ([Wünsch, 2000](#)). PS is a thermo-plastic polymer characterized by high translucency, durability and may be easily dyed. PS as a solid material is used for the production of CDs, toys, toothbrushes, etc. PS is also used for the production of the styrofoam – a material characterized by limited elasticity, expanded or melt-formed. It is produced by rapid heating of PS pellets with a foaming agent. Styrofoam is broadly used in the production of food containers, such as trays, plates, cups. It is also used for food storage and transport, for the production of various packing products, and for the production of toys, clips and office supplies ([Wünsch, 2000](#); [Johannaber and Michaeli, 2004](#); [Domininghaus et al., 2005](#)).

1.2.1. Physical and chemical properties of polystyrene and its toxicological classification

Various international agencies supervise safety and toxicity of PS in everyday use products. Release of styrene monomers into the environment during processes of melting or polymerization is particularly important aspect of that supervision ([Gurman et al., 1987](#)). PS is a moderately thermally stable. Nearly no degradation of pure PS occurs at temperatures below 200 °C however trace amounts of styrene, cumene and ethylbenzene are detected in the air. PS exposure to temperatures over 330 °C results in nearly its complete degradation, with styrene monomer being the main product. When compared to other common synthetic and natural construction materials, products of thermal decomposition of PS seem to be of low toxicity. Amounts of degradation products, including styrene, that may be released from a PS package are associated with a relatively low toxicity of this polymer ([Gurman et al., 1987](#)).

The Environmental Protection Agency (EPA) determined the value of 300 ppm (1000 µg/m³) of styrene as admissible in case of a chronic exposure ([Mutti et al., 1992](#)). Concentrations above that level may be harmful for human health. Styrene levels determined

in polymer industry usually do not exceed 20 ppm ([WHO, 2000](#)), which is much below the determined value of chronic toxicity.

It has been estimated that consumption of styrene from PS is 9 µg/person/day ([Lickly et al., 1995](#)). The admissible daily intake (ADI) reported by the FDA is 90,000 µg/person/day ([FDA, 2002](#)). Therefore, it seems that the use of PS for food and non-food products does not constitute a major problem for human safety and health. A review made by experts for the Harvard Center for Risk Assessment has not demonstrated concerns about contact of food with PS materials ([Cohen et al., 2002](#)).

PS particles are used as model particles in the studies of the effect of characteristic particle surfaces on various biological parameters, because they can be easily synthesized over a broad range of sizes ([Loss et al., 2014](#)). NPs are characterized by higher surface relation to volume, which has an important effect on their reactivity. Due to their size and shape, and various surface modifications, PS-NPs are broadly used in technological and biomedical applications. Modifications of the chemical surface of NPs are of key importance for solubility and durability in biological agents, as well on bio-distribution and bio-compatibility ([Xia et al., 2008](#); [Meng et al., 2009](#)). Bio-compatibility is the property that makes PS broadly used for the production of laboratory equipment and biomedical devices. This property decides also that this compound should not negatively interfere with biological systems. Surface of PS is hydrophobic, and therefore it may be easily modified by, for example, oxidation, producing surfaces highly receptive for cell cultures ([Midwoud et al., 2012](#)). Those surfaces may also be sterilized with UV irradiation and ethylene oxide ([Domininghaus et al., 2005](#)). PS-NPs are broadly used, for example as biosensors, in photonics, and in self-assembling nanostructures ([Loss et al., 2014](#)). Bio-compatibility of PS causes that this substance does not have a negative impact on the interaction of NPs with biological systems. PS-NPs with modified surface are homogenic. They are characterized by low polydispersion index and form stable colloids in biological fluids ([Florence, 2004](#)).

1.3. Degradation of plastic

The number of styrene applications has been constantly growing over last two decades. Despite the fact that the material is recyclable, only a small fraction of waste is utilized. Based on data of the statistics of communal solid waste published by the Environmental Protection Agency in 2005, the total amount of solid PS waste recycled in the US reached the level of nearly 2.6 million tons. PS is not bio-degradable. For that reason disposable products are a huge problem and great source of environment pollution ([Kaplan et al., 1979](#); [Tokawa et al., 2009](#); [Kang et al., 2018](#)). Therefore, degradation methods are sought. In the case of styrene, only its re-use in unchanged form, or incineration, which requires high temperatures reaching 1000 °C, are taken into account. Lasting for 22 years studies of plastic accumulation in the Atlantic Ocean, have not found an no increased amount of this material, despite increased world production ([Law et al., 2010](#)). It was therefore assumed that this is due to microorganisms that can cling to plastic materials drifting on water, using them as a source of food. [Zettler et al. \(2013\)](#) analyzed plastics collected during their cruise over the Sargasso Sea the for presence of microorganisms. The study has demonstrated that various microorganisms clung to analyzed plastic, using their surface as a food source. Moreover, the analysis of rRNA genes allowed identification of bacteria able to degrade hydrocarbons, which confirms that microorganisms play a principal role in degradation of plastic.

The above research has fueled the scientists' interest in discoveries of other microorganisms: fungi and bacteria species that can break down certain plastics. There are some bacteria, so-called

Archaeons that are able to decompose PS, but they are not widely used because of a low productivity of the process. It is known that the strains of *Rhodococcus ruber* and *Actinobacterium* are able to decompose only 0.04–0.57% of PS waste in several weeks (Kaplan et al., 1979; Tokiwa et al., 2009). Japanese scientists focused their attention on the *Ideonella sakaiensis*, the bacteria that shows a strong ability to decompose polyethylene terephthalate, or PET. Cultured on that plastic, the strain produces two enzymes able to hydrolyze PET. The process results in the production of environment-friendly monomers: ethylene glycol and terephthalate acid (Yoshida et al., 2016). Ma et al. (2018) have demonstrated that polyethylene terephthalate hydrolase (PETase) is able to decompose PET at the daily rate of $22.5 = \frac{\text{mg}}{\mu\text{mol/L}}$ PETase.

In another study, Bombelli et al. (2017) have demonstrated that greater wax moth (*Galleria mellonella*) caterpillars were able to degrade polyethylene, constituting 40% of all plastics. One hundred larvae were placed on a plastic bag. It was observed that larvae degraded approximately 92 mg of polyethylene, which was approx. 3%. Products of polyethylene decomposition showing for its bio-degradation were observed in decomposed foil.

Despite discoveries of various organisms able to degrade plastics, scientists also look for novel, bio-degradable and ecological materials, that will undergo rapid bio-degradation with no toxic effect on the environment.

2. Sources of micro- and nanoplastic in the environment

Plastic is responsible for 70% of sea and ocean pollution. Every year, 8 million tons of plastic are released into the sea. Around 10% of plastics production reaches the oceans because of insufficient treatment effectiveness, accidental inputs, littering, illegal dumping and coastal human activity (Waring et al., 2018). Worm et al. (2017) suggested that plastic waste is similar to other persistent pollutants, such as dichlorodiphenyltrichloroethane (DDT) or polychlorinated biphenyls (PCBs), which once threatened a “silent spring” on land. Such a scenario seems now possible in the ocean, where plastic cannot be easily removed, accumulates in organisms and sediments, and persists much longer than on land.

We do not know much about micro-plastic formed in the environment as a result of degradation processes, as well in course of production processes. Micro-plastic particles are less than 5 μm in diameter. Under influence of biological, physical and chemical factors they are degraded into NPs, with diameters of less than 100 nm (Singh and Sharma, 2008; O’Brine and Thompson, 2010).

Both micro- and nanoplastic may be classified in terms of their source as primary and secondary. Primary microplastics, including PS particles are produced by the industry, and are released into the environment (Shim et al., 2018). Primary sources of those particles are: cosmetic products, drugs, paints, as well as medical and electronic devices (Koelman et al., 2015; Efimova et al., 2018). In

cosmetic industry, they are mostly components of face cleansing products, exfoliating agents for hand washing, and peeling formulas (Andrady, 2011). NPs are also released in high-temperature engineering processes (Snopczyński et al., 2009). Other primary sources are plastic packaging producing plants (De Falco et al., 2018). Secondary sources are plastic particles disintegrating into smaller units under physical and chemical processes. They are particles washed from synthetic fibers and released as a result of improper plastic waste management (Figure 3).

There are numerous reports indicating that degradation of plastic leads to release of NPs into the natural environment (Koelman et al., 2015; da Costa et al., 2016; Hernandez et al., 2017). They are found in sludge, which may be a source of these substances in cultivated soil (Habib et al., 1998; Jambeck et al., 2015). Plastic carried by rivers enters oceans and seas in the amount of 8 million tons a year (Jambeck et al., 2015). Microplastics can be formed during mechanical and photo-oxidative degradation. Recent studies have assessed degradation of PS objects (coffee cup lids, single-use plates and polystyrene foams) in the environment by simulating the degradation process with UV-light irradiation (Lambert and Wagner, 2016) or mechanical fragmentation in the sea swash zone with bottom sediments (Efimova et al., 2018). Ekvall et al. (2019) have observed the formation of PS-NPs during the mechanical breakdown of daily-use PS products (coffee cup lids and expanded PS foam).

Studies by Lambert and Wagner (2016) have focused on plastic NPs formed in the process of degradation of a disposable cup cover made of PS. They have found a minor release of NPs (1.26×10^8 particles/mL) during the period of 56 days.

These studies have demonstrated that nanoplastics and microplastics are actually formed in the environment and occur in spherical shapes in various sizes, especially when foamed PS is degraded (Efimova et al., 2018).

3. Presence of plastic particles in the environment and its accumulation in living organisms

Both micro- and NPs of various size have been detected mostly in the aquatic environment, where they are washed from synthetic fibers contained in sludge. Desforges et al. (2014) have demonstrated the presence of plastic micro-particles in waters of the North-Eastern Pacific and in shores of the British Columbia, at the level of 8–9200 particles/ m^3 . Those particles were also detected in rivers of California, at the level of 30–109 particles/ m^3 , and in the Danube river, at the level of approx. 900 particles/L (Moore et al., 2005). It has also been demonstrated that the level of micro-particles in municipal waste water processing plants was 15.1–640 particles/L (Kang et al., 2018).

Microplastics occur in the ground water (Koelmans et al., 2019) because it is not possible to filter all particles present in sewage

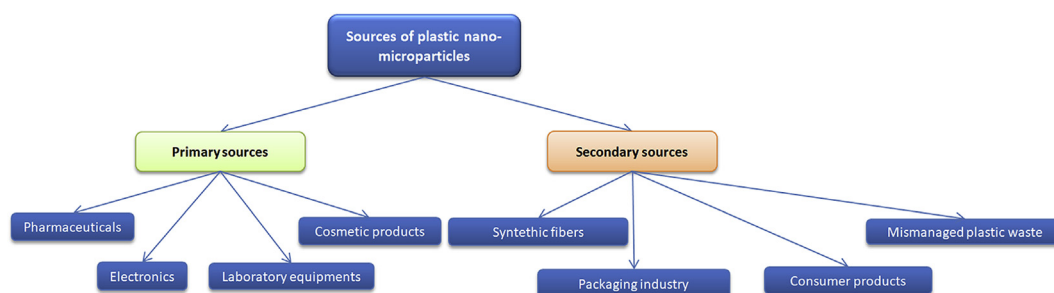


Fig. 3. Primary and secondary sources of nanoplastic in the environment.

treatment plants due to their broad size range (<0.1–5000 μm).

Particles present in water may form aggregates, as demonstrated by Velzeboer et al. (2014) and Della Torre et al. (2014). Velzeboer and co-workers noted that carboxylated PS-NPs (60 nm) formed aggregates reaching the diameter of 361 ± 465.1 nm in sea water, while Della et al. found out that smaller NPs of carboxylated PS (40 nm), formed bigger aggregates the, size of which reached 1764 ± 409 nm.

NPs have been shown to accumulate mostly in sludge. The analysis of sludge from seven waste water processing plants in Ireland demonstrated the micro-particle content ranging from 4196 to 15,385 particles/kg of dry weight (Mahon et al., 2017).

3.1. Presence of nanoplastic in cells and tissues of living organisms

Plastic NPs may enter living organisms with air, food and water, and also through skin. Then they can accumulate in various organs (Hernandez et al., 2017; Revel et al., 2018; Yooeun et al., 2018).

To find out how those particles enter organs and the whole organisms, a study was done on *Danio rerio* embryos. It has been assessed that PS particles with diameters of 25, 50, 250 and 700 nm affect embryos on three different stages of their life. Two exposure routes were used: through the skin - dermal exposure, and through intestinal villi - food exposure. NPs (25 nm, 50 nm), which were administered with food accumulated in selected organs, including eyes. Bigger particles, over 50 nm in diameter, were detected only in the gastrointestinal tract, which indicated that they did not penetrate membranes and reached other tissues of the organism (Pomerena et al., 2017). In another study Lee et al. (2019) studied *Danio rerio* embryos in terms of bioaccumulation and toxicity of PS-NPs alone and with Au ions. They have used particles with diameters of 50, 200 and 500 nm. It has been demonstrated that the smallest particles, 50 nm in diameter, easily penetrated developing embryos, and accumulated in their whole body, and particularly in lipid-rich areas. Presence of PS-NPs has not been shown to have a significant effect on cell death, rate of hatching and the presence of developmental abnormalities. For NPs combined with Au ions, an increased toxicity has been demonstrated, correlated with mitochondrial injury in a dose-dependent and size-dependent manner. The observed toxicity was associated with production of ROS and pro-inflammatory reactions. Pitt et al. (2018), have demonstrated that some nanoplastics with the diameter of 51 nm can penetrate chorionic membrane of *Danio rerio* and accumulate in fish tissues, affecting their behavior and physiology.

In order to precisely assess accumulation of nano-, micro- and macroparticles in eggs and organisms of Medaka fish (*Oryzias latipes*), Kashiwada (2006) used fluorescent NPs of solid latex solution. Fish eggs were treated for 24 h with particles (39.4–42,000 nm). It has been found that particles with a diameter of 474 nm accumulated more intensely in eggs, while 39.4 nm particles accumulated in the yolk and yolk sacs of embryos. Exposure of adult fish to 39.4 nm NPs at the concentration of 10 mg/L resulted in their accumulation mostly in the intestine and gills. Lesser amounts were also found in testes, the liver, blood and the brain animals studied. The presence of 10.5 and 16.5 ng of NPs per mg of blood protein was found respectively in female and male blood of Medaka fish. The analysis has also demonstrated an increased particle - derived fluorescence in fish brains, compared to the control group (although the difference was not statistically significant). Authors concluded that the observation could indicate that NPs were able to penetrate the blood-brain barrier (BBB), and thus accumulated in the brain (Fig. 4).

The BBB is one of the principal protective mechanisms of the central nervous system. It allows penetration of single lipid-soluble particles through capillary endothelium, thus limiting the flow of

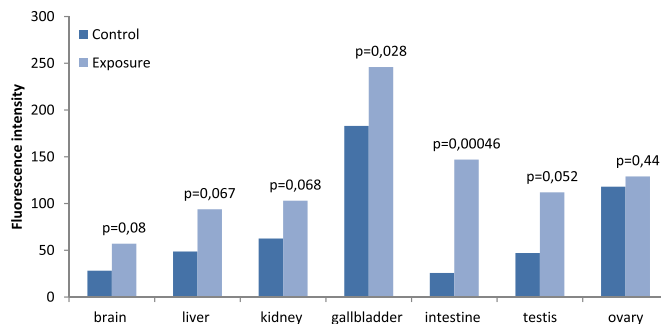


Fig. 4. Distribution of nanoparticles in the See-through Medaka (*Oryzias latipes*) (based on work Kashiwada, 2006).

toxins and pathogens. The BBB is an important border between the neural tissue and circulating blood. Unique and protective properties of this barrier allow maintenance of control over the homeostasis of the brain, as well as over movements of ions and molecules (Zhou et al., 2018). Kashiwada (2006) suggested that plastic NPs would penetrate that barrier in the manner analogous to many other NPs (Zhou et al., 2018) used in medicine. This suggestion has been supported by Mattsson et al. (2017) who demonstrated accumulation of PS-NPs in fish brain. They have demonstrated that small NPs, with the diameter of 53 nm accumulated better than 180 nm particles. NPs accumulation resulted in significant behavioral changes and morphological disorders in fish. Moreover, fish exposed to NPs demonstrated a higher weight loss and contained less water in brain compared to control fish.

Environmental pollutants are usually not only persistent in the environment, but they are also transferred into the human body, causing adverse health effects. The human body is exposed to microplastic through it inhalation with air and dust and by dermal contact with various everyday products (e.g. textiles) (Prata et al., 2020). Inhaled NPs from air accumulate in respiratory tract, pass through the nose and throat and reach lungs. Particles with diameters of less than 10 μm may reach the gas exchange surface and accumulate in alveoli (Oberdorster, 2001; Hoet et al., 2004). Recent research of Cox et al. (2019) have shown that microplastics consumption of humans ranges from 39,000 to 52,000 particles annually depends on age and sex. These estimates increase up to 74,000 and 121,000 when inhalation is taken into consideration.

The above described studies have clearly indicated that the size of particles is of importance for their penetrating abilities, and therefore for their toxicity.

3.2. Accumulation of nanoparticles along the food chain

Many studies have indicate that NPs penetrate living organisms from aquatic environment and accumulate in subsequent links of the food chain (Fig. 5).

Yooeun et al. (2018) studied accumulation of fluorescent plastic NPs in the food chain. The study involved the lowest level of the food chain that is phytoplankton (algae *Chlamydomonas reinhardtii* - a producer), followed by zooplankton (*Daphnia magna* - primary consumer), *Oryzias sinensis* fish (secondary consumer) and *Zacco temminckii* fish (tertiary consumer). *Chlamydomonas reinhardtii* algae were exposed to <100 nm nanoplastic at the level of 50 mg/L. Organisms on higher levels were exposed through their diet only. The microscopic observation have demonstrated that nanoplastic was present on surface of cells of the producer (*Chlamydomonas reinhardtii*), as well as in digestive organs of primary, secondary and tertiary consumers. It has been noted that accumulated nanoplastic had a negative effect on fish activity and caused histopathological

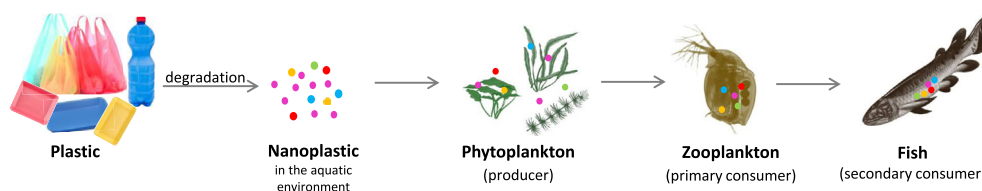


Fig. 5. Accumulation of polystyrene nanoparticles in food chain (based on work Mattsson et al., 2015; Yooeun et al., 2018).

changes in fish liver. It has also been demonstrated that PS-NPs penetrated embryos and were determined in their yolk sac (Yooeun et al., 2018). Similarly Mattsson et al. (2015) demonstrated accumulation of 24 nm and 27 nm PS-NPs in the food chain. Those authors have assessed deposition of NPs in the food chain (algae, Daphnia and fish Crucian carp (*Carassius carassius*)) and their effect on fish behavior and metabolism (fish were the last analyzed link in the food chain). It has been found that accumulated PS-NPs caused some significant changes in the activity and food seeking of *C. carassius*.

Those results seem to be particularly important, as they suggest that NPs present in water reach living organisms at various levels of the food chain.

3.3. Protein binding to the surface of nanoplastics

PS-NPs have the ability to combine with proteins, and to stay dissolved in biological fluids in those combinations. It has been demonstrated that proteins bind to surface of nanoplastics forming the, so-called, protein corona, that defines the biological identity of nanoplastic particles (Jiang et al., 2010; Walkey and Warren, 2012). Composition of the protein corona may depend on physical properties of NPs. Considering bonding strength and exchange rate of proteins bound to the surface of nanomaterials, the corona may be classified as “soft” or “hard”. Soft corona is made of proteins that are loosely bound to NPs and may be easily exchanged. Hard corona is made of proteins strongly bound to those materials. In biological media dispersed NP-protein complexes are recognized by organs or cells (Kokkinopoulou et al., 2012).

It is supposed that the (serum) coronal protein adsorbed on the surface of NPs participates in their interaction with cells. The protein may influence mutual relations between NPs, but also their cellular uptake. Mohr et al. (2014) incubated PS particles with diameters of 80–170 nm with human blood serum. Then, they have analyzed correlations of various parameters, including surface charge, a tendency to aggregate, and absorption of serum proteins with the ability of PS particles to penetrate cells and with their bio-distribution in mice. Those authors have demonstrated that strongly aggregating nano- and microparticles accumulated mostly in the liver, while non-aggregated ones were distributed among all organs.

3.4. The mechanism of uptake of nanoparticles by the cell

Considering size of NPs and the cell type, NPs may be absorbed through phagocytosis, pinocytosis, macro-pinocytosis, or passive transport, and in the consequence they can enter cellular membranes and various biological structures (Fig. 6) (Zhao et al., 2011; Shang et al., 2014).

It has been shown that similarly to lipoproteins, viruses and complex proteins, NPs are contained in vesicles and transported to and from a cell through endocytosis and exocytosis. The most common type of endocytosis is pinocytosis. This process is associated with building a vesicle containing uptake particles in the

cytosol. Those vesicles have receptor proteins that identify particular chemical groups of molecules to be absorbed. Bigger particles are transported in by phagocytosis. The process is realized by specialized cells - macrophages and monocytes. NPs may also be absorbed into the cells by passive transport through the cell membrane. Passive transport is particularly important in case of red blood cells (RBCs), as those cells are not able to perform active endocytosis (Shang et al., 2014). Salvati et al. (2011) have demonstrated that PS-NPs with diameter from 40 to 50 nm could enter A549 line cells through endocytosis. On the other hand, Rossi et al. (2014) have studied the effect of PS materials on the properties of model biological membranes. The analysis have demonstrated that PS-NPs could easily penetrate lipid membranes, which may be associated with adverse effect on membrane function and the cells.

4. Polystyrene toxicity in vitro

Toxicity of NPs is an important question. NPs may influence various factors, including chemical affinity of NPs to numerous biological structures, porousness, increased chemical reactivity of their surface, and a tendency to aggregate (Park et al., 2011; Zhao et al., 2011; Love et al., 2012; Shahbazi et al., 2013).

Schirrinzi et al. (2017) carried out the study to determine the effect of nanoplastics, including PS on generation of reactive oxygen species (ROS) and viability of the cells. Two cell lines were used for the analysis: epithelial HeLa and cerebral T98G. Those cell lines were exposed to PS nano- and microparticles with diameters from 40 to 250 nm, at concentrations ranging from 10 ng/mL to 10 µg/mL. Increased ROS generation caused by PS-NPs has been observed in both cultures. The analysis of cell viability have shown that particles studied had no effect on this parameter (Schirrinzi et al., 2017).

In another study, Anguissola et al., 2014 incubated various cell lines, including 1321N1, HepG2, HEK 293, with NPs with 50 nm in diameter and the final concentrations range from 0.3 to 100 µg/mL for 24 and 72 h, and demonstrated that amine-modified NPs had a cytotoxic effect causing damage to cell membrane. Moreover, NPs triggered apoptosis by activating caspase 9 and two executor caspases 3 and 7. Analyzed NPs caused also morphological changes in mitochondria and lysosomes of analyzed cells.

Murali et al. (2015) have assessed the effect of PSNPs with diameters ranging between 45 and 70 nm, on various types of nerve cells. Metabolic activity of those cells was analyzed directly after exposure to NPs and then after 6 months of storage. The analysis has demonstrated that tested NPs disturbed metabolic activity of the cells in a type-dependent manner. Those changes were a consequence of adsorption of bio-active compounds on particle surface, and of their aggregation. It has also been observed that neurons did not absorb NPs, but glial cells absorbed a high amount of them. After 6 months of storage, an increased toxicity and uptake of PS-NPs were observed.

Another study assessed the kinetics of uptake of non-modified PS-NPs with diameter of 44 nm and 100 nm by human gastric adenocarcinoma cells (AGS). Cell viability and expression of genes participating in regulation of the cell cycle and of inflammatory

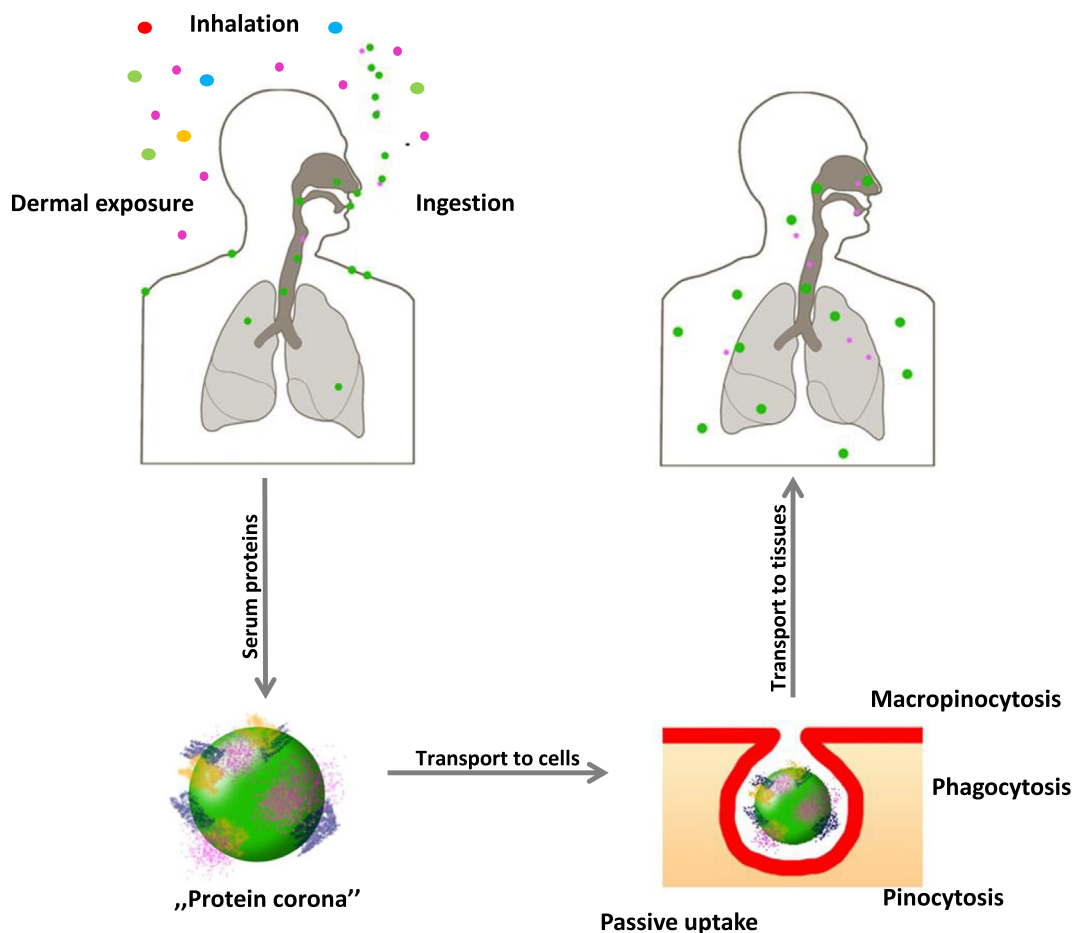


Fig. 6. Nanoparticle uptake by humans and their penetration into cells (based on work Shang et al., 2014; Zhao et al., 2011).

processes were analyzed for that purpose. It has been shown that 44 nm PS-NPs were rapidly and effectively accumulated in the cytosol. It has also been demonstrated that PS-NPs affected viability and morphology of those cells, and their presence led to induction of inflammation. PS-NPs had a significant effect on expression of genes associated with inflammation and the cell cycle (c-Myc, ERK-1, Ki67, CCNE1, p38, p53, IL-8, IL-6, etc.). Smaller particles caused an increase in expression of IL-6 and IL-8, products of which are the most important cytokines participating in pathology of the stomach (Forte et al., 2016).

Barshtein et al. (2011) have studied hemolytic activity of PS-NPs in protein free medium and its modulation by albumin. They have found that treatment of RBCs with PS-NPs induced hemolysis (dose and particle size dependent) in plasma free medium but not in full plasma or in buffer, which contained albumin. Critical albumin concentration was 0.05% wt. The results have shown that hemolytic effect of NPs was strongly modulated by protein concentration in the medium (Barshtein et al., 2011). PS particles (≤ 243 nm) caused also aggregation and endothelial adhesion of RBCs (Barshtein et al., 2016).

Oslakovic et al. (2012) have shown that PS particles (23 nm and 200 nm and 24 nm and 220 nm COOH-modified as well as 57 nm and 340 nm NH_2 -modified) influenced PS-coagulation cascade interactions of human platelets physiology. The PS particles were able to bind to blood plasma coagulation factors VII and IX *in vitro*, leading to a decrease of their actions, and in a consequence, to a decline in thrombin generation.

The ease of penetration of plastic NPs through cell membranes

and their ability to accumulation is a great threat not only for the cell, but also for entire organisms.

5. Toxicity of plastic nanoparticles on living organisms (*in vivo*)

The adverse effect of plastic NPs on microorganisms, plants and animals is more pronounced compared to micro-particles, because lesser diameter facilitates their penetration and accumulation in various tissues and organs (Mattsson et al., 2015).

5.1. The effect on organisms living in the soil: microorganisms

Awet et al. (2018) have investigated the short-term effects (28 days) of environmentally relevant concentrations of PS-NPs on the activity and biomass of soil microbiota, and the functional diversity of soil enzymes in experiment. They have observed a significant reduction of microorganism biomass during the incubation with PS-NPs at the concentration of 100 and 1000 ng/g of dry weight. Reduced activity of dehydrogenase and other enzymes, including: N-(leucine-aminopeptidase), C-(β -glucosidase and cellobiohydrolase), P-(alkaline-phosphatase), have been observed, which indicated a harmful effect of PS-NPs on enzymes and soil microbiota.

5.2. The effect on plankton

Cui et al. (2017) have assessed toxicity of PS-NPs in *Daphnia*

galeata. In individuals exposed to NPs at the concentration of 5 mg/L for 5 days, a significant reduction of reproduction and survival have been observed. A low hatching ratio and abnormal development have been noted for embryos. In another study, [Bhattacharya et al. \(2010\)](#) demonstrated that accumulation of PS-NPs with the diameter of 20 nm and the concentration of 1.8–6.5 mg/L (present as agglomerates) in algae cells led to inhibition of photosynthesis. Analyzed NPs reduced intensity of light reaching cells and reduced air availability. An increased production of ROS was also observed ([Bhattacharya et al., 2010](#)).

5.3. The effect on invertebrates

[Lee et al. \(2013\)](#) have assessed chronic toxicity of PS-NPs with the diameter of 50 nm to copepods belonging to the species of *Tigriopus japonicus*. They have demonstrated that exposure to particles at the concentrations of 12.5 mg/L and 1.25 mg/L resulted in approx. 10% mortality of those invertebrates. In another work, [Della Torre et al. \(2014\)](#) demonstrated that 50 nm amine-modified PS-NPs caused some serious developmental defects at early embryonal stages of sea urchins (*Paracentrotus lividus*). [Zhao et al. \(2017\)](#) observed, the transgenerational toxicity in nematodes *Caenorhabditis elegans* exposed to PS-NPs at the concentrations higher than 100 µg/L. The authors have suggested that observed transgenerational toxicity of the substances studied might be mainly due to the translocation of PS-NPs into reproductive organs such as the gonad, which potentially in turn led to the transfer of these particles to the next generation. Enhancement of intestinal permeability and extension of defecation cycle length was noted, which gave the explanation for the observed accumulation and translocation of PS-NPs in reproductive organs.

The most recent studies published in 2018 demonstrated a significant effect of 100 nm and 500 nm nano- and microparticles on survival, locomotion and development of oxidative stress in soil nematode *C. elegans*. It has been shown that the exposure to PS particles induced a size-dependent toxicity leading to the increase in locomotor behavior of those organisms, and also led to damage of GABAergic and cholinergic neurons. It has also been demonstrated that PS-NPs caused reduced expression of the *gst-4* gene coding the glutathione S-transferase alpha 4 enzyme, which in turn led to the development of oxidative stress ([Lei et al., 2018](#)).

5.4. The effect on vertebrates

In their study of potential toxicity of NPs for fish, [Pitt et al. \(2018\)](#) used the sweet-water species of *Danio rerio*, belonging to the carp family. Fish were exposed to fluorescent PS-NPs at the concentrations of 0.1, 1, 10 ppm for 6 h. Analyzed particles have been shown to accumulate in yolk sac and throughout the whole stage of development migrated to the gastrointestinal tract, i.e. to the gallbladder, the pancreas, the liver, and also to the heart and the brain. It should be underlined, however, that exposure to PS-NPs did not cause significant mortality, changes in mitochondrial energy metabolism, nor deformation, but reduced the heart rate. NPs studied also caused changes in behavior of larvae, including their reduced activity. The study have demonstrated that some nanoplastics are able to penetrate the chorionic membrane of *D. rerio*, and consequently accumulate in fish tissues and affect behavior and physiology of those fish ([Pitt et al., 2018](#)). Similar conclusions have been reached by [Chae et al. \(2018\)](#) and [Mattsson et al. \(2017\)](#). Those authors for the first time noted that PS NPs changed the measured distance covered by fish, and also caused histopathological changes in their livers. Those latter ones demonstrated existence of a correlation between behavioral disorders and incorporation of NPs into the brain.

[Esch et al. \(2012\)](#) analyzed the effect of 50 nm carboxyl NPs on uptake and transport of iron in the intestinal epithelium *in vitro* and the chicken intestinal loop *in vivo*. It has been demonstrated that exposure of intestinal cells to high doses of PS-NPs could impair iron transport. Exposure of chickens to analyzed particles could also cause structural changes in intestinal villi. Moreover, by changing of the properties of the epithelium PS-NPs could also impair absorption of other elements, including copper, zinc, calcium, and other compounds, e.g. vitamins. Those authors have observed that blood of chicken chronically exposed to NPs clotted less efficiently compared to control animals. This phenomenon could be associated with vitamin K deficiency in those birds.

The effect of PS-NPs on the respiratory system of Sprague-Dawley rats was also studied. Animals were exposed to PS particles with diameters of 64 nm, 202 nm and 535 nm. The study has demonstrated a significant migration of neutrophils into the lungs and pneumonia development, which was due to increased activity of lactic dehydrogenase and total protein level. Furthermore increased expression of IL-8 genes in epithelial cells has been observed ([Brown et al., 2001](#)).

[Deng et al. \(2017\)](#) observed tissue distribution of fluorescence PS (5 µm and 20 µm) in mice after oral administration. They also noted accumulation of PS in the liver, kidney and gut with evidence of oxidative stress, energy balance disturbance, and neurotoxicity.

It may be concluded that many studies have indicated the toxic effects of PS-NPs on the digestive, circulatory, nervous or respiratory systems in vertebrates. There are also studies showing that PS-NPs and PS microparticles do not induce toxic effects in animals ([Ašmonaitė et al., 2018](#); [Wang et al., 2019](#)).

6. Carcinogenic properties of styrene

Some reports have shown the carcinogenic effect of styrene, but there are no available data regarding its polymer derivative - polystyrene ([Huff and Infante, 2011](#)).

Presence of styrene and its principal metabolite (styrene - 7, 8-oxide -) was determined in humans exposed to styrene at the concentrations range of 20–414 mg/m³. Studies have demonstrated the presence of styrene in human blood at the concentration of 2.5 µg/mL, and of its metabolite in urine at the concentration of 0.05 µg/L ([Tornero-Velez and Rappaport, 2001](#)).

This compound is not currently classified as carcinogenic by the Environmental Protection Agency (EPA), but was classified as potentially carcinogenic (carcinogenicity class B2) by the International Agency for Research on Cancer (IARC). This classification indicates that the compound may cause cancer in humans, but limited evidence in that regard come from animal studies only ([Loss et al., 2014](#)). Animal studies on styrene carcinogenic potential have provided various results and limited evidence. There are several epidemiological studies suggesting a possible correlation between the exposure to styrene and an increased risk of leukemia and lymphoma in humans ([Thompson et al., 2016](#)). However, those evidence are not unequivocal, because of simultaneous exposure of humans to numerous other chemicals, and insufficient data concerning their levels and exposure times. On the other hand, styrene oxide is a very highly reactive metabolite of styrene that has been demonstrated to be carcinogenic in animals after oral exposure. IARC classified this metabolite as probably carcinogenic for humans (group 2A).

[Conti et al. \(1988\)](#) tested 13-weeks male and female Sprague-Dawley rats exposed to styrene. Styrene was given to animals at doses of 50 and 250 mg/kg b.w. for 4–5 days. An increased tumor formation has not been observed in male rats, but in females the styrene dose of 250 mg/kg b.w. caused a minor number of

malignant and mammary gland tumors. At that dose, styrene caused an approx. 10% reduction of animals survival. Other studies used pregnant mice and their off springs, exposed to a very high dose of styrene - 1350 mg/kg b.w., administered via the gastric tube in olive oil. Lung cancer has been found more often in female, compared to male mice (Ponomarev and Tomatis, 1978).

Further studies used Charles River rats that were treated with styrene at doses of 125 or 250 ppm (mg/L) dissolved in water, but the results of this study were not indicated on an increased risk of cancer in animals studied (Beliles et al., 1985).

7. Conclusions

For many years, we have been observing a rapid increase in plastic production, including PS in the world. This plastic is released into the environment (water, air or soil) in the form of micro- and nanoplastics and occurs in industrialized areas as well as in very clean natural areas like the rocky mountains of the USA. The consequence of this, is the penetration of plastic NPs into living organisms from the lowest (plankton) to the highest trophic level (predators). Accumulation especially in “seafood” such as mussels, shrimps or fish leads to the potential exposure of humans as consumers to the effects of plastic NPs by the oral route. Of course, as we have shown in our paper, human exposure can also result from breathing air polluted with plastic NPs, contaminated drinking water or through skin contact.

Awareness of the above facts should clearly lead to conducting in-depth epidemiological studies on chronic exposure of humans to plastic particles, as well as further *in vitro* and *in vivo* experiments explaining the mechanisms of interaction of plastic NPs with components of living organisms. Such information could support international organizations (including relevant European Union bodies) in active measures to reduce plastic production, stop environmental degradation, and protect the health of living organisms.

Competing financial interests

The authors declare they have no actual or potential competing financial interests.

Declaration of competing interest

The authors declare that they have no known competing financial interests or personal relationships that could have appeared to influence the work reported in this paper.

Acknowledgments

This work was supported by statutory research admitted for Department of Biophysics of Environmental Pollution, University of Lodz.

References

- Andrady, L.A., 2011. Microplastics in the marine environment. *Mar. Pollut. Bull.* 62 (8), 1596–1605.
- Anguissola, S., Garry, D., Salvati, A., O'Brien, J.P., Dawson, A.K., 2014. High content analysis provides mechanistic insights on the pathways of toxicity induced by amine-modified polystyrene nanoparticles. *PLoS One* 9 (9), 1–16.
- Ašmonaitė, G., Sundh, H., Asker, N., Almroth, B., 2018. Rainbow trout maintain intestinal transport and barrier functions following exposure to polystyrene microplastics. *Environ. Sci. Technol.* 52, 14392–14401.
- Awet, T.T., Kohl, Y., Meier, F., Straskraba, S., Grün, A.-L., Ruf, T., Jost, C., Drexler, R., Tunc, E., Emmerling, C., 2018. Effects of polystyrene nanoparticles on the microbiota and functional diversity of enzymes in soil. *Environ. Sci. Eur.* 30 (11), 1–10.
- Barshtein, G., Arbell, D., Yedgar, S., 2011. Hemolytic effect of polymeric nanoparticles: role of albumin. *IEEE Trans. NanoBioscience* 10 (4), 259–261.
- Barshtein, G., Livshits, L., Shvartsman, L.D., Shlomai, N.O., Yedgar, S., Arbell, D., 2016. Polystyrene nanoparticles activate erythrocyte aggregation and adhesion to endothelial cells. *Cell Biochem. Biophys.* 74, 19–27.
- Beliles, R.P., Butala, J.H., Stack, C.R., Makris, S., 1985. Chronic toxicity and three-generation reproduction study of styrene monomer in the drinking water of rats. *Fund. Appl. Toxicol.* 5 (5), 855–868.
- Bhattacharya, P., Lin, S., Turner, P.L., Ke, C.P., 2010. Physical adsorption of charged plastic nanoparticles affects algal photosynthesis. *J. Phys. Chem.* 114 (39), 16556–16561.
- Bombelli, P., Howe, J.C., Bertocchini, F., 2017. Polyethylene bio-degradation by caterpillars of the wax moth *Galleria mellonella*. *Curr. Biol.* 27, R283–R293.
- Brown, D.M., Wilson, M.R., MacNee, W., Stone, V., Donaldson, K., 2001. Size-dependent proinflammatory effects of ultrafine polystyrene particles: a role for surface area and oxidative stress in the enhanced activity of ultrafines. *Toxicol. Appl. Pharmacol.* 175 (3), 191–199.
- Chae, Z., Kim, D., Kim, S.W., An, Z.J., 2018. Trophic Transfer and Individual Impact of Nano-Sized Polystyrene in a Four-Species Freshwater Food Chain.
- Cohen, J.T., Carlson, G., Charnley, G., Coggon, D., Delzell, E., Graham, J.D., Greim, H., Krewski, D., Medinsky, M., Monson, R., Paustenbach, D., Petersen, B., Rappaport, S., Rhomberg, L., Ryan, P.B., Thompson, K.J., 2002. A comprehensive evaluation of the potential health risks associated with occupational and environmental exposure to styrene. *Toxicol. Environ. Health Part B* 5, 1–265.
- Conti, B., Maltoni, C., Perino, G., Ciliberti, A., 1988. Long-term carcinogenicity bioassays on styrene administered by inhalation, ingestion and injection and styrene oxide administered by ingestion in Sprague-Dawley rats, and para-methyl styrene administered by ingestion in Sprague-Dawley rats and Swiss mice. *Ann. N. Y. Acad. Sci.* 534, 203–234.
- Costa, J.P., Santos, P.S.M., Duarte, A.C., Rocha-Santos, T., 2016. Nano plastics in the environment – sources, fates and effects. *Sci. Total Environ.* 566–567, 15–26.
- Cox, D.K., Covernton, A.G., Davies, L.H., Dower, F.J., Juanes, F., Dudas, E.S., 2019. Human consumption of microplastics. *Environ. Sci. Technol.* 1–10.
- Cui, R., Kim, W.S., An, Y., 2017. Polystyrene nanoplastics inhibit reproduction and induce abnormal embryonic development in the freshwater crustacean *Daphnia galeata*. *Sci. Rep.* 1–10.
- De Falco, F., Gullo, M.P., Gentile, G., Di Pace, E., Cocca, M., Gelabert, M., Brouta-Agnès, M., Rovira, A., Escudero, R., Villalba, R., Mossotti, R., Montarsolo, A., Gavignano, S., Tonin, C., Avella, M., 2018. Evaluation of microplastic release caused by textile washing processes of synthetic fabrics. *Environ. Pollut.* 236, 916–925.
- Della Torre, C., Bergami, C., Salvati, A., Faleri, A., Cirino, P., Dawson, K.A., Corsi, I., 2014. Accumulation and embryotoxicity of polystyrene nanoparticles at early stage of development of sea urchin embryos *Paracentrotus lividus*. *Environ. Sci. Technol.* 48 (20), 12302–12311.
- Deng, Y., Zhang, Y., Lemos, B., Ren, H., 2017. Tissue accumulation of microplastics in mice and biomarker responses suggest widespread health risks of exposure. *Sci. Rep.* 7, 46687. <https://doi.org/10.1038/srep46687>.
- Desforges, J.P., Galbraith, M., Dangerfield, N., Ross, P.S., 2014. Widespread distribution of microplastics in subsurface seawater in the NE Pacific Ocean. *Mar. Pollut. Bull.* 79 (1–2), 94–99.
- Dominghaus, H., Eyerer, P., Elsner, P., Hirth, T., 2005. Die Kunststoffe Und Ihre Eigenschaften. Springer Verlag, Berlin, p. 1549.
- Efimova, I., Bagaeva, M., Bagaev, A., Kileso, A., Chubarenko, I.P., 2018. Secondary microplastics generation in the sea swash zone with coarse bottom sediments: laboratory experiments. *Frontiers in Marine Science* 5.
- Ekvall, T.M., Lundqvist, M., Kelpsiene, E., Sileikis, E., Gunnarsson, B.S., Cedervall, T., 2019. Nanoplastic formed during the mechanical breakdown of daily-use polystyrene products. *Nanoscale Adv.* 1, 1055–1061.
- Esch, B.M., Southard, T., Tako, E., 2012. Oral exposure to polystyrene nanoparticles affects iron absorption. *Nat. Nanotechnol.* 1–8.
- Florence, A.T., 2004. Issues in oral nanoparticle drug carrier uptake and targeting. *J. Drug Target.* 12, 65–70.
- FDA (Food and Drug Administration), 2002. The Safety of Styrene-Based Polymers for Food-Contact Use. Polystyrene Packaging Council, Arlington.
- Forde, M., Iachetta, G., Tussellino, M., Carotenuto, R., Prisco, M., De Falco, M., Laforgia, V., Valiante, S., 2016. Polystyrene nanoparticles internalization in human gastric adenocarcinoma cells. *Toxicol. In Vitro* 31, 126–136.
- Gurman, J.L., Baier, L., Levin, B.C., 1987. Polystyrenes: a review of the literature on the products of thermal decomposition and toxicity. *Int. J.* 11, 109–130.
- Habib, D., Locke, C.D., Cannone, J.L., 1998. Synthetic fibres as indicators of municipal sewage sludge, sludge products, and sewage treatment plant effluents. *Water Air Soil Pollut.* 103 (1–4), 1–8.
- Hernandez, L.M., Yousefi, N., Tufenkji, N., 2017. Are there nanoplastics in your personal care products? *Environ. Sci. Technol. Lett.* 4 (7), 280–285.
- Hesler, M., Aengenheister, L., Ellinger, B., Drexler, R., Straskraba, S., Jost, C., Wagner, S., Meier, F., von Briesen, H., Buchel, C., Wick, P., Buerki-Thurnherr, T., Kohl, Y., 2019. Multi-endpoint toxicological assessment of polystyrene nano- and microparticles in different biological models *in vitro*. *Toxicol. Vitro* 61, 104610, 1–15.
- Hoet, P.H.M., Bruske-Hohlfeld, I., Salata, O.V., 2004. Nanoparticles- known and unknown health risk. *J. Nanobiotechnol.* 8 (2), 12, 1.
- Huff, J., Infante, F.P., 2011. Styrene exposure and risk cancer. *Mutagenesis* 26 (5), 583–584.
- Jambeck, R.J., Geyer, R., Wilcox, C., Siegler, R.T., Perryman, M., Andrady, A., Narayan, R., Law, L.K., 2015. Plastic waste inputs from land into ocean. *Science* 347 (6223), 768–771.

- Jiang, X., Weise, S., Hafner, M., Rocker, C., Zhang, F., Wolfgang, J.P., 2010. Quantitative analysis of the protein corona on FePt nanoparticles formed by transferrin binding. *J. R. Soc. Interface* 7, S5–S13.
- Johannaber, F., Michaeli, W., 2004. Handbuch Spritzgießen, fourth ed. Carl Hanser-Verlag, München, pp. 1269–1273.
- Kang, H.J., Park, H.J., Kwon, O.K., Lee, W.S., Jeong, D.H., Ju, B.K., Kwon, J.H., 2018. Occurrence of microplastics in municipal sewage treatment plants: a review. *Environ. Health Toxicol.* 33 (3), e2018013.
- Kaplan, D.L., Hartenstein, R., Sutter, J., 1979. Biodegradation of polystyrene, poly(methyl methacrylate), and phenol formaldehyde. *J. Appl. Environ. Microbiol.* 38, 551–553.
- Kashiwada, S., 2006. Distribution of nanoparticles in the sea-through Medaka (*Oryzias latipes*). *Environ. Health Perspect.* 114 (11), 1697–1702.
- Koelman, A., Besseling, E., Shim, W.J., 2015. Nanoplastics in the aquatic environment. *Critical review. Mar. Anthr. Litt.* 325–340.
- Koelmans, A.A., Nor, N.H.M., Hermens, E., Kooi, M., Mintenig, S.M., De France, J., 2019. Microplastics in freshwaters and drinking water: critical review and assessment of data quality. *Water Res.* 155, 410–422.
- Kokkinopoulou, M., Simon, J., Mailaender, V., Lieberwirth, I., Ladfester, K., 2012. *Physical Chemistry of Polymers*, pp. 71–72.
- Lambert, S., Wagner, M., 2016. Characterisation of nanoplastic during the degradation of polystyrene. *Chemosphere* 145, 265–268.
- Law, L.K., Moret-Ferguson, S., Maximenko, A.N., Proskurowski, G., Peacock, E.E., Hafner, J., Reddy, M.C., 2010. Plastic accumulation in the North Atlantic subtropical gyre. *Science* 1185–1188.
- Lee, K.W., Shim, W.J., Kwon, O.Y., Kang, J.-H., 2013. Size-dependent effects of micro polystyrene nanoparticles in the marine copepod *Tigriopus japonicus*. *Environ. Sci. Technol.* 47, 11278–11283.
- Lee, S.W., Kim, B., Huh, H.Y., Lee, J.-S., 2019. Bioaccumulation of polystyrene nanoplastics and their effect on the toxicity of Au ions in zebrafish embryos. *Nanoscale* 1–13.
- Lei, L., Liu, M., Song, Y., Lu, S., Hu, J., Cao, C., Xie, B., Shi, H., He, D., 2018. Polystyrene (nano)microplastics cause size-dependent neurotoxicity, oxidative damage and other adverse effects in *Caenorhabditis elegans*. *Environ. Sci. Nano* 5 (8).
- Lickly, T.D., Breder, C.V., Rainey, M.L., 1995. A model for estimating the daily dietary intake of a substance from food contact articles: styrene from polystyrene food contact polymers. *Regul. Toxicol. Pharmacol.* 21, 406–417.
- Loss, C., Szyrovetz, T., Musyanovych, A., Mailaender, V., Landfester, K., Nienhaus, U.G., Simmet, T., 2014. Functionalized polystyrene nanoparticles as a platform for studying bio-nano interactions. *Beilstein J. Nanotechnol.* 5, 2403–2412.
- Love, S.A., Maurer-Jones, M.A., Thompson, J.W., Lin, Y.-S., Haynes, C.L., 2012. Assessing nanoparticle toxicity. *Annu. Rev. Anal. Chem.* 5, 181–205.
- Ma, Y., Yao, M., Li, B., Ding, M., He, B., Chen, S., Zhou, X., Yuan, Y., 2018. Enhanced poly(ethylene terephthalate) hydrolase activity by protein engineering. *Engineering* 4 (6), 888–893.
- Mahon, A., O'Connell, B., Healy, M., O'Connor, L., Officer, R., Nash, R., Morrison, L., 2017. Microplastics in sewage sludge: effects of treatment. *Environ. Sci. Technol.* 51, 810–818.
- Mattsson, K., Hansson, L.A., Cedervall, T., 2015. Nano-plastics in the aquatic environment. *Environ. Sci. Process Impacts* 17 (10), 1712–1721.
- Mattsson, K., Johnson, V.E., Malmendal, A., Linse, S., Hansson, L.-A., Cedervall, T., 2017. Brain damage and behavioural disorders in fish induced by plastic nanoparticles delivered through the food chain. *Sci. Rep.* 7 (11452), 1–11.
- Meng, H., Xia, T., George, S., Nel, A.E., 2009. A predictive toxicological paradigm for the safety assessment of nanomaterials. *ACS Nano* 3, 1620–1627.
- Midwood, P.M., Janse, A., Merema, M.T., Groothuis, G.M., Verpoorte, E., 2012. Comparison of biocompatibility and adsorption properties of different plastics for advanced microfluidic cell and tissue culture models. *Anal. Chem.* 84 (9), 3938–3944.
- Mohr, K., Sommer, M., Baier, G., Schottler, S., Okwieka, P., Tenzer, S., Landfester, K., Mailaender, V., Schmidt, M., Meyer, G.R., 2014. Aggregation behavior of polystyrene – nanoparticles in human blood serum and its impact on the in vivo distribution in mice. *J. Nanomed. Nanotechnol.* 5, 1–10.
- Moore, C.J., Lattin, G.L., Zellers, A., 2005. Density of plastic particles found in zooplankton trawls from coastal waters of California to the North Pacific central gyre. In: *Proceedings of the Plastic Debris Rivers to Sea Conference*. Algalita Marine Research Foundation, Long Beach, CA USA.
- Murali, K., Kenesei, K., Li, Y., Demeter, K., Korneyi, Z., Madarasz, E., 2015. Uptake and bio-reactivity of polystyrene nanoparticles is affected by surface modifications, ageing and LPS adsorption: in vitro studies on neural tissue cells. *Nanoscale* 7 (9), 4199–4210.
- Mutti, A., Buzio, C., Perazzoli, F., Bergamaschi, E., Bocchi, M.C., Selis, L., Mineo, F., Franchini, I., 1992. Lymphocyte subpopulations in workers exposed occupationally to styrene. *Med. Lavoro* 83 (2), 167–177.
- O'Brine, T., Thompson, R.C., 2010. Degradation of plastic carrier bags in the marine environment. *Mar. Pollut. Bull.* 60 (12), 2279–2283.
- Oberdorster, G., 2001. Pulmonary effects of inhaled ultrafine particles. *Int. Arch. Occup. Environ. Health* 74 (1), 1–8.
- Oslakovic, C., Cedervall, T., Linse, S., Dahlbäck, B., 2012. Polystyrene nanoparticles affecting blood coagulation. *Nanomedicine* 8 (6), 981–986.
- Park, M.V.D.Z., Neigh, A.M., Vermeulen, J.P., Fonteyne, L.J.J., Verharen, H.W., Briedé, J.J., Loveren, H., Jong, W.H., 2011. The effect of particle size on the cytotoxicity, inflammation, developmental toxicity and genotoxicity of silver nanoparticles. *Biomaterials* 32, 9810–9817.
- Pitt, J.A., Trevisan, R., Massarsky, A., Kozal, J.S., Levin, E.D., Di Giulio, R.T., 2018. Maternal transfer of nanoplastic to offspring in zebrafish (*Danio rerio*): a case study with nanopolystyrene. *Sci. Total Environ.* 1 (643), 324–334.
- Plastics-The Facts, 2017. An Analysis of European Plastics Production, Demand and Waste Data. https://www.plasticseurope.org/application/files/5715/1717/4180/Plastics_the_facts_2017_FINAL_for_website_one_page.pdf.
- Pomeroy, van P., Bruna, N.R., Peijnenburg, W.J.G.M., Vijver, M.G., 2017. Exploring uptake and biodistribution of polystyrene (nano) particles in zebrafish embryos AT different development stages. *Aquat. Toxicol.* 190, 40–45.
- Ponomarev, V., Tomatis, L., 1978. Effects of long-term oral administration of styrene to mice and rats. *Scand. J. Work. Environ. Health* 4, 127–135.
- Prata, P.J.C., da Costa, J.P., Lopes, I., Duarte, A.C., Rocha-Santos, T., 2020. Environmental exposure to microplastics: an overview on possible human health effects. *Sci. Total Environ.* 702, 134455.
- Revel, M., Chatel, A., Mouneyrac, C., 2018. Micro (nano) plastics: a threat to human health? *Curr. Opin. Environ. Sci. Health* 1, 17–23.
- Rossi, G., Barnoud, J., Monticelli, L., 2014. Polystyrene nanoplastics perturb lipid membranes. *J. Phys. Chem. Lett.* 5 (1), 241–246.
- Salvati, A., Aberg, C., dos Santos, T., Varela, J., Pinto, P., Lynch, I., et al., 2011. Experimental and theoretical comparison of intracellular import of polymeric nanoparticles and small molecules: toward models of uptake kinetics. *Nanomed. Nanotechnol. Biol. Med.* 7, 818–826.
- Schirizzi, G.F., Perez-Pomeda, I., Sanchis, J., Rossini, C., Farre, M., Barcelo, D., 2017. Cytotoxic effects of commonly used nanomaterials and microplastics on cerebral and epithelial human cells. *Environ. Res.* 159, 579–587.
- Shahbazi, M.-A., Hamidi, M., Mäkilä, E.M., Zhang, H., Almeida, P.V., Kaasalainen, M., Salonen, J.J., Hirvonen, J.T., Santos, H., 2013. The mechanisms of surface chemistry effects of mesoporous silicon nanoparticles on immunotoxicity and biocompatibility. *Biomaterials* 34, 7776–7789.
- Shang, L., Nienhaus, K., Nienhaus, U.G., 2014. Engineered nanoparticles interacting with cells: size matters. *J. Nanobiotechnol.* 12 (5), 1–11.
- Shim, W.J., Hong, S.H., Eo, S., 2018. Microplastic contamination in aquatic environments. *Marine microplastics. Emerg. Matter Environ. Urg.* 1–26.
- Singh, B., Sharma, N., 2008. Mechanistic implications of plastic degradation. *Polym. Degrad. Stab.* 93 (3), 561–584.
- Snopczyński, T., Góralczyk, K., Czaja, K., Struciński, P., Hernik, A., Korcz, W., Ludwicki, K., 2009. Nanotechnology - possibilities of danger. [in polish] *roczn. PZH* 60 (2), 101–111.
- Thompson, J., Quigley, J., Halfpenny, N., Scott, D., Hawkins, N., 2016. Importance and methods of searching for E-publications ahead of print in systematic reviews. *Evid. Based Med.* 21 (2), 55–59. <https://doi.org/10.1136/ebmed-2015-110374>. Epub 2016 Feb 24.
- Tokiwa, Y., Calabia, B.P., Ugwu, C.U., Aiba, S., 2009. Biodegradability of plastics. *Int. J. Mol. Sci.* 10, 3722–3742.
- Tornero-Velez, R., Rappaport, M.S., 2001. Physiological modeling of the relative contributions of styrene-7,8-oxide derived from direct inhalation and from styrene metabolism to the systemic dose in humans. *Toxicol. Sci.* 64 (2), 151–161.
- Velzeboer, I., Quik, J.T.K., van de Meent, D., Koelmans, A.A., 2014. Rapid settling of nanomaterials due to hetero-aggregation with suspended sediment. *Environ. Toxicol. Chem.* 33, 1766–1773.
- Walkey, D.C., Warren, C.W.C., 2012. Understanding and controlling the interaction of nanomaterials with proteins in a physiological environment. *Chem. Soc. Rev.* 41 (7), 2780–2799.
- Wang, Y., Zhang, D., Zhang, M., Mu, J., Ding, G., Mao, Z., Cao, Y., Jin, F., Cong, Y., Wang, L., Zhang, W., Wang, J., 2019. Effects of ingested polystyrene microplastics on brine shrimp, *Artemia parthenogenetica*. *Environ. Pollut.* 244, 715–722.
- Waring, R.H., Harris, R.M., Mitchell, S.C., 2018. Plastic contamination of the food chain: a threat to human health? *Maturitas* 115, 64–68.
- WHO, 2000. Styrene. Air Quality Guidelines for Europe, second ed. World Health Organization Regional Office for Europe Copenhagen, pp. 1–288.
- Worm, B., Lotze, K.H., Jubinville, I., Wilcox, C., Jambeck, J., 2017. Plastic as a persistent marine pollutant. *Annu. Rev. Environ. Resour.* 42, 1–26.
- Wünsch, J.R., 2000. Polystyrene: Synthesis, Production and Applications. Rapra Technology, Shropshire, pp. 1–28.
- Xia, T., Kovochich, M., Liong, M., Zink, J.J., Nel, A.E., 2008. Cationic polystyrene nanosphere toxicity depends on cell-specific endocytic and mitochondrial injury pathways. *ACS Nano* 2, 85–96.
- Yooeun, C., Dokyung, K., Shin, W.K., Youn-Joo, A., 2018. Trophic transfer and individual impact of Nano-sized polystyrene in a four-species freshwater food chain. *Sci. Rep.* 8, 1–11.
- Yoshida, S., Hiraga, K., Takehana, T., Taniguchi, I., 2016. A bacterium that degrades and assimilates poly(ethylene terephthalate). *Science* 351 (6278), 1196–1199.
- Zettler, E.R., Mincer, T.J., Amaral-Zettler, L.A., 2013. Life in the „plastisphere”: microbial communities on plastic marine debris. *Environ. Sci. Technol.* 47 (13), 7137–7146.
- Zhao, L., Qu, M., Wong, G., Wang, D., 2017. Transgenerational toxicity of nanoplastics in the range of $\mu\text{g L}^{-1}$ in the nematode *Caenorhabditis elegans*. *Environ. Sci.: Nano* 4, 1–11.
- Zhao, Y., Sun, X., Zhang, G., Trewyn, B.G., Slowing, I.I., Lin, V.S.Y., 2011. Interaction of mesoporous silica nanoparticles with human red blood cell membranes: size and surface effects. *ACS Nano* 5, 1366–1375.
- Zhou, Y., Peng, Z., Seven, E.S., Leblanc, R.M., 2018. Crossing the blood-brain barrier with nanoparticles. *J. Contr. Release* 270, 290–303.



Article

Oxidative Properties of Polystyrene Nanoparticles with Different Diameters in Human Peripheral Blood Mononuclear Cells (In Vitro Study)

Kinga Kik, Bożena Bukowska , Anita Krokosz and Paulina Sicińska *

Department of Biophysics of Environmental Pollution, Faculty of Biology and Environmental Protection, University of Lodz, Pomorska Str. 141/143, 90-236 Lodz, Poland; kinga.kik@edu.uni.lodz.pl (K.K.); bozena.bukowska@biol.uni.lodz.pl (B.B.); anita.krokosz@biol.uni.lodz.pl (A.K.)

* Correspondence: paulina.sicinska@biol.uni.lodz.pl

Abstract: With the ongoing commercialization, human exposure to plastic nanoparticles will dramatically increase, and evaluation of their potential toxicity is essential. There is an ongoing discussion on the human health effects induced by plastic particles. For this reason, in our work, we assessed the effect of polystyrene nanoparticles (PS-NPs) of various diameters (29, 44 and 72 nm) on selected parameters of oxidative stress and the viability of human peripheral blood mononuclear cells (PBMCs) in the in vitro system. Cells were incubated with PS-NPs for 24 h in the concentration range of 0.001 to 100 µg/mL and then labeled: formation of reactive oxygen species (ROS) (including hydroxyl radical), protein and lipid oxidation and cell viability. We showed that PS-NPs disturbed the redox balance in PBMCs. They increased ROS levels and induced lipid and protein oxidation, and, finally, the tested nanoparticles induced a decrease in PBMCs viability. The earliest changes in the PBMCs were observed in cells incubated with the smallest PS-NPs, at a concentration of 0.01 µg/mL. A comparison of the action of the studied nanoparticles showed that PS-NPs (29 nm) exhibited a stronger oxidative potential in PBMCs. We concluded that the toxicity and oxidative properties of the PS-NPs examined depended to significant degree on their diameter.

Keywords: polystyrene nanoparticles; ROS; lipid and protein oxidation; apoptosis; cells viability; LC₅₀



Citation: Kik, K.; Bukowska, B.; Krokosz, A.; Sicińska, P. Oxidative Properties of Polystyrene Nanoparticles with Different Diameters in Human Peripheral Blood Mononuclear Cells (In Vitro Study). *Int. J. Mol. Sci.* **2021**, *22*, 4406. <https://doi.org/10.3390/ijms22094406>

Academic Editor: Ying-Jan Wang

Received: 31 March 2021

Accepted: 21 April 2021

Published: 23 April 2021

Publisher's Note: MDPI stays neutral with regard to jurisdictional claims in published maps and institutional affiliations.



Copyright: © 2021 by the authors. Licensee MDPI, Basel, Switzerland. This article is an open access article distributed under the terms and conditions of the Creative Commons Attribution (CC BY) license (<https://creativecommons.org/licenses/by/4.0/>).

1. Introduction

Plastics are now a serious environmental problem in the world. Since the massive production of plastics started in the 1950s, the output has been rising annually. In the 1950s, approximately 1.5 million tons of plastics were produced; the amount has been raised 200-fold up to 299 million tons worldwide in 2013, and from the years 2015 to 2016 from 322 to 335 million tons a year [1]. It has been estimated that the amount of produced plastics may increase significantly and even be doubled in the coming years [2]. Approximately 90% of the total amount of plastics consists of high-density polyethylene, low-density polyethylene, polyvinyl chloride, polystyrene, polypropylene and polyethylene terephthalate [3]. Numerous studies have shown that the degradation of plastic leads to the release of nanoparticles (NPs) into the environment [4,5]. Plastic may be degraded into microparticles (MPs) < 5000 nm (5 µm) in diameter, and further into NPs < 100 nm (0.1 µm) in diameter [6]. Plastic NPs may enter human organisms in food, water, air and through skin. Then, they accumulate in subsequent links of the food chain [7–9].

One of the main plastics used for packaging, commercial and construction purposes is polystyrene (PS) [10]. It is a petroleum-based material obtained by the polymerization of styrene (vinylbenzene) monomers. According to the US Environmental Protection Agency (EPA), the polystyrene manufacturing process is the fifth largest source of hazardous waste. Despite the existing evidence regarding the toxicity of styrene, the styrene polymerization product—polystyrene—is not listed as hazardous in any policy documents.

Plastic nanoparticles, including polystyrene, enter the human body mainly through the digestive and respiratory tracts [11,12]. Depending on the cell type and NP size, they may be transported through phagocytosis, pinocytosis, macro-pinocytosis or absorbed by passive transport, and as a consequence they can enter cellular membranes and various biological structures [13]. In rats, after oral administration, 6% of PS particles (0.87 μm) were detected in the circulation within 15 min [11], whereas oral exposure to polystyrene nanoparticles (1.25 mg kg^{-1} , size 50 nm) resulted in 34% absorption, most probably transported through the mesentery lymph to reach the circulatory system and accumulate mostly in the liver [12]. Moreover, translocation across the mammalian gut into the lymphatic system of various types and sizes of microparticles (between 0.1 and 150 nm) has been demonstrated in studies involving humans (0.2 and 150 nm) [14]. It is known that particles <110 nm can enter the blood stream through the portal vein and particles <20 nm can reach internal organs [15–17]. Crossing the intestinal barrier, particles <100 nm can even be transported into the brain and across the placental barrier [17–22]. Recently, Ragusa et al. (2021) showed in their research the presence of 12 microplastic fragments (ranging from 5 to 10 μm in size), with spheric or irregular shape in four placentas from six placentas investigated in humans [23]. As shown in the above research, inhaled particles can be excreted by mucociliary clearance, but can also settle in the lungs or be absorbed into the bloodstream [17,24]. PS-NPs can enter the circulatory system and thus may interact with all blood components.

There is little data on the effects of polystyrene nanoparticles on blood cells. Studies conducted on workers exposed to styrene showed a decreased percentage of T helper lymphocytes and an increased ratio of suppressor T lymphocytes. These studies demonstrated the immunotoxicity of styrene [25]. Other studies suggest that exposure to styrene may cause lymphoma and leukemia in humans, while polystyrene has not been shown to be carcinogenic [26]. Currently, most studies on the toxicity of plastic particles are animal studies. It was observed that polystyrene induces oxidative stress in *Danio rerio* [27] and mice [28–30] and increases the ROS level in *Daphnia magna* [31].

Insufficient data on the harmful effects of polystyrene nanoparticles prompted us to undertake studies using alternative in vitro tests to elucidate the cellular mechanisms of toxicity. To increase the relevance of these tests for humans, the European Union Reference Laboratory for Alternatives to Animal Testing (EURL-ECVAM) recommends the use of human cells for all in vitro test systems. The source of the cells may be peripheral human blood. It is the first target model for exposure to chemicals of environmental or industrial origin and it provides information on the body's overall response to xenobiotics [32–34].

In our study, we used peripheral human blood mononuclear cells, which were incubated with polystyrene nanoparticles of various sizes (29, 44 and 77 nm) for 24 h in the concentration range of 0.001 to 1000 $\mu\text{g/mL}$. We then assessed the increase in reactive oxygen species levels (including hydroxyl radical), the degree of lipid and protein oxidation and the percentage of viable PBMCs.

2. Results

2.1. Characterization of Polystyrene Nanoparticles

The PS-NPs size distribution in phosphate-buffered saline (pH 7.4) is presented in Figure 1 and Table 1. As we can see, the diameters of the particles indicated by the manufacturer are consistent with the results measured by Dynamic Light Scattering (DLS) method.

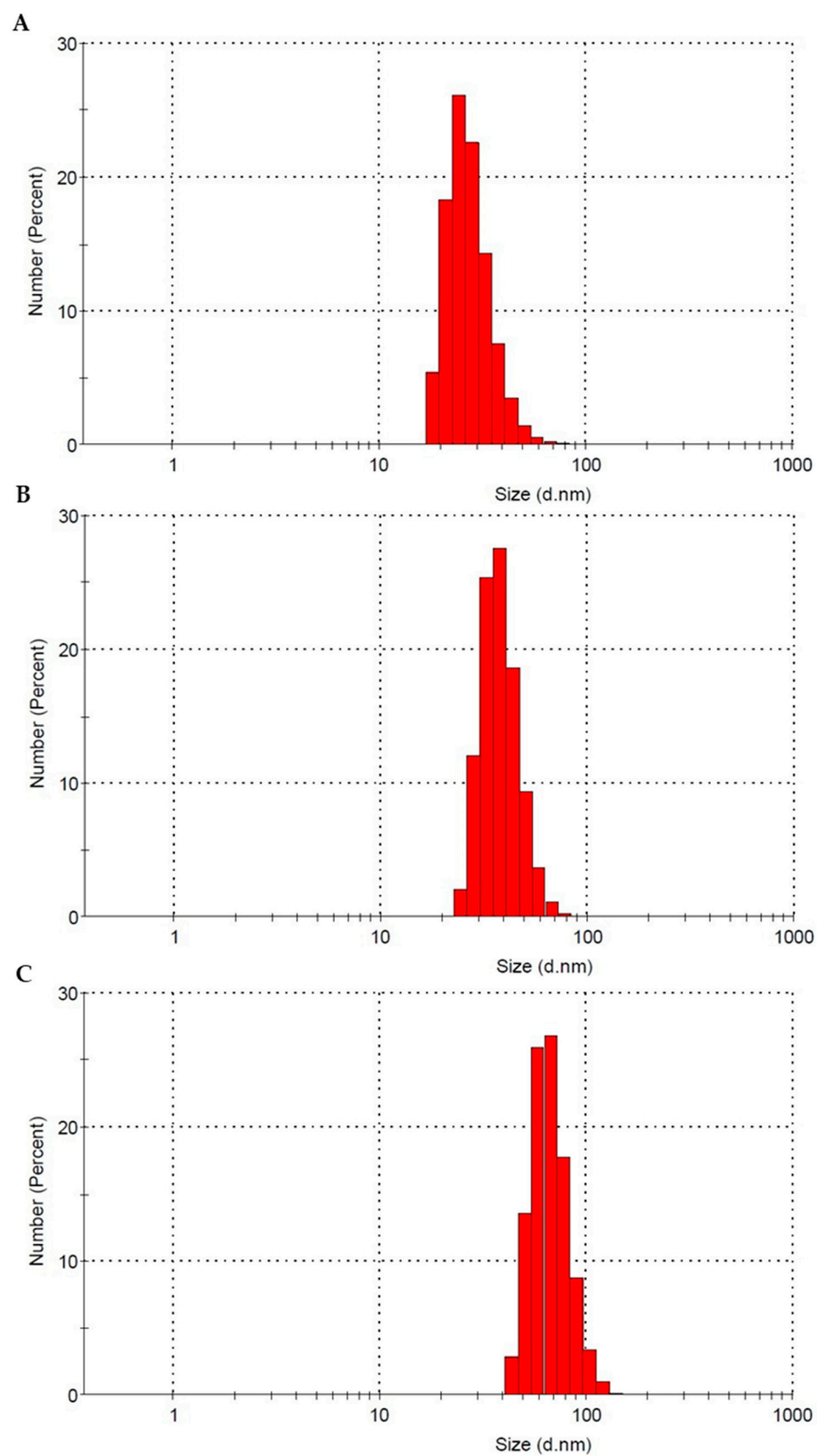


Figure 1. Dynamic light scattering size distribution of the different PS-NPs in phosphate-buffered saline, pH 7.4. Graphs, (A)—29 nm, (B)—44 nm and (C)—72 nm, were prepared by means of the Zetasizer Nano-ZS software.

Table 1. Characterization of PS-NPs size by DLS in phosphate-buffered saline (PBS), pH 7.4.

Diameter in Dicated by Manufacturer	29 nm	44 nm	72 nm
Mean Diameter \pm SD	27.96 \pm 8.03	38.61 \pm 8.61	68.45 \pm 15.19

2.2. Reactive Oxygen Species

24-h incubation of PBMCs with polystyrene nanoparticles showed an increase in ROS in the cells tested. All tested particles caused oxidation of the fluorescent 2'-7'-dichlorodihydrofluorescein probe. Statistically significant changes versus control were caused by PS-NPs with a diameter of 29 and 44 nm, as they increased the production of reactive oxygen species at a concentration of 0.01 $\mu\text{g/mL}$. On the other hand, nanoparticles with a diameter of 72 nm caused statistically significant changes versus control from at the concentration of 0.1 $\mu\text{g/mL}$ (Figure 2).

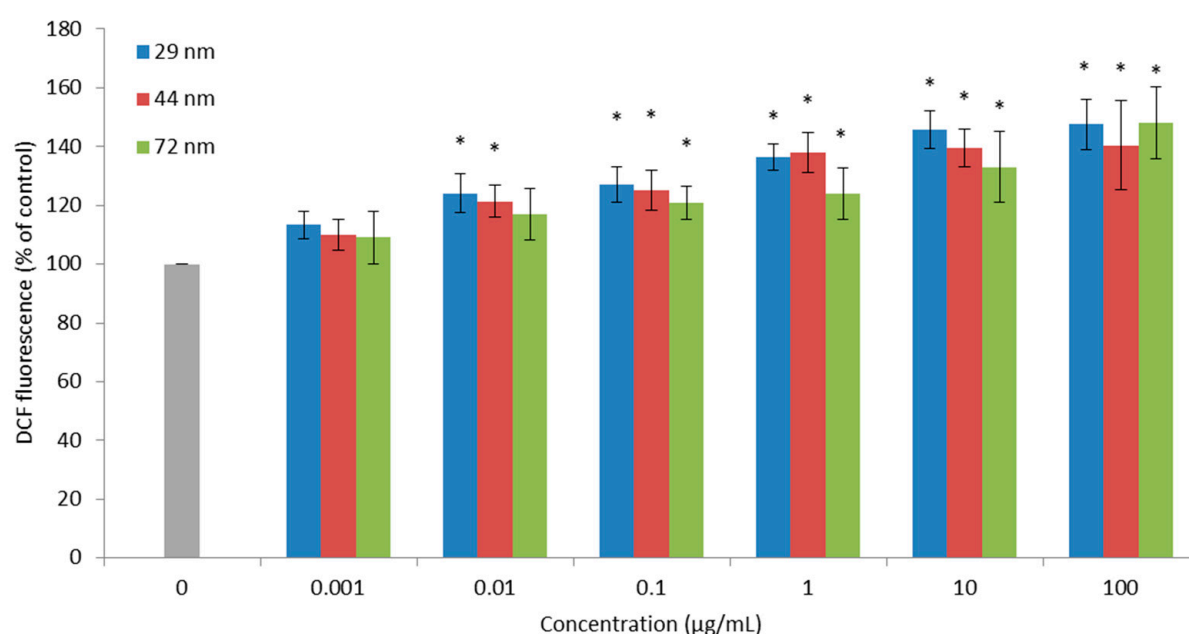


Figure 2. ROS level in PBMCs incubated with PS-NPs of diameter 29, 44 and 72 nm in the concentration range of 0.001 to 100 $\mu\text{g/mL}$ for 24 h ($n = 5$). * $p < 0.05$ indicates statistically significant difference from control; one-way ANOVA and a posteriori Tukey test.

2.3. Hydroxyl Radical Level

The oxidation of 4-hydroxy-phenyl-fluorescein (HPF) is associated with the formation of highly reactive oxygen species including the hydroxyl radical. Statistically significant changes in HPF oxidation were observed after the 24-h incubation of PBMCs with all analyzed nanoparticles, 29, 44 and 72 nm in diameter. It was shown that the largest changes were induced by PS-NPs with the smallest diameter from 1 $\mu\text{g/mL}$. The 44 and 72 nm nanoparticles caused a statistically significant increase in the level of the hydroxyl radical at the concentration of 10 $\mu\text{g/mL}$ (Figure 3).

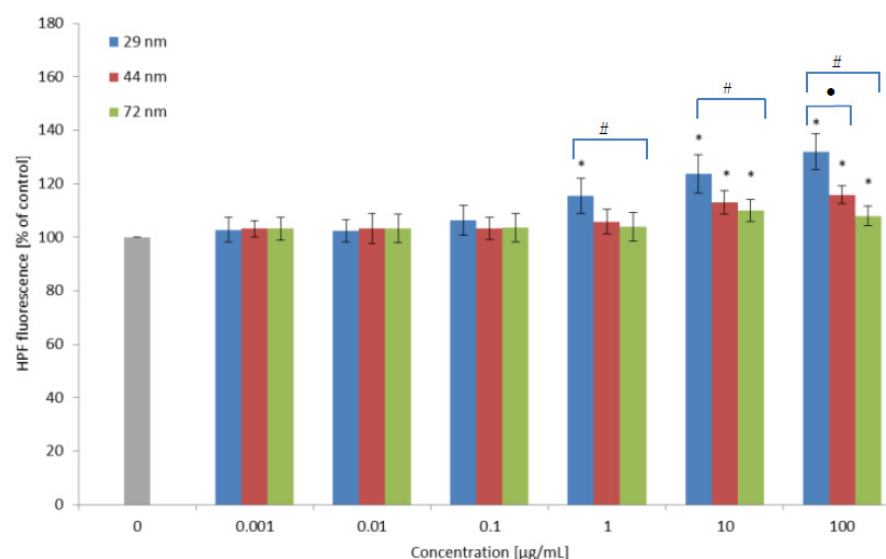


Figure 3. Changes in hydroxyl radical levels of cells incubated with PS-NPs of diameter 29, 44 and 72 nm in the concentration range of 0.001 to 100 µg/mL for 24 h (n = 5). * $p < 0.05$ indicates statistically significant difference from control; (•) statistically significant difference between nanoparticles of size 29 versus 44 nm; (#) statistically significant difference between nanoparticles of size 29 versus 72 nm. One-way ANOVA and a posteriori Tukey test.

2.4. Lipid Peroxidation

Assessment of lipid peroxidation in PBMCs treated with polystyrene nanoparticles of various diameters in the concentration range of 0.001 to 100 µg/mL was performed. All analyzed nanoparticles caused a significant decrease in the fluorescence of cis-parinaric acid. It was shown that the largest changes were shown by nanoparticles with a diameter of 29 nm, which caused a statistically significant decrease in the examined parameters versus the control at the concentration of 0.1 µg/mL. However, in the case of larger polystyrene particles with a diameter of 44 and 72 nm, statistically significant changes versus control were observed at the concentration of 1 µg/mL (Table 2).

Table 2. The level of lipid peroxidation (fluorescence of cis-parinaric acid) and protein oxidation (tryptofan fluorescence) in PBMCs incubated with PS-NPs of diameter 29, 44 and 72 nm in the concentration range of 0.001 to 100 µg/mL for 24 h (n = 5).

Concentration (µg/mL)	Fluorescence of Cis-Parinaric Acid (% of Control)			Tryptofan Fluorescence (% of Control)		
	29 nm	44 nm	72 nm	29 nm	44 nm	72 nm
0	100	100	100	100	100	100
0.001	96.83 ± 5.09	97.86 ± 5.86	98.30 ± 4.99	95.65 ± 5.28	96.28 ± 6.36	98.38 ± 7.34
0.01	94.80 ± 6.50	95.81 ± 6.27	95.13 ± 6.91	94.39 ± 6.71	95.97 ± 7.01	97.46 ± 5.71
0.1	83.30 ± 5.60 *	94.00 ± 6.83	95.31 ± 6.99	86.19 ± 5.82 *	94.66 ± 6.71	98.56 ± 7.51
1	79.04 ± 4.77 *	91.03 ± 5.89 *	89.46 ± 4.41 *	82.88 ± 7.01 *	89.29 ± 7.25 *	95.06 ± 6.57 *
10	76.21 ± 4.63 *	83.32 ± 5.45 *	85.56 ± 5.93 *	83.00 ± 5.53 *	87.92 ± 4.45 *	83.75 ± 5.42 *
100	74.23 ± 4.08 *	77.29 ± 7.45 *	74.22 ± 5.60 *	83.31 ± 4.47 *	84.88 ± 5.98 *	78.86 ± 4.81 *

* $p < 0.05$ indicates statistically significant difference from control; one-way ANOVA and a posteriori Tukey test.

2.5. Protein Damages

All tested nanoparticles were reported to cause oxidative damage to proteins in lymphocytes after 24 h of incubation. The 29 and 44 nm nanoparticles induced a statistically significant decrease in tryptophan fluorescence at the concentrations of 0.1 and 1 µg/mL, respectively, compared to the control sample. In the case of the largest nanoparticles, the changes were statistically significant from 10 µg/mL (Table 2).

2.6. Cell Apoptosis

All PS-NPs increased the number of apoptotic cells. Nanoparticles of 29 nm in diameter starting from the concentration of 1 $\mu\text{g}/\text{mL}$ caused a statistically significant increase in the number of apoptotic cells. However, nanoparticles with a size of 44 and 72 nm starting from the concentrations of 10 and 100 $\mu\text{g}/\text{mL}$, respectively, caused an increase in the number of apoptotic PBMCs (Figure 4).

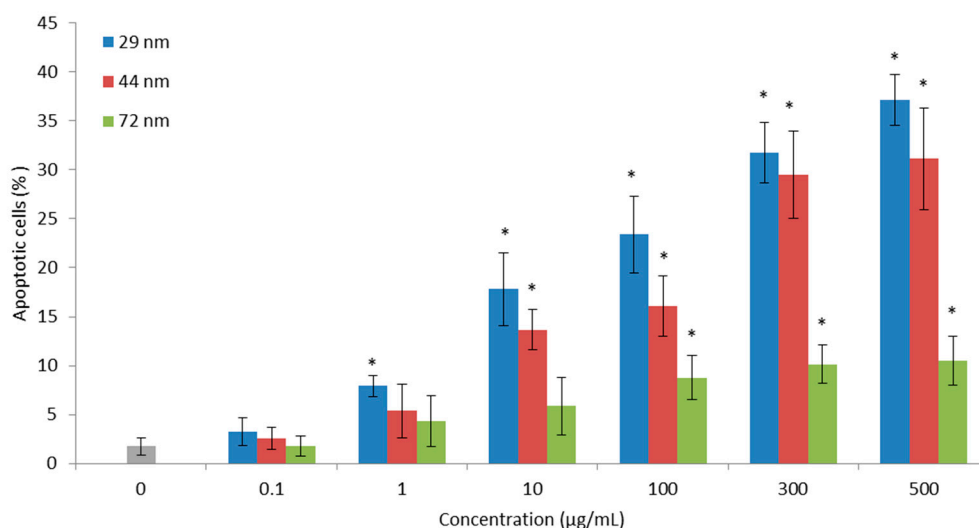


Figure 4. Percentage of apoptotic PBMCs incubated for 24 h with PS-NPs of diameter 29, 44 and 72 nm in the concentration range from 0.01 to 500 $\mu\text{g}/\text{mL}$ ($n = 5$). * $p < 0.05$ indicates statistically significant difference from control; one-way ANOVA and a posteriori Tukey test.

2.7. Cell Viability

All analyzed PS-NPs decreased PBMC viability. The greatest changes of the examined parameters were observed in cells incubated with nanoparticles with a diameter of 29 nm. Statistically significant changes for nanoparticles with diameters of 29 and 44 nm were at the concentration of 500 $\mu\text{g}/\text{mL}$. The largest nanoparticles with a diameter of 72 nm caused a small but statistically significant decrease in the number of cells only at the concentration of 1000 $\mu\text{g}/\text{mL}$ (Figure 5).

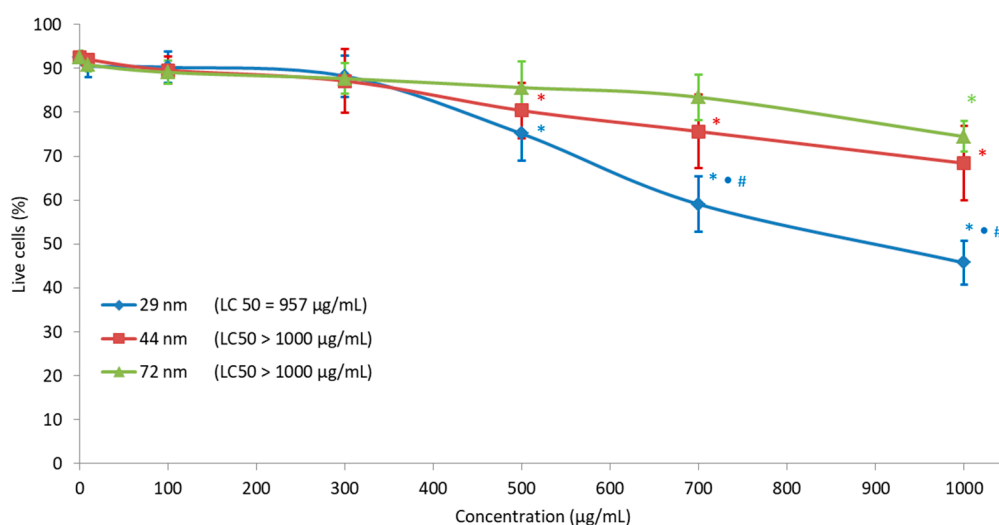


Figure 5. Percentage of cell viability incubated with PS-NPs with a diameter of 29, 44 and 72 nm in the concentration range of 10 to 1000 $\mu\text{g}/\text{mL}$ for 24 h ($n = 5$). * $p < 0.05$ indicates statistically significant difference from control; (•) statistically significant difference between nanoparticles of the size 29 versus 44 nm; (#) statistically significant difference between nanoparticles of the size 29 versus 72 nm. One-way ANOVA and a posteriori Tukey test.

3. Discussion

Nano- and microplastics, once regarded as inert particles without toxicity, are now seen as potentially harmful to organisms depending on exposure conditions and organism susceptibility [35–37]. The high surface area of plastic particles may be responsible for oxidative stress, cytotoxicity and particle translocation to other tissues, while their persistent nature limits their removal from the organism, leading to chronic inflammation [38]. As shown in the literature, nano- and microplastic particles can induce the production of ROS. The formation of free radicals on NP/MP surfaces occurs by photooxidation or UV radiation through cross-linking reactions [39]. Free radicals that have been generated along the polymer chain can then bind to atmospheric oxygen and lead to the formation of polymeric peroxy radicals, while continuing to form secondary polymeric alkyl radicals [3]. Currently, the studies on oxidative stress induced by PS-NPs have been conducted mainly on animals [40–43], while there have been only a few in vitro studies performed [44–46].

Our research showed that PS-NPs after 24 h of incubation with PBMCs in the concentration range of 0.001 to 100 µg/mL caused an increase in ROS at a concentration of 0.01 µg/mL for PS-NPs with a size of 29 and 44 nm, while for nanoparticles with a size of 72 nm a comparable increase in ROS was observed from 0.1 µg/mL (Figure 2). In the case of the hydroxyl radical, a statistically significant increase was observed from the concentration of 1 µg/mL for the smallest polystyrene nanoparticles, while for the remaining nanoparticles, a statistically significant increase was observed only at the concentration of 10 µg/mL (Figure 3). Similar increases in ROS under the influence of PS-NPs were observed by Schirizzi et al., 2017, measuring ROS formation in cells in cerebral (T98G) and epithelial (HeLa) human cells after exposure to PS-MPs (10 nm) and PS-NPs (40 and 250 nm) at 10 mg/L [46]. Positive effects were reported by Poma et al. (2019) in the human fibroblast Hs27 cell line by using a total ROS assay kit. The increase in ROS was observed after short exposure times (less than 30 min) [44]. In contrast, other researchers did not notice ROS formation in human intestinal Caco-2 cells after exposure to PS-NPs for 24 h [45]. These negative findings are in agreement with the results reported by Rubio et al. (2020) for THP-1 cells, where no effects in ROS production were noted. Mild positive effects were observed in Raji-B cells incubated for 3 h with the highest concentration of PS-NPs of 50 µg/mL. In another study, PS-NPs were able to induce a significant increase in intracellular ROS levels in TK6 cells. The authors suggested that the effects induced by PS-NPs can be strongly dependent on the type of the cells used [47]. PS-NPs caused also an increase in ROS and changes in the activity of antioxidant enzymes in organisms such as *Daphnia pulex* [40,41], marine bacteria (*Halomonas alkaliphila*) [42] and *Danio rerio* [43]. Liu et al. (2020; 2021) conducted a study on *Daphnia pulex*. The organism was exposed to 75 nm in diameter polystyrene nanoparticles at concentrations of 0.1, 0.5, 1 and 2 mg/L. It was observed that the analyzed nanoparticles induced a ROS level increase at concentrations of 0.5, 1 and 2 mg/L, and increased the content of hydrogen peroxide (H₂O₂) and activated the MAPK-HIF-1/NFκB pathway in the study organisms. Increased expression of the MAPK pathway genes was demonstrated at the lowest concentrations of nanoplastics. Moreover, a decrease in the activity of antioxidant enzymes, i.e., catalase (CAT) and total and copper-zinc superoxide dismutase (SOD, CuZnSOD) was found [40,41]. The formation of oxidative stress in sea bacteria (*Halomonas alkaliphila*) exposed to polystyrene nanoparticles and amine-modified nanoparticles of 55 and 50 nm in diameter, respectively, and an initial concentration of 10 g/L was also demonstrated. Amine-modified plastic particles caused higher oxidative stress than unmodified particles [42]. The latest research showed that exposure of adult zebrafish (*Danio rerio*) to 70 nm NP-PS at doses of 0.5 and 1.5 ppm for 7 days resulted in their accumulation in tissues, among others in the liver, intestines, brain and gonads, lead to disorders of lipid and energy metabolism and induced oxidative stress [43]. In other studies, an increase in the activity of CAT, SOD and GSH enzymes in visceral fat, gills and mantle was observed in *Corbicula fluminea* mussels exposed to 80 nm polystyrene nanoparticles at concentrations of 0.1, 1 and 5 mg/L [48].

The toxicity of nanoplastic particles may be dependent on their ability to translocate across the gut, enter the systemic circulation, penetrate cells and interact with biological macromolecules, such as lipids and proteins [21].

As a result of the fragmentation of microparticles into nanoparticles, the surface-to-weight ratio increases, which enables their penetration directly through lipid membranes [3]. In addition, recent studies have shown that nano- and microparticles of plastics increase cellular oxidative stress, which in turn may lead to the lipid peroxidation (LPO) of cell membranes [19,49], and consequently to the loss of plasma membrane integrity and intracellular membranes [50]. Therefore, in the next step, we checked whether polystyrene nanoparticles of different sizes affected the lipid oxidation in PBMCs.

Our research showed a statistically significant increase in lipid peroxidation at a concentration of 0.1 µg/mL in the case of polystyrene nanoparticles with a size of 29 nm, while nanoparticles with a size of 44 and 72 nm caused similar statistically significant changes at the concentration of 1 µg/mL (Table 2). Furthermore, Zheng et al. 2019 showed that 50 nm polystyrene nanoparticles increased the level of malondialdehyde (MDA) in rat hepatocytes, being a marker of lipid peroxidation [51]. Other studies reported a significant increase in lipid peroxidation in the muscle and brain tissue of sea bass (*Dicentrarchus labrax*) after 24-h exposure to microplastics at a concentration of 0.69 mg/L [18,19,52]. In turn, Ribeiro et al. (2017) demonstrated the formation of oxidative damage in *Scrobicularia plana* following exposure to 20 µm polystyrene microparticles at the concentration of 1 mg/L. This analysis demonstrated a slight increase in the LPO level [53]. Another study showed an increase in MDA in green discus fish exposed to microplastic at concentrations of 0, 50 and 500 µg/L [54]. Despite the above-mentioned studies, other authors observed that exposure to plastic microparticles did not induce lipid peroxidation in sea shellfish (*Mytilus edulis*) [55].

As a result of lipid peroxidation, aldehydes are formed, which can act cytotoxically [56] and lead to the inhibition of the activity of some transport proteins and membrane enzymes [57]. The process of protein oxidation may cause reversible and irreversible damage depending on the source of ROS and the type of oxidants [58]. Free radicals attack the main polypeptide chain and side chains of amino acid residues as a result of aromatic hydroxylation or thioloxidation [59]. Usually, aromatic amino acids (tyrosine, tryptophan and phenylalanine) and sulfur amino acids (methionine and cysteine) are damaged [58]. Cysteine and methionine, which contain active sulfur atoms, are the most susceptible to oxidation [60]. Oxidants attack the protein backbone, thereby causing protein conformational changes and fragmenting these structures. Induced by oxidation, intermolecular bridges can change the proteolytic properties of proteins and cause their aggregation [59].

Therefore, we also analyzed the level of oxidative changes in PBMCs proteins under the influence of polystyrene nanoparticles of different sizes. On the basis of the decrease in tryptophan fluorescence, we found that the smallest nanoparticles (29 nm) caused statistically significant changes at the concentration of 0.1 µg/mL, while nanoparticles with a diameter of 44 and 72 nm only at a concentration ten times higher (1 µg/mL) (Table 2).

Research by Holloczki and Gehrke (2019) showed that 5 nm nanoplastics interacted with proteins, thereby changing their key secondary structure and leading to their denaturation. It was also observed that amino acids containing side chains, i.e., tryptophan and phenylalanine, can be adsorbed on the surface of nanoplastics. Moreover, these studies suggest that a strong NP–amino acid interaction may disrupt protein folding [61]. Other studies have looked at the effect of NP on human plasma. A strong affinity of plasma proteins with the analyzed particles was demonstrated. Formation of a protein corona measuring 100 to 600 nm was observed in plasma. This analysis also showed that the interaction of proteins with nanoparticles caused conformational changes as well as protein denaturation [62]. In the latest research, scientists analyzed the effect of 150 µg/mL PS-NPs on bovine protein serum. It was proved that bovine serum albumin was maintained on the surface of the tested particles during the initial phase of internalization, which could protect the cell membrane against damage caused by polystyrene nanoparticles. Lysoso-

mal cytotoxicity was also observed in this study due to the degradation of the protein corona [63].

Accumulation of ROS, oxidized protein or lipid products in the cell impairs the functions of the cell, which in turn may lead to its apoptosis [64–66]. Thubagere et al. (2010) suggested that the cause of the apoptosis in cells treated with NPs may be the accumulation of H_2O_2 [67]. Other studies have shown that accumulation of NPs in lysosomes plays a central role in the cell death, leading to swelling of the lysosomes and the release of cathepsins into the cytosol, which ultimately propagates damage to the mitochondria with subsequent activation of apoptosis [68].

In the next step, we conducted quantitative analysis of the apoptosis of PBMCs treated with PS-NPs. Our results show that PS-NPs caused a statistically significant increase in the number of apoptotic cells, which was dependent on the concentration of tested NPs. Importantly, the earliest changes were caused by the smallest NPs, starting from a concentration of 1 $\mu\text{g/mL}$ (Figure 4). The concentration-dependent apoptotic effect of PS-NPs has also been demonstrated in the studies conducted on the human epithelial carcinoma cell line (A431) [69] and RAW264.7 cells [70]. In another study, researchers showed that PS-NPs induced apoptosis of human lung epithelial cells A549. They observed that PS-NPs induced the significant up-regulation of pro-apoptotic proteins such as DR5, caspase-3, caspase-8, caspase-9 and cytochrome c, which revealed that PS-NPs triggered a TNF- α -associated apoptosis pathway [71].

At the end, we determined the percentage of viable cells after 24 incubations of PBMCs with polystyrene nanoparticles of different sizes, and we made an attempt to determine the lethal concentration (LC_{50}). Our research has shown that nanoparticles with a size of 29 and 44 nm cause a statistically significant decrease in viability from the concentration of 500 $\mu\text{g/mL}$ by 25% and 20%, respectively, while nanoparticles with a size of 72 nm cause a similar statistically significant decrease in viability only at the concentration of 1000 $\mu\text{g/mL}$. We also determined the LC_{50} for PBMCs under the influence of polystyrene nanoparticles of different sizes. LC_{50} for nanoparticles with a size of 29 nm was 957 $\mu\text{g/mL}$, while for nanoparticles with a size of 44 and 72 nm it was >1000 $\mu\text{g/mL}$ (Figure 5). Rubio et al. (2020) also investigated changes in the viability of three selected cell-lines after PS-NP exposure. The cells THP-1, TK6 and Raji-B were exposed for 24 and 48 h to a range of the concentrations of PS-NPs, up to 200 $\mu\text{g/mL}$. The authors observed only mild cytotoxic effects of studied particles at their highest tested concentration in two types of cells: TK6 and Raji-B [47].

Summing up, we found the pro-oxidative effect of the analyzed PS-NPs in human PBMCs. The effect was dependent on the diameter of the NPs, which may affect their different ability to enter the cells. The largest effects were shown for the smallest NPs, of 29 nm. A similar effect was observed by Xu et al. (2019), who incubated the human alveolar epithelial A549 cell line with NPs of 25 and 70 nm. The authors showed that smaller PS-NPs were rapidly internalized by the cell and caused greater changes in the tested parameters [71].

Due to the occurrence of oxidative, unfavorable processes caused by polystyrene nanoparticles, their accumulation in the tissues of mammals and humans may have negative long-term consequences, and requires further detailed research.

4. Materials and Methods

4.1. Biological Material

The study was conducted on peripheral blood mononuclear cells. Peripheral human blood mononuclear cells were collected from a leucocyte–buffy coat from the blood of healthy donors. Blood was collected by employees of Blood Bank in Lodz, Poland, from volunteering donors and then was subjected to laboratory diagnostics. PBMCs were isolated from the leucocyte–buffy coat separated from blood bought from the Regional Centre of Blood Donation and Blood Treatment in Lodz, Poland. Blood was collected from 25 healthy individuals (non-smoking donors with no known illness, aged 18–30).

Department of Biophysics of Environmental Pollution, University of Lodz, purchases blood for research based on the agreement of Blood Donation and Healing. Blood Bank in Lodz is accredited by Health Minister (No BA/2/2004) in the field of taking blood and separating its ingredients. The research was approved by the Bioethics Committee of the University of Lodz (Resolution No. 8/KBBN-UŁ/II/2019 (08.04.2019)).

4.2. Chemical Standards

Standards of PS-NPs (diameter: 29, 44 and 72 nm) were purchased from Polysciences Europe GmbH. PBS buffer was used to dissolve compounds. Fluorescent markers, i.e., 3'-(p-hydroxyphenyl)-fluorescein (HPF) to measure the level of the hydroxyl radical, 6-carboxy-2',7'-dichlorodihydro-fluorescein diacetate (H₂DCFDA-AM) used for ROS analysis, propidium iodide (PI) and calcein-AM for cell viability assessment and cis-parinaric acid were purchased from the company Molecular Probes (USA). FITC Annexin V Apoptosis Detection Kit (BD Pharmingen™) was purchased from BD Biosciences (USA). Lymphocyte separation medium (LSM) (1.077 g/cm) and RPMI 1640 medium were bought from Biotech. Potassium chloride (KCl), sodium chloride (NaCl), sodium hydrogen phosphate (Na₂HPO₄), potassium dihydrogen phosphate (KH₂PO₄), ammonium chloride (NH₄Cl), sodium hydrogen carbonate (NaHCO₃), ethylenediaminetetraacetic acid (EDTA) and other chemicals were purchased from Sigma.

4.3. Characterization of Polystyrene Nanoparticles

The average diameters of PS-NPs were measured by dynamic light scattering (DLS) using Zetasizer Nano-ZS (Malvern Instruments, Malvern, UK). Samples were measured at 25 °C in phosphate-buffered saline (PBS), pH 7.4, in plastic cuvettes. The analysis was made using the Malvern Instruments software. The refraction factor for PBS was assumed to be 1.50. Detection wavelength was 633 nm, and detection angle was 90°.

4.4. Obtaining Leucocytes

The buffy coat was centrifuged (3000 rpm, 10 min, at 20 °C) to remove plasma. Then, the lymphocyte layer was harvested. PBMCs were isolated using LSM, a mixture of Ficoll® and sodium diatrizoate (Hypaque) (density 1.077 g/mL) by centrifugation at 600 × g for 30 min at 20 °C. After centrifugation, PBMCs were harvested and resuspended in 3 mL of red blood cell lysis buffer and incubated for 5 min at 20 °C, then PBS was added, followed by centrifugation at 200 × g for 15 min at 20 °C. The supernatant was collected and cells deposited on the bottom of the tube were washed with RPMI medium containing L-glutamine and 10% fetal bovine serum and subjected to another centrifugation at 200 × g for 15 min. The final density of cells used for the study was 1 × 10⁶ cells/mL [72].

4.5. Determination of Reactive Oxygen Species Levels

Changes in the level of reactive oxygen species formed were assessed based on the analysis of the oxidation of 5'-carboxy-2',7'-dichlorodihydrofluorescein diacetate. This marker is nonpolar and therefore it can enter a cell. While penetrating the cell membrane, it is cleaved by membrane esterase to a nonfluorescent compound dichlorodihydrofluorescein, which under the influence of ROS is oxidized to 2',7'-dichlorofluorescein (DCF), emitting green fluorescence. After 24 h of incubation of PBMCs with a suspension of polystyrene nanoparticles, the samples were centrifuged (3000 rpm, 10 min, at 4 °C) and suspended in PBS and the marker was added to the final concentration of 2.5 μM. The mixture was incubated for 15 min in the dark at 37 °C. ROS level analysis was performed with the flow cytometer (LSR® II from Becton-Dickinson, San Jose, CA, USA) at an excitation wavelength of 490 nm and an emission of 530 nm for a total number of 10,000 counts [73].

4.6. Determination of Hydroxyl Radical Level

The principle of the analysis of the level of hydroxyl radical is the oxidation of the 3'-(p-hydroxyphenyl)-fluorescein probe as a result of the interaction with highly reactive

oxygen species (mainly hydroxyl radicals). The reaction produces fluorescein that emits green fluorescence at the wavelength of 515 nm [74]. After 24 h of incubation of PBMCs with a suspension of polystyrene nanoparticles, samples were centrifuged (3000 rpm, 4 °C) and were suspended in PBS, and the marker was added to the final concentration of 2 µM. Prepared samples were then incubated for 15 min at 37 °C in the dark. The flow cytometer (LSR[®] II from Becton-Dickinson, San Jose, CA, USA) was used for a total number of 10,000 events.

4.7. Lipid Peroxidation

Lipid peroxidation was analyzed by measuring the fluorescence of cis-parinaric acid at an excitation of 320 nm and emission of 432 nm. In the first step, cis-parinaric acid was added to the suspension of lymphocytes, to obtain the final concentration of 5 µM in sample, and incubated for 1 h at 37 °C in the dark, which allowed incorporation of the acid into the cell membrane [75]. After 24 h of incubation of PBMCs with a suspension of polystyrene nanoparticles, samples were centrifuged (3000 rpm, 4 °C) and were suspended in PBS, and the marker was added to the final concentration of 2 µM. Samples were centrifuged (600× g, 10 min, at 4 °C) to remove an excess of cis-parinaric acid. Remaining cells were suspended in RPMI medium and subjected to another 24-h incubation with analyzed compounds. The above analysis was performed using a 96-well microplate reader (Cary Eclipse Fluorescence Spectrophotometer–Varian, Australia).

4.8. Protein Oxidation

Protein oxidation was assessed by measuring tryptophan fluorescence at an excitation of 295 nm and emission of 335 nm. Fluorescent properties of proteins result from the presence of aromatic amino acids in their structure, e.g., tryptophan [76]. A decrease in fluorescence of the analyzed samples resulted from oxidative damage of tryptophan, as well as damage of proteins in PBMCs membrane. After 24 h of incubation of PBMCs with a suspension of polystyrene nanoparticles, samples were centrifuged (3000 rpm, 4 °C) and were suspended in PBS, and the marker was added to the final concentration of 2 µM. Samples were centrifuged (600× g, 10 min, at 4 °C). Supernatant was discarded and lymphocytes were suspended in RPMI medium with L-glutamine. Protein damage analysis was performed in 96-well plates using the microplate reader (Cary Eclipse Fluorescence Spectrophotometer–Varian, Australia).

4.9. Detection of Apoptosis

The samples were incubated with a suspension of polystyrene nanoparticles in final concentrations ranging from 0.1 to 500 µg/mL for 24 h at 37 °C in total darkness. The test was carried out in accordance with the instructions of the manufacturer. The cells were stained with PI and fluorescein conjugated with Annexin V in Annexin-binding buffer for 15 min at room temperature in total darkness. The samples were analyzed by flow cytometry (LSR[®] II from Becton-Dickinson, San Jose, CA, USA) with excitation at 488 nm to visualize fluorescein and PI fluorescence at maxima of 525 and 617 nm, respectively [72].

4.10. Analysis of Cells Viability of PBMC

Cell viability analysis was performed with calcein-AM and propidium iodide. Calcein-AM is hydrolyzed to a hydrophilic, highly fluorescent calcein, which is retained inside living cells [77]. In living cells, calcein ester emits strong green fluorescent light at an excitation of 490 nm and an emission of 515 nm, which demonstrates its fluorescent properties that calcein itself does not have. PI, on the other hand, is a marker of dead cells with two positive charges. This dye enters dead cells and binds to DNA, emitting red fluorescent light, which can be excited by a wavelength of 535 nm and an emission of 617 nm. After 24 h of incubation of PBMCs with a suspension of polystyrene nanoparticles, samples were centrifuged (3000 rpm, 4 °C) and were suspended in PBS, and the marker was added to the final concentration of 2 µM. Samples were centrifuged (100× g, 10 min,

4 °C) and then the marker mix (PI and calcein-AM) was added. Finally, the samples were incubated in the dark for 15 min, transferred to ice, and their fluorescence was measured. The total number of counts per sample was 10,000. Cell viability analysis using the above stains was performed on the flow cytometer (LSR[®] II from Becton-Dickinson, San Jose, CA, USA).

4.11. Statistical Analysis

The assays were performed on blood from 5 donors (5 experiments were conducted), whereas for each donor, the experimental point was a mean value of at least 3 replications. The results are shown as mean \pm SD. Multiple comparisons among the group mean differences were analyzed by one-way analysis of variance (ANOVA) followed by Tukey's post-hoc test. Tukey test was used as a post-hoc test. When the p value was lower than 0.05, the differences were considered statistically significant (*). Statistical analysis was conducted using STATISTICA software ver.13 (StatSoft Inc., Tulsa, OK, USA).

5. Conclusions

This study for the first time illustrates the action of polystyrene nanoparticles on human PBMCs.

Polystyrene nanoparticles increased ROS levels, including hydroxyl radical, as well as induced the oxidation of lipids and proteins.

The pro-oxidative effects of PS-NPs resulted in an increase in apoptosis and decrease in PBMC viability.

Observed changes in PBMCs incubated with PS-NPs depended on their size. A comparison of the actions of PS-NPs showed that the smallest nanoparticles (29 nm) exhibited the strongest oxidative potential in PBMCs

Changes in the parameters studied occurred at very low PS-NPs concentrations (0.01 μ g/mL), which may potentially be found in the human body as a result of environmental exposure.

Author Contributions: Conceptualization, K.K.; methodology, K.K.; formal analysis, K.K.; project administration, P.S.; visualization, P.S.; wrote the manuscript, K.K., B.B. and P.S.; supervised project, B.B.; analysis in DLS, A.K. All authors have read and agreed to the published version of the manuscript.

Funding: This work was financed by a statutory research admitted by the Department of Biophysics of Environmental Pollution, University of Lodz (number B211000000191.01).

Institutional Review Board Statement: The investigation was approved by the Bioethics Committee of the University of Lodz (Resolution No. 8/KBBN-UŁ/II/2019 (08.04.2019)).

Informed Consent Statement: Leucocyte-buffy coat was purchased from Blood Bank in Lodz, Poland. All procedures related to blood donation were executed at the Regional Centre of Blood, Donation and Blood Treatment in Lodz, Poland. The blood donor recruitment was at the Centre, according to national legal procedures and European Union regulations (incl. the regulation (EU) 2016/679 of the European Parliament and of the Council of 27 April 2016 on the protection of natural persons regarding the processing of personal data and on the free movement of such data).

Data Availability Statement: Not applicable.

Conflicts of Interest: The authors declare no conflict of interest.

References

1. Plastics Europe. Plastics—The Facts. 2017. Available online: https://www.plasticseurope.org/application/files/5715/1717/4180/Plastics_the_facts_2017_FINAL_for_website_one_page.pdf (accessed on 25 March 2021).
2. Hesler, M.; Aengenheister, L.; Ellinger, B.; Drexel, R.; Straskraba, S.; Jost, C.; Wagner, S.; Meier, F.; von Briesen, H.; Buchel, C.; et al. Multi-endpoint toxicological assessment of polystyrene nano- and microparticles in different biological models in vitro. *Toxicol. Vitro* **2019**, *61*, 104610. [CrossRef]
3. Hu, M.; Palić, D. Micro- and nano-plastics activation of oxidative and inflammatory adverse outcome pathways. *Redox Biol.* **2020**, *37*, 1–16. [CrossRef]

4. Koelman, A.; Besseling, E.; Shim, W. Nanoplastics in the aquatic environment. Critical review. *Mar. Anthropol. Litter* **2015**, 325–340. [\[CrossRef\]](#)
5. Efimova, I.; Bagaeva, M.; Bagaev, A.; Kileso, A.; Chubarenko, I. Secondary microplastics generation in the sea swash zone with coarse bottom sediments: Laboratory experiments. *Front. Mar. Sci.* **2018**, 5, 1–15. [\[CrossRef\]](#)
6. Mason, S.A.; Garneau, D.; Sutton, R.; Chu, Y.; Ehmann, K.; Barnes, J.; Fink, P.; Papazissimos, D.; Rogers, D.L. Microplastic pollution is widely detected in US municipal wastewater treatment plant effluent. *Environ. Poll.* **2016**, 218, 1045–1054. [\[CrossRef\]](#)
7. Yooeun, C.; Dokyung, K.; Shin, W.K.; Youn-Joo, A. Trophic transfer and individual impact of Nano-sized polystyrene in a four-species freshwater food chain. *Sci. Rep.* **2018**, 8, 1–11.
8. Mattsson, K.; Hansson, L.; Cedervall, T. Nanoplastics in the aquatic environment. *Environ. Sci. Proc. Imp.* **2015**, 17, 1712–1721.
9. Kik, K.; Bukowska, B.; Sicińska, P. Polystyrene nanoparticles: Sources, occurrence in the environment, distribution in tissues, accumulation and toxicity to various organisms. *Environ. Pollut.* **2020**, 262, 114297. [\[CrossRef\]](#) [\[PubMed\]](#)
10. Farely, A.T.; Shaw, C.I. Polystyrene as Hazardous Household Waste. In *Household Hazardous Waste Management*; IntechOpen: London, UK, 2017; pp. 44–60. [\[CrossRef\]](#)
11. Eyles, J.; Alpar, H.; Field, W.; Lewis, D.; Keswick, M. The transfer of polystyrene microspheres from the gastrointestinal tract to the circulation after oral administration in the rat. *J. Pharm. Pharmacol.* **1995**, 47, 561–565. [\[CrossRef\]](#) [\[PubMed\]](#)
12. Jani, P.; Halbert, G.; Langridge, J.; Florence, A. Nanoparticle uptake by the rat gastrointestinal mucosa: Quantification and particle size dependency. *J. Pharm. Pharmacol.* **1990**, 42, 821–826. [\[CrossRef\]](#) [\[PubMed\]](#)
13. Shang, L.; Nienhaus, K.; Nienhaus, U.G. Engineered nanoparticles interacting with cells: Size matters. *J. Nanobiotechnology* **2014**, 12, 1–11. [\[CrossRef\]](#)
14. Hussain, N.; Jaitley, V.; Florence, A. Recent advances in the understanding of uptake of microparticulates across the gastrointestinal lymphatics. *Adv. Drug Deliv. Rev.* **2001**, 23, 107–142. [\[CrossRef\]](#)
15. European Food Safety Authority (EFSA). Presence of microplastics and nanoplastics in food, with particular focus on seafood. *EFSA J.* **2016**, 14, 1–30.
16. Smith, M.; Love, C.D.; Rochman, M.C.; Neff, A.R. Microplastics in seafood and the implications for human health. *Curr. Environ. Health Rep.* **2018**, 5, 375–386. [\[CrossRef\]](#) [\[PubMed\]](#)
17. Wright, S.; Kelly, F. Plastic and human health: A micro issue? *Environ. Sci. Technol.* **2017**, 51, 6634–6647. [\[CrossRef\]](#) [\[PubMed\]](#)
18. Barboza, A.G.L.; Vethaak, D.A.; Lavorante, O.B.R.B.; Lundebye, K.; Guilhermino, L. Marine microplastics debris: An emerging issue for food security, food safety and human health. *Mar. Pollut. Bull.* **2018**, 133, 336–348. [\[CrossRef\]](#) [\[PubMed\]](#)
19. Barboza, A.G.L.; Vieira, R.L.; Branco, V.; Carvalho, C.; Guilhermino, L. Microplastics increase mercury bioconcentration in gills and bioaccumulation in the liver, and cause oxidative stress and damage in *Dicentrarchus labrax* juveniles. *Sci. Rep.* **2018**, 8, 15655. [\[CrossRef\]](#)
20. Betzer, O.; Shilo, M.; OPOCHINSKY, R.; Barnoy, E.; Motiei, M.; Okun, E.; Yadid, G.; Popovtzer, R. The effect of nanoparticle size on the ability to cross the blood-brain barrier: An in vivo study. *Nanomedicine* **2017**, 12, 1533–1546. [\[CrossRef\]](#)
21. Bouwmeester, H.; Hollman, H.C.P.; Peters, B.J.H. Potential health impact of environmentally released micro- and nanoplastics in the human food production chain: Experiences from nanotoxicology. *Environ. Sci. Technol.* **2015**, 49, 8932–8947. [\[CrossRef\]](#) [\[PubMed\]](#)
22. Wick, P.; Malek, A.; Manser, P.; Meili, D.; Maeder-Althaus, X.; Diener, L.; Diener, P.-A.; Zisch, A.; Krug, F.H.; von Mandach, U. Barrier capacity of human placenta for nanosized materials. *Environ. Health Perspect.* **2010**, 118, 432–436. [\[CrossRef\]](#)
23. Ragusa, A.; Svelato, A.; Santacroce, C.; Catalano, P.; Notarstefano, V.; Carnevali, O.; Papa, F.; Rongioletti, A.C.M.; Baiocco, F.; Draghi, S.; et al. Plasticenta: First evidence of microplastics in human placenta. *Environ. Int.* **2021**, 146, 106274.
24. Prata, J. Airborne microplastics: Consequences to human health? *Environ. Pollut.* **2018**, 234, 115–126. [\[CrossRef\]](#)
25. Mutti, A.; Buzio, C.; Perazzoli, F.; Bergamaschi, E.; Bocchi, M.C.; Selis, L.; Mineo, F.; Franchini, I. Lymphocyte subpopulations in workers exposed occupationally to styrene. *Med. Lav.* **1992**, 83, 167–177. [\[PubMed\]](#)
26. Thompson, J.; Quigley, J.; Halfpenny, N.; Scott, D.; Hawkins, N. Importance and methods of searching for E-publications ahead of print in systematic reviews. *Evid. Based Med.* **2016**, 21, 55–59. [\[CrossRef\]](#) [\[PubMed\]](#)
27. Lu, Y.; Zhang, Y.; Deng, Y.; Jiang, W.; Zhao, Y.; Geng, J.; Ding, L.; Ren, H.-Q. Uptake and accumulation of polystyrene microplastics in zebrafish (*Danio rerio*) and Toxic effects in the Liver. *Environ. Sci. Technol.* **2016**, 50, 4054–4060. [\[CrossRef\]](#) [\[PubMed\]](#)
28. Deng, Y.; Zhang, Y.; Lemos, B.; Ren, H. Tissue accumulation of microplastics in mice and biomarker responses suggest widespread health risks of exposure. *Sci. Rep.* **2017**, 7, 46687. [\[CrossRef\]](#) [\[PubMed\]](#)
29. Deng, Y.; Zhang, Y.; Qiao, R.; Bonilla, M.M.; Yang, X.; Ren, H.; Lemos, B. Evidence that microplastics aggravate the toxicity of organophosphorus flame retardants in mice (*Mus musculus*). *J. Hazard. Mater.* **2018**, 357, 348–354. [\[CrossRef\]](#)
30. Yang, Y.F.; Chen, C.Y.; Lu, T.H.; Liao, C.M. Toxicity-based toxicokinetic/toxicodynamic assessment for bioaccumulation of polystyrene microplastics in mice. *J. Hazard. Mater.* **2019**, 366, 703–713. [\[CrossRef\]](#)
31. Lin, W.; Jiang, R.; Hu, S.; Xiao, X.; Wu, J.; Wei, W.; Xiong, Y. Investigating the toxicities of different functionalized polystyrene nanoplastics on *Daphnia magna*. *Ecotoxicol. Environ. Saf.* **2019**, 180, 509–516. [\[CrossRef\]](#)
32. Gennari, A.; Ban, M.; Braun, A.; Casati, S.; Corsini, E.; Dastyk, J.; Descotes, J.; Hartung, T.; Hooghe-Peters, R.; House, R. The use of in vitro systems for evaluating immunotoxicity: The report and recommendations of an ECVAM workshop. *J. Immunotoxicol.* **2005**, 2, 61–83. [\[CrossRef\]](#)

33. Tulinska, J.; Kazimirova, A.; Kuricova, M.; Barancokova, M.; Liskova, A.; Neubauerova, E.; Drlickova, M.; Ciampor, F.; Vavra, I.; Bilanicova, D.; et al. Immunotoxicity and genotoxicity testing of PLGA-PEO nanoparticles in human blood cell model. *Nanotoxicology* **2015**, *9*, 33–43. [\[CrossRef\]](#)
34. Dusinska, M.; Tulinska, J.E.; Yamani, N.; Kuricova, M.; Liskova, A.; Rollerova, E.; Rundén-Pran, E.; Smolkova, B. Immunotoxicity, genotoxicity and epigenetic toxicity of nanomaterials: New strategies for toxicity testing? *Food Chem. Toxicol.* **2017**, *109*, 797–811. [\[CrossRef\]](#)
35. Galloway, T. Micro- and Nano-plastic and Human Health. In *Marine Anthropogenic Litter*; Bergmann, M., Gutow, L., Klages, M., Eds.; Springer: Berlin/Heidelberg, Germany, 2015; pp. 343–366.
36. Dayem, A.A.; Hossain, K.M.; Lee, B.S.; Kim, K.; Saha, K.S.; Yang, M.-G.; Choi, Y.H.; Cho, G.-S. The role of Reactive Oxygen species (ROS) in the biological activities of metallic nanoparticles. *Int. J. Mol. Sci.* **2017**, *18*, 120. [\[CrossRef\]](#)
37. Yin, L.; Liu, H.; Cui, H.; Chen, B.; Li, L.; Wu, F. Impacts of polystyrene microplastics on the behavior and metabolism in a marine demersal teleost, black rockfish (*Sebastes schlegelii*). *J. Hazard. Mater.* **2019**, *380*, 120861. [\[CrossRef\]](#)
38. He, Y.; Li, J.; Chen, J.; Miao, X.; Li, G.; He, Q.; Xu, H.; Li, H.; Wei, Y. Cytotoxic effects of polystyrene nanoplastics with different surface functionalization on human HepG2 cells. *Sci. Total Environ.* **2020**, *723*, 138180. [\[CrossRef\]](#)
39. Yousif, E.; Haddad, R. Photodegradation and photostabilization of polymers especially polystyrene: Review. *Springerplus* **2013**, *398*, 1–32. [\[CrossRef\]](#)
40. Liu, Z.; Li, Y.; Perez, E.; Jiang, Q.; Chen, Q.; Yang, J.; Huang, Y.; Yang, Y.; Zhao, Y. Polystyrene nanoplastic induces oxidative stress, immune defense, and glycometabolism change in *Daphnia pulex*: Application of transcriptome profiling in risk assessment of nanoplastics. *J. Hazard. Mater.* **2021**, *402*, 123778. [\[CrossRef\]](#)
41. Liu, Z.; Huang, Y.; Jiao, Y.; Chen, Q.; Wu, D.; Yu, P.; Li, Y.; Cai, M.; Zhao, Y. Polystyrene nanoplastic induces ROS production and affects the MAPK-HIF-1/NFkB-mediated antioxidant system in *Daphnia pulex*. *Aquat. Toxicol.* **2020**, *220*, 105420. [\[CrossRef\]](#) [\[PubMed\]](#)
42. Sun, X.; Chen, B.; Li, Q.; Liu, N.; Xia, B.; Zhu, L.; Qu, K. Toxicities of polystyrene nano- and microplastics toward marine bacterium *Halomonas alkaliphila*. *Sci. Total Environ.* **2018**, *642*, 1378–1385. [\[CrossRef\]](#) [\[PubMed\]](#)
43. Sarasamma, S.; Audira, G. Nanoplastics Cause Neurobehavioral Impairments, Reproductive and Oxidative Damages, and Biomarker Responses in *Zebrafish*: Throwing up Alarms of Wide Spread Health Risk of Exposure. *Int. J. Mol. Sci.* **2020**, *21*, 1410. [\[CrossRef\]](#) [\[PubMed\]](#)
44. Poma, A.; Vecchiotti, G.; Colafarina, S.; Zarivi, O.; Aloisi, M.; Arrizza, L.; Chichiricò, G.; Di Carlo, P. In vitro genotoxicity of polystyrene nanoparticles on the human fibroblast Hs27 cell line. *Nanomaterials* **2019**, *9*, 1299. [\[CrossRef\]](#)
45. Cortés, C.; Domenech, J.; Salazar, M.; Pastor, S.; Marcos, R.; Hernández, A. Nanoplastics as a potential environmental health factor: Effects of polystyrene nanoparticles on human intestinal epithelial Caco-2 cells. *Environ. Sci. Nano* **2020**, *7*, 272–285. [\[CrossRef\]](#)
46. Schirinzi, G.F.; Perez-Pomeda, I.; Sanchis, J.; Rossini, C.; Farre, M.; Barcelo, D. Cytotoxic effects of commonly used nanomaterials and microplastics on cerebral and epithelial human cells. *Environ. Res.* **2017**, *159*, 579–587. [\[CrossRef\]](#)
47. Rubio, L.; Barguill, I.; Domenech, J.; Marcos, R.; Hernández, A. Biological effects, including oxidative stress and genotoxic damage, of polystyrene nanoparticles in different human hematopoietic cell lines. *J. Hazard. Mater.* **2020**, *398*, 122900. [\[CrossRef\]](#)
48. Li, Z.; Feng, C.; Wu, Y.; Guo, X. Impacts of nanoplastics on bivalve: Fluorescence tracing of organ accumulation, oxidative stress and damage. *J. Hazard. Mater.* **2020**, *392*, 122418. [\[CrossRef\]](#) [\[PubMed\]](#)
49. Alomar, C.; Sureda, A.; Capo, X.; Guijarro, B.; Tejada, S.; Deudero, S. Microplastic ingestion by *Mullus surmuletus* Linnaeus, 1758 fish and its potential for causing oxidative stress. *Environ. Res.* **2017**, *159*, 135–142. [\[CrossRef\]](#) [\[PubMed\]](#)
50. Moor, A.C.E. Signaling pathways in cell death and survival after photodynamic therapy. *J. Photochem. Photobiol. B* **2000**, *57*, 1–13. [\[CrossRef\]](#)
51. Zheng, T.; Yuan, D.; Liu, C. Molecular toxicity of nanoplastics involving in oxidative stress and desoxyribonucleic acid damage. *J. Mol. Recognit.* **2019**, *32*, 1–7. [\[CrossRef\]](#) [\[PubMed\]](#)
52. Barboza, A.G.L.; Vieira, R.L.; Branco, V.; Figueiredo, N.; Carvalho, F.; Carvalho, C.; Guilhermino, L. Microplastics cause neurotoxicity, oxidative damage and energy-related changes and interact with the bioaccumulation of mercury in the European seabass, *Dicentrarchus labrax* (Linnaeus, 1758). *Aquat. Toxicol.* **2018**, *195*, 49–57. [\[CrossRef\]](#) [\[PubMed\]](#)
53. Ribeiro, F.; Garcia, R.A.; Pereira, P.B.; Fonseca, M.; Mestre, C.N.; Fonseca, G.T.; Ilharco, M.L.; Bebianno, J.M. Microplastics effects in *Scrobicularia plana*. *Mar. Pollut. Bull.* **2017**, *122*, 379–391. [\[CrossRef\]](#) [\[PubMed\]](#)
54. Wen, B.; Jin, R.S.; Chen, Z.Z.; Gao, Z.J.; Liu, N.Y.; Liu, H.J.; Feng, S.X. Single and combined effects of microplastics and cadmium on the cadmium accumulation, antioxidant defence and innate immunity of the discus fish (*Symphysodon aequifasciatus*). *Environ. Pollut.* **2018**, *243*, 462–471. [\[CrossRef\]](#) [\[PubMed\]](#)
55. Paul-Pont, I.; Lacroix, C.; Fernandez, G.C.; Hegaret, H.; Lambert, C.; Le Goïc, N.; Frere, L.; Cassone, L.-A.; Sussarellu, R.; Fabioux, C.; et al. Exposure of marine mussels *Mytilus* spp. to polystyrene microplastics: Toxicity and influence on fluoranthene bioaccumulation. *Environ. Pollut.* **2016**, *216*, 724–737. [\[CrossRef\]](#) [\[PubMed\]](#)
56. Nowis, D.; Legat, M.; Grzela, T.; Niderla, J.; Wilczek, E.; Wilczynski, G.M.; Glodkowska, E.; Mrowka, P.; Issat, T.; Dulak, J.; et al. Heme oxygenase-1 protects tumor cells against photodynamic therapy-mediated cytotoxicity. *Oncogene* **2006**, *25*, 3365–3374. [\[CrossRef\]](#)
57. Kulbacka, J.; Saczko, J.; Chwiłkowska, A. Stres oksydacyjny w procesach uszkodzenia komórek. *Pol. Merk. Lek.* **2009**, *44*, 1–4.
58. Levine, L.R.; Stadtman, R.E. Oxidative modification of proteins during aging. *Exp. Gerontol.* **2001**, *36*, 1495–1502. [\[CrossRef\]](#)

-
59. Zhang, W.; Xiao, S.; Ahn, U.D. Protein oxidation: Basic principles and implications for meat quality. *Crit. Rev. Food Sci. Nat.* **2013**, *53*, 1191–1201. [[CrossRef](#)]
60. Shacter, E. Quantification and significance of protein oxidation in biological Samales. *Drug Metab. Rev.* **2000**, *32*, 307–326. [[CrossRef](#)]
61. Hollóczki, O.; Gehrke, S. Nanoplastics can change the secondary structure of proteins. *Sci. Rep.* **2019**, *9*, 16013. [[CrossRef](#)]
62. Gopinath, M.P.; Saranya, V.; Vijayakumar, S.; Meera, M.M.; Ruprekha, S.; Kunal, R.; Pranay, A.; Thomas, J.; Mukherjee, A.; Chandrasekaran, N. Assessment on interactive prospectives of nanoplastics with plasma proteins and the toxicological impacts of virgin, coronated and environmentally released-nanoplastics. *Sci. Rep.* **2019**, *9*, 8860. [[CrossRef](#)] [[PubMed](#)]
63. Tan, Y.; Zhu, X.; Wu, D.; Song, E.; Song, Y. Compromised Autophagic Effect of Polystyrene Nanoplastics Mediated by protein corona was recovered after lysosomal degradation of corona. *Environ. Sci. Technol.* **2020**, *54*, 11485–11493. [[CrossRef](#)]
64. Davies, M.J. Singlet oxygen-mediated damage to proteins and its consequences. *Biochem. Biophys. Res. Commun.* **2003**, *305*, 761–770. [[CrossRef](#)]
65. Davies, M.J. The oxidative environment and protein damage. *Biochim. Biophys. Acta* **2005**, *1703*, 93–109. [[CrossRef](#)]
66. Gracanin, M.; Hawkins, L.C.; Pattison, I.D.; Davies, J.M. Singlet-oxygen-mediated amino acid and protein oxidation: Formation of tryptophan peroxides and decomposition products. *Free Radic. Biol. Med.* **2009**, *47*, 92–102. [[CrossRef](#)] [[PubMed](#)]
67. Thubagere, A.; Reinhard, B. Nanoparticle-induced apoptosis propagates through hydro-gen-peroxide-mediated bystander killing: Insights from a human intestinal epithelium in vitro model. *ACS Nano* **2010**, *4*, 3611–3622. [[CrossRef](#)] [[PubMed](#)]
68. Wang, F.; Bexiga, M.; Anguissola, S.; Boya, P.; Simpson, J.C.; Salvati, A.; Dawson, K.A. Time resolved study of cell death mechanisms induced by amine-modified polystyrene nanoparticles. *Nanoscale* **2013**, *5*, 10868–10876. [[CrossRef](#)] [[PubMed](#)]
69. Phuc, L.; Taniguchi, A. Polystyrene Nanoparticles Induce Apoptosis or Necrosis with or without Epidermal Growth Factor. *J. Nanosci. Nanotechnol.* **2019**, *19*, 4812–4817. [[CrossRef](#)] [[PubMed](#)]
70. Hu, Q.; Wang, H.; He, C.; Jin, Y.; Fu, Z. Polystyrene nanoparticles trigger the activation of p38 MAPK and apoptosis via inducing oxidative stress in zebrafish and macrophage cells. *Environ. Pollut.* **2021**, *269*, 116075. [[CrossRef](#)]
71. Xu, M.; Halimu, G.; Zhang, Q.; Song, Y.; Fu, X.; Li, Y.; Zhang, H. Internalization and toxicity: A preliminary study of effects of nanoplastic particles on human lung epithelial cell. *Sci. Total Environ.* **2019**, *1*, 133794. [[CrossRef](#)]
72. Sicińska, P. Di-n-butyl phthalate, butylbenzyl phthalate, and their metabolites exhibit different apoptotic potential in human peripheral blood mononuclear cells. *Food Chem. Toxicol.* **2019**, *133*, 110750. [[CrossRef](#)]
73. Sicińska, P.; Mokra, K.; Wozniak, K.; Michałowicz, J.; Bukowska, B. Genotoxic risk assessment and mechanism of DNA damage induced by phthalates and their metabolites in human peripheral blood mononuclear cells. *Sci. Rep.* **2021**, *11*, 1658. [[CrossRef](#)] [[PubMed](#)]
74. Setsukinai, K.I.; Urano, Y.; Katsuko, K.; Majima, H.; Nagano, T. Development of novel fluorescence probes that can reliably detect reactive oxygen species and distinguish specific species. *J. Biol. Chem.* **2002**, *278*, 3170–3175. [[CrossRef](#)] [[PubMed](#)]
75. Steenbergen, R.; Drummen, G.; den Kamp, J.O.; Post, J. The use of cis-parinaric acid to measure lipid peroxidation in cardiomyocytes during ischemia reperfusion. *Biochim. Biophys. Acta* **1997**, *1330*, 127–137. [[CrossRef](#)]
76. Vivian, J.T.; Callis, P.R. Mechanisms of tryptophan fluorescence shifts in 858 proteins. *Biophys. J.* **2001**, *80*, 2093–2109. [[CrossRef](#)]
77. Papadopoulos, G.N.; Dedoussis, V.G.; Spanakos, G.; Gritzapis, D.A.; Baxeavanis, N.C.; Papamichail, M. An improved fluorescence assay for the determination of lymphocyte-mediated cytotoxicity using flow cytometry. *J. Immunol. Methods* **1994**, *177*, 101–111. [[CrossRef](#)]



Polystyrene nanoparticles: the mechanism of their genotoxicity in human peripheral blood mononuclear cells

Kinga Malinowska, Bożena Bukowska, Ireneusz Piwoński, Marek Foksiński, Aneta Kisielewska, Ewelina Zarakowska, Daniel Gackowski & Paulina Sicińska

To cite this article: Kinga Malinowska, Bożena Bukowska, Ireneusz Piwoński, Marek Foksiński, Aneta Kisielewska, Ewelina Zarakowska, Daniel Gackowski & Paulina Sicińska (2022) Polystyrene nanoparticles: the mechanism of their genotoxicity in human peripheral blood mononuclear cells, *Nanotoxicology*, 16:6-8, 791-811, DOI: [10.1080/17435390.2022.2149360](https://doi.org/10.1080/17435390.2022.2149360)

To link to this article: <https://doi.org/10.1080/17435390.2022.2149360>



© 2022 The Author(s). Published by Informa UK Limited, trading as Taylor & Francis Group.



Published online: 25 Nov 2022.



[Submit your article to this journal](#)



Article views: 229



[View related articles](#)



[View Crossmark data](#)

ARTICLE



Polystyrene nanoparticles: the mechanism of their genotoxicity in human peripheral blood mononuclear cells

Kinga Malinowska^a, Bożena Bukowska^a, Ireneusz Piwoński^b, Marek Foksiński^c, Aneta Kisielewska^b, Ewelina Zarakowska^c, Daniel Gackowski^c and Paulina Sicińska^a

^aDepartment of Biophysics of Environmental Pollution, Faculty of Biology and Environmental Protection, University of Lodz, Lodz, Poland; ^bDepartment of Materials Technology and Chemistry, Faculty of Chemistry, University of Lodz, Lodz, Poland; ^cDepartment of Clinical Biochemistry, Faculty of Pharmacy, Collegium Medicum in Bydgoszcz, Nicolaus Copernicus University in Toruń, Bydgoszcz, Poland

ABSTRACT

Plastic nanoparticles are widely spread in the biosphere, but health risk associated with their effect on the human organism has not yet been assessed. The purpose of this study was to determine the genotoxic potential of non-functionalized polystyrene nanoparticles (PS-NPs) of different diameters of 29, 44, and 72 nm in human peripheral blood mononuclear cells (PBMCs) (*in vitro*). To select non-cytotoxic concentrations of tested PS-NPs, we analyzed metabolic activity of PBMCs incubated with these particles in concentrations ranging from 0.001 to 1000 µg/mL. Then, PS-NPs were used in concentrations from 0.0001 to 100 µg/mL and incubated with tested cells for 24 h. Physico-chemical properties of PS-NPs in media and suspension were analyzed using dynamic light scattering (DLS), atomic force microscopy (AFM), scanning electron microscopy (SEM) and zeta potential. For the first time, we investigated the mechanism of genotoxic action of PS-NPs based on detection of single/double DNA strand-breaks and 8-oxo-2'-deoxyguanosine (8-oxodG) formation, as well as determination of oxidative modification of purines and pyrimidines and repair efficiency of DNA damage. Obtained results have shown that PS-NPs caused a decrease in PBMCs metabolic activity, increased single/double-strand break formation, oxidized purines and pyrimidines and increased 8oxodG levels. The resulting damage was completely repaired in the case of the largest PS-NPs. It was also found that extent of genotoxic changes in PBMCs depended on the size of tested particles and their ζ -potential value.

ARTICLE HISTORY

Received 5 August 2022
Revised 14 November 2022
Accepted 15 November 2022

KEYWORDS

Polystyrene nanoparticles; peripheral blood mononuclear cells; DNA strand-breaks; 8-oxo-2'-deoxyguanosine; oxidation of purines; oxidation of pyrimidines

1. Introduction

Long-term exposure to certain chemicals can cause DNA damage. The most common types of DNA lesions are single strand breaks (SSBs), double strand breaks (DSBs), oxidative modification of DNA bases, and adducts formation (Christmann and Kaina 2013). They can be induced both by exogenous factors: UV radiation, ionization, and various types of chemicals, and endogenous factors, such as metabolic and replication stresses resulting in the formation of reactive oxygen species (ROS) (Felgentreff et al. 2021).

Nanoplastics (NPs) and microplastics (MPs) resulting from decomposition of large pieces of plastic are pollutants of global concern. Until recently, it has been considered that the diameter of plastic

NPs should not exceed 100 nm, although in the latest reports the diameter of 1000 nm has been assumed as the upper limit (Gigault et al. 2018; Rakowski and Grzelak 2020; Mitrano, Wick, and Nowack 2021). MPs are plastic particles up to 5 mm in diameter (Hartmann et al. 2019). In this work, we have adopted a traditional size of particles referring to NPs, which should not exceed a diameter of above 100 nm. Among the above-mentioned particles, polypropylene (PP) and polyethylene (PE) NPs are commonly found in the environment, while polystyrene nanoparticles (PS-NPs) are determined in smaller amounts. Polystyrene is produced by polymerization of styrene monomers and it is the fifth leading thermoplastic material on the global market. This polymer is widely used in the

CONTACT Kinga Malinowska ✉ kinga.malinowska@edu.uni.lodz.pl Department of Biophysics of Environmental Pollution, Faculty of Biology and Environmental Protection, University of Lodz, Pomorska 141/143 St., 90-236 Lodz, Poland

© 2022 The Author(s). Published by Informa UK Limited, trading as Taylor & Francis Group.

This is an Open Access article distributed under the terms of the Creative Commons Attribution-NonCommercial-NoDerivatives License (<http://creativecommons.org/licenses/by-nc-nd/4.0/>), which permits non-commercial re-use, distribution, and reproduction in any medium, provided the original work is properly cited, and is not altered, transformed, or built upon in any way. The terms on which this article has been published allow the posting of the Accepted Manuscript in a repository by the author(s) or with their consent.

production of food packaging, automotive industry, electronics, household appliances, and more (ChemicalSafetyFacts.org 2020). The key to understanding the potential toxicity of NPs is their physico-chemical properties, that is, size, shape, and surface charge. We used PS-NPs because they are commercially available in different size and well-characterized by their size, shape, and lack of functionalization to understand the principles of polymer chemistry. Additionally, using scanning electron microscopy (SEM), atomic force microscopy (AFM), and dynamic light scattering (DLS), we confirmed the size and shape of the tested particles. Additionally, we performed zeta potential measurements.

More and more studies on PS-NPs have focused on the assessment of their toxic effects to humans. This is a consequence of previous reports stating that they can penetrate into human organisms, translocate through biological barriers, enter cells environment (Xu et al. 2019; Z. Liu et al. 2021; Hwang et al. 2022) and interact with the cells of the immune system (including lymphocytes) (Rubio et al. 2020).

For this reason, PS-NPs as a model of non-functionalized particles with the smallest diameters (29, 44, and 72 nm) penetrating into the cells were selected for more detailed analyzes and evaluation of molecular mechanism of their genotoxic action.

As shown by numerous studies on animals, plastic particles (especially NPs) after penetrating organisms, may be accumulated in trace amounts in the spleen, liver, thymus, lungs, heart, reproductive organs, and the brain (European Food Safety Authority (EFSA) 2016; Prüst, Meijer, and Westerink 2020; Hwang et al. 2022). The main source of human exposure to plastic particles is consumption of contaminated food, primarily seafood (Hantoro et al. 2019; Toussaint et al. 2019). In addition, microplastics have also been detected in milk, honey, table salt, and mineral water (Auta, Emenike, and Fauziah 2017; Horton et al. 2017; Cox et al. 2019, Kutralam-Muniasamy et al. 2020). Campanale et al. (2020) proved that plastic particles with a diameter less than 2.5 μm can reach the gastrointestinal (GI) tract by ingestion and be internalized by the GI cells by endocytosis. Plastic particles with a diameter of 50–500 μm were found in feces, and their number was approximately 20 per 10 μg of feces. Thanks to this analysis, it was estimated that 90,000

of these particles are released in the feces annually (van Raamsdonk et al. 2020). Other studies have indicated the presence of 12 microplastics fragments ranging from 5 to 10 μm in diameter in women placentas (Ragusa et al. 2021).

Plastic particles also enter the human body through the respiratory system and, to a lesser extent, through the skin (Enyoh et al. 2020). Particles have also been shown to be adsorbed by the lung epithelium (Asgharian, Hofmann, and Miller 2001; Smith et al. 2002). Enaud et al. (2020) proved that particles, after getting into the circulatory system, showed immunological effect on the so-called gut–lung axis. It has been estimated that the daily human exposure to plastic particles ranges from 26 to 130 (Facciola et al. 2021). Recently, Leslie et al. (2022) showed the presence of plastic particles in human blood. Blood from 22 volunteers was tested, and the presence of particles was found in 17 of tested participants. The concentration of these xenobiotics reached as much as 12 $\mu\text{g}/\text{mL}$ of blood, while the concentration of the analyzed PS alone was 4.8 $\mu\text{g}/\text{mL}$. In this study on a small group of donors, the mean blood concentration of plastic particles was 1.6 $\mu\text{g}/\text{mL}$ (Leslie et al. 2022). However, a question arises here whether the presence of such high particle concentrations in the blood of people is an indisputable fact or an effect of contamination of the sample during collection and preparation, which has yet to be clarified. Under conditions of high exposure or high individual sensitivity, MPs can cause inflammatory changes resulting from their possible interaction with tissues. There are a small number of publications on the interaction of PS-NPs with leukocytes. Rubio et al. (2020) studied the effect of PS-NPs with a diameter of about 50 nm on the population of immune cells. They used three different human leukocyte lines for analysis, including Raji-B (B lymphocytes), TK6 (lymphoblasts), and THP-1 (monocytes). The study showed low toxicity, ROS production, and genotoxicity of NPs in Raji-B and TK6 cells with less uptake of NPs. No side effects were observed in monocytes, although uptake of the tested particles was higher in this cell type. In another study, mice were exposed to MPs with a diameter of 10–150 μm at concentrations of 20 and 200 $\mu\text{g}/\text{g}$ for 5 weeks. In tested animals, a decreased percentage of regulatory T cells and an increased percentage of Th17

cells in splenocytes were noted. In addition, there was a change in the level of inflammatory interleukin 1 α (IL1 α) and the granulocyte colony stimulating factor G-CSF (Li et al. 2020).

The results we have obtained so far, have shown that tested PS-NPs disturbed the redox balance, increased the total level of ROS and highly ROS (a hydroxyl radical), as well as induced lipid and protein oxidation in human PBMCs (Kik et al. 2021). Our recent study on the genotoxic potential of PS-NPs is justified considering the results obtained so far, which demonstrated an increase in ROS, in particular hydroxyl radical level, which may contribute to DNA damage.

The aim of this research was to determine the mechanism of interaction of plastic PS-NPs with human peripheral blood mononuclear cells (PBMCs). PBMCs due to large nucleus, and a key role playing in the immune system are very often used in the studies that evaluate genotoxic potential of various xenobiotics. Therefore, we assessed the effect of PS-NPs of different diameters (29, 44, and 72 nm) on DNA damage and repair in human PBMCs. Genotoxic damage can contribute to disorders of the immune system, which can lead to the development of cancer or autoimmune diseases (e.g. asthma, allergy; Farhat et al. 2011). In addition, PBMCs participate in the transport of xenobiotics that is why the analysis of the mechanism of interaction of PS-NPs with this cell type is fully justified (Santovito, Cervella, and Delpero 2014).

For this research, we used non-functionalized PS-NPs of different (small) diameters, which, as shown in previous studies, can enter the cells (Z. Liu et al. 2021) and are well-characterized in terms of their size and shape, in order to check whether these NPs can cause genotoxic effects. Our research can therefore be the starting point for further analyzes of environmentally relevant particles. In order to assess genotoxic potential of tested PS-NPs, we used mainly comet assay (single-cell gel electrophoresis) and chromatography (8-oxodG level). The cells were incubated with PS-NPs in concentrations ranging from 0.0001 to 100 $\mu\text{g/mL}$ for 24 h. Preliminary studies also assessed the effect of PS-NPs (0.0001–1000 $\mu\text{g/mL}$) on the metabolic activity of PBMCs after 24 h exposure in order to select their concentrations that do not alter cell viability, and consequently may be used in genotoxicity tests. A

range of PS-NPs concentrations was used, which corresponded (with the exception of 100 $\mu\text{g/mL}$) to plastic levels that were found in human blood (Leslie et al. 2022).

2. Materials and methods

2.1. Chemical standards

Standards of non-functionalized PS-NPs were purchased from Polysciences Europe GmbH. Restriction enzymes, that is, Endonuclease III (EndoIII) and DNA-formamidopyrimidine glycosidase (Fpg) were used for detection of oxidatively modified purines and pyrimidines, respectively (New England Biolabs). Nuclease P1 and Shrimp Alkaline Phosphatase (rSAP) were used to detect 8-OHdG and were purchased from New England Biolabs. 3-(4,5-dimethylthiazol-2-yl)-2,5 diphenyl-tetrazolium bromide (MTT), DMF, and sodium dodecyl sulfate (SDS) were used to assess the metabolic activity of PBMCs and were purchased in Sigma-Aldrich (St Louis, MA, USA) and (ROTH). Other reagents: Lymphocyte Separation Medium (1.077 g/mL) and RPMI medium 1640 were bought in Biowest and Biotech. Type I agarose and type XI agarose, EDTA, Triton, fetal bovine serum needed for the assessment of DNA damage were supplied from Sigma-Aldrich, USA. The remaining reagents, that is, NaCl, NaOH, TRIS, sodium acetate, and HEPES were purchased from POCh (Poland) and Roth (Germany).

2.2. Physico-chemical characterization of polystyrene nanoparticles

Taking into account recent reports indicating that in order to obtain comparable results, in-depth characterization of material (microplastics) is needed (Ramsperger et al. 2022), we decided to perform physico-chemical tests of PS-NPs. We took photos using AFM and SEM and assessed PS-NPs hydrodynamic size using the DLS technique. PS-NPs were diluted in water and in RPMI medium to study their size by DLS and zeta potential. Non-functionalized PS-NPs suspensions of various diameters were diluted in RPMI medium to study their biological effects, while tested NPs diluted in water were used to assess their physical properties by AFM and SEM.

Diluted water suspensions of PS-NPs were deposited on silicon wafers prior to AFM and SEM

imaging. A piece of silicon wafer was cleaned in ethanol and dried in a flow of pure air. Freshly cleaned wafers were placed vertically in a cuvette containing diluted water suspension of PS-NPs of given size and allowed to slowly evaporate for 2–3 days. Next, wafers with deposited NPs were withdrawn and dried in ambient conditions.

The AFM measurements were performed on Bruker Dimension Icon (Billerica, Massachusetts, USA) operating in tapping mode in ambient air. A non-contact Tespa V2 cantilever from Bruker operating at resonance frequency $\nu = 324$ kHz was used. Typical image size was $2\ \mu\text{m} \times 2\ \mu\text{m}$.

Field Emission Scanning Electron Microscopy (FE-SEM) imaging was carried out using a FEI NovaNano SEM 450 microscope (Hillsboro, OR, USA) equipped with a Schottky gun operating in immersion mode using a through lens detector (TLD) at 5 kV voltage. Typical magnification was $150,000\times$.

Dynamic Light Scattering (DLS) measurements - stability and hydrodynamic size of PS-NPs labeled as A (29 nm), B (44 nm), and C (72 nm) were performed using a DLS (Litesizer 500, Particle Analyzer, Anton Paar, Graz, Austria), equipped with a laser of wavelength of 658 nm as the light source and scattering angle $\theta = 173^\circ$. Samples in water were measured without filtering in a quartz cuvette at 25°C , while in RPMI at 37°C .

The zeta potentials of the PS-NPs ($c = 500\ \mu\text{g/mL}$) were measured using a Malvern Instruments Zetasizer Nano-ZS (Malvern Instruments Ltd., Malvern, UK). Samples in electric field were prepared in capillary cells (DTS1061). Measurement was carried out at 37°C in water and RPMI at pH 7.4 with 5 repetitions. The zeta potential value was calculated directly from the Helmholtz–Smoluchowski equation using Malvern software (Sze et al. 2003).

2.3. Biological material

Human peripheral blood mononuclear cells (PBMCs) were used for this study. PBMCs were isolated from the buffy coat purchased at the Regional Center for Blood Donation and Treatment in Lodz, Poland. The purchase of blood for research is possible thanks to the contract concluded between the Institute of Biophysics of Environmental Pollution, University of Lodz, and the aforementioned Blood Donation Center. Blood Bank employees receive a coat of

leukocytes and platelets through the preparation of whole blood from healthy, nonsmoking donors aged 18–30 years. The blood bank in Lodz is authorized to collect blood and separate its components based on the accreditation of the Minister of Health (No. BA/2/2004). The experiments described in this study were approved by the Bioethics Committee of University of Lodz (Resolution No. 8/KBBN-UŁ/II/2019 (08/04/2019)).

2.3.1. PBMCs isolation

The isolation of PBMCs took place in several stages. In the first stage, the buffy coat was centrifuged ($600\times g$, 10 min, 20°C), which allowed for the removal of plasma and collection of the resulting PBMCs layer. Further isolation was performed by centrifugation ($600\times g$, 30 min, 20°C) of the blood on a Lymphocyte Separation Medium with a density of $1.077\ \text{g/mL}$. After centrifugation, the resulting lymphocyte ring was collected, to which 3 mL of erythrocyte lysis buffer (150 mM NH_4Cl , 10 mM NaHCO_3 , 1 mM EDTA, pH 7.4) was added. The samples were incubated for 5 min at 20°C and supplemented with 6.5 mL of PBS. The cells were centrifuged again ($200\times g$, 15 min, 20°C). In the final step, the supernatant was collected, and the cells attached to the bottom of the tube were washed twice with RPMI medium containing L-glutamine and 10% fetal bovine serum. Then, centrifugation was performed ($200\times g$, 15 min, 20°C). The final PBMCs density used for the experiments was 5×10^4 cells/mL.

2.3.2. Isolation of DNA and determination of the 8-oxo-2'-deoxyguanosine (8-oxodG) in DNA isolates

The analyzes were performed using a method described earlier by Gackowski et al. (2016) and Starczak et al. (2021) with some modifications. DNA extraction and hydrolysis to deoxynucleosides: briefly, a pellet of frozen cells was dispersed in ice-cold buffer B, pH 8.0 containing Tris-HCl (10 mmol/L), Na_2EDTA (5 mmol/L), and deferoxamine mesylate (0.15 mmol/L). SDS solution was added (to a final concentration of 0.5%), and the mixture was gently mixed using a polypropylene Pasteur pipette. Samples were incubated at 37°C for 30 min. Proteinase K was added to a final concentration of 1 mg/mL and incubated at 37°C for 1 h. The mixture was cooled to 4°C , transferred to Phase Lock

Gel – Light tubes. The mixture of phenol, chloroform, and isoamyl alcohol (25:24:1) was added (1:1 v/v) and vortexed vigorously. After extraction, the aqueous phase was treated with a chloroform:isoamyl alcohol mixture (24:1). The supernatant was treated with two volumes of cold ethanol to precipitate high molecular weight nucleic acids. The precipitate was removed with a plastic spatula, washed with 70% (v/v) ethanol and dissolved in 50 μ L Milli-Q grade deionized water. The samples were mixed with 200 mM ammonium acetate containing 0.2 mM ZnCl_2 , pH 4.6 (1:1 v/v). Nuclease P1 (200 U, New England Biolabs, Ipswich, MA, USA) and tetrahydrouridine (10 μ g/sample) were added to the mixture and incubated at 37 °C for 1 h. Subsequently, 10% (v/v) NH_4OH and 6 U of shrimp alkaline phosphatase (rSAP, New England Biolabs, Ipswich, MA, USA) were added, and the samples were incubated for 1 h at 37 °C. Finally, all the hydrolysates were ultra-filtered prior to injection.

2.4. Biological properties of PS-NPs

2.4.1. Analysis of cell viability

The cytotoxic effect of the investigated PS-NPs was determined by a standard MTT method, based on the reduction of yellow 3-(4,5-dimethylthiazol-2-yl)-2,5 diphenyl-tetrazolium bromide (MTT) by cellular reductase, mainly mitochondria succinate dehydrogenase. The reduction of MTT to formazan is possible due to the NAD(P)H-dependent oxidoreductase enzymes that are present in living cells. Insoluble formazan crystals are dissolved in the solubilization buffer. The study was performed in a 96-well plate after 24 h of incubation of PS-NPs with PBMCs at a density of 1×10^5 cells/well. After this time, 20 μ L of MTT was added and the cells were incubated for 3–4 h. Then 100 μ L of 20% SDS and 50% DMF were added and the incubation was also carried out for 24 h. In the next step, the contents of the wells were poured into the sink and 100 μ L of DMSO was added per well. The absorbance was measured at 570 nm with a spectrophotometer.

2.4.2. Single cell gel electrophoresis (comet assay), as a technique for detecting single/double DNA strand breaks and their repair

Using this technique, the cells were immersed in low melting point agarose and placed on

microscopic slides coated with normal melting point agarose and then lysed. Slides were then dipped in the expanding buffer. Released DNA was submitted to 20 min electrophoresis in alkaline conditions in which 17 V and 32–115 A current were applied. In neutral conditions electrophoresis was carried out for 60 min at the 9 V and 98 A current. After electrophoresis, all slides were dried and stained with 40 μ L DAPI at 2 μ g/mL, centrifuged prior to use for 15 min at $219 \times g$ at 4 °C. A Zeiss Axio Scope. A1 fluorescence microscope (Carl Zeiss Microscopy GmbH, Germany) with an AxioCam MR microscope camera was used to observe the comets. DNA damage was viewed using the ZEN blue program, at $20 \times$ magnification. LUCIA Comet Assay v.7.60 (Laboratory Imaging, Prague, Czech Republic) software was used to count the comets. For each concentration, at least 50 comets were counted, so, for one donor the total number of comets was approx. 1000 (7 concentrations \times 50 comets \times 3 types of NPs). The mean value of DNA in the comet's tail was taken as the DNA damage index (Tail DNA%; Tice et al. 2000; Woźniak and Błasiak 2003).

2.4.3. Single and double DNA strand breaks measured by the alkaline and neutral versions of the comet test

The comet assay enables the identification of single/double DNA strand-breaks according to the procedure of Singh et al. (1988) and Singh and Stephens (1997) with some modifications (Klaude et al. 1996). After 24 h of exposure of PBMCs to PS-NPs, the samples were centrifuged at $112 \times g$ for 5 min at 4 °C. The cells were immersed in 0.75% low melting point (LMP) agarose and placed on microscopic slides coated with 0.5% normal melting point (NMP) agarose. The slides prepared in this way were placed in the lysis buffer (2.5 M NaCl, 0.1 M EDTA, 10 mM Tris, 1% Triton X-100, pH 10) for 1.5 h at 4 °C. After the lysis had been completed, the slides were rinsed 2–3 times with the expanding buffer (300 mM NaOH and 1 mM EDTA, pH > 13) and left in this buffer for 20 min. Then, fresh electrophoretic buffer (300 mM NaOH and 1 mM EDTA) was prepared and electrophoresis in alkaline conditions was performed for 20 min. For the detection of double-stranded lesions, the neutral version of the comet assay was applied, with a buffer consisting of 100 mM of TRIS and 300 mM of sodium

acetate, pH 9. The duration of electrophoresis in the neutral version was 60 min.

2.4.4. Oxidative modification of purines and pyrimidines

Modification of the comet assay using restriction enzymes, i.e. endonuclease III (EndoIII) and formamidopyrimidine DNA glycosylase (Fpg) allows for detection of oxidatively modified purines and pyrimidines, respectively. The course of the experiment after the 24-h incubation of the tested cells with NPs was the same as in section 2.4.1, up to cell lysis. After lysis, slides were washed several times with HEPES buffer (40 mM HEPES-KOH, 0.5 mM Na₂EDTA, 0.1 KCl, 0.2 mg/mL BSA, pH 9). Then, 50 µL of a buffer containing 1 U EndoIII or Fpg was applied to each slide. Slides were covered with coverslips and incubated at 37 °C for 30 min in a moist chamber. Finally, the coverslips used in the previous step were removed. The obtained results of DNA strand breaks formation and DNA base oxidation were expressed as percent of DNA in the comet tail versus the concentration of the individual tested substance. For this analysis, the alkaline version of the comet assay was used. Based on literature data, we decided to use 1 U of each enzyme per gel, which guaranteed their utilization in excess (therefore, the calibration curve was not prepared; Czarny et al. 2015).

2.4.5. Detection of 8-oxodG: 2D-UPLC-MS/MS analysis

DNA hydrolysates were spiked with an internal standard [¹⁵N₅]-8-oxo-2'-deoxyguanosine ([¹⁵N₅]-8-oxodG) at a volumetric ratio of 4:1 to a final concentration of 50 fmol/µL. Chromatographic separation was performed with a Waters ACQUITY 2D-UPLC system with a photodiode array detector for the first dimension of the 2D-chromatography (used for quantification of the unmodified deoxonucleosides) and a Xevo TQ-S tandem quadrupole mass spectrometer (used for the second dimension of the 2D-chromatography to analyze 8-oxodG). The at-column dilution technique was used between the first and second dimensions to improve the retention on the trap/transfer column. Separation was performed with a gradient elution for 10 min using a mobile phase of 0.05% acetate (A) and acetonitrile (B) (0.7–5% B for 5 min, column washing with 30%

acetonitrile and re-equilibration with 99% A for 3.6 min). The flow rate for the second dimension was 0.3 mL/min. The separation was performed with a gradient elution for 10 min using a mobile phase of 0.01% acetate (A) and methanol (B) (1–50% B for 4 min, isocratic flow of 50% B for 1.5 min, and re-equilibration with 99% A until the next injection). All samples were analyzed with three to five technical replicates, of which the technical mean was used for further calculation. Mass spectrometric detection was performed using a Waters Xevo TQ-S or TQ-XS tandem quadrupole mass spectrometer equipped with an electrospray ionization source. Collision-induced dissociation was obtained using argon 6.0 at 3×10^{-6} bar pressure as the collision gas. Transition patterns for all the analyzed compounds and the specific detector settings were determined using the MassLynx 4.1 IntelliStart feature set in a quantitative mode to ensure the best signal-to-noise ratio and a resolution of 1 at MS1 and 0.75 at MS2 (Gackowski et al. 2016).

2.4.6. DNA repair

RPMI 1640 medium with L-glutamine heated to 37 °C was added to cells exposed to PS-NPs for 24 h. DNA repair was assessed by the extent of residual DNA damage detection at each time point (0, 30, 60, 90, and 120 min) using the alkaline version of the comet assay. The samples were prepared as described above.

2.5. Statistical analysis

The Shapiro-Wilk test was used to verify the results for normality. In the next step, one-way analysis of variance (ANOVA) and Tuckey's post-hoc test were performed to assess the significance of differences between the means. Reproducibility of the results was obtained by carrying out tests in five replications (blood from five donors). From the results, average of at least three repetitions is drawn. Only for chromatographic analysis, the unpaired Student's *t* test (two-tailed) was used. The results are presented as mean ± SD. All tests were performed at the level of significance of the data $\alpha = 0.05$. Statistical analyzes were performed with the Statistica 13 software (StatSoft Inc., Tulsa, OK, USA).

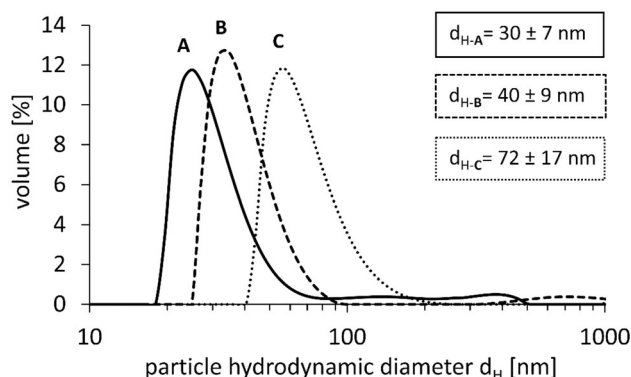


Figure 1. DLS size distribution by the volume of A, B, and C PS-NPs.

3. Results

3.1. Physico-chemical characterization of PS

In order to confirm the shape, size, and behavior of PS-NPs in a suspension and as-deposited on the substrate surface, two types of microscopy techniques, dynamic scattering physical method and analysis of zeta potential were used.

3.1.1. PS-NPs characterization by DLS

DLS measurements were performed to characterize the hydrodynamic diameter and size distribution of PS-NPs in water (Figure 1). The measurements in water revealed that PS-NPs formed stable suspensions, which exhibited homogenous size distribution. The hydrodynamic particle size in water (d_H) equaled to $d_{H-A} = 30 \pm 7$ nm, $d_{H-B} = 40 \pm 9$ nm, and $d_{H-C} = 72 \pm 17$ nm, and corresponded well to size of NPs provided by the manufacturer: 29, 44, and 72 nm, respectively.

We obtained different results when analyzing PS-NPs in the cellular medium containing albumin. The hydrodynamic particle size (d_H) in RPMI medium equaled to $d_{H-A} = 95 \pm 4$ nm, $d_{H-B} = 60 \pm 5$ nm, and $d_{H-C} = 63 \pm 5$ nm.

The agglomeration of PS-NPs would be visible in DLS measurements as additional peaks at larger dimensions (sizes). In our measurements in water and in buffer (Kik et al. 2021) such peaks were not visible and only signals from particles having defined size were visible indicating that PS-NPs did not form agglomerates in water.

Differently, agglomeration of PS-NPs in RPMI medium was observed, especially in the case of the smallest particles. For 26 nm PS-NPs, we observed 3

Table 1. The size of PS-NPs obtained by measurement with DLS, AFM, and SEM techniques.

PS NPs	(nm)	(nm)	(nm)
manufacturer	29	44	72
AFM	~ 24	~ 41	~ 72
SEM	26 ± 4	40 ± 5	70 ± 4
DLS in water	30 ± 7	40 ± 9	72 ± 17
DLS in RPMI	95 ± 4	60 ± 5	63 ± 5
Peak 1	179 ± 13	49 ± 3	61 ± 3
Peak 2	28 ± 2	1953 ± 3040	–
Peak 3	4576 ± 759	–	–

peaks and a diameter 3 times greater than declared by the manufacturer (Table 1).

3.1.2. PS-NPs characterization by AFM

AFM images of PS-NPs deposited on Si surface showing their morphology and approximated size are presented in Figure 2. It was found that PS-NPs were unevenly distributed over the Si surface. Most of them formed local close-packed agglomerates, due to the strong inter-particle and surface-particle attracting interactions. However, part of the particles were also visible as single objects. Estimated heights of selected PS-NPs (marked by blue lines in AFM images and presented as cross-sectional graphs) were: 24, 44, and 72 nm. AFM imaging revealed that the size of PS-NPs did not change much independently whether the measurement was performed on samples prepared as a deposit on the surface in the air or in a suspension by DLS. Moreover, obtained size was practically the same as a size of PS-NPs obtained in DLS technique in water.

3.1.3. PS-NPs characterization by SEM

Further analysis of PS-NPs deposited on Si wafer was performed with the use of FE-SEM. Figure 3 presents images of PS-NPs at magnifications of 150 k \times (left column) and PS-NPs size distribution (right column). It was found that PS-NPs form various flat nanostructures depending of their size. Small-size PS-NPs (29 nm) were visible mostly as separated single objects and as agglomerates exhibiting irregular shapes at low number. PS-NPs having medium size formed closely packed meander-like structures. Finally, the largest PS-NPs formed two-dimensional islands having the size of several microns built of closely inter-connected particles. The organization of these particles on the surface indicated for strong interactions of PS-NPs with a substrate but also between individual particles due to adhesive

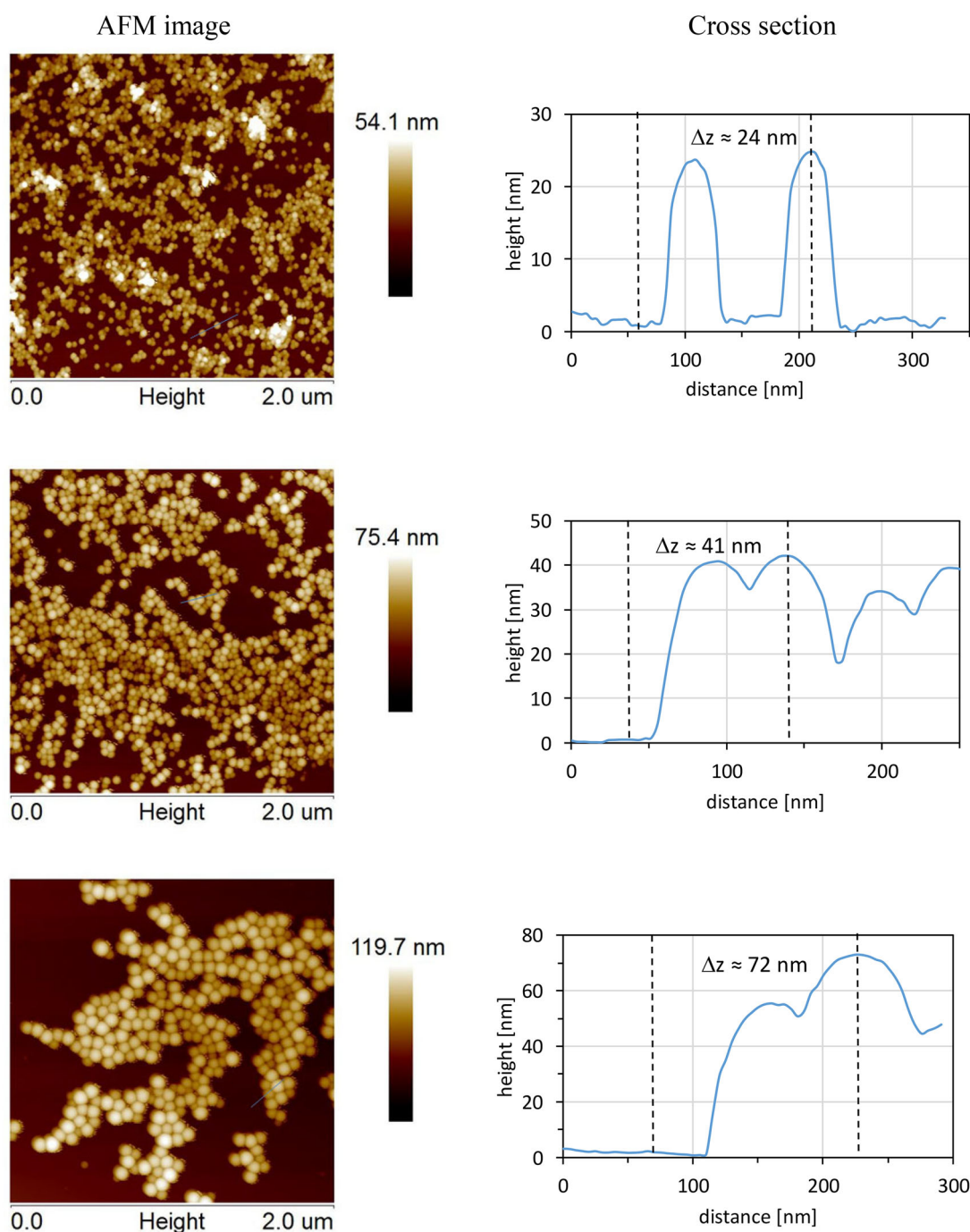


Figure 2. AFM images and corresponding cross-sectional profiles of selected PS-NPs.

interactions occurring during and after deposition. The average size distribution of PS-NPs from SEM images is presented on histograms and corresponds to the results obtained in DLS and AFM measurements. The size of NPs obtained by application of various techniques is gathered in Table 1.

3.1.4. Differences in particles' ζ -potentials

We measured the ζ -potentials at pH 7.4 of each particle type after their incubation in water and in

RPMI medium (Table 2). The incubation of all tested PS-NPs in RPMI medium showed a significant change in ζ -potential dependently on the particle size from -41 ± 3 mV (for the smallest particles of 29 nm) to -56 ± 2 mV (for the largest particles of 71 nm). In contrast, the absolute value of ζ -potential in the water slightly lowered with increasing diameter from -40 ± 1 mV (for the smallest particles of 29 nm) to -36 ± 1 mV (for the largest particles of 72 nm; Table 2).

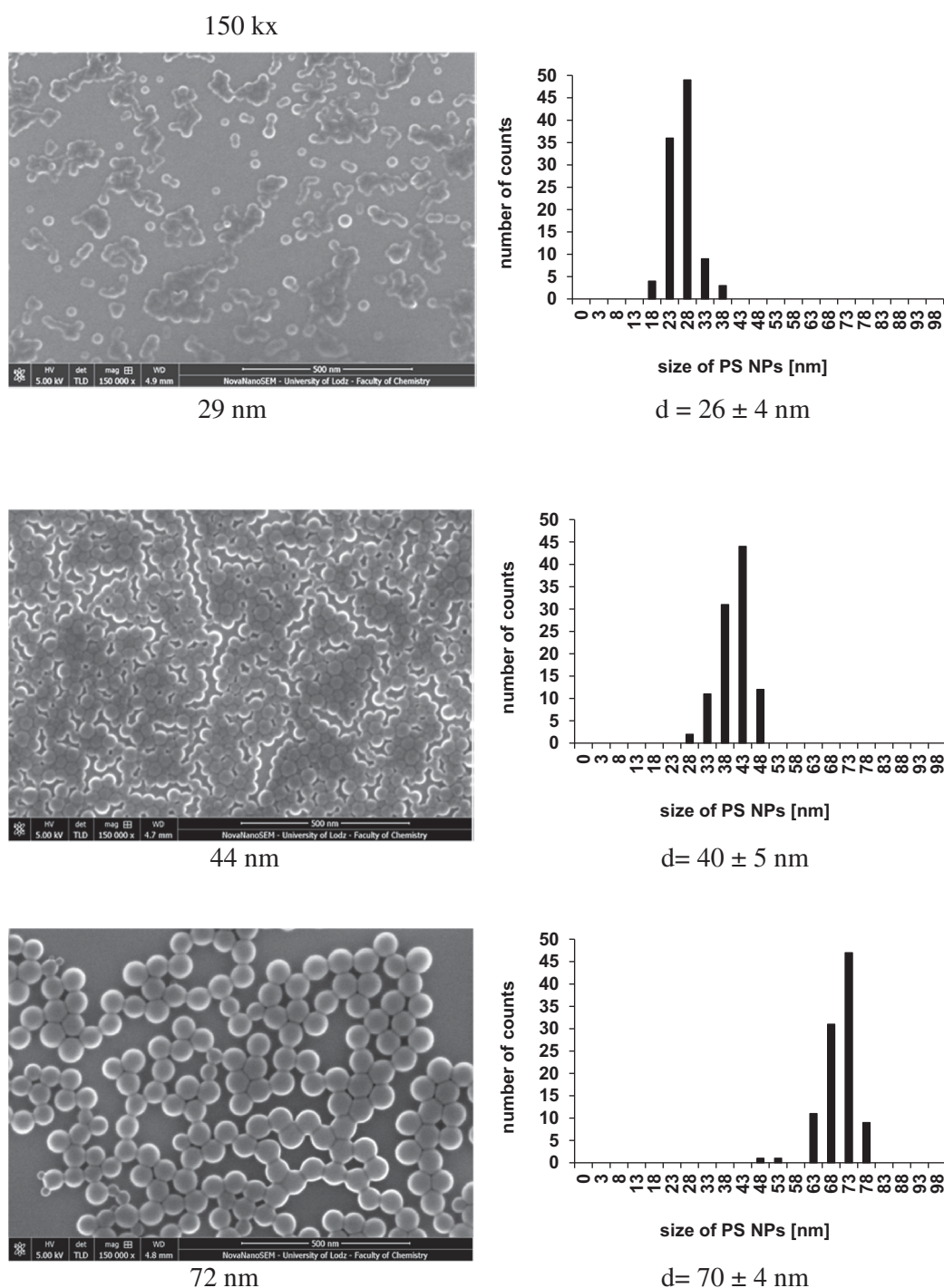


Figure 3. SEM images of nanostructures built of PS-NPs of different sizes (left column). PS-NPs size distribution (right column).

Table 2. The level of ζ -potential of PS-NPs in water and in cell medium (RPMI), pH 7.4.

PS NPs	(nm)	(nm)	(nm)
manufacturer	29	44	72
ζ -potential in water (mV)	-40 ± 1	-38 ± 1	-36 ± 1
ζ -potential in RPMI (mV)	-41 ± 3	-45 ± 2	-56 ± 2

3.2. MTT assay

Metabolic activity of PBMCs after 24-h exposure to PS-NPs was assessed by means of the tetrazole salt

reduction test (MTT test). The research showed a statistically significant decrease in metabolic activity for all tested particles. NPs with a diameter of 29 nm caused a decrease in the tested parameter from the concentration of 300 $\mu\text{g/mL}$, while NPs with a diameter of 44 and 72 nm from the concentration of 500 $\mu\text{g/mL}$ depleted the examined parameter (Figure 4). The IC_{50} concentration was determined (Figure 4). The IC_{50} concentration for

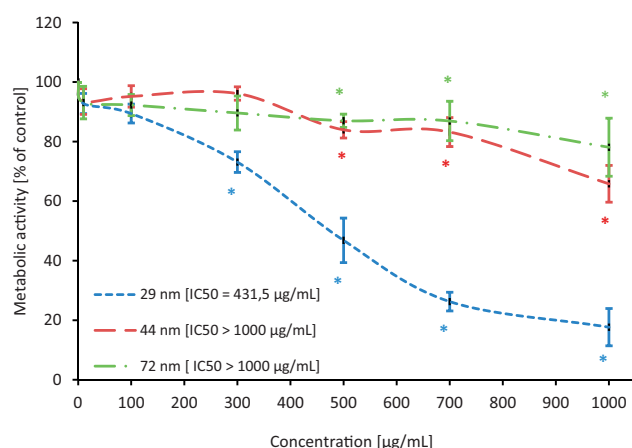


Figure 4. The level of metabolic activity of human PBMCs incubated with PS-NPs of 29, 44, and 72 nm in diameter in the range of concentrations of 10–1000 µg/mL for 24 h. Statistically significant changes for $p < 0.05^*$ ($n = 5$).

the smallest NPs was 431.5 µM, while for the 44 and 72 nm NPs it was over 1000 µM. Based on determined viability, PS-NPs at the concentrations that did not significantly change cell viability (≤ 100 µg/mL) were taken for further analysis.

3.3. Single and double DNA strand break: alkaline and neutral version of the comet assay

Formation of single (SSBs) and double DNA strand breaks (DSBs) was assessed in PBMCs incubated for 24 h with PS-NPs in concentrations ranging of 0.0001–100 µg/mL. All tested NPs caused DNA single/double-strand breaks formation. NPs with a diameter of 29 nm caused statistically significant changes in DNA integrity from the concentration of 0.01 µg/mL, while NPs with a diameter of 44 and 72 nm from the concentrations of 0.1 and 10 µg/mL caused DNA damage, respectively (Figure 5).

The level of DNA damage in tested cells (expressed as % of DNA in comet tail) after their exposure to the highest concentration (100 µg/mL) of PS-NPs was 23.15 ± 1.89 for 29 nm NPs, as well as 13.88 ± 2.43 and 6.93 ± 1.23 for 44 and 72 nm PS-NPs, respectively, as shown in Figure 6.

DSBs, which are one of the most destructive forms of DNA helix damage, were detected after exposure of PBMCs to the smallest NPs (29 nm) at 10 and 100 µg/mL (% of DNA in comet tail – 3.44 ± 0.93 and 8.22 ± 1.13 , respectively) and PS-NPs of intermediate size (44 nm) at 100 µg/mL (% of DNA in comet tail – 6.08 ± 0.66). No changes in

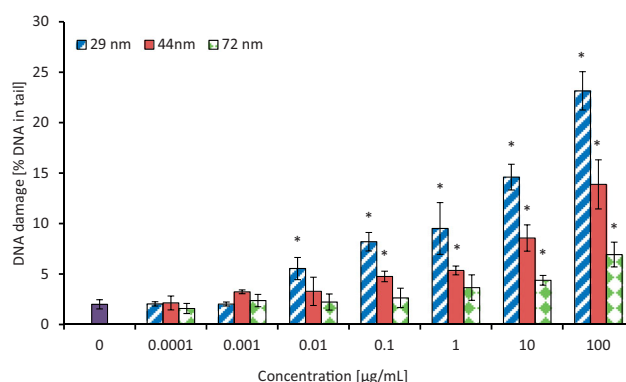


Figure 5. The level of DNA strand-breaks in human PBMCs incubated for 24 h with PS-NPs of 29, 44, and 72 nm in diameter in the range of concentrations of 0.0001–100 µg/mL. Statistically significant changes for $p < 0.05^*$ ($n = 5$).

double-stranded lesions were found after PBMCs treatment with NPs with a diameter of 72 nm (% of DNA in the tail – 3.74 ± 1.36 versus control cells – $1.91 \pm 0.54\%$; Figure 7). The comparison of the tested substances showed that PS-NPs with a diameter of 29 nm caused the highest level of DNA strand breaks formation in human PBMCs.

3.4. Oxidative modifications of purines and pyrimidines

Detection of oxidative DNA damage involving purines and pyrimidines oxidation was done after exposure of PBMCs to PS-NPs in concentrations range from 0.0001 to 100 µg/mL for 24 h. The cells were then treated with repair enzymes: endonuclease III (EndoIII) or formamidopyrimidine N-glycosylase (Fpg). The analysis of this parameter showed the formation of oxidized purine and pyrimidine bases in PBMCs after their treatment with tested PS-NPs with a higher level of oxidative damage detected by the inclusion of Fpg (Figures 8 and 9). A statistically significant increase in the level of purine oxidation occurred in PBMCs treated with the smallest NPs (29 nm) from the concentration of 0.01 µg/mL, while bigger particles (44 and 72 nm) increased this parameter from 10 and 100 µg/mL, respectively. After treatment of the cells with EndoIII, the increase in the level of pyrimidine oxidation occurred at higher PS-NPs concentrations in comparison to samples treated with Fpg. It was found that NPs of 29 nm increased pyrimidine oxidation from 10 µg/mL, while NPs of bigger sizes (44 and 72 nm) raised this parameter from 100 µg/mL.

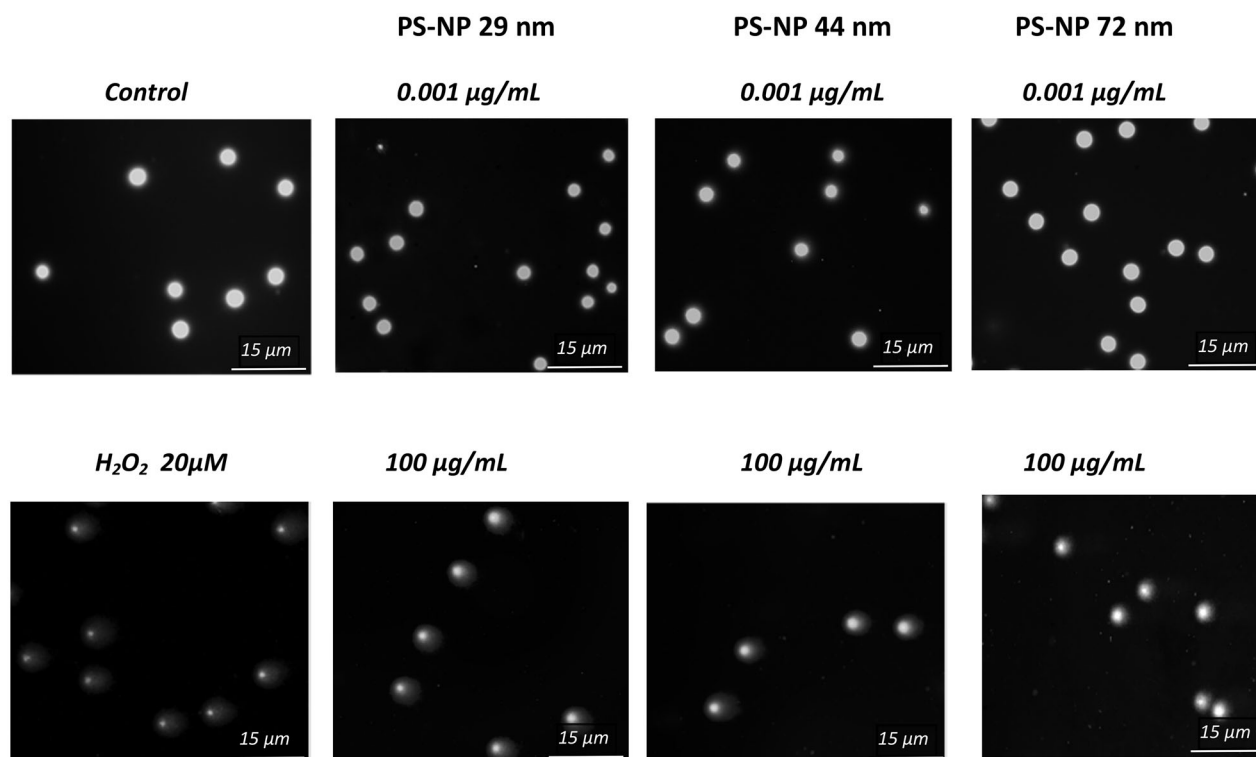


Figure 6. Selected photos showing the level of single and double strand-breaks (DNA in comet tail) in human PBMCs incubated for 24 h with PS-NPs of 29, 44, and 72 nm in diameter at two selected concentrations of 0.001 and 100 µg/mL versus the control. Photos were taken with a Zeiss Axio Scope. A1 fluorescence microscope.

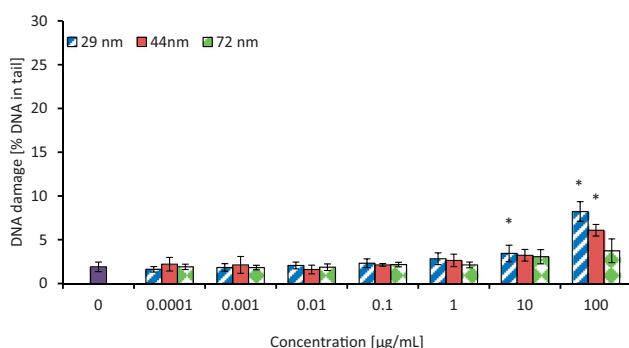


Figure 7. The level of DNA double strand-breaks in human PBMCs incubated for 24 h with PS-NPs of 29, 44, and 72 nm in diameter in the range of concentrations of 0.0001–100 µg/mL. Statistically significant changes for $p < 0.05^*$ ($n = 5$).

The presence of oxidized bases was expressed as % of DNA in the comet tail.

3.5. Detection of 8-oxodG

The most important DNA oxidation biomarkers are oxidized products of guanine and deoxyguanosine, which include 8-oxo-2'-deoxyguanosine (8-oxodG). To detect 8-oxodG, PBMCs were exposed to PS-NPs in concentration range from 0.0001 to 100 µg/mL

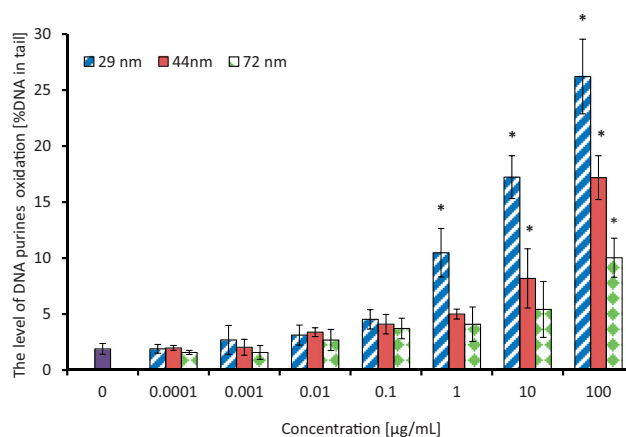


Figure 8. The level of DNA purines oxidation in human PBMCs (analysis by means of alkaline version of the comet assay with formamidopyrimidine-DNA glycosylase). The cells were incubated for 24 h with PS-NPs of 29, 44, and 72 nm in diameter in the range of concentrations of 0.0001–100 µg/mL. The value of comet tail (damaged DNA) in the presence of either enzyme for different concentrations of PS-NPs was reduced by the value obtained in comet assay without the enzyme (value for enzymatic buffer for the appropriate concentration of PS-NPs). Statistically significant changes for $p < 0.05^*$ ($n = 5$).

for 24 h. The cells were subsequently frozen. In the next stage, DNA isolation was performed, as described in the Section 2.1.2, and the tested

parameter was determined in the obtained DNA isolates. Two-dimensional (2D) liquid chromatography was used for the 8-oxodG analysis. Changes in the tested parameter were observed only after PBMCs exposure to the smallest size NPs. A statistically significant increase in 8-oxodG occurred from their concentration of 0.1 $\mu\text{g/mL}$ (Figure 10).

3.6. DNA repair

The time course of DNA damage repair kinetics of SSBs and DSBs was carried out after 24 h of the exposure of PBMCs to PS-NPs, which, after particles removal, were resuspended in heated RPMI 1640

medium with L-glutamine. The cells were post-incubated at 37 °C at selected time intervals (30, 60, 90, and 120 min). The resulting DNA damage caused by the largest NPs was completely repaired, and significant extent of DNA damage repair was observed in PBMCs treated with NPs with a diameter of 29 and 44 nm. A statistically significant decrease in DNA damage occurred in PBMCs treated with 29 and 44 nm NPs after 30 min of post-incubation, while in the case of 72 nm particles after 60 min of post-incubation (Figure 11).

DNA damage in PBMCs, amounting to 24.43% ($t = 0$ min) caused by the smallest NPs, decreased to 6.72% ($t = 120$ min), which showed that there was no complete DNA repair.

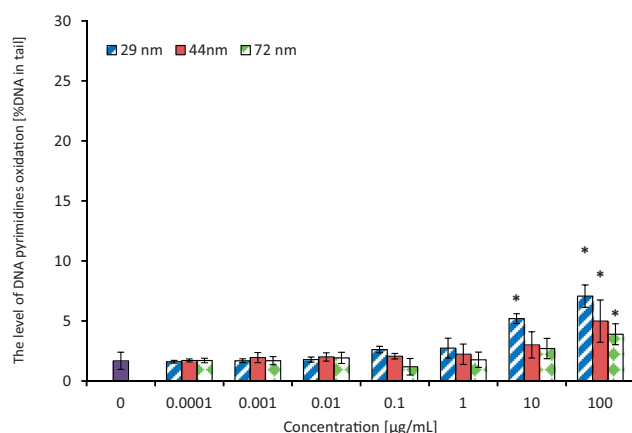


Figure 9. The level of DNA pyrimidines oxidation in human PBMCs (analysis by means of alkaline version of the comet assay with endonuclease III). PBMCs were incubated for 24 h with PS-NPs of 29, 44, and 72 nm in diameter in the range of concentrations of 0.0001–100 $\mu\text{g/mL}$. The value of comet tail (damaged DNA) in the presence of either enzyme for different concentrations of PS-NPs was reduced by the value obtained in comet assay without the enzyme (value for enzymatic buffer for the appropriate concentration of PS-NPs). Statistically significant changes for $p < 0.05^*$ ($n = 5$).

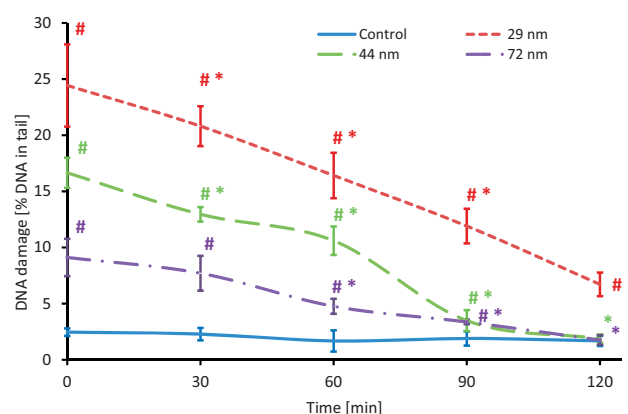


Figure 11. Time course of the repair kinetics of DNA damage (SSBs and DSBs), measured as DNA in comet tail of PBMCs treated for 24 h with PS-NPs of 29, 44, and 72 nm in diameter in the concentration of 100 $\mu\text{g/mL}$, and then post-incubated for 2 h in medium deprived of tested particles. (*) Statistically significant different from control ($p < 0.05$). (#) Statistically significant different from time "0" for individual PS-NPs size ($p < 0.05$). Each value represents the mean \pm SD ($n = 5$).

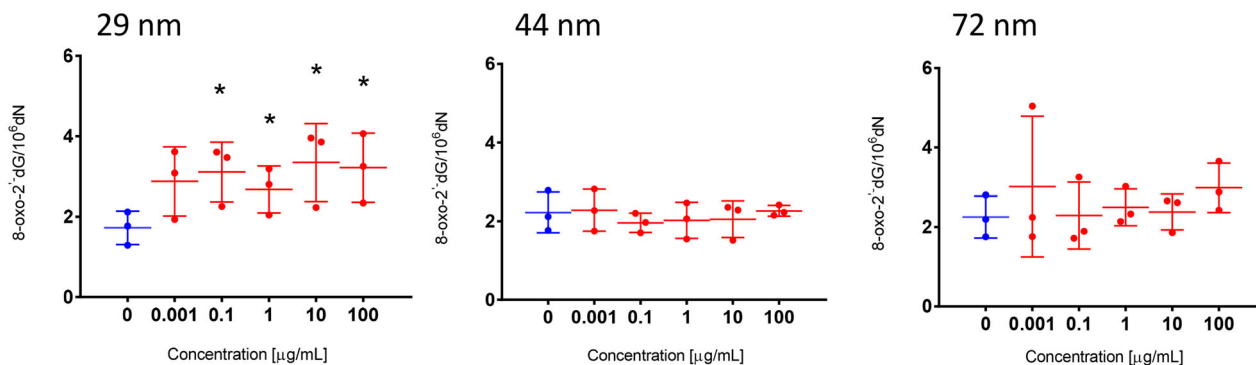


Figure 10. The level of 8-oxodG in human PBMCs. PBMCs were incubated for 24 h with PS-NPs of 29, 44, and 72 nm in diameter in the range of concentrations of 0.0001–100 $\mu\text{g/mL}$. Statistically significant changes for $p < 0.05^*$ ($n = 3$).

For particles with a diameter of 44 nm, DNA damage decreased from 16.65 ($t=0$ min) to 1.88% ($t=120$ min), which was comparable to damage level (2.45%) in control samples. Similarly, slight damage induced by 72 nm NPs was completely repaired: from 9.11 ($t=0$ min) to 1.75% ($t=120$ min).

4. Discussion

Environmental xenobiotics can cause genome instability as a result of significant chromosome rearrangements, such as polyploidy, aneuploidy, gene amplification, DNA strand breaks, and disruptions in repair of these breaks. In addition, they induce changes in genes that regulate cell growth and proliferation, and thus may lead to neoplastic transformations (Tubbs and Nussenzweig 2017; Alimba et al. 2021), therefore the mechanism of genotoxic action of PS-NPs on PBMCs appears to be key in assessing their toxicity.

Damage to human DNA leads to disturbances in numerous cellular processes, which may result in various disorders, including cancer development. The assessment of genotoxic potential of xenobiotics influencing human organisms is crucial for the evaluation of human safety. Some reports have shown carcinogenic effect of styrene, but there are no available data regarding its polymer derivative - polystyrene (Huff and Infante 2011). Animal studies on carcinogenic potential of styrene have provided conflicting results and limited evidence. There are several epidemiological studies suggesting a possible association between the exposure to styrene and an increased risk of leukemia and lymphoma in humans (Thompson et al. 2016). However, those pieces of evidence are not unequivocal, because of the simultaneous exposure of humans to numerous other chemicals, and insufficient data concerning their levels and exposure times.

There is no study that has assessed genotoxic mechanism of action of PS-NPs or other plastic NPs in any cell type. Therefore, we decided for the first time to determine genotoxic effect of non-functionalized PS-NPs of different diameters on human PBMCs, focusing on single and double strand-breaks formation, oxidative damage to purines and pyrimidines, and changes in 8-oxo-2'-deoxyguanosine level and repair capacity of the resulting DNA damage.

PS-NPs may accumulate in the human body and exert toxicity by inducing or enhancing an immune response. Chronic exposure is anticipated to be of greater concern due to the accumulative effects of PS-NPs action that could occur in the human body. This is expected to be dose-dependent, and a robust evidence base of exposure levels is currently lacking (Wright and Kelly 2017). The exposure of humans to plastic and PS (determined even in the placenta of women, Ragusa et al. 2021) and far insufficient data on the adverse effects of these substances, persuade us to conduct studies that assess toxic effects of PS-NPs on human blood cells and describe the underlying mechanisms of their action. PS particles are usually used as model substances in the studies of the effect of characteristic particle surfaces on various biological parameters, because they can be easily synthesized over a broad range of sizes. NPs are characterized by a higher surface in relation to their volume, which has an important effect on their reactivity (Xia et al. 2008).

Questions about the genotoxicity of plastic particles are constantly arising. Avio et al. (2015) suggest that MPs can induce genomic instability through DNA damage, such as DNA strand breaks and micronucleus formation or chromosomal aberrations. According to some scientific reports, MPs can cause DNA damage both through direct interactions with genetic material and indirect interactions, such as ROS or toxic ions formation. It was shown that exposure of NIH 3T3 cells to cationic functionalized PS-NPs caused changes during mitosis in their cell cycle, leading to an extension of the G0/G1 phase, which in turn led to DNA damage (Hu and Palić 2020). In other studies, increased chromosomal aberrations have been observed in plant root meristematic cells (Maity et al. 2020) and mammalian cell lines (Poma et al. 2019; Rubio et al. 2020). Alimba et al. (2021) proved that plastic particles could reduce gene transcription and increase DNA fragmentation. Recent studies by Sarma et al. (2022) showed a reduction in the mitotic index in PBMCs after exposure to PS-NPs at high concentrations (500, 1000, and 2000 $\mu\text{g/mL}$). They also observed a significant increase in micronucleus formation, percent of cytostasis, and a decrease in the nuclear division rate. This analysis showed that PS-NPs cytotoxicity was related to oxidative stress,

genotoxic activity, and genomic instability. Other studies have shown DNA damage in the blood cells of marine organisms, including *Scrobicularia plana* and *Mytilus galloprovincialis* after exposure to PS and polyethylene microparticles at 0.5, 5, and 50 µg/mL (Avio et al. 2015; Ribeiro et al. 2017).

The above reports provide evidence that MPs and NPs can directly or indirectly interact with DNA and cause damage to the genetic material in various organisms. So far, a lot of studies have been done on indirect mechanisms of NPs–DNA interaction, including PS-NPs, which have shown oxidative stress induction by generating intracellular ROS (mainly in animals) (Sun et al. 2018; Liu et al. 2020; L. Liu et al. 2021; Sarasamma et al. 2020; Horie and Tabei 2021). Similarly, our previous studies revealed that the exposure of PBMCs to PS-NPs increased ROS, including hydroxyl radical level and caused lipids and protein oxidation that could lead to loss of homeostasis, and consequently DNA damage (Kik et al. 2021). Verster and Bouwman (2018) proved that most of the studied lung tissues with neoplastic changes contained microplastics. Taking into account the above mentioned studies, which have shown the induction of ROS by PS-NPs, which are responsible for numerous DNA lesions, we decided to evaluate genotoxic properties of these substances.

An increase in ROS level, especially the hydroxyl radical, may result in the formation of an 8-oxo-2'-deoxyguanosine (8-oxodG) derivative. Therefore, using the 2D-UPLC-MS/MS analysis, we determined 8-oxodG formation in PBMCs exposed to PS-NPs. We observed 8-oxodG formation, but only under the influence of the smallest NPs with a diameter of 29 nm from the concentration of 0.1 µg/mL (Figure 10). 8-oxodG is considered to be the most sensitive and useful marker of DNA oxidative damage, which can be found in many tissues and fluids because it readily penetrates into the blood (Nemtsova et al. 2022). It is well-established that 8-oxodG is highly mutagenic; it mispairs with adenine during DNA replication and causes GC to AT conversion, which is the most frequent type of spontaneous mutation (Dizdaroglu et al. 2002; Ma et al. 2016). 8-oxodG is by far the most extensively studied change occurs as a consequence of oxidative DNA damage (Mangal et al. 2009). Sokmen et al. (2019) found that PS-NPs with a diameter of 20 nm were dispersed throughout the entire brain area of *Danio*

rerio. Moreover, in these fish species, 8-oxodG occurred in neuronal cells of the brain tissue.

It is known that there is a link between DNA strand breakage and DNA base modifications (Toyokuni and Sagripanti 1996). Therefore, we analyzed DNA single and double-strand breaks formation using the alkaline version of the comet assay, and exclusively double-strand breaks using the neutral version of this assay. For this purpose, we used PS-NPs in the concentrations range from 0.0001 to 100 µg/mL. We showed that 24 h of incubation of PBMCs with PS-NPs (29 nm) from the concentration of 0.01 µg/mL led to significant static increase in DNA damage (SSBs and DSBs formation) in the alkaline conditions. For PS-NPs with a diameter of 44 and 72 nm, the increase in this parameter was observed from their concentration of 0.1 and 10 µg/mL, respectively (Figure 5). On the other hand, using the neutral version of the comet assay, we observed an increase in the level of very undesirable DSBs in PBMCs exposed to the smallest NPs from their concentration of 10 µg/mL. These results correlated with the formation of 8-oxodG only in tests with PS-NPs with a diameter of 29 nm (Figure 7).

In the next stage of the study, we examined the level of oxidative damage to DNA purines and pyrimidines with modified comet assay using the enzymes Fpg and EndoIII. We showed much greater damage to purines than to pyrimidines caused by all tested NPs. The most profound changes were found in purines of PBMCs exposed to the smallest NPs, which also correlated with DSBs and 8-oxodG formation (Figures 8, 9).

DNA damage in human white blood cells, such as lymphocytes, monocytes, and polymorphonuclear cells after *ex vivo* exposure to various PS-NPs concentrations (0–100 µg/mL) was also observed by Ballesteros et al. (2020). They showed notable differences in the basal levels of DNA damage between various cells subpopulations. The highest level of DNA strand breaks measured with the alkaline version of the comet assay was observed in polymorphonuclear cells (% of tail DNA – 36.86 ± 9.94), while damage in monocytes and lymphocytes was 29.31 ± 9.39 % and 20.24 ± 3.61 %, respectively, after exposure to PS-NPs at their concentrations of <50 µg/mL. At the concentrations of

50 and 100 µg/mL, DNA breakage increased only in monocytes and polymorphonuclear cells.

Similarly, the analysis by Zheng, Yuan, and Chunguang (2019) showed DNA damage in rat liver cells (C57BL6-J) exposed to PS-NPs at 5 and 10 µM. Other researchers detected DNA damage in the Hs27 (human fibroblasts) cell line exposed to PS-NPs at 75 µg/mL using the cytokine block micronucleus (CBMN) assay (Poma et al. 2019). In turn, Vecchiotti et al. (2021) showed the formation of micronuclei in colorectal adenocarcinoma cells (HCT116) exposed to high concentrations (800 and 1200 µg/mL) of PS-NPs (100 nm), which indicated their low genotoxic potential. In addition, they observed formation of nuclear buds and protrusions of nucleoplasm. Other studies used white carp (*Ctenopharyngodon idella*), which was exposed to PS-NPs at 0.04, 34, and 34 µg/L for 20 days. The results showed DNA damage in red blood cells of studied fish (Guimarães et al. 2021). Subsequent studies conducted by Alaraby et al. (2022) revealed a significant increase in the level of DNA damage in *Drosophila* larvae exposed to PS particles at doses of 0.4 and 2 mg/g of food. They also showed that the exposure to NPs with a diameter of 50 nm induced a higher level of DNA damage than in the case of particles with a diameter of 200 and 500 nm. The above mentioned results are consistent with other studies by Gopinath et al. (2019), Shah et al. (2020), and Brandts et al. (2018) who showed that damage to the genetic material increased along with increasing doses of PS-NPs given to *Allium cepa*, *Ctenopharyngodon Idella*, and *Mytilus galloprovincialis*.

There are also studies showing the lack of genotoxic effect of plastic particles in various cell types. Studies by Cortés et al. (2020) showed no significant effect of micro and nano PS at concentrations range from 25 to 200 µg/mL on DNA integrity in Caco-2 intestinal cells. These studies were confirmed by Domenech et al. (2021) who did not notice any DNA damage in Caco-2 cells after long-term exposure to PS-NPs. Additionally, they used a modified version of the comet assay using the enzyme Fpg, which showed no tendency to increase oxidative DNA lesions. Similarly, Cole et al. (2020) did not observe DNA damage in mussels (*Mytilus* spp.) exposed to PS-NPs with a diameter of 50 nm at 500 ng/mL.

In the last step of our study, the repair of damaged DNA in PBMCs after incubation with tested NPs was assessed. It was found that damage caused by PS-NPs of 44 and 72 nm was effectively repaired within 2 h (Figure 11). In contrast, damage caused by the smallest NPs was not completely removed. Human DNA is constantly exposed to damage, which is why all living cells in the process of evolution developed various mechanisms of DNA repair, including base mismatch repair (MMR), base excision repair (BER), and nucleotide excision repair (NER). Repair by splitting non-homogeneous ends of DNA (NHEJ) and homologous recombination (HR) can also be distinguished (Carriere et al. 2017). Damage related to the presence of 8-oxodG is mostly repaired by the BER pathway. This modified DNA base is repaired by glycosylases, for example, OGG1 (Krokan, Standal, and Slupphaug 1997). The MMR pathway also plays an important role in the case of DNA damage caused by NPs. It can eliminate mutations caused by these particles, for example, repairs 8-oxodG formed as a result of guanine oxidation (Carriere et al. 2017). In the case of NER, DNA damage is repaired by the global genomic NER (GG-NER) and the NER is linked to transcription (Marteijn et al. 2014). DSBs can be repaired with NHEJ or HR, thanks to the presence of the p53 binding protein (Nakamura et al. 2006). NHEJ mechanism repairs double-stranded damage in a pathway dependent on POLµ and POLλ polymerases (Carriere et al. 2017).

In summary, tested PS-NPs caused SSBs and DSBs formation, induced oxidation of purines and pyrimidines and increased the level of 8-oxodG. The presence of the derivative 8-oxodG, and oxidation of purines and pyrimidines, as well as substantial ROS and hydroxyl radicals formation (Kik et al. 2021) indicate that radical mechanism is involved in the action of tested particles.

We have shown that among the non-functionalized PS-NPs, those with the smallest diameter exhibited the strongest genotoxicity, which was probably associated with their easiest penetration into tested cells, as reported by Xu et al. (2019), Z. Liu et al. (2021), and Hwang et al. (2022).

Xu et al. (2019) incubated the human alveolar epithelial A549 cell line with NPs in diameter of 25 and 70 nm and showed that smaller PS-NPs were rapidly internalized by these cells and caused

greater changes in examined parameters. Similarly, studies by Z. Liu et al. (2021) revealed that PS-NPs with a diameter of 50 and 500 nm entered the cells through active endocytosis due to hydrophobic interactions and van der Waals forces, as well as through passive penetration of the membrane resulting from the division of PS-NPs in the water-phospholipid system. It was proven that the smallest NPs (50 nm) were transported by RBL-2H3 cells (rat basophilic leukemia cells) *via* clathrin, caveolin, and macropinocytosis pathways, while larger particles (500 nm) were transported by macropinocytosis. Liu and coworkers also observed that PS-MPs with a size of 5000 nm were not adsorbed on the cell because of their too large size, which hindered their diffusion into the membrane surface. In addition, they showed that masses of the internalized PS50 inside the cells and the excreted PS50 outside the cells were both higher than the masses of PS500, indicating that the smaller particles more easily entered or leaved the cells than did their larger counterparts. According to the above mentioned study, the size of NPs may affect, among others on the kinetics and transport or the amount of particles that are taken up by the cells. Recently, Hwang et al. (2022) observed that PS-NPs of 50 nm, unlike 100 nm ones, circulated in the blood vessels and accumulated in the brains of zebrafish larvae.

The value of zeta potential is very significant in PS-NPs toxicity. Musyanovych et al. (2011) suggested that surface charge is very important for internalization particles by cells. They showed that PS-NPs with an anionic surfactant with a ζ -potential of -60 mV were internalized by HeLa cells more often than NPs stabilized with a nonionic surfactant having a ζ -potential of -5 mV. This was in agreement with the study of Ramsperger et al. (2022) who observed that PS microplastic particles (3 μ m) from Polysciences (P-MPP) with higher absolute value of negative potential zeta were more often covered by cellular membranes than PS microplastic particles (3 μ m) from Micromod (MMPP), and therefore internalized by J774A.1 and ImKC macrophages. Additionally, it has been proven that particles showing a higher absolute value of negative ζ -potential induced a more significant metabolic response in a sensitive cell line and more strongly altered cell proliferation, especially at their higher concentrations.

These observations do not agree with our results, which indicate that if the particles are made of the same polymer, non-functionalized, but differ only in size, the effect is the opposite depending on the absolute value of the negative zeta potential. Increasing size of tested PS-NPs was correlated with increasing absolute value of negative zeta potential in RPMI medium, but it was not associated with higher particle cytotoxicity and genotoxicity (even weakened them). The smallest tested nanoparticles (26 nm), showed the strongest cytotoxicity and genotoxicity and had the lowest absolute value of negative zeta potential (-40.86 ± 2.77 mV), while the largest particles had the highest absolute value of negative zeta potential (-56 ± 2 mV) and exhibited the lowest cytotoxicity and genotoxicity. We observed an increase in absolute value of negative zeta potential of tested PS-NPs diluted in RPMI medium compared to those suspended in water. Probably, the observed changes in ζ -potential recorded after incubation of the particles in cell culture media may indicate on the formation of a protein corona (Partikel et al. 2019). Protein corona increases the diameter of the particle, but also changes the composition of the surface of the nanoparticles, and these changes affect biodistribution, efficacy, and toxicity of these substances (Breznica, Koliqi, and Daka 2020). The obtained diameter measured by DLS for the smallest particles (26 nm) in RPMI medium containing albumin was three times greater than that measured in water and declared by the manufacturer. The diameter of the largest 72 nm particles, measured by DLS, was the closest to that obtained in water, as well as declared by the manufacturer. Also, Gopinath et al. (2019) showed that coronated-NPs with increased protein conformational changes caused higher genotoxic and cytotoxic effects in human blood cells than the virgin-NPs.

Summing up, we observed genotoxic changes in PBMCs incubated with PS-NPs (probably present in human organisms), which may raise concerns about the health of humans exposed to these substances. On the other hand, obtained data showed that tested PS-NPs caused mainly SSBs formation. Moreover, DNA damage, which was the most strongly induced by the smallest PS-NPs was repaired to a large extent, while DNA damage

caused by tested NPs with a diameter of 44 and 72 nm was totally removed.

5. Conclusion

Non-functionalized PS-NPs induced SSBs and DSBs formation in PBMCs, caused oxidation of purines and pyrimidines and increased the level of 8-oxodG. The formation of the derivative 8-oxodG and oxidation of purines and pyrimidines indicate the radical mechanism of action of the tested PS-NPs. We have observed that PS-NPs with the smallest diameter and the lowest absolute value of negative zeta potentials exhibited the strongest cytotoxicity and genotoxicity, which was probably associated with their easiest penetration into tested cells.

Acknowledgment

The authors are thankful to Katarzyna Miłowska (Department of General Biophysics) that performed the measurements ζ -potential of the PS-NP using a Malvern Instruments Zetasizer Nano-ZS.

Author contributions

K.M., B.B. and P.S. planned the experiments. K.M., P.S., E.Z., D.G., M.F., I.P. and A.K. carried out the experimental part; K.M.; B.B., P.S., E.Z., D.G., M.F., I.P. and A.K. analyzed the data; K.M., and P.S. carried out the statistical analysis, K.M., P.S. and I.P., prepared tables/figures/photos; K.M.; B.B., P.S., M.F., I.P. wrote the final manuscript.

Disclosure Statement

No potential conflict of interest was reported by the author(s).

Funding

The research was conducted within the framework of National Science Center, Poland, Project No. 2021/41/N/NZ7/02049.

References

- Alaraby, M., D. Abass, J. Domenech, A. Hernández, and R. Marcos. 2022. "Hazard Assessment of Ingested Polystyrene Nanoplastics in *Drosophila Larvae*." *Environmental Science: Nano* 9 (5): 1845–1857. doi:10.1039/D1EN01199E
- Alimba, G. C., C. Faggio, S. Sivanesan, L. A. Ogunkanmi, and K. Krishnamurthi. 2021. "Micro(Nano)-Plastics in the Environment and Risk of Carcinogenesis: Insight into Possible Mechanisms." *Journal of Hazardous Materials*. 416 (7): 126143. doi:10.1016/j.jhazmat.2021.126143
- Asgharian, B., W. Hofmann, and F. J. Miller. 2001. "Mucociliary Clearance of Insoluble Particles from the Tracheobronchial Airways of the Human Lung." *Journal of Aerosol Science* 32 (6): 817–832. doi:10.1016/S0021-8502(00)00121-X
- Auta, H., Emenike, C, and Fauziah, S. 2017. "Distribution and Importance of Microplastics in the Marine Environment: A Review of the Sources, Fate, Effects, and Potential Solution." *Environment International* 102: 165–176. doi:10.1016/j.envint.2017.02.013
- Avio, C. G., S. Gorbi, M. Milan, M. Benedetti, D. Fattorini, G. d'Errico, M. Pauletto, L. Bargelloni, and F. Regoli. 2015. "Pollutants Bioavailability and Toxicological Risk from Microplastics to Marine Mussels." *Environmental Pollution (Barking, Essex : 1987)* 198: 211–222. doi:10.1016/j.envpol.2014.12.021
- Ballesteros, S., J. Domenech, I. Barguilla, C. Cortés, R. Marcos, and A. Hernández. 2020. "Genotoxic and Immunomodulatory Effects in Human White Blood Cells after ex Vivo Exposure to Polystyrene Nanoplastics." *Environmental Science: Nano* 7 (11): 3431–3446. doi:10.1039/D0EN00748J
- Brandts, I., M. Teles, A. P. Gonçalves, A. Barreto, L. Franco-Martinez, A. Tvarijonaviciute, M. A. Martins, A. M. V. M. Soares, L. Tort, and M. Oliveira. 2018. "Effects of Nanoplastics on *Mytilus Galloprovincialis* after Individual and Combined Exposure with Carbamazepine." *The Science of the Total Environment* 643 (643): 775–784. doi:10.1016/j.scitotenv.2018.06.257
- Breznica, P., R. Koliqi, and A. Daka. 2020. "A Review of the Current Understanding of Nanoparticles Protein Corona Composition." *Medicine and Pharmacy Reports* 93 (4): 342–350.
- Campanale, C., C. Massarelli, I. Savino, V. Locaputo, and V. F. Uricchio. 2020. "A Detailed Review Study on Potential Effects of Microplastics and Additives of Concern on Human Health." *International Journal of Environmental Research and Public Health* 17 (4): 1212. doi:10.3390/ijerph17041212
- Carriere, M., S. Sauvaigo, T. Douki, and J.-L. Ravanat. 2017. "Impact of Nanoparticles on DNA Repair Processes: current Knowledge and Working Hypotheses." *Mutagenesis* 32 (1): 203–213. doi:10.1093/mutage/gew052
- ChemicalSafetyFacts.org. 2020. [Accessed 3 Aug 2022]. <https://www.chemicalsafetyfacts.org/polystyrene/>
- Christmann, M, and B. Kaina. 2013. "Transcriptional Regulation of Human DNA Repair Genes following Genotoxic Stress: trigger Mechanisms, Inducible Responses and Genotoxic Adaptation." *Journal of Biological Chemistry* 283: 1–5.
- Cole, M., C. Liddle, G. Consolandi, C. Drago, C. Hird, P. K. Lindeque, and T. S. Galloway. 2020. "Microplastics, Microfibres and Nanoplastics Cause Variable Sub-Lethal Responses in Mussels (*Mytilus Spp.*)." *Marine Pollution Bulletin* 160: 111552. doi:10.1016/j.marpolbul.2020.111552

- Cortés, C., J. Domenech, M. Salazar, S. Pastor, R. Marcos, and A. Hernandez. 2020. "Nanoplastics as a Potential Environmental Health Factor: Effects of Polystyrene Nanoparticles on Human Intestinal Epithelial Caco-2 Cells." *Environmental Science: Nano* 7 (1): 272–285. doi:10.1039/C9EN00523D
- Cox, D. K., A. G. Covernton, L. H. Davies, F. J. Dower, F. Juanes, and S. E. Dudas. 2019. "Human Consumption of Microplastics." *Environmental Science & Technology* 53 (12): 7068–7074. doi:10.1021/acs.est.9b01517
- Czarny, P., D. Kwiatkowski, D. Kacperska, D. Kawczyńska, M. Talarowska, A. Orzechowska, A. Bielecka-Kowalska, J. Szemraj, P. Gaandstrokecki, and T. Śliwiński. 2015. "Elevated Level of DNA Damage and Impaired Repair of Oxidative DNA Damage in Patients with Recurrent Depressive Disorder." *Medical Science Monitor* 6 (21): 412–418.
- Dizdaroğlu, M., P. Jaruga, M. Birincioglu, and H. Rodriguez. 2002. "Free Radical-Induced Damage to DNA: Mechanisms and Measurement." *Free Radic. Free Radical Biology & Medicine* 32 (11): 1102–1115. doi:10.1016/S0891-5849(02)00826-2
- Domenech, J., M. de Britto, A. Velázquez, S. Pastor, A. Hernández, R. Marcos, and C. Cortés. 2021. "Long-Term Effects of Polystyrene Nanoplastics in Human Intestinal Caco-2 Cells." *Biomolecules* 11 (10): 1442. doi:10.3390/biom11101442
- Enaud, R., R. Prevel, E. Ciarlo, F. Beaufile, G. Wieërs, B. Guery, and L. Delhaes. 2020. "The Gut-Lung Axis in Health and Respiratory Diseases: A Place for Inter-Organ and Inter-Kingdom Crosstalks." *Front Cell Infect Microbiol. Frontiers* 10: 9.
- Enyoh, E. C., L. Shafea, W. A. Verla, N. E. Verla, W. Qingyue, T. Chowdhury, and M. Paredes. 2020. "Microplastics Exposure Routes and Toxicity Studies to Ecosystems: An Overview." *Environmental Analysis, Health and Toxicology* 35 (1): e2020004. doi:10.5620/eaht.e2020004
- European Food Safety Authority (EFSA). 2016. "Presence of Microplastics and Nanoplastics in Food, with Particular focus on Seafood." *EFSA Journal* 14: 1–30.
- Facciola, A., G. Visalli, P. M. Ciarello, and A. Di Pietro. 2021. "A Newly Emerging Airborne Pollutants: current Knowledge of Health Impact of Micro and Nanoplastics." *International Journal of Environmental Research and Public Health* 18 (6): 2997. [Mismatch] doi:10.3390/ijerph18062997
- Farhat, S., C. Silva, M. Orione, L. Campos, A. Sallum, and A. Braga. 2011. "Air Pollution in Autoimmune Rheumatic Diseases: A Review." *Autoimmunity Reviews* 11 (1): 14–21. doi:10.1016/j.autrev.2011.06.008
- Felgentreff, K., C. Schuetz, U. Baumann, C. Klemann, D. Viemann, S. Ursu, E.-M. Jacobsen, et al. 2021. "Differential DNA Damage Response of Peripheral Blood Lymphocyte Populations." *Frontiers in Immunology* 12: 739675. doi:10.3389/fimmu.2021.739675
- Gackowski, D., M. Starczak, E. Zarakowska, M. Modrzejewska, A. Szpila, Z. Banaszkiwicz, and R. Olinski. 2016. "Accurate, Direct, and High-through Put Analyses of a Broad Spectrum of Endogenously Generated DNA Base Modifications with Isotope-Dilution Two-Dimensional Ultraperformance Liquid Chromatography with Tandem Mass Spectrometry: Possible Clinical Implication." *Analytical Chemistry* 88 (24): 12128–12136. doi:10.1021/acs.analchem.6b02900
- Gigault, J., A. T. Halle, M. Baudrimont, P.-Y. Pascal, F. Gauffre, T.-L. Phi, H. El Hadri, B. Grassl, and S. Reynaud. 2018. "Current Opinion: What is a Nanoplastic?" *Environmental Pollution (Barking, Essex : 1987)* 235: 1030–1034. doi:10.1016/j.envpol.2018.01.024
- Gopinath, P. M., V. Saranya, S. Vijayakumar, M. Mythili Meera, S. Ruprekha, R. Kunal, A. Pranay, J. Thomas, A. Mukherjee, and N. Chandrasekaran. 2019. "Assessment on Interactive Prospectives of Nanoplastics with Plasma Proteins and the Toxicological Impacts of Virgin, Coronated and Environmentally Released-Nanoplastics." *Scientific Reports* 9 (1): 15. doi:10.1038/s41598-019-45139-6
- Guimarães, B. T. A., Estrela, N. F., Pereira, S. P., de Andrade Vieira, E. J., de Lima Rodrigues, S. A., Silva, G. F, and Malafaia, G. 2021. "Toxicity of Polystyrene Nanoplastics in *Ctenopharyngodonidella* Juveniles: A Genotoxic, Mutagenic and Cytotoxic Perspective." *The Science of the Total Environment* 752: 141937. doi:10.1016/j.scitotenv.2020.141937
- Hantoro, I., Löhr, A. J., Van Belleghem, F. G. A. J., Widianarko, B. and Ragas, A. M. J. 2019. "Microplastics in Coastal Areas and Seafood: implications for Food Safety." *Food Additives & Contaminants. Part A, Chemistry, Analysis, Control, Exposure & Risk Assessment* 36 (5): 674–711. doi:10.1080/19440049.2019.1585581
- Hartmann, B. N., T. Hüffer, C. R. Thompson, M. Hassellöv, A. Verschoor, R. A. Dugaard, S. Rist, et al. 2019. "Are we Speaking the Same Language? Recommendations for a Definition and Categorization Framework for Plastic Debris." *Environmental Science & Technology* 53 (3): 1039–1047. doi:10.1021/acs.est.8b05297
- Horie, M, and Y. Tabei. 2021. "Role of Oxidative Stress in Nanoparticles Toxicity." *Free Radical Research* 55 (4): 331–342. doi:10.1080/10715762.2020.1859108
- Horton, A. A., Walton, A., Spurgeon, J. D., Lahive, E, and Svendsen, C. 2017. "Microplastics in Freshwater and Terrestrial Environments: evaluating the Current Understanding to Identify the Knowledge Gaps and Future Research Priorities." *The Science of the Total Environment* 586: 127–141. doi:10.1016/j.scitotenv.2017.01.190
- Hu, M, and D. Palić. 2020. "Micro-and Nano-Plastics Activation of Oxidative and Inflammatory Adverse Outcome Pathways." *Redox Biology* 37: 101620. doi:10.1016/j.redox.2020.101620
- Huff, J, and F. P. Infante. 2011. "Styrene Exposure and Risk Cancer." *Mutagenesis* 26 (5): 583–584. doi:10.1093/mutage/ger033
- Hwang, K. S., Y. Son, S. S. Kim, D. S. Shin, S. H. Lim, J. Y. Yang, H. N. Jeong, B. H. Lee, and M. A. Bae. 2022. "Size-

- Dependent Effects of Polystyrene Nanoparticles (PS-NPs) on Behaviors and Endogenous Neurochemicals in Zebrafish Larvae." *International Journal of Molecular Sciences* 23 (18): 10682. doi:10.3390/ijms231810682
- Kik, K., B. Bukowska, A. Krokosz, and P. Sicińska. 2021. "Oxidative Properties of Polystyrene Nanoparticles with Different Diameters in Human Peripheral Blood Mononuclear Cells (In Vitro Study)." *International Journal of Molecular Sciences* 22 (9): 4406. doi:10.3390/ijms22094406
- Klaude, M., S. Eriksson, J. Nygren, and G. Ahnstrom. 1996. "Polyribose Polymerase Deficient V79 Chinese Hamster, the Comet Assay: mechanisms and Technical Cell Line." *International Journal of Oncology* 17: 955–962.
- Krokan, H. E., R. Standal, and G. Slupphaug. 1997. "DNA Glycosylases in the Base Excision Repair of DNA." *Biochemical Journal* 325 (1): 1–16. doi:10.1042/bj3250001
- Kutralam-Muniasamy, G., F. Pérez-Guevara, I. Elizalde-Martínez, and V. Shruti. 2020. "Branded Milks- Are They Immune from Microplastics Contamination?" *The Science of the Total Environment* 714: 136823. doi:10.1016/j.scitotenv.2020.136823
- Leslie, A. H., van Velzen, M. J. M., Brandsma, H. S., Vethaak, D. A., Garcia-Vallejo, J. J. and Lamoree, M. H. 2022. "Discovery and Quantification of Plastic Particle Pollution in Human Blood." *Environment International* 163: 107199. doi:10.1016/j.envint.2022.107199
- Li, B., Y. Ding, X. Cheng, D. Sheng, Z. Xu, Q. Rong, J. Wu, H. Zhao, X. Ji, and Y. Zhang. 2020. "Polyethylene Microplastics Affect the Distribution of Gut Microbiota and Inflammation Development in Mice." *Chemosphere* 244: 125492. doi:10.1016/j.chemosphere.2019.125492
- Liu, Z., Y. Huang, Y. Jiao, Q. Chen, D. Wu, P. Yu, Y. Li, M. Cai, and Y. Zhao. 2020. "Polystyrene Nanoplastic Induces ROS Production and Affects the MAPK-HIF-1/NFkB-Mediated Antioxidant System in *Daphnia pulex*." *Aquatic Toxicology (Amsterdam, Netherlands)* 220: 105420. doi:10.1016/j.aquatox.2020.105420
- Liu, L., K. Xu, B. Zhang, Y. Ye, Q. Zhang, and W. Jiang. 2021. "Cellular Internalization and Release of Polystyrene Microplastics and Nanoplastics." *The Science of the Total Environment* 779: 146523. doi:10.1016/j.scitotenv.2021.146523
- Liu, Z., Y. Li, E. Pérez, Q. Jiang, Q. Chen, Y. Jiao, Y. Huang, Y. Yang, and Y. Zhao. 2021. "Polystyrene Nanoplastic Induces Oxidative Stress, Immune Defense, and Glycometabolism Change in *Daphnia pulex*. Application of Transcriptome Profiling in Risk Assessment of Nanoplastics." *Journal of Hazardous Materials* 402: 123778. doi:10.1016/j.jhazmat.2020.123778
- Ma, B., M. Jing, P. Villalta, J. R. Kapphahn, R. S. Montezuma, A. D. Ferrington, and I. Stepanov. 2016. "Simultaneous Determination of 8-Oxo-2'-Deoxyguanosine and 8-Oxo-2'-Deoxyadenosine in Human Retinal DNA by Liquid Chromatography Nanoelectrospray-Tandem Mass Spectrometry." *Scientific Reports* 6 (1): 22375. doi:10.1038/srep22375
- Maity, S., A. Chatterjee, R. Guchhait, S. De, and K. Pramanick. 2020. "Cytogenotoxic Potential of a Hazardous Material, Polystyrene Microparticles on *Allium Cepa* L." *Journal of Hazardous Materials* 385: 121560. doi:10.1016/j.jhazmat.2019.121560
- Mangal, D., D. Vudathala, H.-J. Park, H. S. Lee, M. T. Penning, and I. A. Blair. 2009. "Analysis of 7,8-Dihydro-8-Oxo-2'-Deoxyguanosine in Cellular DNA during Oxidative Stress." *Chemical Research in Toxicology* 22 (5): 788–797. 2009doi: 10.1021/tx800343c
- Marteijn, J. A., H. Lans, W. Vermeulen, and J. H. Hoeijmakers. 2014. "Understanding Nucleotide Excision Repair and Its Roles in Cancer and Ageing." *Nature Reviews Molecular Cell Biology* 15 (7): 465–481. doi:10.1038/nrm3822
- Mitrano, M., P. Wick, and B. Nowack. 2021. "Placing Nanoplastics in the Context of Global Plastic Pollution." *Nature Nanotechnology* 16 (5): 491–500. doi:10.1038/s41565-021-00888-2
- Musyanovych, A., J. Dausend, M. Dass, P. Walther, V. Mailander, and K. Landfester. 2011. "Criteria Impacting the Cellular Uptake of Nanoparticles: A Study Emphasizing Polymer Type and Surfactant Effects." *Acta Biomaterialia* 7 (12): 4160–4168. doi:10.1016/j.actbio.2011.07.033
- Nakamura, K., W. Sakai, T. Kawamoto, R. T. Bree, N. F. Lowndes, S. Takeda, and Y. Taniguchi. 2006. "Genetic Dissection of Vertebrate 53BP1: A Major Role in Non-Homologous End Joining of DNA Double Strand Breaks." *DNA Repair* 5 (6): 741–749. doi:10.1016/j.dnarep.2006.03.008
- Nemtsova, V., A. Shalimova, O. Kolesnikova, O. Vysotska, V. Zlatkina, and N. Zhelezniakova. 2022. "Prognostic Value of Plasma 8-Oxo-2'-Deoxyguanosine Levels in Cardio Vascular Complications Formation in Comorbidity of Arteria Hypertension and Type 2 Diabetes Mellitus." *Arterial Hypertension* 19 (997): 1–12.
- Partikel, K., R. Korte, D. Mulac, H. U. Humpf, and K. Langer. 2019. "Serum Type and Concentration Both Affect the Protein-Corona Composition of PLGA Nanoparticles." *Beilstein Journal of Nanotechnology* 10: 1002–1015. doi:10.3762/bjnano.10.101
- Poma, A., G. Vecchiotti, S. Colafarina, O. Zarivi, M. Aloisi, L. Arrizza, G. Chichiriccò, and P. Di Carlo. 2019. "In Vitro Genotoxicity of Polystyrene Nanoparticles on the Human Fibroblast Hs27 Cell Line." *Nanomaterials* 9 (9): 1299–1213. doi:10.3390/nano9091299
- Prüst, M., J. Meijer, and R. H. S. Westerink. 2020. "The Plastic Brain: Neurotoxicity of Micro- and Nanoplastics. Part FibreToxicol." *BioMed Central* 17: 1–16.
- Ragusa, A., A. Svelato, C. Santacroce, P. Catalano, V. Notarstefano, O. Carnevali, F. Papa, et al. 2021. "Plasticenta: First Evidence of Microplastics in Human Placenta." *Environment International* 146: 106274. doi:10.1016/j.envint.2020.106274
- Rakowski, M., and A. Grzelak. 2020. "A New Occupational and Environmental Hazard- Nanoplastic." *Medycyna Pracy* 71 (6): 743–756. doi:10.13075/mp.5893.00990

- Ramsperger, A. F. R. M., J. Jasinski, M. Völkl, T. Witzmann, M. Meinhart, V. Jérôme, W. P. Kretschmer, et al. 2022. "Supposedly Identical Microplastic Particles Substantially Differ in Their Material Properties Influencing Particle-Cell Interactions and Cellular Responses." *Journal of Hazardous Materials* 425: 127961. doi:10.1016/j.jhazmat.2021.127961
- Ribeiro, F., R. A. Garcia, P. B. Pereira, M. Fonseca, C. N. Mestre, G. T. Fonseca, M. L. Ilharco, and M. J. Bebianno. 2017. "Microplastics Effects in *Scrobicularia Plana*." *Marine Pollution Bulletin* 122 (1-2): 379–391. doi:10.1016/j.marpolbul.2017.06.078
- Rubio, L., I. Barguilla, J. Domenech, R. Marcos, and A. Hernandez. 2020. "Biological Effects, Including Oxidative Stress and Genotoxic Damage, of Polystyrene Nanoparticles in Different Human Hematopoietic Cell Lines." *Journal of Hazardous Materials* 398: 122900. doi:10.1016/j.jhazmat.2020.122900
- Santovito, A., P. Cervella, and M. Delperio. 2014. "Chromosomal Damage in Peripheral Blood Lymphocytes from Nurses Occupationally Exposed to Chemicals." *Human & Experimental Toxicology* 33 (9): 897–903. doi:10.1177/0960327113512338
- Sarasamma, S., G. Audira, P. Siregar, N. Malhotra, Y.-H. Lai, S.-T. Liang, J.-R. Chen, K. H.-C. Chen, and C.-D. Hsiao. 2020. "Nanoplastics Cause Neurobehavioral Impairments, Reproductive and Oxidative Damages and Biomarker Responses in Zebrafish: Throwing up Alarms of Wide Spread Health Risk of Exposure." *International Journal of Molecular Sciences* 21 (4): 1410. doi:10.3390/ijms21041410
- Sarma, K. D., R. Dubey, M. R. Samarth, S. Shubham, P. Chowdhury, M. Kumawat, V. Verma, R. R. Tiwari, and K. Manoj. 2022. "The Biological Effects of Polystyrene Nanoplastics on Human Peripheral Blood Lymphocytes." *Nanomaterials* 12 (10): 1632. doi:10.3390/nano12101632
- Shah, N., A. Khan, N. Habib Khan, and M. Khisroon. 2020. "Genotoxic Consequences in Common Grass Carp (*Ctenopharyngodon Idella*, (Valenciennes, 1844)) Exposed to Selected Toxic Metals." *Biological Trace Element Research* 199: 305–314.
- Singh, N. P., McCoy, T.M., Tice, R. R. and Schneider, L. E. 1988. "Simple Technique for Quantitation of Low Levels of DNA Damage in Individual Cells." *Experimental Cell Research*. 175 (1): 184–191. doi:10.1016/0014-4827(88)90265-0
- Singh, N. P, and E. R. Stephens. 1997. "Microgel Electrophoresis: Sensitivity, Mechanisms and DNA Electrostretching." *Mutation Research* 383 (2): 167–175. doi:10.1016/S0921-8777(96)00056-0
- Smith, J. R. H., G. Etherington, A. L. Shutt, and M. J. Youngman. 2002. "A Study of Aerosol Deposition and Clearance from the Human Nasal Passage." *Annals of Occupational Hygiene* 46: 309–313.
- Sökmen, T. Ö., Sulukan, E., Türkoğlu, M., Baran, A., Özkaraca, M., Buğrahan Ceyhan, S. 2020. "Polystyrene nanoplastics (20 nm) are able to bioaccumulate and cause oxidative DNA damages in the brain tissue of zebrafish embryo (Danio rerio)." *NeuroToxicology* 77: 51–59,doi:10.1016/j.neuro.2019.12.010.
- Starczak, M., M. Gawronski, R. Olinski, and D. Gackowski. 2021. "Quantification of DNA Modifications Using Two-Dimensional Ultraperformance Liquid Chromatography Tandem Mass Spectrometry (2D-UPLC-MS/MS)." *Methods in Molecular Biology (Clifton, N.J.)* 2198: 91–108. doi:10.1007/978-1-0716-0876-0_8
- Sun, X., B. Chen, Q. Li, N. Liu, B. Xia, L. Zhu, and K. Qu. 2018. "Toxicities of Polystyrene Nano- and Microplastics toward Marine Bacterium *Halomonas alkaliphila*." *The Science of the Total Environment* 642: 1378–1385. doi:10.1016/j.scitotenv.2018.06.141
- Sze, A., D. Erickson, L. Ren, and D. Li. 2003. "Zeta-Potential Measurement Using the Smoluchowski Equation and the Slope of the Current-Time Relationship in Electroosmotic Flow." *Journal of Colloid and Interface Science* 261 (2): 402–410. doi:10.1016/S0021-9797(03)00142-5
- Thompson, J., J. Quigley, N. Halfpenny, D. Scott, and N. Hawkins. 2016. "Importance and Methods of Searching for e-Publications a Head of Print in Systematic Reviews." *Evidence-Based Medicine* 21 (2): 55–59. doi:10.1136/ebmed-2015-110374
- Tice, R. R., E. Agurell, D. Anderson, B. Burlinson, A. Hartmann, H. Kobayashi, Y. Miyamae, E. Rojas, J.-C. Ryu, and F. Y. Sasaki. 2000. "Single Cell Gel/Comet Assay: Guidelines for in Vitro and in Vivo Genetic Toxicology Testing." *Environmental and Molecular Mutagenesis* 35 (3): 206–221. doi:10.1002/(SICI)1098-2280(2000)35:3<206::AID-EM8>3.0.CO;2-J
- Toussaint, B., B. Raffael, A. Angers-Loustau, D. Gilliland, V. Kestens, M. Petrillo, M. I. Rio-Echevarria, and G. van den Eede. 2019. "Review of Micro- and Nanoplastic Contamination in the Food Chain." *Food Additives & Contaminants. Part A, Chemistry, Analysis, Control, Exposure & Risk Assessment* 36 (5): 639–673. doi:10.1080/19440049.2019.1583381
- Toyokuni, S, and L.-J. Sagripanti. 1996. "Association between 8-Hydroxy-2'-Deoxyguanosine Formation and DNA Stand Break Mediated by Copper and Iron." *Free Radical Biology and Medicine* 6: 859–864.
- Tubbs, A, and A. Nussenzweig. 2017. "Endogenous DNA Damage as a Source of Genomic Instability in Cancer." *Cell* 168 (4): 644–656. doi:10.1016/j.cell.2017.01.002
- van Raamsdonk, L. W. D., M. van der Zande, A. A. Koelmans, R. L. A. P. Hoogenboom, R. J. B. Peters, M. J. Groot, M. C. A. A. Peijnenburg, and A. J. Y. Weesepeel. 2020. "Current Insights into Monitoring, Bioaccumulation, and Potential Health Effects of Microplastics Present in the Food Chain." *Foods* 9 (1): 72. doi:10.3390/foods9010072
- Vecchiotti, G., S. Colafarina, M. Aloisi, O. Zarivi, P. Di Carlo, and A. Poma. 2021. "Genotoxicity and Oxidative Stress Induction by Polystyrene Nanoparticles in the Colorectal Cancer Cell Line HCT116." *PloS One* 16 (7): e0255120. doi:10.1371/journal.pone.0255120
- Verster, C, and H. Bouwman. 2018. "Contextualization of Airborne Microplastic Pollution in the South African

- Environment." In Proceedings of the 2018 Conference of the National Association for Clean Air. Riverside Sun, Vanderbijlpark, Gauteng.
- Woźniak, K., and J. Błasiak. 2003. "In Vitro Genotoxicity of Lead Acetate: induction of Single and Double DNA Strand Breaks and DNA-Protein Cross-Links." *Mutation Research* 535 (2): 127–139. doi:[10.1016/S1383-5718\(02\)00295-4](https://doi.org/10.1016/S1383-5718(02)00295-4)
- Wright, L. S, and J. F. Kelly. 2017. "Plastic and Human Health: A Micro Issue?" *Environmental Science & Technology* 51 (12): 6634–6647. doi:[10.1021/acs.est.7b00423](https://doi.org/10.1021/acs.est.7b00423)
- Xia, T., M. Kovichich, M. Liong, J. Zink, and A. Nel. 2008. "Cationic Polystyrene Nanosphere Toxicity Depends on Cell-Specific Endocytic and Mitochondrial Injury Pathways." *ACS Nano* 2 (1): 85–96. doi:[10.1021/nn700256c](https://doi.org/10.1021/nn700256c)
- Xu, M., G. Halimu, Q. Zhang, Y. Song, X. Fu, Y. Li, Y. Li, and H. Zhang. 2019. "Internalization and Toxicity: A Preliminary Study of Effects of Nanoplastic Particles on Human Lung Epithelial Cell." *The Science of the Total Environment* 694: 133794. doi:[10.1016/j.scitotenv.2019.133794](https://doi.org/10.1016/j.scitotenv.2019.133794)
- Zheng, T., D. Yuan, and L. Chunguang. 2019. "Molecular Toxicity of Nanoplastics Involving in Oxidative Stress and Desoxyribonucleic Acid Damage." *Journal of Molecular Recognition : JMR* 32 (11): e2804. doi:[10.1002/jmr.2804](https://doi.org/10.1002/jmr.2804)



The effects of non-functionalized polystyrene nanoparticles of different diameters on the induction of apoptosis and mTOR level in human peripheral blood mononuclear cells

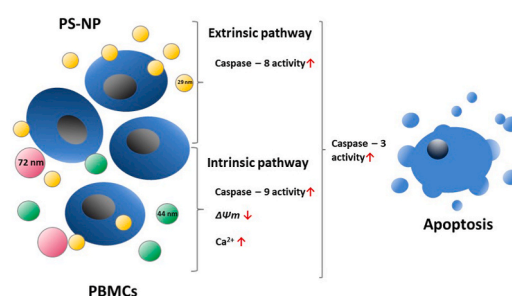
Kinga Malinowska, Paulina Sicińska, Jaromir Michałowicz, Bożena Bukowska^{*}

University of Lodz, Faculty of Biology and Environmental Protection, Department of Biophysics of Environmental Pollution, 141/143 Pomorska St., 90-236, Lodz, Poland

HIGHLIGHTS

- Polystyrene nanoparticles (PS-NPs) triggered apoptosis in peripheral blood mononuclear cells.
- PS-NPs of 29, 44, and 72 nm raised cytosolic calcium ion level and reduced mitochondrial potential.
- PS-NPs of 44 nm and 72 nm induced caspase-9 and -3, activating mitochondrial pathway of apoptosis.
- PS-NPs of 29 nm activated both extrinsic and intrinsic pathway of apoptosis.
- Apoptotic changes and an increase of mTOR level depended on the size of the tested NPs.

GRAPHICAL ABSTRACT



ARTICLE INFO

Handling editor: Giulia Guerriero

Keywords:

Apoptosis
Caspases
Transmembrane mitochondrial potential
Cytosolic calcium ion
Plastic

ABSTRACT

Particles of various types of plastics, including polystyrene nanoparticles (PS-NPs), have been determined in human blood, placenta, and lungs. These findings suggest a potential detrimental effect of PS-NPs on blood-stream cells. The purpose of this study was to assess the mechanism underlying PS-NPs-induced apoptosis in human peripheral blood mononuclear cells (PBMCs). Non-functionalized PS-NPs of three diameters: 29 nm, 44 nm, and 72 nm were studied used in this research. PBMCs were isolated from human leukocyte-platelet buffy coat and treated with PS-NPs at concentrations ranging from 0.001 to 200 µg/mL for 24 h. Apoptotic mechanism of action was evaluated by determining the level of cytosolic calcium ions, as well as mitochondrial transmembrane potential, and ATP levels. Furthermore, detection of caspase-8, -9, and -3 activation, as well as mTOR level was conducted. The presence of apoptotic PBMCs was confirmed by the method of double staining of the cells with propidium iodide and FITC-conjugated Annexin V. We found that all tested NPs increased calcium ion and depleted mitochondrial transmembrane potential levels. The tested NPs also activated caspase-9 and caspase-3, and the smallest NPs of 29 nm of diameter also activated caspase-8. The results clearly showed that apoptotic changes and an increase of mTOR level depended on the size of the tested NPs, while the smallest particles caused the greatest alterations. PS-NPs of 26 nm of diameter activated the extrinsic pathway (increased caspase-8 activity), as well as intrinsic (mitochondrial) pathway (increased caspase-9 activity, raised calcium ion level, and decreased transmembrane mitochondrial potential) of apoptosis. All PS-NPs increased mTOR level at

^{*} Corresponding author.

E-mail address: bozena.bukowska@biol.uni.lodz.pl (B. Bukowska).

<https://doi.org/10.1016/j.chemosphere.2023.139137>

Received 25 April 2023; Received in revised form 31 May 2023; Accepted 3 June 2023

Available online 5 June 2023

0045-6535/© 2023 Elsevier Ltd. All rights reserved.

the concentrations smaller than those that induced apoptosis and its level returned to control value when the process of apoptosis escalated.

Author contributions statement

Conceptualization, K.M and B.B.; methodology, K.M. and P.S.; validation, B.B., K.M. and P.S.; formal analysis, K.M. and B.B.; investigation, K. M. and P.S.; resources, B.B. and K.M.; data curation, B.B. and K.M.; writing–original draft preparation, K.M., B.B., P.S., J.M., writing–review and editing, K.M., B.B., P.S. and J.M.; visualization, K.M. and B.B.; supervision, B.B.; project administration, B.B.; funding acquisition, B.B. All authors have read and agreed to the published version of the manuscript.

1. Introduction

One of the very important topics in ecotoxicology is the assessment of risks resulting from the potential adverse impact of microplastics (MPs, diameter < 5 µm) and nanoplastics (NPs, diameter < 0.1 µm) on living organisms. The above-mentioned particles are used in many industries, for example pharmaceutical and cosmetic, as well as in laboratories (Dalela et al., 2015; Hernandez et al., 2017; Wang et al., 2018) and are derived from the decomposition of plastic that contaminates the environment. The occurrence of MPs and NPs has been reported in water, soil, air, and food (Gasperi et al., 2018; Song et al., 2018; Zhang and Liu, 2018), which results resulting in their penetration into cells and tissues of plants, animals, and humans. The most common route of human exposure to plastic NPs is associated with food ingestion. Numerous studies have shown that plastic particles accumulate in the marine food chain (EFSA Panel on Contaminants in the Food Chain, 2016; Hernandez et al., 2019; Yee et al., 2021).

NPs penetrate the biological barriers of living organisms and accumulate in their tissues (Geiser and Kreyling, 2010; Prata, 2018). Most of NPs ingested orally pass through the gastrointestinal tract being absorbed through the gastrointestinal tract barrier (Kreyling et al., 2017). Nevertheless, translocation of various types and sizes of particles (between 0.1 and 150 nm) through the mammalian gut into the lymphatic system has been demonstrated in studies involving humans (Hussain, 2001). After crossing the intestinal barrier, the particles of < 100 nm can even be transported into the brain (Wright and Kelly, 2017), as well as through the placental barrier (Graefmueller et al., 2015). The tissue distribution of fluorescent PS particles of 5 µm and 20 µm in mice after oral administration resulted in accumulation in the kidney, liver, and intestine with manifestation of, disturbance of energy balance, oxidative stress and neurotoxicity (Deng et al., 2017).

Another route of the exposure of humans to nanoplastic particles is air inhalation. Inhaled nanoparticles can be eliminated by mucociliary clearance, but can also settle in the lungs or be absorbed in the circulation (Geiser and Kreyling, 2010). Inhaled microplastic particles can promote various lung diseases by inducing inflammation (Lu et al., 2022). The dermal route has also been recognized as one of the routes of human exposure to plastic particles. Plastic NPs with a diameter less than 40 nm have been shown to enter the body through the epidermis (Schneider et al., 2009; Vogt et al., 2006). Recently, Leslie et al. (2022) showed the presence of plastic in the blood of 17 out of 22 people tested. Furthermore, the latest study of a cohort of 196 people confirmed the presence of nanoplastics in peripheral blood of all tested people (Salvia et al., 2023).

The presence of plastic particles in the human body can cause cell damage and possibly induce immune effects (Rawle et al., 2022; Yin et al., 2023). Some studies have shown that PS-NPs can alter the function of the immune system. PS-NPs of about 50 nm in diameter were studied in Raji B, TK6 (lymphocytes), and THP-1 (monocytes) immune cells (Rubio et al., 2020). They observed low PS-NPs toxicity, a small rise in

ROS formation, and low gene toxicity of Raji-B and TK6 cells. Another research work (Forte et al., 2016) assessed the inflammatory processes of human gastrointestinal cancer cells using PS-NPs of 44 nm and 100 nm in diameter, showing that 44 nm PS-NPs influenced cell viability and shape, and that their presence caused inflammation. PS-NPs have also been shown to alter the expression of genes connected with inflammation and the cell cycle. Smaller particles increased the expression of interleukin- 6 (IL-6) and IL-8, which are considered to be the most important cytokines implicated in the pathology of the stomach. In another study, Li et al. (2022) observed that nanoplastic inhibited the expression of activated T-cell markers on the surface of T-cells, whereas inhibiting CD8⁺ T-cell differentiation, and the expression of T-cell cytokines in spleen lymphocytes. A series of key signal molecules implicated in activation and function of T cells were severely influenced after exposure to nanoplastics. In a recent study conducted by Jing et al. (2022) mice exposed to PS-MPs and PS-NPs (10 µm, 5 µm and 80 nm) at doses of 60 g (42 days of intragastric administration) revealed that these particles exhibited hemostatic toxicity. They noticed a disturbance in bone marrow cell distribution, a depletion in colony formation, self-renewal, differentiation capability, and a rise in lymphocytes. PS-NPs and PS-MPs also interfered with the intestinal microbiota, metabolism, and inflammation, all of which were connected with hematotoxicity, showing that the abnormal hematochemical-cytokine axes of the intestinal microbiota could be the key pathway for plastic particles-induced hematopoietic lesion.

Hence, potential interactions between blood cells, including PBMCs and PS-NPs present in blood, may have biological consequences. Due to the large number of PBMCs in the circulation and their essential role in the immune system, these cells are often used as model cells in the studies evaluating toxicity of xenobiotics (Santovito et al., 2014; Sarma et al., 2022; Singh et al., 2006). Accelerating PBMCs apoptosis is associated with ill-healthy changes in the immune system, including weakened immunity (Chu et al., 2021; Weinberg et al., 2004), which can lead to autoimmune diseases (type 1 diabetes, asthma, allergies) and cancer (Hallit and Salameh, 2017; Ratomski et al., 2007).

Apoptosis is programmed cell death, which is responsible for the elimination of damaged or ageing cells from the organism without inflammatory reactions. When apoptosis occurs, biochemical and morphological changes lead to phagocytosis of the cell by macrophages (Elmore, 2007). It has been shown that xenobiotics are able to trigger apoptosis, which can lead to accelerated cells elimination, and consequently results in development of various disorders, e.g. autoimmune diseases (Favaloro et al., 2012; Pallardy et al., 1999). The extrinsic apoptotic pathway is triggered by a death ligand binding to a death receptor, such as TNF-α to TNFR1, while the intrinsic, also called mitochondrial pathway of apoptosis shifts the balance in the Bcl-2 family towards proapoptotic members. The p53 protein activated by DNA damage may impel these two pathways through the Bid protein (Haupt et al., 2003).

As a result of missing data on the mechanism of proapoptotic action of PS-NPs in human PBMCs, we decided to conduct such research. In our previous study (Kik et al., 2021) the degree of apoptosis in human PBMCs treated for 24 h with PS-NPs was determined by flow cytometry using propidium iodide (PI) and fluorescein (FITC) conjugated with Annexin V. All tested NPs increased the number of apoptotic PBMCs, while PS-NPs of 29 nm more strongly than NPs of 44 nm and 72 nm changed examined parameter.

In this study, PBMCs were incubated with PS-NPs of different diameters (29 nm, 44 nm and 72 nm) for 24 h in the concentration range from 0.001 to 100 µg/mL (in ATP level detection up to 200 µg/mL). Changes in the number of apoptotic cells were determined by the double

staining of PBMCs with PI and FITC-conjugated Annexin V, and the proapoptotic mechanism of action of PS-NPs was assessed by detection of ATP level, the levels of cytosolic calcium ions and transmembrane mitochondrial potential, as well as caspase-8, -9, and -3 activation. We also investigated the activation of mammalian rapamycin target protein (mTOR) pathway by measuring the level of this protein. mTOR is a serine/threonine kinase implicated in the regulation of various cell processes, such as cell energy metabolism, as well as regulation of autophagy and apoptosis (Wang et al., 2022).

2. Materials and methods

2.1. Chemicals

Standards of non-functionalized PS-NPs were purchased from Poly-science Europe GmbH. PBMCs separation medium (LSM) (1.077 g/cm³) and RPMI 1640 medium with L-glutamine were bought from Cytogen (Germany). HBSS solution, bovine serum albumin, bovine calf serum, penicillin streptomycin, pluronic F-127, valinomycin, camptothecin, caspase-3 and caspase-8 fluorometric assay kits, caspase-9 chromogenic substrate, and caspase-9 inhibitor were purchased from Sigma-Aldrich (USA). MitoTracker Red CMXRos were bought from Molecular Probes (USA). Fluo-3/AM was bought from MoBiTec (Germany). ATP kit was purchased from Thermo Fisher Scientific (USA) and mTOR ELISA Kit (USA) from Novus Biologicals Biotechnie Brand.

2.2. Biological material

Human peripheral blood mononuclear cells (PBMCs) were isolated from the leukocyte-buffy coat purchased from the Regional Centre for Blood Donation and Treatment (RCBDT) in Lodz, Poland. The purchase of blood for this research was possible due to the contract concluded between the University of Lodz and the mentioned RCBDT. Leukocyte-buffy coat was isolated by bank employees from whole blood obtained from healthy, non-smoking donors. The Lodz Blood Bank is accredited by the Minister of Health (No. BA/2/2004) and our described experiments have been approved by the Bioethics Committee of the University of Lodz (Resolution No. 8/KBBN-UŁ/II/2019 (08/04/2019)).

2.2.1. Isolation of PBMCs

In the first step of isolation of the PBMCs, the buffy coat was centrifuged (600×g, 10 min, 20 °C), which allowed for the removal of plasma and collection of the resulting layer of the PBMCs. The PBMCs were then layered on lymphocyte separation medium (density of 1.077 g/cm³) and centrifuged (600×g, 30 min, 20 °C). PBMCs were collected, and a volume of 3 mL of erythrocyte lysis buffer (150 mM NH₄Cl, 10 mM NaHCO₃, 1 mM EDTA, pH 7.4) was added to PBMCs suspension. The cells were incubated for 5 min at 20 °C and supplemented with a volume of 6.5 mL of PBS. The samples were then centrifuged again (200 g x, 15 min, 20 °C). The supernatant was collected and the PBMCs attached to the bottom of the tube were rinsed twice using RPMI medium (with L-glutamine) and centrifuged (200×g, 15 min, 20 °C). PBMCs with a density of 5 × 10⁴ cells/mL were used for the experiments.

2.3. Physico-chemical characterization of non-functionalized PS-NPs

The evaluation of the characteristic of non-functionalized PS-NPs with different diameters of 26 nm, 44 nm and 72 nm was carried out in our previous studies (Kik et al., 2021; Malinowska et al., 2022). In our earlier study, we evaluated the hydrodynamic size of non-functionalized PS-NPs using the dynamic light scattering technique (DLS) (Kik et al., 2021; Malinowska et al., 2022), and showed photos of tested NPs made with an atomic force microscope (AFM) and scanning electron microscope (SEM) (Malinowska et al., 2022) (doi.org/10.1080/17435390.2022.2149360). It was found that PS-NPs formed local close-packed agglomerates, due to the strong

inter-particle and surface-particle attracting interactions. However, part of the particles were also visible as single objects. The diameters of the PS-NPs showed by the manufacturer were comparable with obtained by the DLS method (30 ± 7 nm, 40 ± 9 nm; 72 ± 17 nm (Malinowska et al., 2022)) in water and 27.96 ± 8.03 nm; 38.61 ± 8.61 nm; 68.45 ± 15.19 nm in phosphate-buffered saline (Kik et al., 2021) as well as AFM (24 nm; 41 nm; 72 nm (Malinowska et al., 2022)) and SEM (26 ± 4 nm, 40 ± 5 nm; 70 ± 4 nm (Malinowska et al., 2022)) microscopy in water. We also determined the zeta potential at pH 7.4 in RPMI medium, in which the tested NPs were suspended. We observed a substantial alteration in the zeta potential depending on the particle diameters. The absolute level of negative ζ-potential in the RPMI increased with the elevated particle diameter from −41 ± 3 mV (for the smallest particles of 26 nm) to −56 ± 2 mV (for the largest particles of 72 nm) (Malinowska et al., 2022).

2.4. Apoptosis methods

2.4.1. Annexin V-FITC/PI double-staining test

The expression of PS in the outer leaflet of membrane of the apoptotic cells was determined by annexin V-FITC apoptosis detection kit (Sigma-Aldrich). In addition, propidium iodide (PI) uptake was used to detect early apoptosis, late apoptosis, or necrosis induced by PS-NPs in PBMCs. The cells after incubation, were resuspended in RPMI medium to obtain the final concentration of 104 per mL. One microliter of Annexin V-FITC and 2 μL of PI were (1 μM each) added to the cells suspension, which was incubated for 10 min at room temperature in the dark. The samples were examined under a fluorescence microscope (Nikon Eclipse 800). The obtained photos are presented in the manuscript.

2.4.2. Cytosolic calcium ions level

The Fluo-3/AM fluorescent probe was utilized for the detection of calcium ion level in the cytosol. After the conjugation of calcium ions, the probe shows a bright green fluorescence. The detection was done according to the manufacturer's protocol (Fluo-3/AM, MoBiTec, Germany). PBMCs were treated with different sized PS-NPs (29 nm, 44 nm, and 77 nm) in concentrations ranging from 0.001 to 10 μg/mL for 24 h at 37 °C in total darkness. The subsequent steps of sample handling were as described by Kwiatkowska et al. (2020). The samples were determined by flow cytometry (LSR II, Becton Dickinson) with excitation at 488 nm to show the Fluo-3 fluorescence at 525 nm. The FMC gate on PBMCs was established for data acquisition, and the data were recorded for a total of 10,000 cells per sample.

2.4.3. Mitochondrial transmembrane potential (ΔΨ_m)

The MitoLite Red CMXRos fluorescent probe was used for the detection of ΔΨ_m. This probe is a cationic dye that is capable of entering living cells and bioaccumulating in mitochondria, depending on the ΔΨ_m level. The probe is capable of remaining in mitochondria as it contains thiol-reactive chloromethyl moieties. PBMCs were incubated with PS-NPs of different sizes (29 nm, 44 nm and 77 nm) in at the concentrations ranging from 0.001 to 100 μg/mL for 24 h at 37 °C in total darkness. After incubation, the probes were centrifuged (300 g) for 5 min at 4 °C. The supernatant was removed, and the PBMCs were resuspended in PBS and stained with MitoLite CMXRos at 1 μM for 20 min at 37 °C in total darkness. MitoLite CMXRos fluorescence in the probes (excitation/emission maxima: 579/599 nm) was measured in 96-well plates using a microplate reader (Cary Eclipse, Varian) (Kwiatkowska et al., 2020).

2.4.4. Caspase-8, -9 -3 activation

The process of apoptosis is regulated directly and indirectly by caspases. Analysis of caspase-3, caspase-8 and caspase-9 activation was done according to Barańska et al. (2022). The analysis of caspase-3 and -8 was carried out according to the manufacturer's protocols (Caspase-3

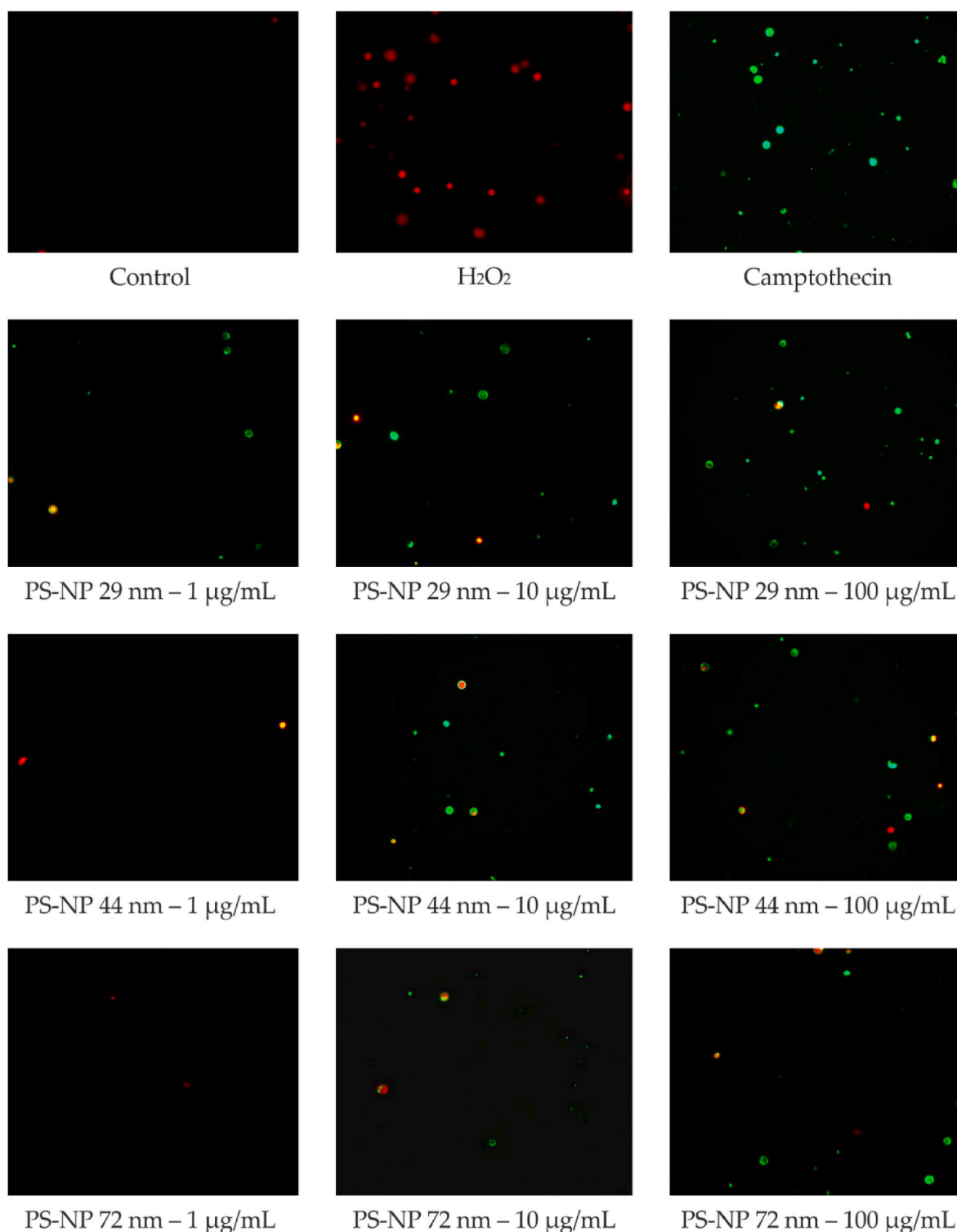


Fig. 1. Annexin V-FITC/propidium iodide double-staining assay. PBMCs after treatment with PS-NPs, were stained with FITC-Annexin V (green stained cells) and propidium iodide (red stained cells), and then analyzed by fluorescence microscopy (Zeiss Axio Scope) at 100 × magnification.

Assay Kit, Fluorometric Caspase-8 Assay Kit, Sigma-Aldrich). These fluorometric assays are based on the hydrolysis of the peptide substrates acetyl-Asp-Glu-Val-Asp-7-amino-4-methylcoumarin (Ac-DEVD-AMC) by caspase-3 and acetyl-Ile-Glu-Thr-Asp-7-amino-4-methylcoumarin (Ac-IETD-AMC) by caspase-8. As a result, a release of the fluorescent 7-amino-4-methylcoumarin (AMC) moiety occurs that exhibits fluorescence (excitation/emission maxima: 360/460 nm).

The Colorimetric evaluation of caspase-9 activity was done

according to the manufacturer's protocol (Caspase-9 Colorimetric Activity Assay Kit, LEHD Sigma-Aldrich). Caspase-3 hydrolyses the substrate acetyl-Leu-Glu-His-Asp-p-nitroaniline (Ac-LEHD-pNA) to p-nitroaniline (p-NA) (absorption at 405 nm). Camptothecin (10 mM) was used as a positive control in assays of caspases determination. The determination of caspase-3 and -8 activities was done using a fluorescent microplate reader (Fluoroskan Ascent FL, Labsystem, Thermo-Fisher, Waltham, MA, USA), while the detection of caspase-9 activity was

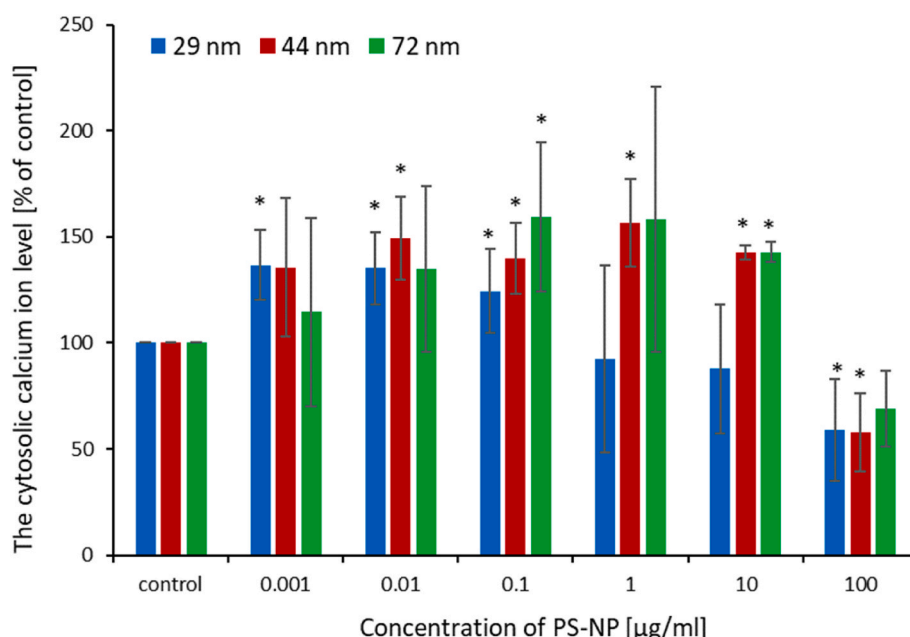


Fig. 2. Changes in the level of cytosolic calcium ions in human PBMCs caused by different sized non-functionalized PS-NPs. Each value represents the mean \pm SD obtained from 4 independent experiments (4 donors), while the mean value was obtained from at least 3 replications for each donor. Significantly different from control (*) $P < 0.05$; Student's t-test for a single sample.

conducted performed using an absorbance microplate reader (BioTek ELx808, Bio-Tek).

2.4.5. The level of mTOR

The level of serine/threonine protein kinase mTOR was tested using the human ELISA Kit (Catalogue # NBP2-50064, 100 assays, stored at 4 °C). Novus's mTOR ELISA kit is a sandwich ELISA assay for quantitative measurement of human mTOR in cell culture supernatants. Absorbance values proportional to the amount of mTOR were read at 405 nm using an microplate reader (BioTek, Synergy H1) and the standard curve was used for calculations.

2.4.6. Determination of the level of adenosine-5'-triphosphate (ATP)

The method of detection of ATP level was done according to procedures described previously (Kwiatkowska et al., 2020). The ATP level in the cells was detected by bioluminescence measurement at 560 nm using recombinant luciferase and its substrate, D-luciferin. The oxy-luciferin formed returning from its excited state to the its base state emitted luminescence that was determined using a fluorescent microplate reader (Fluoroskan Ascent FL, Labsystem, Thermo-Fisher, Waltham, MA, USA).

2.4.7. Statistical analysis

Data were shown as the average and standard deviation (SD); $n =$

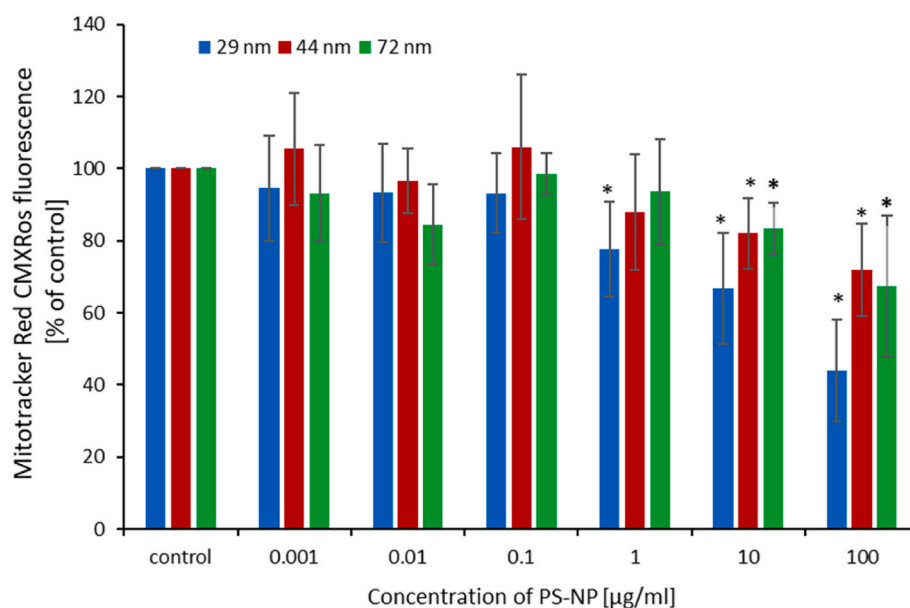


Fig. 3. Changes in transmembrane mitochondrial potential ($\Delta\Psi_m$) in human PBMCs caused by different sized non-functionalized PS-NPs. Each value represents the mean \pm SD obtained from 4 independent experiments (4 blood donors), while mean value was achieved from at least 3 replications for each donor. Significantly different from control (*) $P < 0.05$; Student's t-test for a single sample.

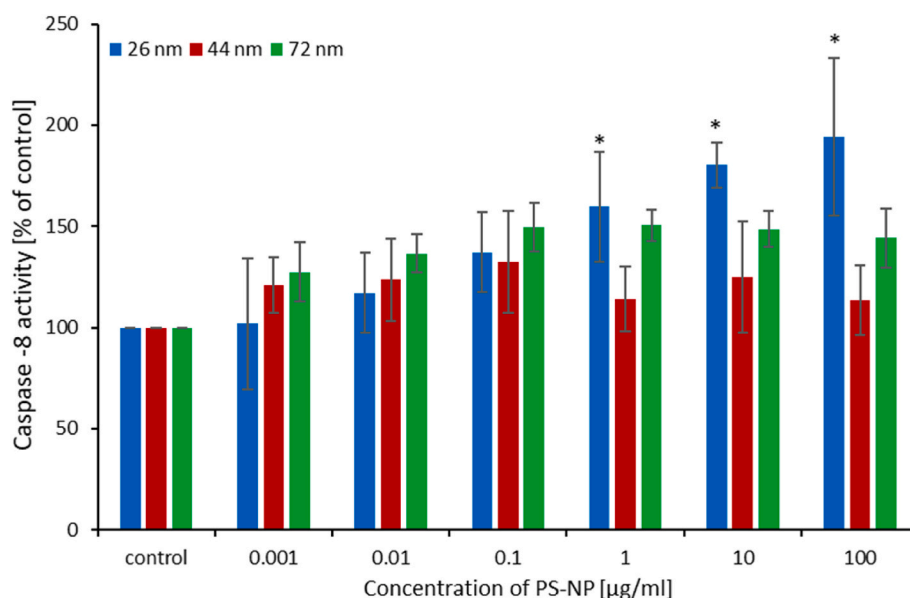


Fig. 4. Changes in caspase-8 activity in human PBMCs caused by different sized non-functionalized PS-NPs. Each value represents the mean \pm SD obtained from 3 independent experiments (3 blood donors), while mean value was obtained from at least 2 replications for each donor. Significantly different from control (*) $P < 0.05$; two-way ANOVA and a posteriori Tukey test.

3–6 (3–6 blood donors). Statistical analysis was conducted using Statistica v.13.1 (Dell Inc., Tulsa, OH, USA). The Shapiro-Wilk test was employed to test for normality, and the Brown-Forsythe's test was used to verify variance homogeneity. Statistical significance was tested using two-way ANOVA or one-way ANOVA followed by a post hoc Tukey's test. In some cases, the Student's t-test was used for a single sample. The results were considered statistically significant when $P < 0.05$.

3. Results

3.1. Annexin V-FITC/PI double-staining test

Microscopic analysis confirmed the formation of apoptotic cells, which were detected by flow cytometry in our previous study (Kik et al.,

2021). The type of cell death induced by PS-NPs was investigated by annexin V-FITC/PI test. Analysis of PBMCs after PS-NPs treatment revealed mainly the presence of apoptotic cells (green stained cells) and to a very small extent necrotic cells (red stained cells) (Fig. 1) (All photos are in supplementary materials). The highest number of apoptotic cells was observed after treatment of PBMCs with PS-NPs at 29 nm from the concentration of 1 $\mu\text{g/mL}$. In turn, for NPs of 44 nm, a significant increase in the percentage of apoptotic cells was observed from the concentration of 10 $\mu\text{g/mL}$, while for NPs of 70 nm from the concentration of 100 $\mu\text{g/mL}$. Two positive controls were used to induce necrotic and apoptotic cell death. Hydrogen peroxide (100 μM) was added to induce necrotic cell death, which was visualized by staining the cells with propidium iodide (red fluorescence), whereas camptothecin (10 mM) was added to induce apoptotic cell death, which was visualized by

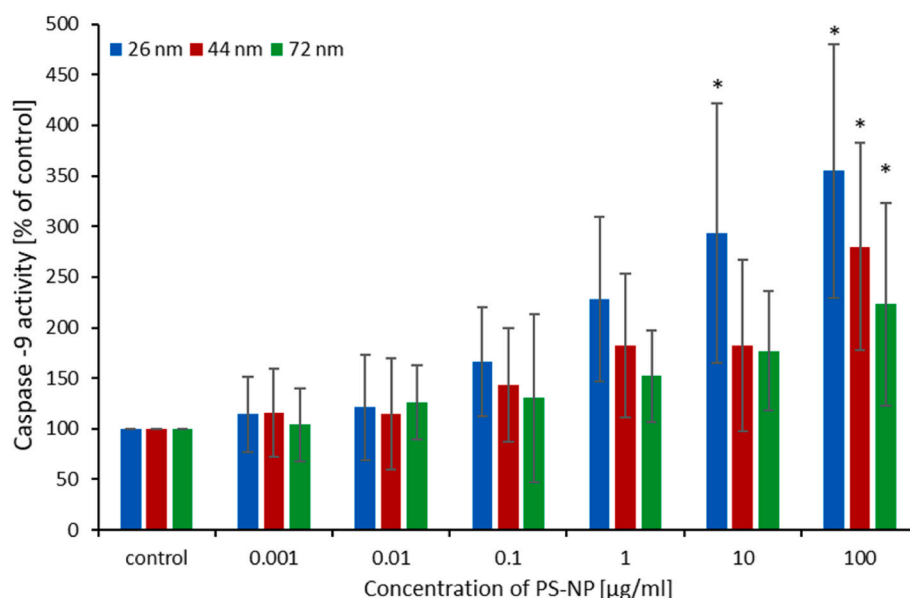


Fig. 5. Changes in caspase-9 activity in human PBMCs induced by different sized non-functionalized PS-NPs. Each value represents the mean \pm SD obtained from 6 independent experiments (6 blood donors), while mean value was obtained from at least 2 replications from each donor. Significantly different from control (*) $P < 0.05$; two-way ANOVA and a posteriori Tukey test.

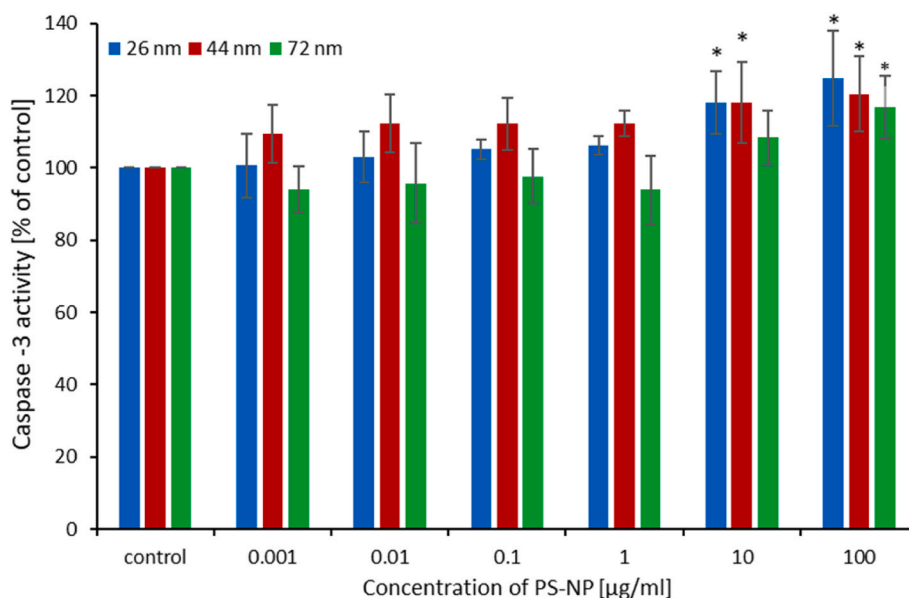


Fig. 6. Changes in caspase-3 activity in human PBMCs induced by different sized non-functionalized PS-NPs. Each value represents the mean \pm SD obtained from 5 independent experiments (5 blood donors), while mean value was obtained from at least 2 replications for each donor. Significantly different from control (*) $P < 0.05$; one-way and a posteriori Tukey test.

staining the cells with annexin V-FITC (green fluorescence).

3.2. Cytosolic calcium ions level

A statistically significant increase in calcium ion level was observed for all tested PS-NPs. PS-NPs of 29 nm and 44 nm increased this parameter from the concentrations of 0.001–0.1 $\mu\text{g/mL}$ and from 0.01 to 10 $\mu\text{g/mL}$, respectively. The highest PS-NPs of 72 nm increased this parameter at the concentrations of 0.1 and 10 $\mu\text{g/mL}$. Furthermore, a decrease in calcium ion level was observed at the highest concentration of 100 $\mu\text{g/mL}$ of PS-NPs tested, but it was statistically significant only for particles of 29 nm and 44 nm (Fig. 2).

3.3. Mitochondrial transmembrane potential ($\Delta\Psi_m$)

A statistically significant decrease in transmembrane mitochondrial potential was observed after incubation of PBMCs with different diameters of PS-NPs ($P < 0.05$). PS-NPs of 29 nm in diameter induced changes in tested parameter from the concentration of 1 $\mu\text{g/mL}$ (a decrease to $78\% \pm 13\%$ versus control), while PS-NPs of 44 nm and 72 nm in diameter induced alterations from the concentration of 10 $\mu\text{g/mL}$ (a decrease to $82\% \pm 10\%$ versus control and to $83\% \pm 7\%$ versus control respectively) (Fig. 3).

3.4. Caspase-8, -9 -3 activation

Caspase-8 is the initiator caspase of programmed cell death and is involved in the receptor pathway of apoptosis. This study showed that only PS-NPs of 29 nm in diameter activated caspase-8 in human PBMCs at the concentration of 1 $\mu\text{g/mL}$ (an increase to $160\% \pm 27\%$ versus control; $P < 0.05$), 10 $\mu\text{g/mL}$ (an increase to $180\% \pm 11\%$ versus control; $P < 0.01$), and 100 $\mu\text{g/mL}$ (an increase to $194\% \pm 39\%$ versus control; $P < 0.001$). Other NPs did not activate this enzyme (Fig. 4). Furthermore, the differences in caspase-8 activity were statistically significant between samples containing tested NPs of 72 nm, 44 nm and 29 nm at the concentrations of 10 $\mu\text{g/mL}$ and 100 $\mu\text{g/mL}$ ($P < 0.02$).

Then, we measured the activity of caspase-9, which is the initiator caspase of programmed cell death in the mitochondrial pathway of apoptosis. PS-NPs of 29 nm at the concentrations of 10 $\mu\text{g/mL}$ and 100 $\mu\text{g/mL}$ caused an increase in caspase-9 activation in tested cells after 24

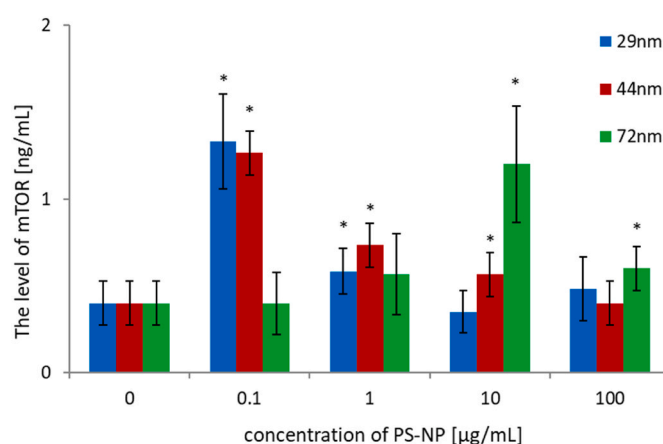


Fig. 7. Changes in the level of mTOR in human PBMCs incubated by different-sized non-functionalized PS-NPs in the concentrations ranging from 0.1 to 100 $\mu\text{g/mL}$ for 24 h. Data were presented as the mean \pm SD obtained from 6 measurements, mean value of at least 1 replications (6 donors). Significantly different from control (*) $P < 0.05$; Student's t-test for a single sample.

h of incubation (an increase to $290\% \pm 132\%$ versus control and to $355\% \pm 125\%$ versus control, respectively). PS-NPs of 44 nm and 72 nm increased the activity of this enzyme only at 100 $\mu\text{g/mL}$ (an increase to $280\% \pm 102\%$ versus control and to $223\% \pm 101\%$ versus control, respectively) (Fig. 5). Differences in caspase-9 activity were statistically significant between samples containing NPs of 72 nm and 29 nm at the concentrations of 10 $\mu\text{g/mL}$ ($P < 0.02$) and 100 $\mu\text{g/mL}$ ($P < 0.001$).

We also detected caspase-3 activation, which is an executioner caspase of apoptosis. It was found that after 24 h of incubation, PS-NPs of 29 nm ($P < 0.001$) and 44 nm ($P < 0.02$) at the concentrations of 10 $\mu\text{g/mL}$ (an increase to $118\% \pm 9\%$ versus control and to $118\% \pm 11\%$ versus control, respectively) and 100 $\mu\text{g/mL}$ (an increase to $125\% \pm 13\%$ versus control and to $120\% \pm 10\%$ versus control, respectively) increased caspase-3 activation in the tested cells (Fig. 6). PS-NPs of 72 nm in diameter activated caspase-3 at their highest concentration of 100 $\mu\text{g/mL}$ (an increase to $117\% \pm 9\%$ versus control, $P > 0.05$). The differences in caspase-3 activity were not statistically significant between

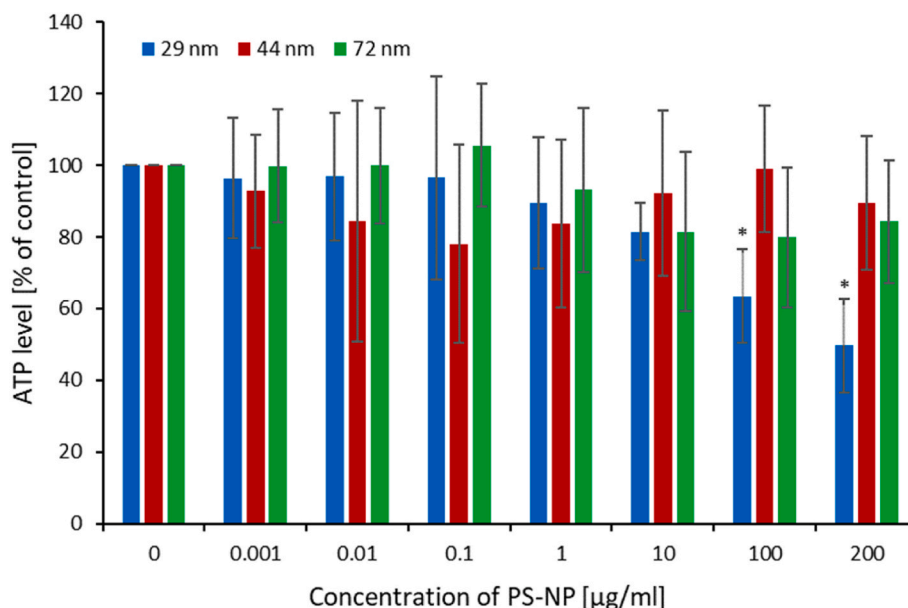


Fig. 8. Changes in ATP level in human PBMCs incubated with different-sized non-functionalized PS-NPs in the concentrations ranging from 0.001 to 200 µg/mL for 24 h. Each value represents the mean \pm SD obtained from 5 experiments (5 blood donors), while mean value was obtained from at least 3 replications for each donor. Significantly different from control (*) $P < 0.05$; one-way ANOVA and a posteriori Tukey test.

the samples containing tested NPs of 72 nm and 44 nm, as well as 26 nm in the concentrations of 10 µg/mL and 100 µg/mL ($P > 0.05$) (two-way ANOVA and a posteriori Tukey test).

3.5. mTOR level

A statistically significant increase in the level of mTOR was observed after incubation of PBMCs with different-sized PS-NPs. PS-NPs of 29 nm diameters caused an increase in the level of mTOR at the concentrations range from 0.1 to 1 µg/mL ($P < 0.05$), while PS-NPs of 44 nm raised the parameter studied at the concentrations of 0.1 µg/mL to 10 µg/mL ($P < 0.05$). The biggest NPs of 72 nm of diameters increased mTOR level at their highest concentrations of 10 µg/mL and 100 µg/mL ($P < 0.05$) (Fig. 7).

3.6. ATP level

PS-NPs of 29 nm of diameter decreased the ATP level at the concentrations of 100 µg/mL and 200 µg/mL in human PBMCs (a decrease to $63\% \pm 13\%$ versus control, and to $50\% \pm 13\%$ versus control, respectively). Other tested NPs did not change this parameter (Fig. 8). No differences in ATP level between different-sized NPs were found ($P > 0.05$) (two-way ANOVA and a posteriori Tukey test).

4. Discussion

Apoptosis is one of the key processes involved in the cell cycle, hormone-dependent atrophy, embryonic development, normal immune function, and chemical-induced cell death (Elmore, 2007). Several studies have shown that PS-NPs interact with cell membranes, resulting in alterations in membrane integrity, disturbances in ion transport, and signal transduction (Elliott, 2017; Jin et al., 2019; Pinsino et al., 2017). The response to nanoplastic toxicity plays a major role in cellular organelles, mainly mitochondria, whose main role is to produce ATP. Mitochondria are responsible for processes, such as bioenergetics, cell signaling, and biosynthesis. Mitochondria produce reactive oxygen species (ROS) and redox compounds, as well as store calcium ions, therefore, they act as regulators of various related signaling pathways, which can contribute to many pathologies (Marciniak, 2017; Schwarz

and Blower, 2016). It has been proven that dysregulation of mitochondrial functions plays a key role in the pathogenesis and development of numerous types kinds of diseases, including cancer, metabolic syndromes, cardiovascular disease, obesity, neurodegenerative diseases, and may accelerate the aging process. These reports are were confirmed by the studies of Ly et al. (2003) who showed that mitochondrial dysfunction, resulting in the collapse of the transmembrane potential, is a parameter that can determine apoptosis induction, although most studies have shown that apoptotic triggering reduces the total level of ATP in the cell to some extent (Heiden et al., 1999; Lieberthal et al., 1998; Nomura et al., 1999; Waterhouse et al., 2001; Wu et al., 2019). Furthermore, Pinton et al. (2008) showed that calcium ions accumulated in the mitochondria and the endoplasmic reticulum are important secondary messengers in the control of apoptotic cell death.

Due to the lack of sufficient data on the mechanism of proapoptotic action of PS-NPs on PBMCs, we decided to conduct such research. Furthermore, we also taken into account our preliminary analysis, which showed that PS-NPs at 29 nm in diameter caused about 8% increase in the number (expressed as a percent) of apoptotic cells already at the concentration of 1 µg/mL (vs. control 2%), whereas PS-NPs at 44 nm induced apoptotic changes from the concentration of 10 µg/mL (14%). Moreover, At the highest tested concentration of 100 µg/mL, PS-NPs of 29 nm, 44 nm and 72 nm increased the number of apoptotic cells up to 23%, 16% and 9%, respectively (Kik et al., 2021).

In the first stage of our analysis, using Annexin V-FITC/PI double staining assay, we confirmed the induction of apoptosis under the influence of the tested NPs, which was previously determined using flow cytometry (Kik et al., 2021). The highest increase in the number of apoptotic cells was observed after treatment of the PBMCs with PS-NPs of 29 nm, then NPs of 44 nm, and finally NPs of 70 nm.

Then, we examined changes in the level of cytosolic calcium ions and changes in mitochondrial transmembrane potential ($\Delta\Psi_m$) in tested cells incubated with examined PS-NPs in the concentrations range from 0.001 to 100 µg/mL for 24 h. A statistically significant increase in the level of cytosolic calcium ions was observed in PBMCs incubated with all tested NPs at low concentrations of 0.001–0.1 µg/mL (Fig. 2). The calcium ion is an important regulator of apoptosis. An increase in Ca^{2+} mitochondrial uptake results in a change in mitochondrial depolarization, and then the opening of the mitochondrial permeability transition

pore (mPTP), which leads to apoptotic cell death. Calcium ions can also activate calpains, which cleave various proteins from the BCL-2 family (D'Orsi et al., 2012; Hajnóczky et al., 2003; Sukumaran et al., 2021). Our results indicated an increase in calcium ion level at the concentrations lower than those that caused changes in other apoptotic parameters, indicating that this process preceded the entire cascade of apoptotic changes.

We also observed a statistically significant decrease in mitochondrial transmembrane potential in cells treated with all tested particles. NPs with a diameter of 29 nm caused changes in $\Delta\Psi_m$ from the concentration of 1 $\mu\text{g/mL}$, while larger particles induced alterations in this parameter from the concentration of 10 $\mu\text{g/mL}$. Tang et al. (2022) studied the effect of PS-NPs of 50 nm at the concentrations of 20, 50, 100 and 200 $\mu\text{g/mL}$ on SHY-5Y human neuroblastoma cells. This analysis showed that PS-NPs caused mitochondrial damage resulting from increased release of lactate dehydrogenase, inhibition of cell proliferation, stimulation of oxidative stress response, increased Ca^{2+} level, and apoptosis. In addition, they observed a decrease in of the mitochondrial transmembrane potential and the level of adenosine triphosphate level in examined cells. Other studies have revealed that the exposure of human astrocytoma cells to modification with 50 nm diameter of PS-NPs amines modifications caused mitochondrial damage to the mitochondria, and consequently led to their apoptotic death (Wang et al., 2013). Another study also confirmed the above findings. Lu et al. (2022) proved that PS-NPs with a diameter of 20 nm at the concentration of 80 $\mu\text{g/mL}$ could disrupt the integrity of the cell membrane in Caco-2 cells. In these studies, a significant increase in ROS level was observed, which was associated with the loss of mitochondrial transmembrane potential. Other researchers have also observed an increase in the level of ROS and NADPH₄ oxidase (NOX-4-ROS generator, located in the mitochondria and the endoplasmic reticulum) in A549 lung epithelial cells treated with PS-NPs (Halimu et al., 2022). Mitochondrial damage, such as suppression of mitochondrial respiration and changes in mitochondrial transmembrane potential, has been also reported in human liver cells exposed to PS-NPs of 80 nm (Lin et al., 2022). Many other studies have also confirmed that plastic particles induce mitochondrial disorders (Florance et al., 2022; Wang et al., 2021; Zhang et al., 2022).

ROS also play a central role in cell signaling and in regulation of the main pathways of apoptosis mediated by mitochondria, death receptors, and the endoplasmic reticulum. Elevated levels of cytosolic calcium ions and increased ROS formation are known to reduce electrolyte transport across the mitochondrial membrane, leading to the opening of PTP and reduction of $\Delta\Psi_m$ (Wacquier et al., 2020). Finally, various proapoptotic proteins are released, activating the mitochondrial death pathway (Moungjaroen et al., 2006; Oliveira et al., 2019). ROS can bind to death receptors containing the death domain (DD) and initiate the extrinsic pathway of apoptosis (Zhang et al., 2005). Studies of PS-NPs have indicated the induction of oxidative stress by these molecules by through generating intracellular ROS (Liu et al., 2020; Sarasamma et al., 2020). In the study of Li et al. (2022), the exposure of mice to plastic NPs led to apoptosis induction, an increase in the expression of proteins associated with this process, ROS production, and alterations in mitochondrial transmembrane potential in spleen lymphocytes. Furthermore, Hu et al. (2021) showed that the fluorescent PS-NPs with a diameter of 42 nm activated the p38 MAPK signaling pathway in RAW 264.7 cells of Zebrafish *rerio* larvae, which showed that they induced apoptosis. Also, our previous results (Kik et al., 2021) showed that the NPs tested increased ROS level and caused the oxidation of lipids and proteins in human PBMCs. The consequence of these processes may be DNA lesions, such as single/double-strand breaks formation, purines and pyrimidines oxidation, and 8-oxo-dG creation (only PS-NPs of 29 nm of diameter) (Malinowska et al., 2022). These oxidative changes, which increase ROS level, and DNA damage can induce apoptosis directly through the DNA damage reaction (DDR). DDR promotes apoptosis and prevents the spread of abnormal cells. The tumor suppressor protein p53 is one of the most important molecules that control DNA damage. P53 is capable of

inducing apoptosis by interacting with apoptotic protein Bax and block this process through antiapoptotic factor Bcl2 (Baran et al., 2014). Schmidt et al. (2023) showed that after acute exposure to nano- and microplastic PS, the expression pattern of the p53 tumor suppressor protein increased in murine skin cells.

The process of apoptosis is strictly regulated by enzymes in the cysteine protease group, the so-called caspases. Early markers of programmed cell death, include caspases-8 and caspase-9 activation classified as initiating and caspase-3 classified as executive (Elmore, 2007). That is why, we measured their activity next. For this purpose, we incubated PBMCs with PS-NPs in the concentrations range from 0.001 to 100 $\mu\text{g/mL}$. We observed that only PS-NPs with a diameter of 29 nm caused statistically significant changes in the activity of all studied caspases. On the other hand, particles with diameters of 44 nm and 72 nm caused changes in the activity of caspase-9 and caspase-3, while they did not activate caspase -8. Xu et al. (2019) evaluated the effects of 25 nm and 70 nm PS-NPs on a human alveolar epithelial cell line A549. They observed that the tested NPs induced a significant change (up-regulation) in the expression of proapoptotic proteins, i.e., caspases-3, -8, and -9 and cytochrome c, which resulting in apoptosis. Furthermore, research conducted by Liu et al. (2022) showed that PS-NPs of 50 nm, 500 nm and 5 μm triggered apoptosis in rat basophilic leukemia (RBL-2H3) cells. They observed that antiapoptotic genes (Bcl-2) were down-regulated, and proapoptotic Bax and caspase-3 genes were up-regulated. PS-NPs by induction of oxidative stress led to mitochondrial and lysosomal damage, arrested disturbed the cell cycle in the G0/G1 phase, and caused apoptosis. In other studies, PS-NPs have been shown to induce apoptosis in mouse cell lines (L. Liu et al., 2022), and mouse intestinal epithelial cells (Liang et al., 2022). Banerjee et al. (2021) studied the effect of PS-NPs with a size of 50–5000 nm in the concentrations range of 0.1–100 $\mu\text{g/mL}$ on gastric epithelial cells (SNU-1). Exposure of SNU-1 to PS-NPs was shown to increase caspase-8 and caspase-3 activities. Additionally, the tested particles changed the levels of BAX and Bcl-2, which play a significant role in the progression of apoptosis (Kale et al., 2018). Other researchers have shown that up-regulation of BAX results in apoptotic cell death as a result of damage to the outer mitochondrial membrane (permeabilization). Bcl-2 inactivates BAX, thus performing a pro- or anti-apoptotic function (Boersma et al., 1997; Olsson and Zhivotovsky, 2011; Westphal et al., 2014). Bexiga et al. (2011) observed activation of caspases 3/7 and caspase-9 in the human astrocytoma cell line exposed to PS-NPs. These results suggested that PS-NPs may have mediated cell death through an apoptotic mechanism associated with mitochondrial damage. Subsequent studies revealed that in male rats exposed to PS-NPs at a dose of 3 mg/kg/day, there was an increase in the expression of genes associated with apoptosis (Yasin et al., 2022). They observed positive expression of caspase 3.

We also revealed that caspase-8 activity increased after the incubation of PBMCs with the smallest 26 nm NPs. These particles also caused the largest oxidative changes (Kik et al., 2021) and most strongly increased ROS level (Malinowska et al., 2022). This high ROS increase was likely to activate the external pathway of apoptotic cell death. It has been shown that ROS activates transmembrane death receptors, such as Fas, TRAIL-R1/2 and TNF-R1. Apoptosis mediated by death receptor involves the recruitment of the adapter proteins FADD and procaspase-8 or-10 to the cytoplasmic surface of the receptor to form death-inducing signal complex (DISC). This results in the activation of caspase-8/-10 that can directly activate caspases-3/-6/-7, and induce apoptosis. Caspases-8/-10 are also capable of dividing Bid into tBid, which activates a pathway of crosstalk between the death receptor and the mitochondria. tBid moves to mitochondria and blocks the anti-apoptotic activity of Bcl-2 and Bcl-XL, thus activating Bax and Bak. This results in the release of cytochrome c and the Smac/Diablo into the cytosol, and activation of the intrinsic apoptosis pathway (Redza-Dutordoir and Averill-Bates, 2016).

mTOR acts as a master switch of cell catabolism and anabolism.

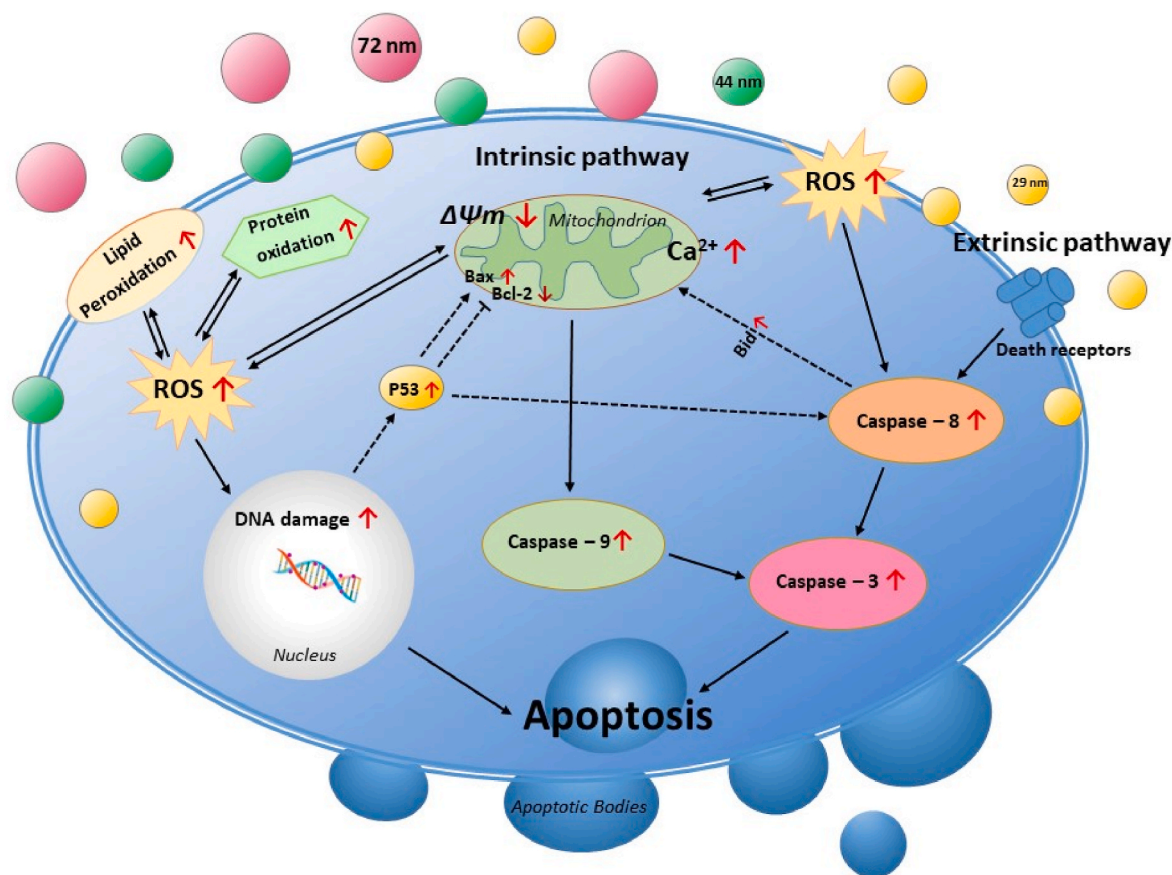


Fig. 9. Proposed mechanism of apoptosis induction in PBMCs based on the obtained results in this study and previously published results by our team (continuous arrow) and suggested changes based on literature data (dashed arrow). All tested PS-NPs induced apoptosis by the involvement of the mitochondrial pathway (increase of cytosolic Ca^{2+} level, decrease of transmembrane mitochondrial potential, activation of caspase-9 and -3). Moreover, the smallest NPs of 29 nm of diameter increased caspase-8 activity, activating the external pathway of apoptosis, probably through a high increase in ROS level induction. All PS-NPs tested increased ROS level, lipid and protein peroxidation (Kik et al., 2021), and consequently caused DNA damage (Malinowska et al., 2022), which probably due to increased p53 level induced apoptosis.

mTOR was recently found to have profound effect on apoptosis control. mTOR is a serine/threonine kinase, which transfers signals by direct phosphorylation or by inhibiting PP2A phosphatase (Castedo et al., 2002). Cytokines, growth factors, such as insulin, nutrients, including amino acids, glucose, and nucleotides, as well as, cellular stressors, including ROS and hypoxia are capable of regulating of mTOR activation in T cells (Huang et al., 2020). Microplastics may influence reproductive function of male by activating various signaling pathways, such as mTOR (Dubey et al., 2022; Wei et al., 2021). mTOR signaling is regulated by Ca^{2+} binding proteins, particularly calmodulin (Amemiya et al., 2023; Li et al., 2016). We observed an increase in the level of cytosolic calcium in tested PBMCs incubated already with low concentrations of NPs, which could be a cause of mTOR activation. We noticed an increase in mTOR level in PBMCs exposed to PS-NPs concentrations lower than those, which triggered apoptosis (0.1 $\mu\text{g/mL}$ - 26 nm; 0.1 $\mu\text{g/mL}$ and 1 $\mu\text{g/mL}$ - 44 nm and 10 $\mu\text{g/mL}$ - 72 nm) or at the concentrations that had negligible effect on apoptosis (1 $\mu\text{g/mL}$ - 26 nm; 10 $\mu\text{g/mL}$ - 44 nm and 100 $\mu\text{g/mL}$ for 72 nm). Where a significant increase in apoptosis was found, the mTOR level returned to the control value (10 $\mu\text{g/mL}$ and 100 $\mu\text{g/mL}$ - 26 nm; 100 $\mu\text{g/mL}$ - 44 nm). Thus, the reduction of elevated mTOR levels resulted in an intensification of apoptosis (Saxton and Sabatini, 2017). The induction of the mTOR protein that we observed at low PS-NPs concentrations is in agreement with the data published by Wang et al. (2022) and Castedo et al. (2002). Wang et al. (2022) showed that mTOR modulates apoptosis of endoplasmic CD4⁺T cells induced by stress through ROS in septic immunosuppression. Castedo et al. showed

that mTOR kinase contributes to apoptosis induced by the HIV-1 Env glycoprotein of the HIV-1 virus (Castedo et al., 2002). The immunofluorescence methods used by them showed that the mTOR kinase protein was accumulated in the nucleus of synaptic cells, before the phosphorylation of P53 protein. After P53 phosphorylation, the next step of apoptosis in these cells was to activate BAX protein, increase mitochondrial permeability, release cytochrome c and activate cascade of caspases.

The studies have shown that the total level of ATP (Budd et al., 2000; Leist et al., 1997) remains unchanged in the early stages of apoptosis, and Lu et al. (2022) even suggested that the prerequisite for apoptotic cell death is an increase in ATP levels in the cytosol. In our studies, we did not noted observed elevated ATP level, but only a decrease in this parameter after exposure of PBMCs to the highest concentrations (100 $\mu\text{g/mL}$ and 200 $\mu\text{g/mL}$) of the smallest NPs of 29 nm. Apoptosis is an active process that requires energy and the primary energy carrier in mitochondria is ATP, which is essential for all living cells. Researchers have suggested that intracellular ATP levels may modulate externalization of phosphatidylserine during apoptosis and indicated to ATP-dependent translocation of aminophospholipids in this process (Gleiss et al., 2002). Imamura et al. (2020) showed that cytosolic ATP affects caspase-3 activation, and this process usually ends within 2 h. Programmed cell death occurs when ATP is depleted, but only when there is sufficient energy in the cell to activate the pathways that mediate and induce cell death (Imamura et al., 2020). If a decrease in ATP level is constant, it can lead to necrosis. A decrease in metabolic

activity in PBMCs measured by the MTT test under the influence of PS-NPs with a diameter of 29 nm was shown in previous studies but only from their high concentration of 300 µg/mL (Malinowska et al., 2022), while a decrease in cell viability (necrotic changes) (stained with calcein and PI measured by the cytometric method) occurred even from the concentration of 500 µg/mL (Kik et al., 2021). A decreased ATP level was also observed in mouse GC-2 cells and in various regions of the mouse brain after exposure to PS-NPs (Liang et al., 2022; T. Liu et al., 2022).

In summary, the PS-NPs studied induced apoptosis by the involvement of the mitochondrial pathway; although the smallest NPs of 29 nm in diameter also activated the external pathway, probably via induction high ROS level (Fig. 9). Similarly, as in our previous studies on the pro-oxidative and genotoxic potential, the greatest apoptotic effects were provoked by the smallest PS-NPs of 29 nm, when compared to PS-NPs of larger diameter (72 nm). Furthermore, we have demonstrated an increase in mTOR level preceding apoptosis, and its return to control value as a result of enhanced apoptosis.

5. Conclusion

1. Tested PS-NPs induced apoptosis by the involvement of the mitochondrial pathway by increasing the cytosolic Ca^{2+} level, decreasing of transmembrane mitochondrial potential, and activating caspase-9 and caspase-3.
2. The smallest PS-NPs of 29 nm in diameter also increased caspase-8 activity, activating the extrinsic pathway of apoptosis.
3. An increase in the level of mTOR was observed before apoptosis was triggered, and its level returned to control value, when apoptosis escalated.
4. Apoptotic changes and an increase in mTOR level depended on the size of the tested NPs. The largest changes were induced by the smallest nanoparticles with a diameter of 29 nm.
5. Apoptotic changes were noted at PS-NPs concentrations that are unlikely to be found in the blood of people who are environmentally exposed to these particles.

Funding

This work was financed by a statutory research admitted by Department of Biophysics of Environmental Pollution, University of Lodz (number B211100000191.01).

Declaration of competing interest

The authors declare that they have no known competing financial interests or personal relationships that could have appeared to influence the work reported in this paper.

Data availability

Data will be made available on request.

Appendix A. Supplementary data

Supplementary data to this article can be found online at <https://doi.org/10.1016/j.chemosphere.2023.139137>.

References

- Amemiya, Y., Maki, M., Shibata, H., Takahara, T., 2023. New insights into the regulation of mTOR signaling via Ca^{2+} -binding proteins. *IJMS* 24, 3923. <https://doi.org/10.3390/ijms24043923>.
- Banerjee, A., Billey, L.O., Shelver, W.L., 2021. Uptake and toxicity of polystyrene micro/nanoplastics in gastric cells: effects of particle size and surface functionalization. *PLoS One* 16, e0260803. <https://doi.org/10.1371/journal.pone.0260803>.
- Baran, K., Rodriguez, D., Green, D., 2014. The DNA damage response mediates apoptosis and tumor suppression. In: Wu, H. (Ed.), *Cell Death*. Springer New York, New York, NY, pp. 135–165. https://doi.org/10.1007/978-1-4614-9302-0_7.
- Barańska, A., Bukowska, B., Michałowicz, J., 2022. Determination of apoptotic mechanism of action of tetrabromobisphenol A and tetrabromobisphenol S in human peripheral blood mononuclear cells: a comparative study. *Molecules* 27, 6052. <https://doi.org/10.3390/molecules27186052>.
- Bexiga, M.G., Varela, J.A., Wang, F., Fenaroli, F., Salvati, A., Lynch, I., Simpson, J.C., Dawson, K.A., 2011. Cationic nanoparticles induce caspase 3-, 7- and 9-mediated cytotoxicity in a human astrocytoma cell line. *Nanotoxicology* 5, 557–567. <https://doi.org/10.3109/17435390.2010.539713>.
- Boersma, A.W.M., Nooter, K., Burger, H., Kortland, C.J., Stoter, G., 1997. Bax upregulation is an early event in cisplatin-induced apoptosis in human testicular germ-cell tumor cell line NT2, as quantitated by flow cytometry. *Cytometry* 27, 275–282. [https://doi.org/10.1002/\(SICI\)1097-0320\(19970301\)27:3<275::AID-CYTO10>3.0.CO;2](https://doi.org/10.1002/(SICI)1097-0320(19970301)27:3<275::AID-CYTO10>3.0.CO;2).
- Budd, S.L., Tennen, L., Lishnak, T., Lipton, S.A., 2000. Mitochondrial and extramitochondrial apoptotic signaling pathways in cerebrocortical neurons. *Proc. Natl. Acad. Sci. U.S.A.* 97, 6161–6166. <https://doi.org/10.1073/pnas.100121097>.
- Castedo, M., Ferri, K.F., Kroemer, G., 2002. Mammalian target of rapamycin (mTOR): pro- and anti-apoptotic. *Cell Death Differ.* 9, 99–100. <https://doi.org/10.1038/sj.cdd.4400978>.
- Chu, C.-M., Chiu, L.-C., Yu, C.-C., Chuang, L.-P., Kao, K.-C., Li, L.-F., Wu, H.-P., 2021. Increased death of peripheral blood mononuclear cells after TLR4 inhibition in sepsis is not via TNF/TNF receptor-mediated apoptotic pathway. *Mediat. Inflamm.* 2021, 1–9. <https://doi.org/10.1155/2021/2255017>.
- Dalela, M., Shrivastav, T.G., Kharbada, S., Singh, H., 2015. pH-sensitive biocompatible nanoparticles of paclitaxel-conjugated poly(styrene-co-maleic acid) for anticancer drug delivery in solid tumors of syngeneic mice. *ACS Appl. Mater. Interfaces* 7, 26530–26548. <https://doi.org/10.1021/acsami.5b07764>.
- Deng, Y., Zhang, Y., Lemos, B., Ren, H., 2017. Tissue accumulation of microplastics in mice and biomarker responses suggest widespread health risks of exposure. *Sci. Rep.* 7, 46687. <https://doi.org/10.1038/srep46687>.
- D'Orsi, B., Bonner, H., Tuffy, L.P., Düssmann, H., Woods, I., Courtney, M.J., Ward, M.W., Prehn, J.H.M., 2012. Calpains are downstream effectors of bax-dependent excitotoxic apoptosis. *J. Neurosci.* 32, 1847–1858. <https://doi.org/10.1523/JNEUROSCI.2345-11.2012>.
- Dubey, I., Khan, S., Kushwaha, S., 2022. Developmental and reproductive toxic effects of exposure to microplastics: a review of associated signaling pathways. *Front. Toxicol.* 4, 901798. <https://doi.org/10.3389/ftox.2022.901798>.
- EFSA Panel on Contaminants in the Food Chain (CONTAM), 2016. Presence of microplastics and nanoplastics in food, with particular focus on seafood. *EFSA J.* 14, 14501. <https://doi.org/10.2903/j.efsa.2016.4501>.
- Elliott, J., 2017. Toward achieving harmonization in a nanocytotoxicity assay measurement through an interlaboratory comparison study. *ALTEX* 201–218. <https://doi.org/10.14573/altex.1605021>.
- Elmore, S., 2007. Apoptosis: a review of programmed cell death. *Toxicol. Pathol.* 35, 495–516. <https://doi.org/10.1080/01926230701320337>.
- Favaloro, B., Allocati, N., Graziano, V., Di Ilio, C., De Laurenzi, V., 2012. Role of apoptosis in disease. *Aging* 4, 330–349. <https://doi.org/10.18632/aging.100459>.
- Florance, I., Chandrasekaran, N., Gopinath, P.M., Mukherjee, A., 2022. Exposure to polystyrene nanoplastics impairs lipid metabolism in human and murine macrophages in vitro. *Ecotoxicol. Environ. Saf.* 238, 113612. <https://doi.org/10.1016/j.ecoenv.2022.113612>.
- Forde, M., Iachetta, G., Tussellino, M., Carotenuto, R., Prisco, M., De Falco, M., Laforgia, V., Valiante, S., 2016. Polystyrene nanoparticles internalization in human gastric adenocarcinoma cells. *Toxicol. Vitro* 31, 126–136. <https://doi.org/10.1016/j.tiv.2015.11.006>.
- Gasper, J., Wright, S.L., Dris, R., Collard, F., Mandin, C., Guerrouache, M., Langlois, V., Kelly, F.J., Tassin, B., 2018. Microplastics in air: are we breathing it in? *Curr. Opin. in Environ. Sci. Health* 1, 1–5. <https://doi.org/10.1016/j.coesh.2017.10.002>.
- Geiser, M., Kreyling, W.G., 2010. Deposition and biokinetics of inhaled nanoparticles. *Part. Fibre Toxicol.* 7, 2. <https://doi.org/10.1186/1743-8977-7-2>.
- Gleiss, B., Gogvadze, V., Orrenius, S., Fadeel, B., 2002. Fas-triggered phosphatidylserine exposure is modulated by intracellular ATP. *FEBS (Fed. Eur. Biochem. Soc.) Lett.* 519, 153–158. [https://doi.org/10.1016/S0014-5793\(02\)02743-6](https://doi.org/10.1016/S0014-5793(02)02743-6).
- Grafmueller, S., Manser, P., Diener, L., Diener, P.-A., Maeder-Althaus, X., Maurizi, L., Jochum, W., Krug, H.F., Buerki-Thurnherr, T., von Mandach, U., Wick, P., 2015. Bidirectional transfer study of polystyrene nanoparticles across the placental barrier in an ex vivo human placental perfusion model. *Environ. Health Perspect.* 123, 1280–1286. <https://doi.org/10.1289/ehp.1409271>.
- Hajnóczky, G., Davies, E., Madesh, M., 2003. Calcium signaling and apoptosis. *Biochem. Biophys. Res. Commun.* 304, 445–454. [https://doi.org/10.1016/S0006-291X\(03\)00616-8](https://doi.org/10.1016/S0006-291X(03)00616-8).
- Halimu, G., Zhang, Q., Liu, L., Zhang, Z., Wang, X., Gu, W., Zhang, B., Dai, Y., Zhang, H., Zhang, C., Xu, M., 2022. Toxic effects of nanoplastics with different sizes and surface charges on epithelial-to-mesenchymal transition in A549 cells and the potential toxicological mechanism. *J. Hazard Mater.* 430, 128485. <https://doi.org/10.1016/j.jhazmat.2022.128485>.
- Hallit, S., Salameh, P., 2017. Exposure to toxics during pregnancy and childhood and asthma in children: a pilot study. *JEGH* 7, 147. <https://doi.org/10.1016/j.jegh.2017.04.004>.
- Haupt, S., Berger, M., Goldberg, Z., Haupt, Y., 2003. Apoptosis - the p53 network. *J. Cell Sci.* 116, 4077–4085. <https://doi.org/10.1242/jcs.00739>.

- Heiden, M.G.V., Chandel, N.S., Schumacker, P.T., Thompson, C.B., 1999. Bcl-xL prevents cell death following growth factor withdrawal by facilitating mitochondrial ATP/ADP exchange. *Mol. Cell* 3, 159–167. [https://doi.org/10.1016/S1097-2765\(00\)80307-X](https://doi.org/10.1016/S1097-2765(00)80307-X).
- Hernandez, L.M., Xu, E.G., Larsson, H.C.E., Tahara, R., Maisuria, V.B., Tufenkji, N., 2019. Plastic teabags release billions of microparticles and nanoparticles into tea. *Environ. Sci. Technol.* 53, 12300–12310. <https://doi.org/10.1021/acs.est.9b02540>.
- Hernandez, L.M., Yousefi, N., Tufenkji, N., 2017. Are there nanoplastics in your personal care products? *Environ. Sci. Technol. Lett.* 4, 280–285. <https://doi.org/10.1021/acs.estlett.7b00187>.
- Hu, Q., Wang, H., He, C., Jin, Y., Fu, Z., 2021. Polystyrene nanoparticles trigger the activation of p38 MAPK and apoptosis via inducing oxidative stress in zebrafish and macrophage cells. *Environ. Pollut.* 269, 116075 <https://doi.org/10.1016/j.envpol.2020.116075>.
- Huang, H., Long, L., Zhou, P., Chapman, N.M., Chi, H., 2020. mTOR signaling at the crossroads of environmental signals and T-cell fate decisions. *Immunol. Rev.* 295, 15–38. <https://doi.org/10.1111/imr.12845>.
- Hussain, N., 2001. Recent advances in the understanding of uptake of microparticles across the gastrointestinal lymphatics. *Adv. Drug Deliv. Rev.* 50, 107–142. [https://doi.org/10.1016/S0169-409X\(01\)00152-1](https://doi.org/10.1016/S0169-409X(01)00152-1).
- Imamura, H., Sakamoto, S., Yoshida, T., Matsui, Y., Penuela, S., Laird, D.W., Mizukami, S., Kikuchi, K., Kakizuka, A., 2020. Single-cell dynamics of pannexin-1-facilitated programmed ATP loss during apoptosis. *Elife* 9, e61960. <https://doi.org/10.7554/eLife.61960>.
- Jin, Y., Lu, L., Tu, W., Luo, T., Fu, Z., 2019. Impacts of polystyrene microplastic on the gut barrier, microbiota and metabolism of mice. *Sci. Total Environ.* 649, 308–317. <https://doi.org/10.1016/j.scitotenv.2018.08.353>.
- Jing, J., Zhang, L., Han, L., Wang, J., Zhang, W., Liu, Z., Gao, A., 2022. Polystyrene micro-/nanoplastics induced hematopoietic damages via the crosstalk of gut microbiota, metabolites, and cytokines. *Environ. Int.* 161, 107131 <https://doi.org/10.1016/j.envint.2022.107131>.
- Kale, J., Osterlund, E.J., Andrews, D.W., 2018. BCL-2 family proteins: changing partners in the dance towards death. *Cell Death Differ.* 25, 65–80. <https://doi.org/10.1038/cdd.2017.186>.
- Kik, K., Bukowska, B., Krokosz, A., Sicińska, P., 2021. Oxidative properties of polystyrene nanoparticles with different diameters in human peripheral blood mononuclear cells (in vitro study). *IJMS* 22, 4406. <https://doi.org/10.3390/ijms22094406>.
- Kreyling, W.G., Holzwarth, U., Haberl, N., Kozempel, J., Hirn, S., Wenk, A., Schleh, C., Schäffler, M., Lipka, J., Semmler-Behnke, M., Gibson, N., 2017. Quantitative biokinetics of titanium dioxide nanoparticles after intravenous injection in rats: Part 1. *Nanotoxicology* 11, 434–442. <https://doi.org/10.1080/17435390.2017.1306892>.
- Kwiatkowska, M., Michałowicz, J., Jarosiewicz, P., Pingot, D., Sicińska, P., Huras, B., Zakrzewski, J., Jarosiewicz, M., Bukowska, B., 2020. Evaluation of apoptotic potential of glyphosate metabolites and impurities in human peripheral blood mononuclear cells (in vitro study). *Food Chem. Toxicol.* 135, 110888 <https://doi.org/10.1016/j.fct.2019.110888>.
- Leist, M., Single, B., Castoldi, A.F., Kühnle, S., Nicotera, P., 1997. Intracellular adenosine triphosphate (ATP) concentration: a switch in the decision between apoptosis and necrosis. *J. Exp. Med.* 185, 1481–1486. <https://doi.org/10.1084/jem.185.8.1481>.
- Leslie, H.A., van Velzen, M.J.M., Brandsma, S.H., Vethaak, A.D., Garcia-Vallejo, J.J., Lamoree, M.H., 2022. Discovery and quantification of plastic particle pollution in human blood. *Environ. Int.* 163, 107199 <https://doi.org/10.1016/j.envint.2022.107199>.
- Li, R.-J., Xu, J., Fu, C., Zhang, J., Zheng, Y.G., Jia, H., Liu, J.O., 2016. Regulation of mTORC1 by lysosomal calcium and calmodulin. *Elife* 5, e19360. <https://doi.org/10.7554/eLife.19360>.
- Li, Yuqi, Xu, M., Zhang, Z., Halimu, G., Li, Yongqiang, Li, Yansheng, Gu, W., Zhang, B., Wang, X., 2022. In vitro study on the toxicity of nanoplastics with different charges to murine splenic lymphocytes. *J. Hazard Mater.* 424, 127508 <https://doi.org/10.1016/j.jhazmat.2021.127508>.
- Liang, B., Huang, Y., Zhong, Y., Li, Z., Ye, R., Wang, B., Zhang, B., Meng, H., Lin, X., Du, J., Hu, M., Wu, Q., Sui, H., Yang, X., Huang, Z., 2022. Brain single-nucleus transcriptomics highlights that polystyrene nanoplastics potentially induce Parkinson's disease-like neurodegeneration by causing energy metabolism disorders in mice. *J. Hazard Mater.* 430, 128459 <https://doi.org/10.1016/j.jhazmat.2022.128459>.
- Lieberthal, W., Menza, S.A., Levine, J.S., 1998. Graded ATP depletion can cause necrosis or apoptosis of cultured mouse proximal tubular cells. *Am. J. Physiol. Ren. Physiol.* 274, F315–F327. <https://doi.org/10.1152/ajprenal.1998.274.2.F315>.
- Lin, S., Zhang, H., Wang, C., Su, X.-L., Song, Y., Wu, P., Yang, Z., Wong, M.-H., Cai, Z., Zheng, C., 2022. Metabolomics reveal nanoplastic-induced mitochondrial damage in human liver and lung cells. *Environ. Sci. Technol.* 56, 12483–12493. <https://doi.org/10.1021/acs.est.2c03980>.
- Liu, L., Liu, B., Zhang, B., Ye, Y., Jiang, W., 2022. Polystyrene micro(nano)plastics damage the organelles of RBL-2H3 cells and promote MOAP-1 to induce apoptosis. *J. Hazard Mater.* 438, 129550 <https://doi.org/10.1016/j.jhazmat.2022.129550>.
- Liu, T., Hou, B., Wang, Z., Yang, Y., 2022. Polystyrene microplastics induce mitochondrial damage in mouse GC-2 cells. *Ecotoxicol. Environ. Saf.* 237, 113520 <https://doi.org/10.1016/j.ecoenv.2022.113520>.
- Liu, Z., Huang, Y., Jiao, Y., Chen, Q., Wu, D., Yu, P., Li, Y., Cai, M., Zhao, Y., 2020. Polystyrene nanoplastic induces ROS production and affects the MAPK-HIF-1/NFκB-mediated antioxidant system in *Daphnia pulex*. *Aquat. Toxicol.* 220, 105420 <https://doi.org/10.1016/j.aquatox.2020.105420>.
- Lu, K., Zhan, D., Fang, Y., Li, L., Chen, G., Chen, S., Wang, L., 2022. Microplastics, potential threat to patients with lung diseases. *Front. Toxicol.* 4, 958414 <https://doi.org/10.3389/ftox.2022.958414>.
- Lu, Z., Zhang, Y., He, L., Zhou, C., Hong, P., Qian, Z.-J., Ju, X., Sun, S., Li, C., 2022. Nanoplastics induce more severe apoptosis through mitochondrial damage in Caco-2 cells compared to sub-micron plastics (preprint). <https://doi.org/10.21203/rs.3.rs-1417473/v1>.
- Ly, J.D., Grubb, D.R., Lawen, A., 2003 [No title found] *Apoptosis* 8, 115–128. <https://doi.org/10.1023/A:1022945107762>.
- Malinowska, K., Bukowska, B., Piwoński, I., Foksiński, M., Kisielska, A., Zarakowska, E., Gackowski, D., Sicińska, P., 2022. Polystyrene nanoparticles: the mechanism of their genotoxicity in human peripheral blood mononuclear cells. *Nanotoxicology* 1–21. <https://doi.org/10.1080/17435390.2022.2149360>.
- Marciniak, S.J., 2017. Endoplasmic reticulum stress in lung disease. *Eur. Respir. Rev.* 26, 170018 <https://doi.org/10.1183/16000617.0018-2017>.
- Moungjaroen, J., Nimmannit, U., Callery, P.S., Wang, L., Azad, N., Lipipun, V., Chanvorachote, P., Rojanasakul, Y., 2006. Reactive oxygen species mediate caspase activation and apoptosis induced by lipoic acid in human lung epithelial cancer cells through bcl-2 down-regulation. *J. Pharmacol. Exp. Therapeut.* 319, 1062–1069. <https://doi.org/10.1124/jpet.106.110965>.
- Nomura, K., Imai, H., Koumura, T., Arai, M., Nakagawa, Y., 1999. Mitochondrial phospholipid hydroperoxide glutathione peroxidase suppresses apoptosis mediated by a mitochondrial death pathway. *J. Biol. Chem.* 274, 29294–29302. <https://doi.org/10.1074/jbc.274.41.29294>.
- Oliveira, M. de S., Barbosa, M.I.F., de Souza, T.B., Moreira, D.R.M., Martins, F.T., Villarreal, W., Machado, R.P., Doriguetto, A.C., Soares, M.B.P., Bezerra, D.P., 2019. A novel platinum complex containing a piplartine derivative exhibits enhanced cytotoxicity, causes oxidative stress and triggers apoptotic cell death by ERK/p38 pathway in human acute promyelocytic leukemia HL-60 cells. *Redox Biol.* 20, 182–194. <https://doi.org/10.1016/j.redox.2018.10.006>.
- Olsson, M., Zhivotovsky, B., 2011. Caspases and cancer. *Cell Death Differ.* 18, 1441–1449. <https://doi.org/10.1038/cdd.2011.30>.
- Pallardy, M., Biola, A., Lebre, H., Bréard, J., 1999. Assessment of apoptosis in xenobiotic-induced immunotoxicity. *Methods* 19, 36–47. <https://doi.org/10.1006/meth.1999.0825>.
- Pinsino, A., Bergami, E., Della Torre, C., Vannuccini, M.L., Addis, P., Secci, M., Dawson, K.A., Matranga, V., Corsi, I., 2017. Amino-modified polystyrene nanoparticles affect signalling pathways of the sea urchin (*Paracentrotus lividus*) embryos. *Nanotoxicology* 11, 201–209. <https://doi.org/10.1080/17435390.2017.1279360>.
- Pinton, P., Giorgi, C., Siviero, R., Zecchini, E., Rizzuto, R., 2008. Calcium and apoptosis: ER-mitochondria Ca²⁺ transfer in the control of apoptosis. *Oncogene* 27, 6407–6418. <https://doi.org/10.1038/nc.2008.308>.
- Prata, J.C., 2018. Airborne microplastics: consequences to human health? *Environ. Pollut.* 234, 115–126. <https://doi.org/10.1016/j.envpol.2017.11.043>.
- Ratomski, K., Skotnicka, B., Kasprzycka, E., Żelazowska-Rutkowska, B., Wysocka, J., Anisimowicz, S., 2007. Ocena odsetka limfocytów CD19+CD5+ w przerosłych migdałkach gardłowych u dzieci chorych na wysiękowe zapalenie ucha środkowego. *Otolaryngol. Pol.* 61, 962–966. [https://doi.org/10.1016/S0030-6657\(07\)70561-9](https://doi.org/10.1016/S0030-6657(07)70561-9).
- Rawle, D.J., Dumenil, T., Tang, B., Bishop, C.R., Yan, K., Le, T.T., Suhrbier, A., 2022. Microplastic consumption induces inflammatory signatures in the colon and prolongs a viral arthritis. *Sci. Total Environ.* 809, 152212 <https://doi.org/10.1016/j.scitotenv.2021.152212>.
- Redza-Dutoroir, M., Averill-Bates, D.A., 2016. Activation of apoptosis signalling pathways by reactive oxygen species. *Biochim. Biophys. Acta Mol. Cell Res.* 1863, 2977–2992. <https://doi.org/10.1016/j.bbamcr.2016.09.012>.
- Rubio, L., Barguilla, I., Domenech, J., Marcos, R., Hernández, A., 2020. Biological effects, including oxidative stress and genotoxic damage, of polystyrene nanoparticles in different human hematopoietic cell lines. *J. Hazard Mater.* 398, 122900 <https://doi.org/10.1016/j.jhazmat.2020.122900>.
- Salvia, R., Rico, L.G., Bradford, J.A., Ward, M.D., Olszowy, M.W., Martínez, C., Madrid-Aris, A.D., Grifols, J.R., Ancochea, Á., Gomez-Muñoz, L., Vives-Pi, M., Martínez-Cáceres, E., Fernández, M.A., Sorigue, M., Petriz, J., 2023. Fast-screening flow cytometry method for detecting nanoplastics in human peripheral blood. *MethodsX* 10, 102057. <https://doi.org/10.1016/j.mex.2023.102057>.
- Santovito, A., Cervella, P., Delperio, M., 2014. Chromosomal damage in peripheral blood lymphocytes from nurses occupationally exposed to chemicals. *Hum. Exp. Toxicol.* 33, 897–903. <https://doi.org/10.1177/0960327113512338>.
- Sarasamma, S., Audira, G., Siregar, P., Malhotra, N., Lai, Y.-H., Liang, S.-T., Chen, J.-R., Chen, K.H.-C., Hsiao, C.-D., 2020. Nanoplastics cause neurobehavioral impairments, reproductive and oxidative damages, and biomarker responses in zebrafish: throwing up alarms of wide spread health risk of exposure. *IJMS* 21, 1410. <https://doi.org/10.3390/ijms21041410>.
- Sarma, D.K., Dubey, R., Samarth, R.M., Shubham, S., Chowdhury, P., Kumawat, M., Verma, V., Tiwari, R.R., Kumar, M., 2022. The biological effects of polystyrene nanoplastics on human peripheral blood lymphocytes. *Nanomaterials* 12, 1632. <https://doi.org/10.3390/nano12101632>.
- Saxton, R.A., Sabatini, D.M., 2017. mTOR signaling in growth, metabolism, and disease. *Cell* 168, 960–976. <https://doi.org/10.1016/j.cell.2017.02.004>.
- Schmidt, A., da Silva Brito, W.A., Singer, D., Mühl, M., Berner, J., Saadati, F., Wolff, C., Miebach, L., Wende, K., Bekeschus, S., 2023. Short- and long-term polystyrene nano- and microplastic exposure promotes oxidative stress and divergently affects skin cell architecture and Wnt/beta-catenin signaling. *Part. Fibre Toxicol.* 20, 3. <https://doi.org/10.1186/s12989-023-00513-1>.
- Schneider, M., Stracke, F., Hansen, S., Schaefer, U.F., 2009. Nanoparticles and their interactions with the dermal barrier. *Derm. Endocrinol.* 1, 197–206. <https://doi.org/10.4161/derm.1.4.9501>.

- Schwarz, D.S., Blower, M.D., 2016. The endoplasmic reticulum: structure, function and response to cellular signaling. *Cell. Mol. Life Sci.* 73, 79–94. <https://doi.org/10.1007/s00018-015-2052-6>.
- Singh, R.P., Kumar, S., Nada, R., Prasad, R., 2006. Evaluation of copper toxicity in isolated human peripheral blood mononuclear cells and its attenuation by zinc: ex vivo. *Mol. Cell. Biochem.* 282, 13. <https://doi.org/10.1007/s11010-006-1168-2>.
- Song, Y.K., Hong, S.H., Eo, S., Jang, M., Han, G.M., Isobe, A., Shim, W.J., 2018. Horizontal and vertical distribution of microplastics in Korean coastal waters. *Environ. Sci. Technol.* 52, 12188–12197. <https://doi.org/10.1021/acs.est.8b04032>.
- Sukumaran, P., Nascimento Da Conceicao, V., Sun, Y., Ahamad, N., Saraiva, L.R., Selvaraj, S., Singh, B.B., 2021. Calcium signaling regulates autophagy and apoptosis. *Cells* 10, 2125. <https://doi.org/10.3390/cells10082125>.
- Tang, Q., Li, T., Chen, K., Deng, X., Zhang, Q., Tang, H., Shi, Z., Zhu, T., Zhu, J., 2022. PS-NPs induced neurotoxic effects in SHSY-5Y cells via autophagy activation and mitochondrial dysfunction. *Brain Sci.* 12, 952. <https://doi.org/10.3390/brainsci12070952>.
- Vogt, A., Combadiere, B., Hadam, S., Stieler, K.M., Lademann, J., Schaefer, H., Autran, B., Sterry, W., Blume-Peytavi, U., 2006. 40nm, but not 750 or 1,500nm, nanoparticles enter epidermal CD1a+ cells after transcutaneous application on human skin. *J. Invest. Dermatol.* 126, 1316–1322. <https://doi.org/10.1038/sj.jid.5700226>.
- Wacquier, B., Combettes, L., Dupont, G., 2020. Dual dynamics of mitochondrial permeability transition pore opening. *Sci. Rep.* 10, 3924. <https://doi.org/10.1038/s41598-020-60177-1>.
- Wang, F., Bexiga, M.G., Anguissola, S., Boya, P., Simpson, J.C., Salvati, A., Dawson, K.A., 2013. Time resolved study of cell death mechanisms induced by amine-modified polystyrene nanoparticles. *Nanoscale* 5, 10868. <https://doi.org/10.1039/c3nr03249c>.
- Wang, H., Chen, J., Bai, G., Han, W., Guo, R., Cui, N., 2022. mTOR modulates the endoplasmic reticulum stress-induced CD4+ T cell apoptosis mediated by ROS in septic immunosuppression. *Mediat. Inflamm.* 2022, 1–11. <https://doi.org/10.1155/2022/6077570>.
- Wang, L., Xie, X., Cao, T., Bosset, J., Bakker, E., 2018. Surface-doped polystyrene microsensors containing lipophilic solvatochromic dye. *Transducers. Chem. Eur. J.* 24, 7921–7925. <https://doi.org/10.1002/chem.201800077>.
- Wang, Y.-L., Lee, Y.-H., Hsu, Y.-H., Chiu, I.-J., Huang, C.-C.-Y., Huang, C.-C., Chia, Z.-C., Lee, C.-P., Lin, Y.-F., Chiu, H.-W., 2021. The kidney-related effects of polystyrene microplastics on human kidney proximal tubular epithelial cells HK-2 and male C57BL/6 mice. *Environ. Health Perspect.* 129, 057003. <https://doi.org/10.1289/EHP7612>.
- Waterhouse, N.J., Goldstein, J.C., von Ahsen, O., Schuler, M., Newmeyer, D.D., Green, D. R., 2001. Cytochrome C maintains mitochondrial transmembrane potential and ATP generation after outer mitochondrial membrane permeabilization during the apoptotic process. *JCB (J. Cell Biol.)* 153, 319–328. <https://doi.org/10.1083/jcb.153.2.319>.
- Wei, Y., Zhou, Y., Long, C., Wu, H., Hong, Y., Fu, Y., Wang, J., Wu, Y., Shen, L., Wei, G., 2021. Polystyrene microplastics disrupt the blood-testis barrier integrity through ROS-Mediated imbalance of mTORC1 and mTORC2. *Environ. Pollut.* 289, 117904. <https://doi.org/10.1016/j.envpol.2021.117904>.
- Weinberg, A., Jessor, R.D., Edelstein, C.L., Bill, J.R., Wohl, D.A., 2004. Excess apoptosis of mononuclear cells contributes to the depressed cytomegalovirus-specific immunity in HIV-infected patients on HAART. *Virology* 330, 313–321. <https://doi.org/10.1016/j.virol.2004.09.017>.
- Westphal, D., Kluck, R.M., Dewson, G., 2014. Building blocks of the apoptotic pore: how Bax and Bak are activated and oligomerize during apoptosis. *Cell Death Differ.* 21, 196–205. <https://doi.org/10.1038/cdd.2013.139>.
- Wright, S.L., Kelly, F.J., 2017. Plastic and human health: a micro issue? *Environ. Sci. Technol.* 51, 6634–6647. <https://doi.org/10.1021/acs.est.7b00423>.
- Wu, B., Wu, X., Liu, S., Wang, Z., Chen, L., 2019. Size-dependent effects of polystyrene microplastics on cytotoxicity and efflux pump inhibition in human Caco-2 cells. *Chemosphere* 221, 333–341. <https://doi.org/10.1016/j.chemosphere.2019.01.056>.
- Xu, M., Halimu, G., Zhang, Q., Song, Y., Fu, X., Li, Yongqiang, Li, Yansheng, Zhang, H., 2019. Internalization and toxicity: a preliminary study of effects of nanoplastic particles on human lung epithelial cell. *Sci. Total Environ.* 694, 133794. <https://doi.org/10.1016/j.scitotenv.2019.133794>.
- Yasin, N.A.E., El-Naggar, M.E., Ahmed, Z.S.O., Galal, M.K., Rashad, M.M., Youssef, A.M., Elleithy, E.M.M., 2022. Exposure to Polystyrene nanoparticles induces liver damage in rat via induction of oxidative stress and hepatocyte apoptosis. *Environ. Toxicol. Pharmacol.* 94, 103911. <https://doi.org/10.1016/j.etap.2022.103911>.
- Yee, M.S.-L., Hii, L.-W., Looi, C.K., Lim, W.-M., Wong, S.-F., Kok, Y.-Y., Tan, B.-K., Wong, C.-Y., Leong, C.-O., 2021. Impact of microplastics and nanoplastics on human health. *Nanomaterials* 11, 496. <https://doi.org/10.3390/nano11020496>.
- Yin, B., Wang, D., Zhang, Y., Lu, H., Hou, L., Guo, T., Zhao, H., Xing, M., 2023. Polystyrene microplastics promote liver inflammation by inducing the formation of macrophages extracellular traps. *J. Hazard Mater.* 452, 131236. <https://doi.org/10.1016/j.jhazmat.2023.131236>.
- Zhang, G.S., Liu, Y.F., 2018. The distribution of microplastics in soil aggregate fractions in southwestern China. *Sci. Total Environ.* 642, 12–20. <https://doi.org/10.1016/j.scitotenv.2018.06.004>.
- Zhang, M., Shi, J., Huang, Q., Xie, Y., Wu, R., Zhong, J., Deng, H., 2022. Multi-omics analysis reveals size-dependent toxicity and vascular endothelial cell injury induced by microplastic exposure in vivo and in vitro. *Environ. Sci.: Nano* 9, 663–683. <https://doi.org/10.1039/D1EN01067K>.
- Zhang, N., Hartig, H., Dzhalalov, I., Draper, D., He, Y.W., 2005. The role of apoptosis in the development and function of T lymphocytes. *Cell Res.* 15, 749–769. <https://doi.org/10.1038/sj.cr.7290345>.

Appendix A. Supplementary data

Supplementary data to this article can be found online at <https://doi.org/10.1016/j.chemosphere.2023.139137>.

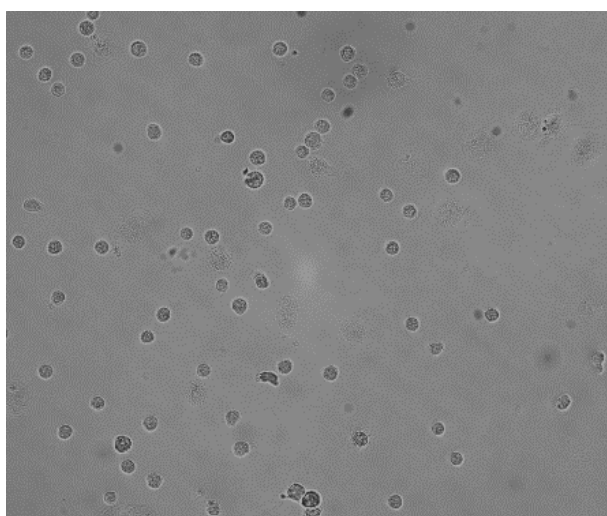
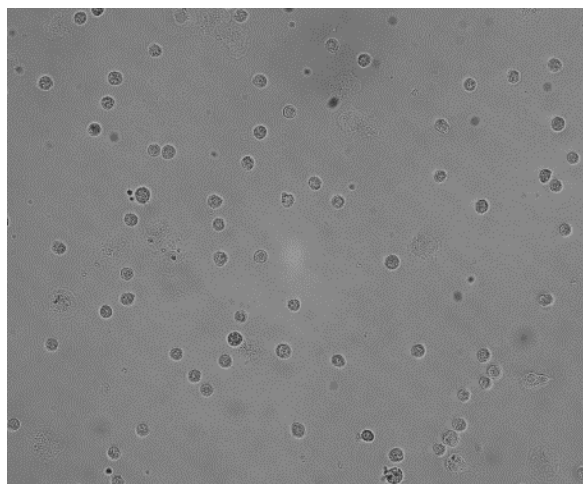
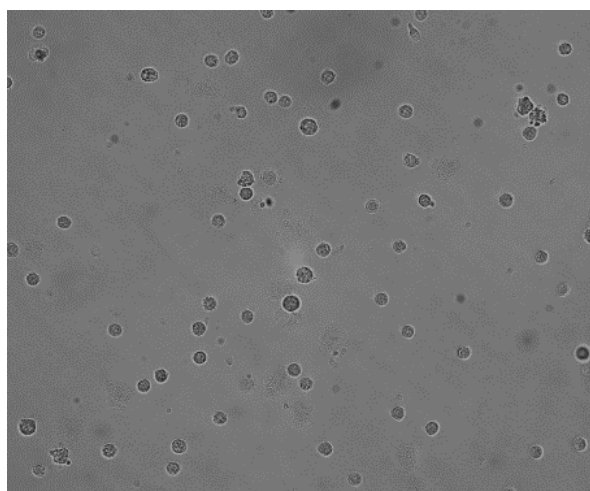
The effects of non-functionalized polystyrene nanoparticles of different diameters on the induction of apoptosis and mTOR level in human peripheral blood mononuclear cells

Kinga Malinowska¹, Paulina Sicińska¹, Jaromir Michałowicz¹ and Bożena Bukowska^{1*}

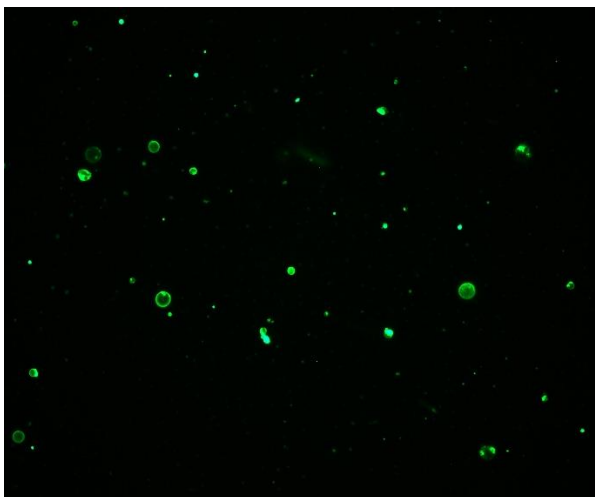
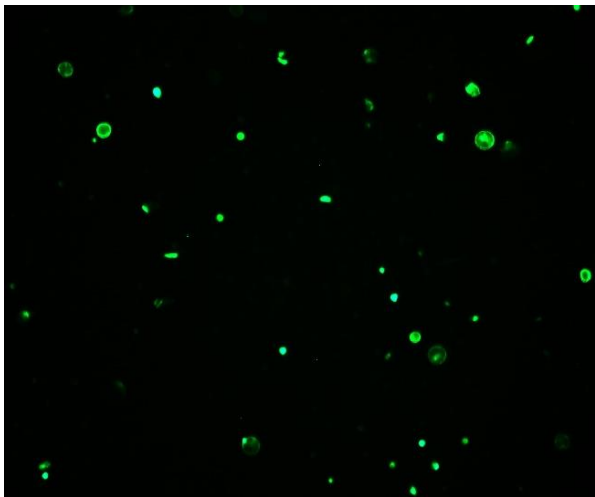
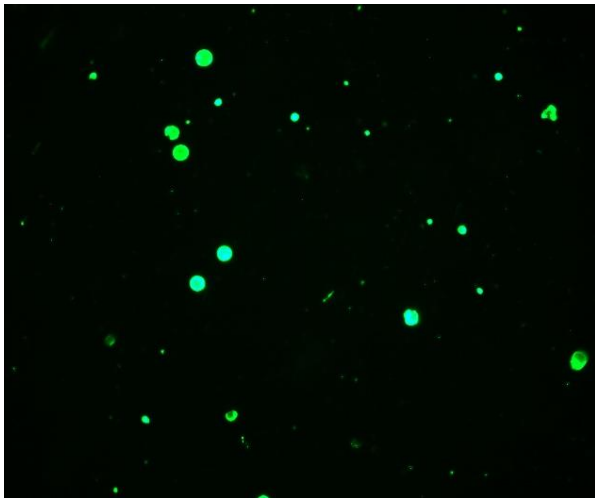
¹University of Lodz, Faculty of Biology and Environmental Protection, Department of Biophysics of Environmental Pollution, 141/143 Pomorska St., 90–236 Lodz, Poland;

*Correspondence: bozena.bukowska@biol.uni.lodz.pl

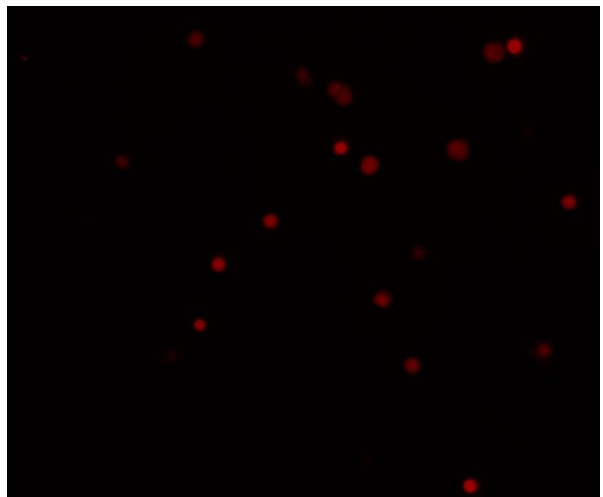
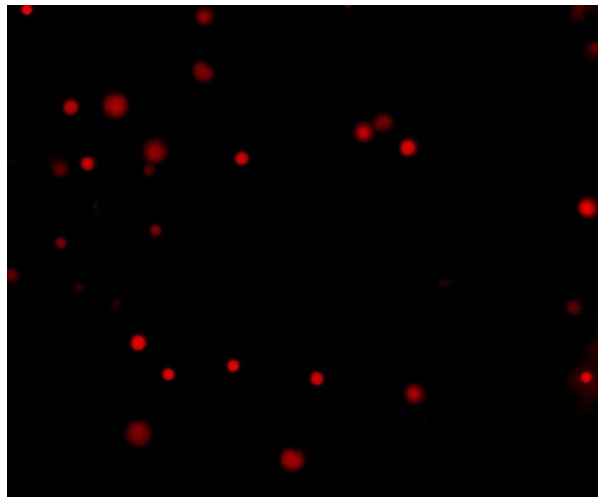
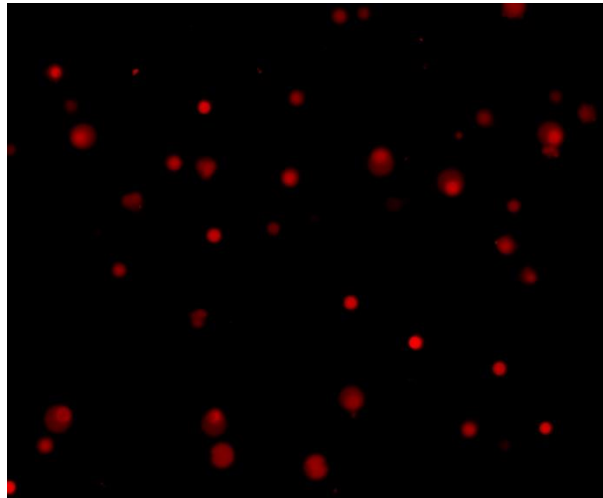
PBMCs (Photo „white”)



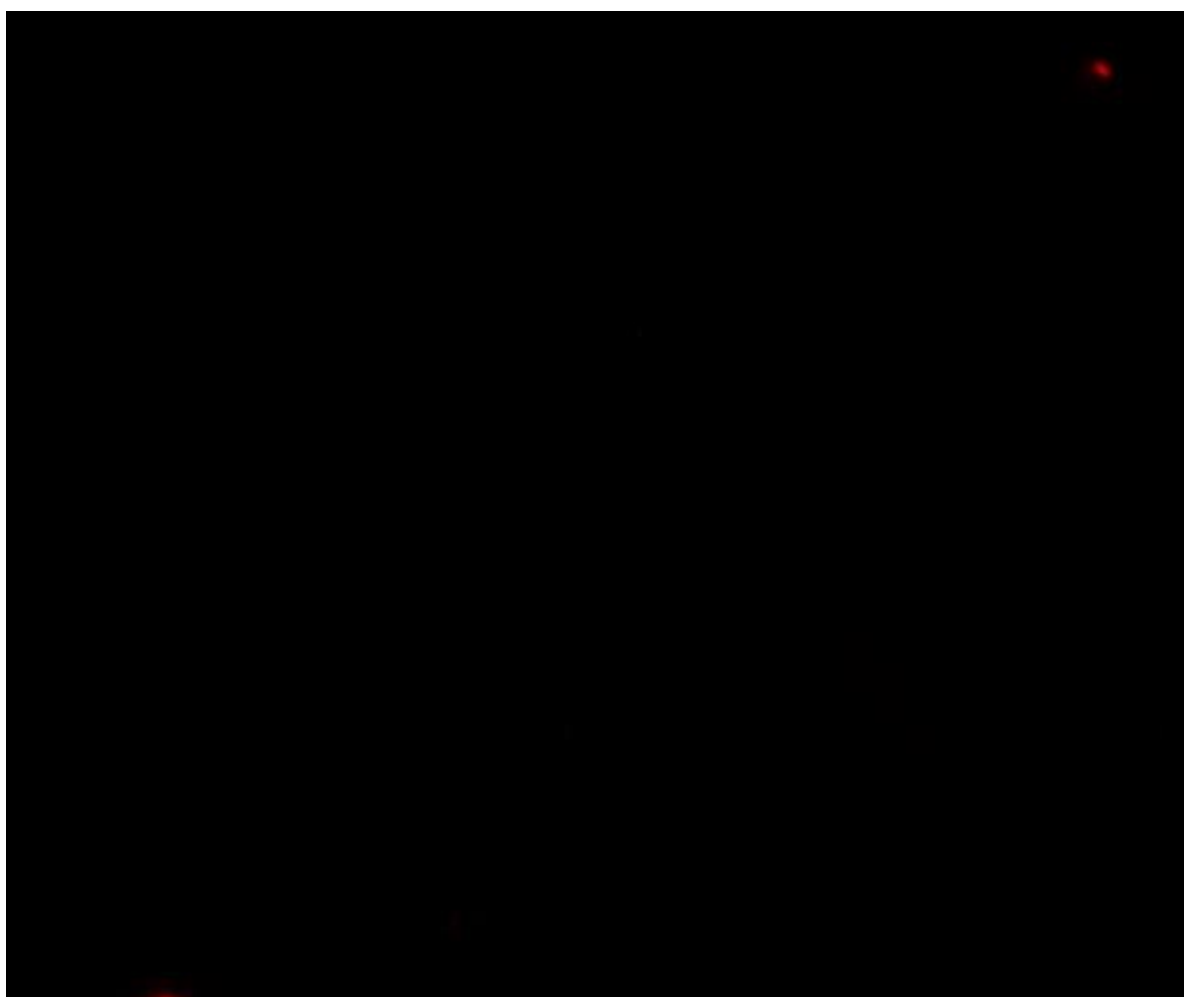
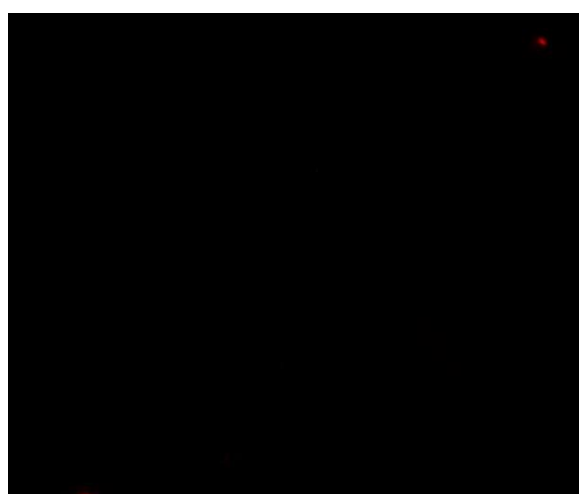
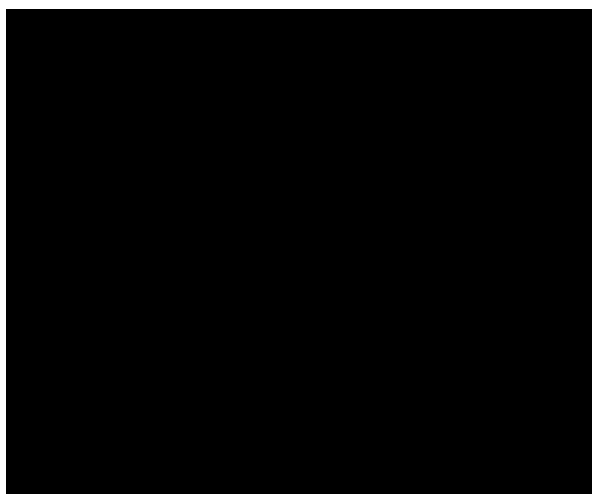
Camptothecin 20 mM
(aneksyna V)

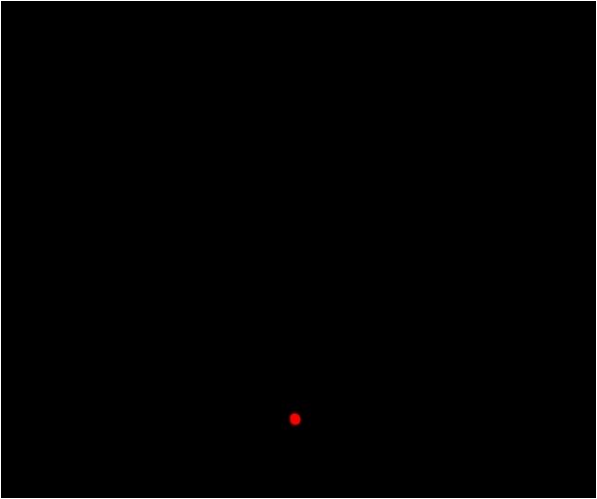
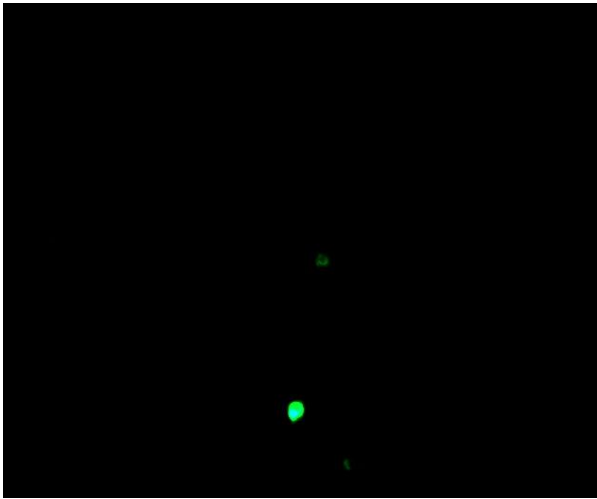
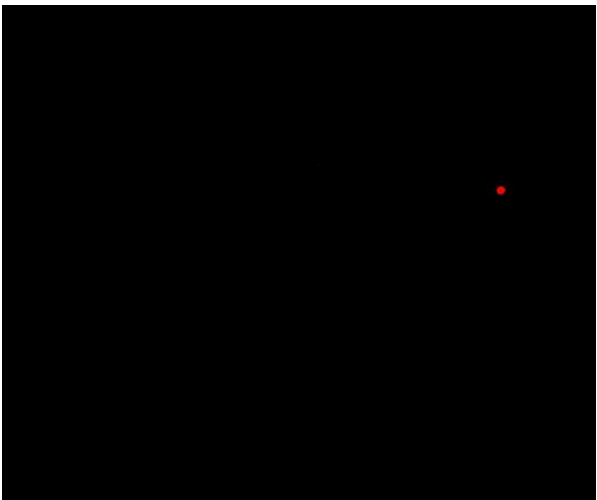
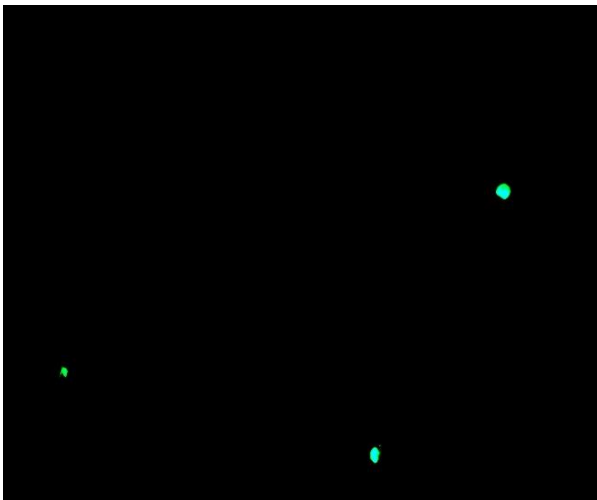
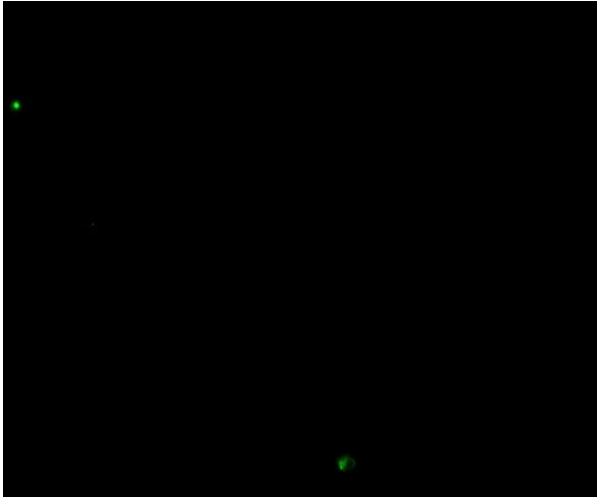


Hydrogen peroxide 100 μ M
(propidium iodide)

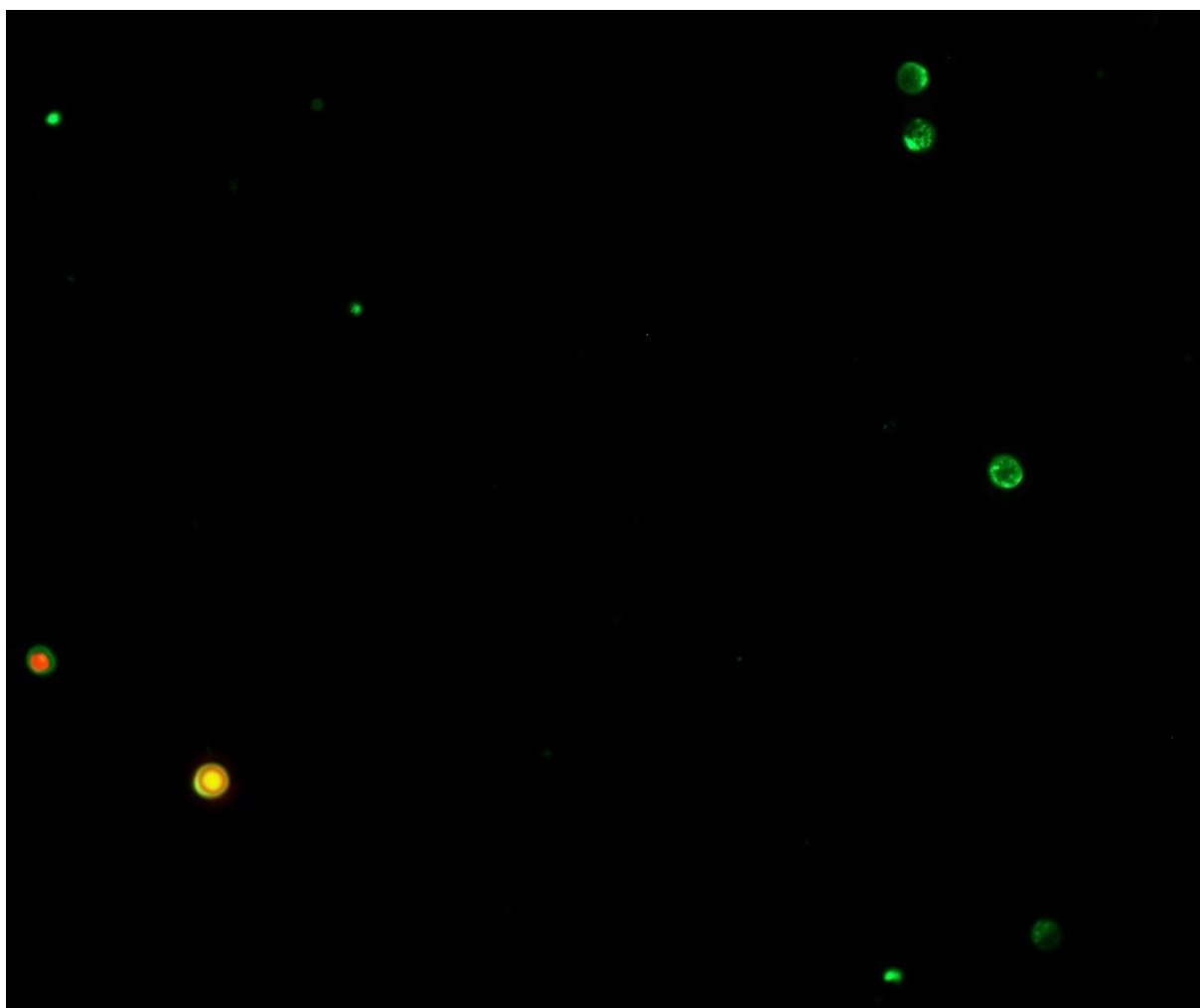
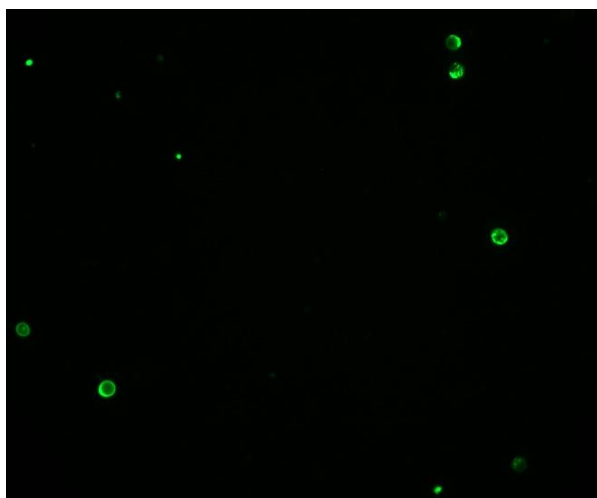


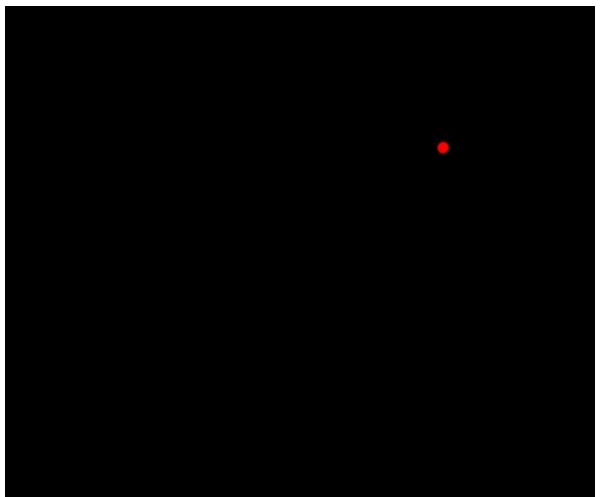
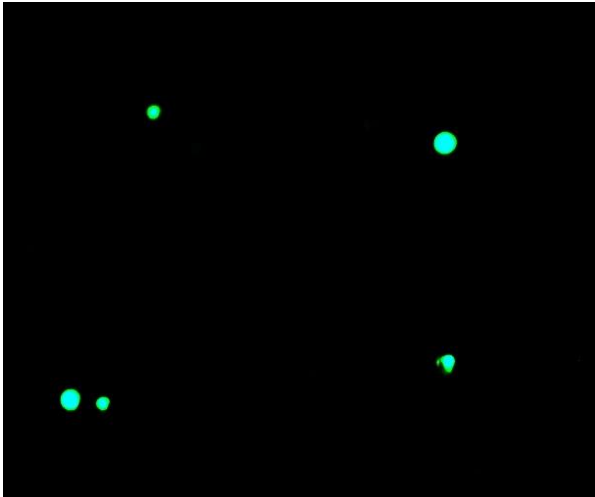
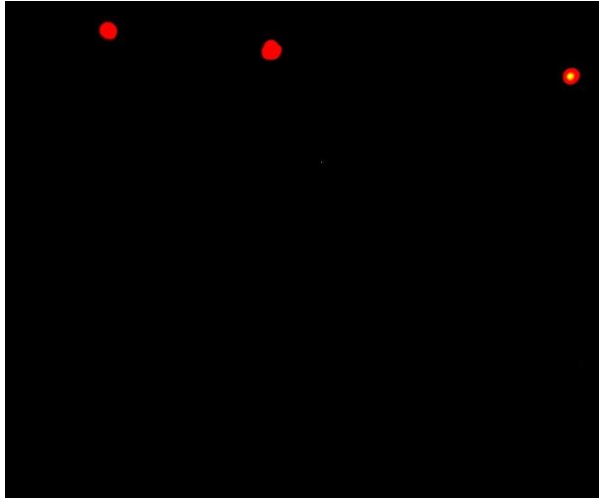
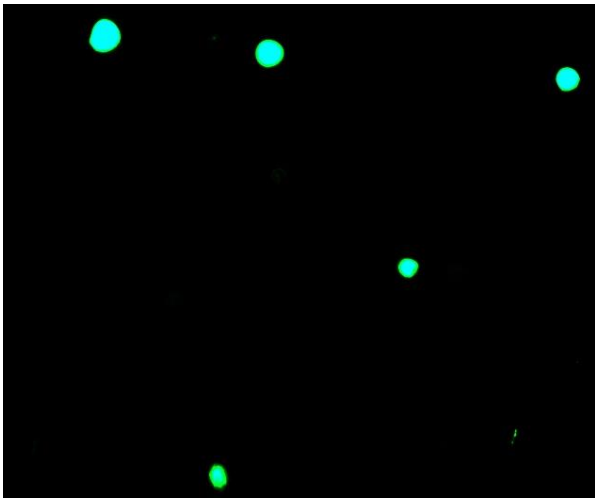
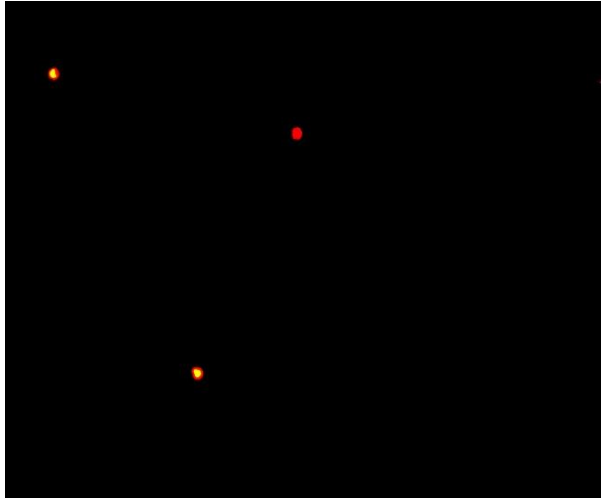
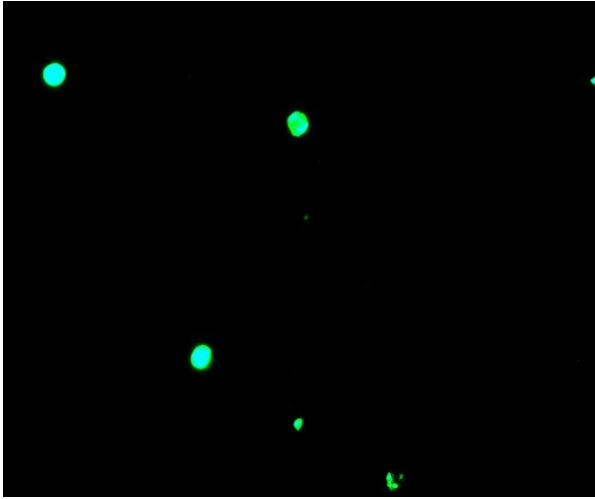
CONTROL PBMCs

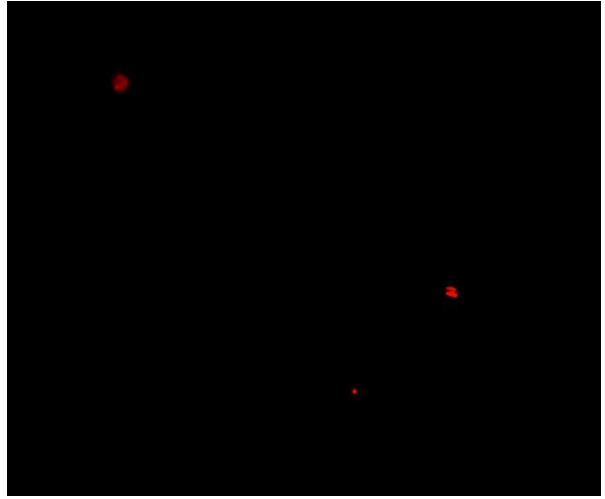
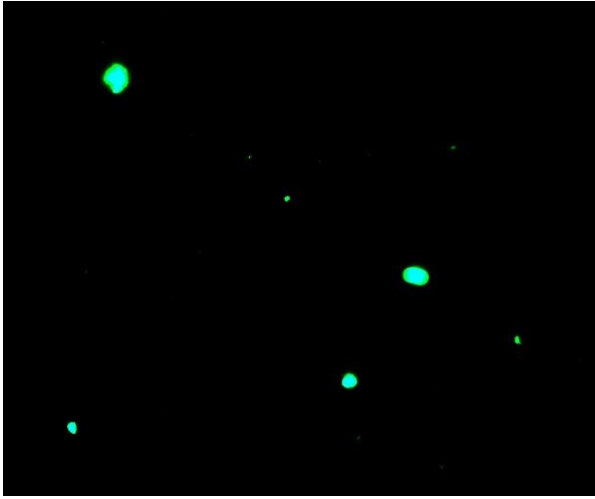




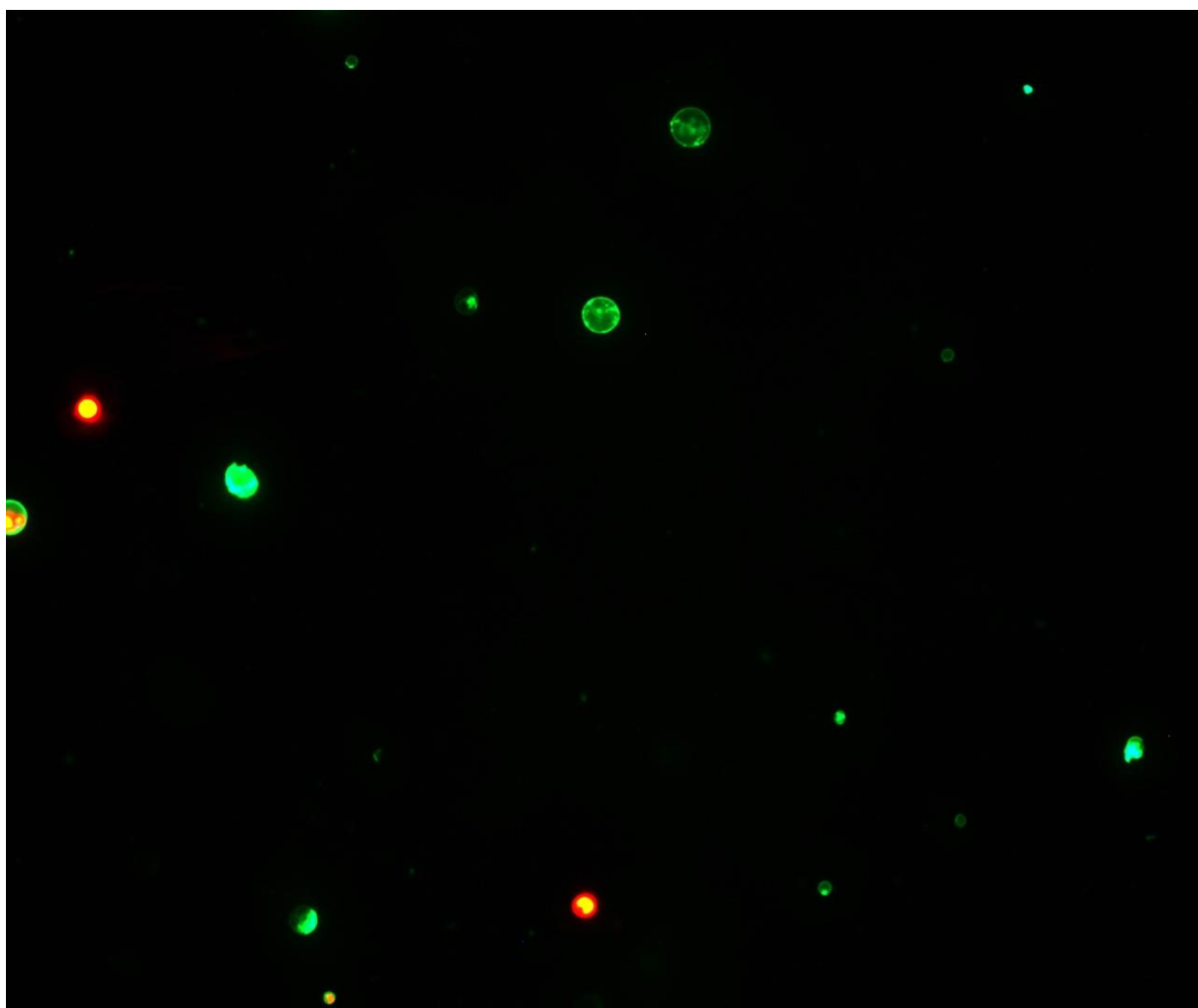
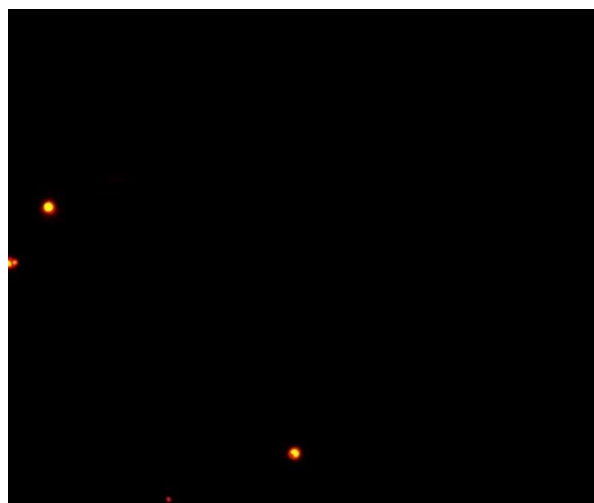
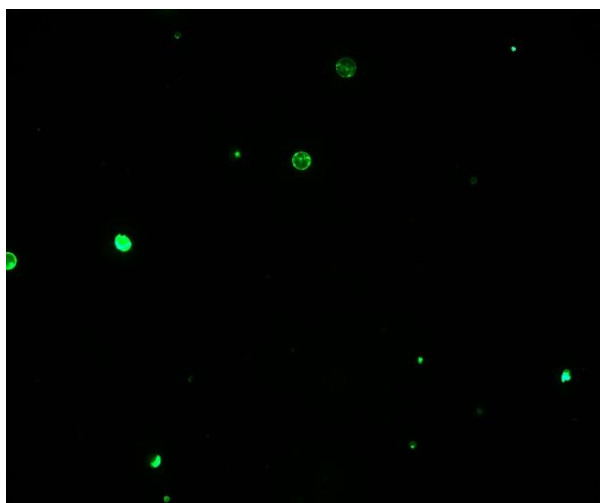
29 nm 1 $\mu\text{g/ml}$

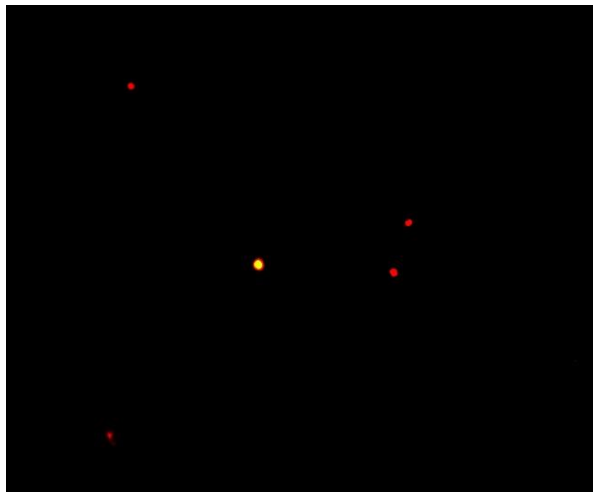
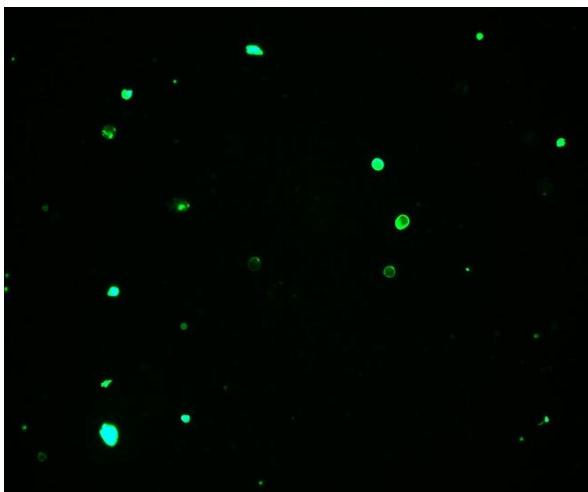
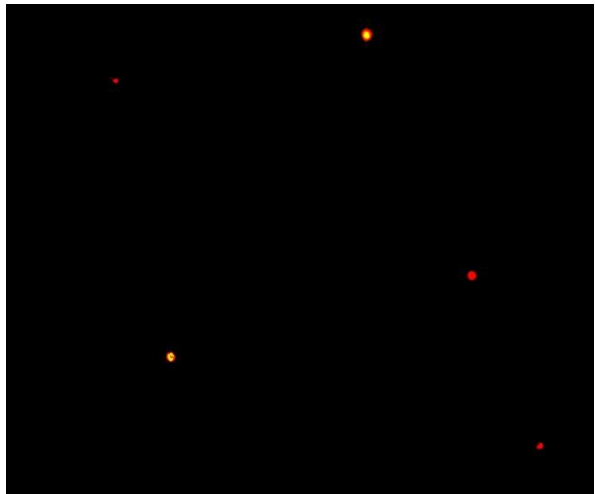
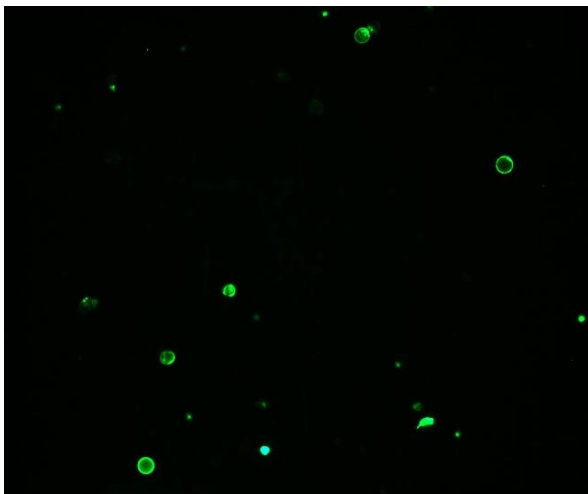
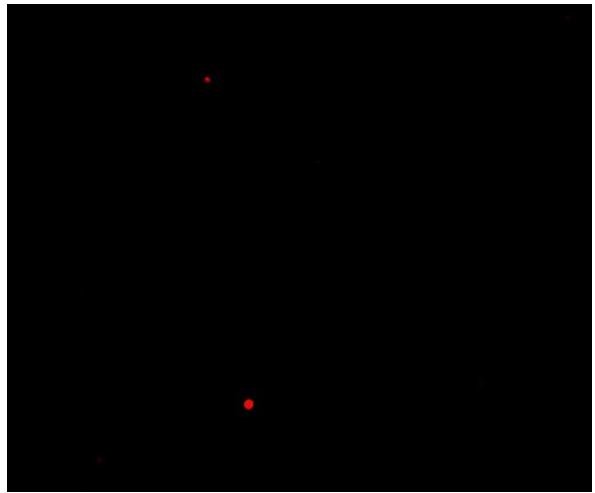
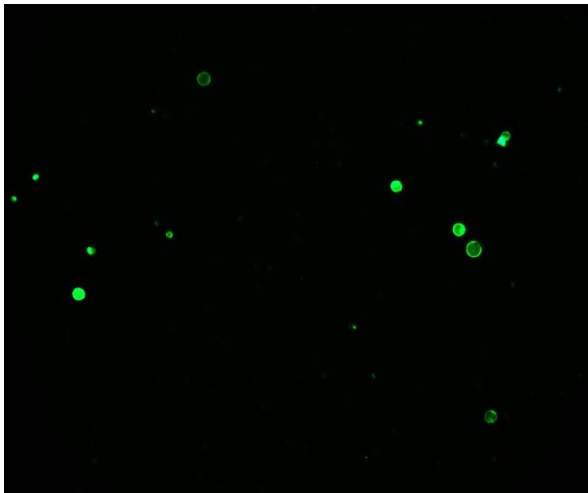


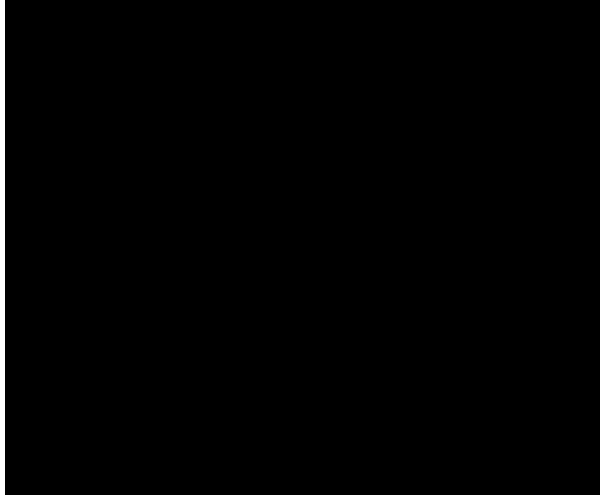
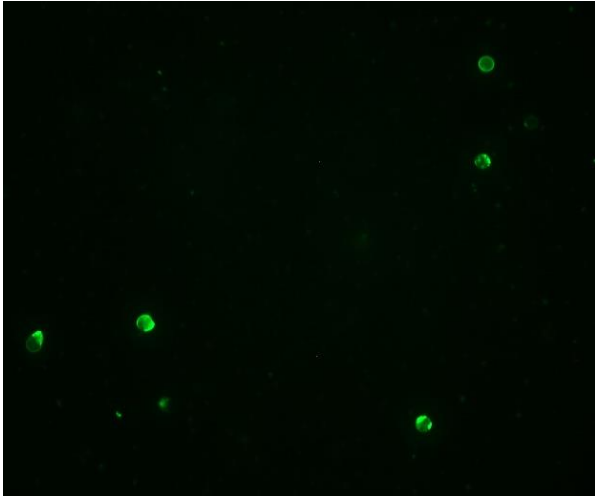




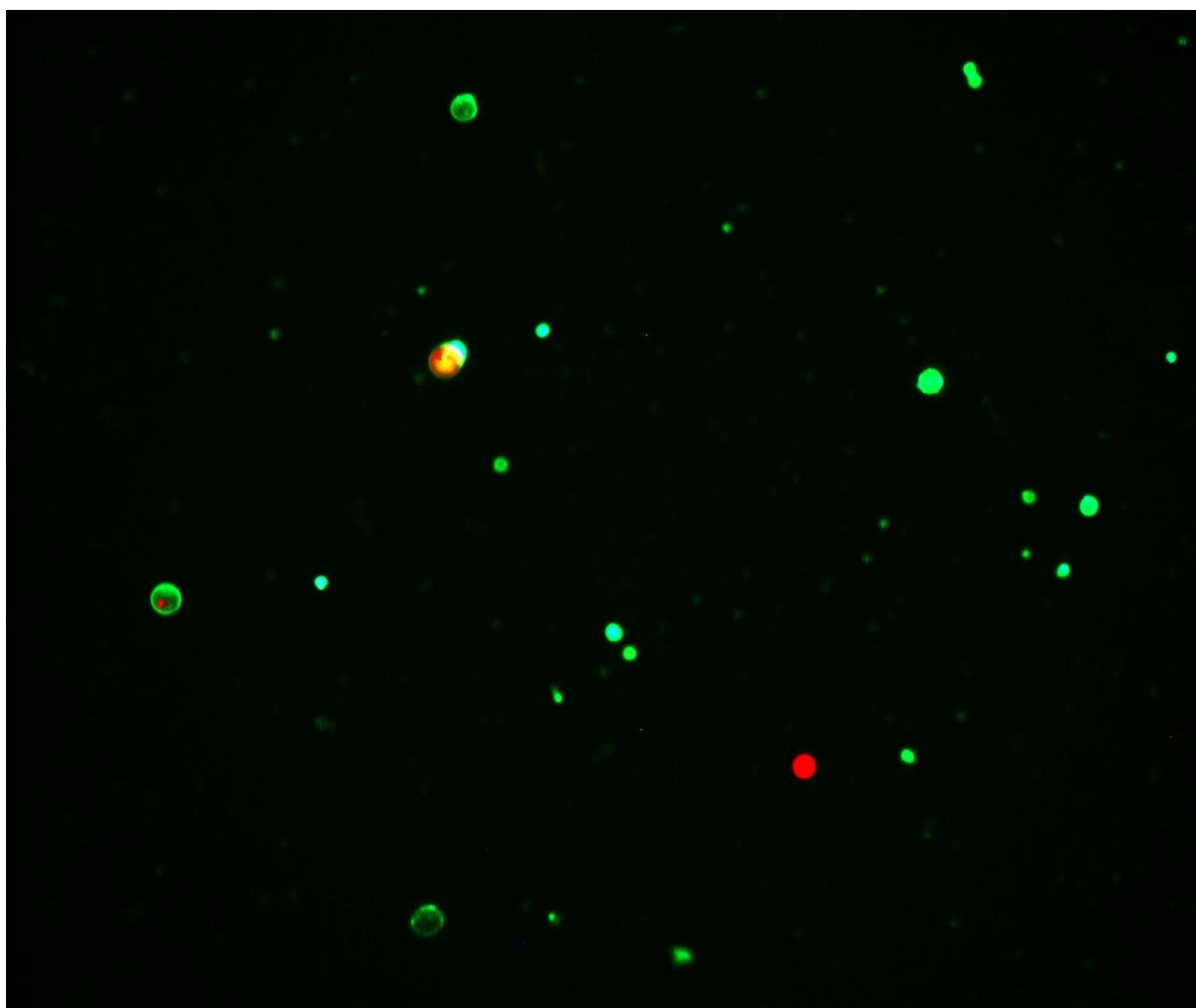
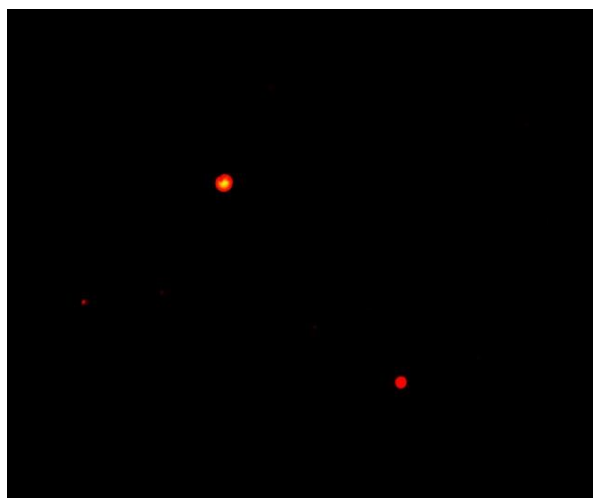
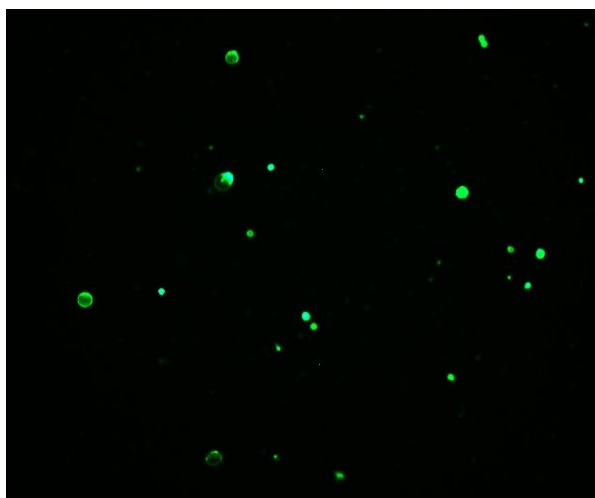
29 nm 10 $\mu\text{g/ml}$

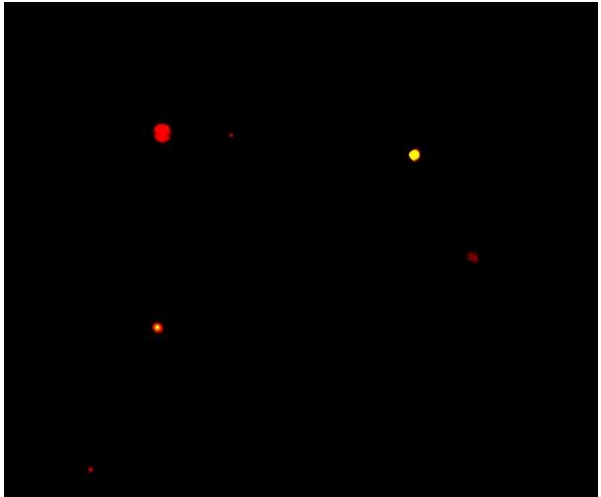
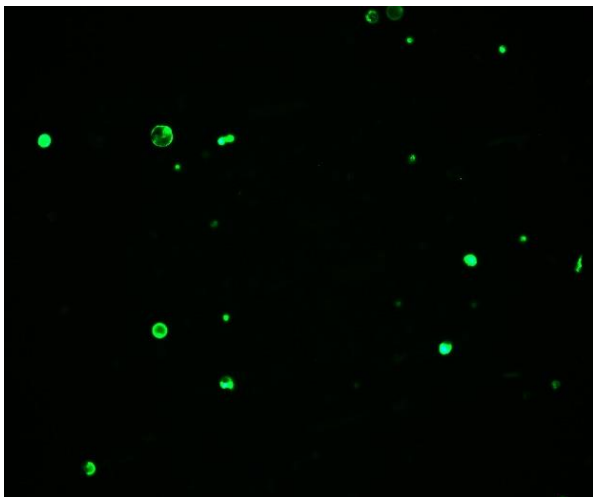
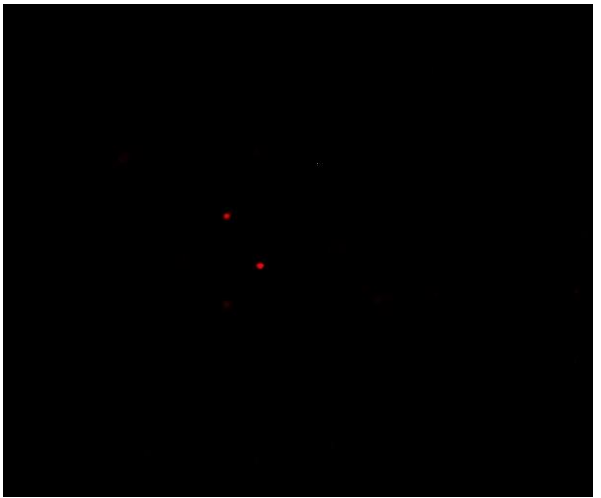
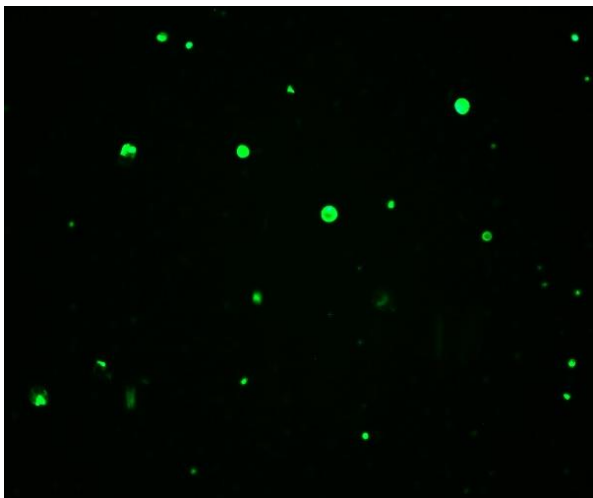
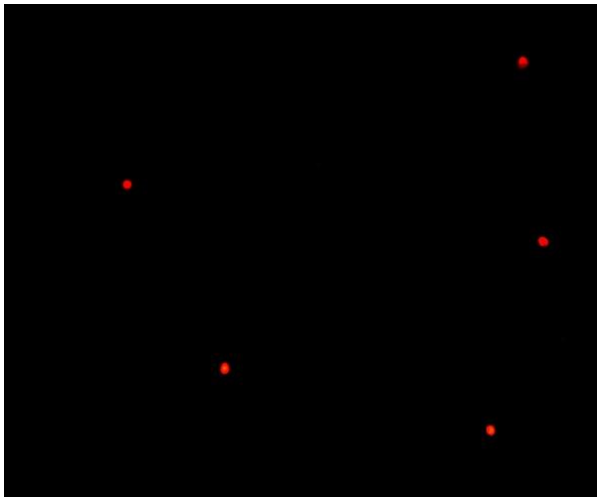
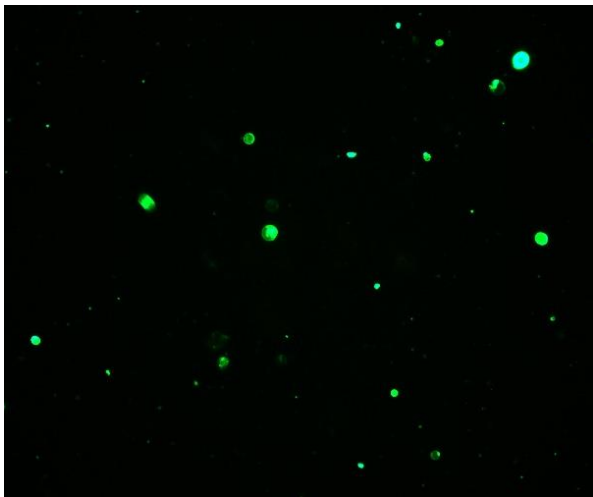


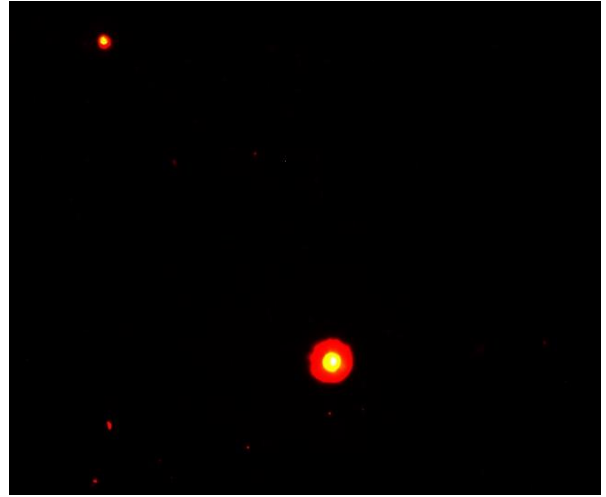
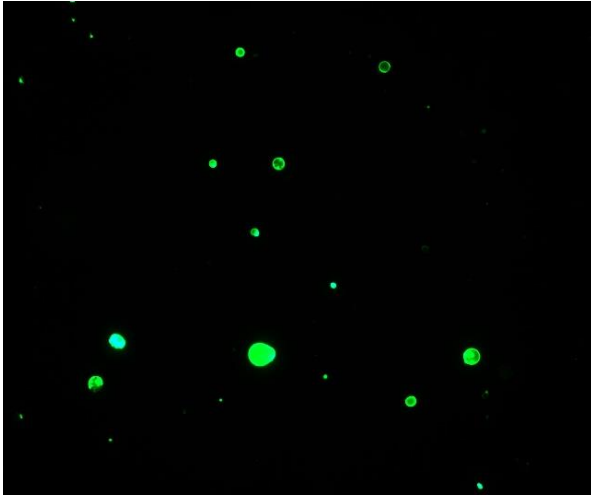




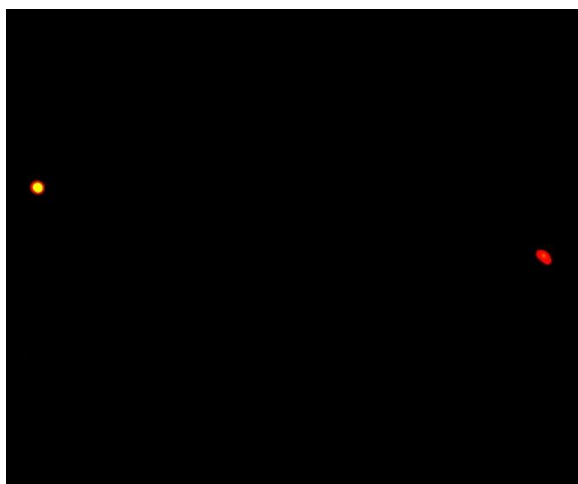
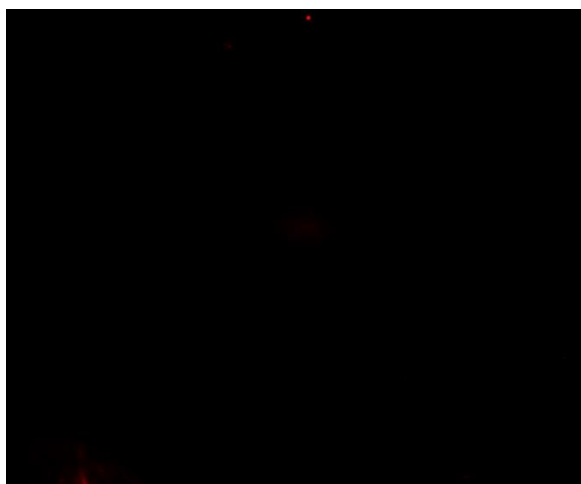
29 nm 100 $\mu\text{g/ml}$

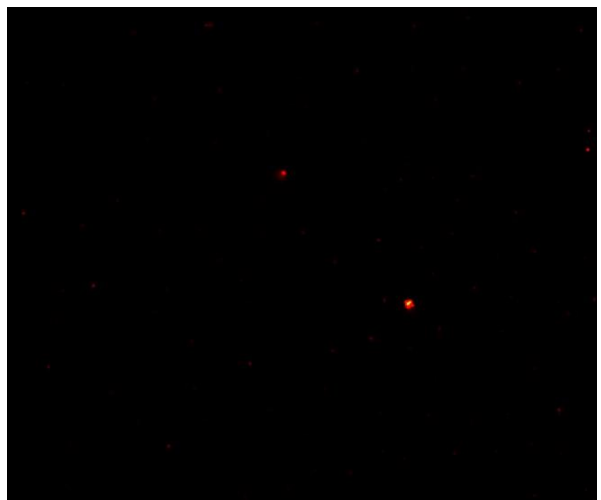
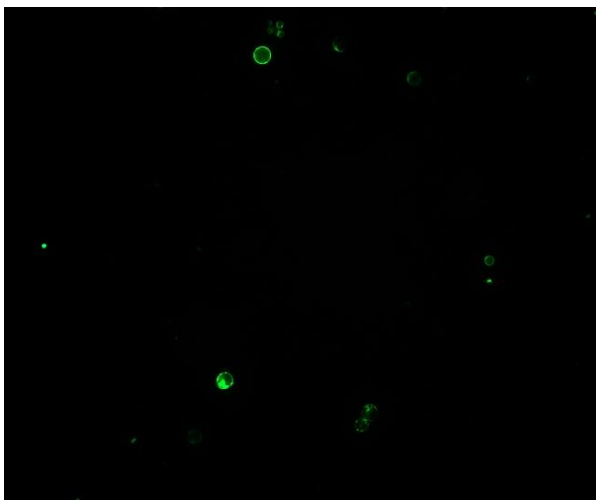
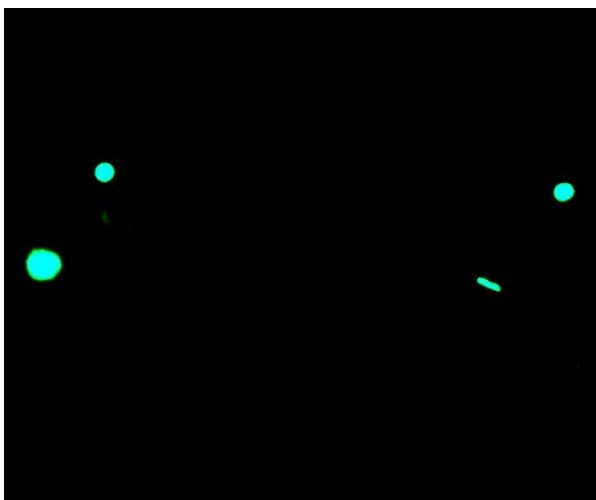
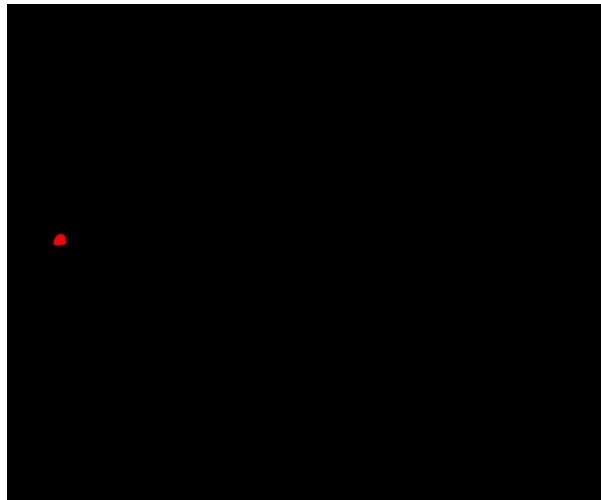
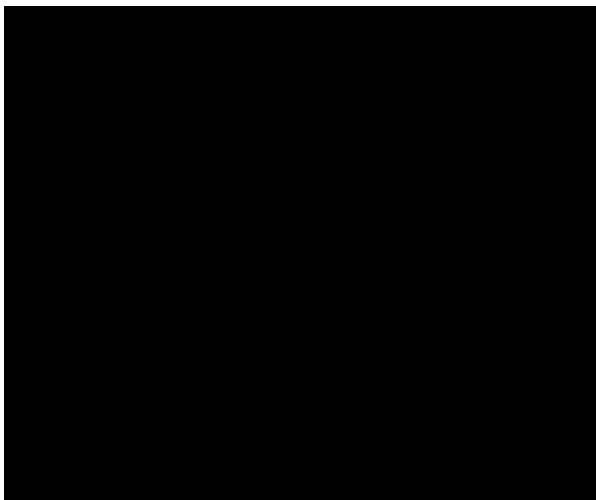


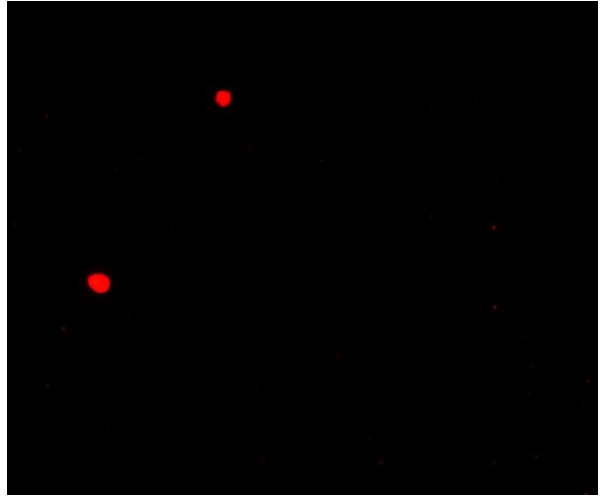
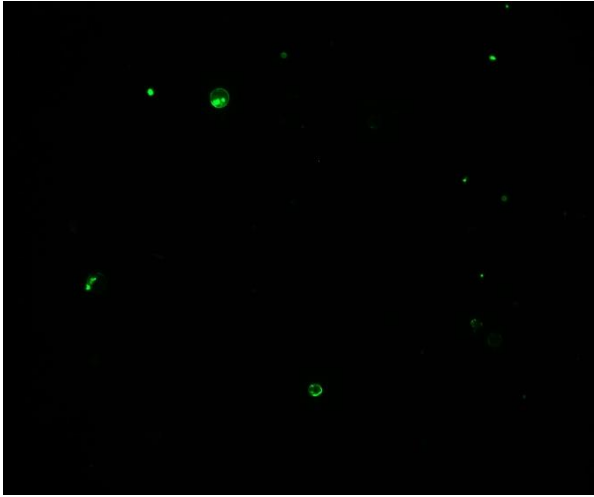




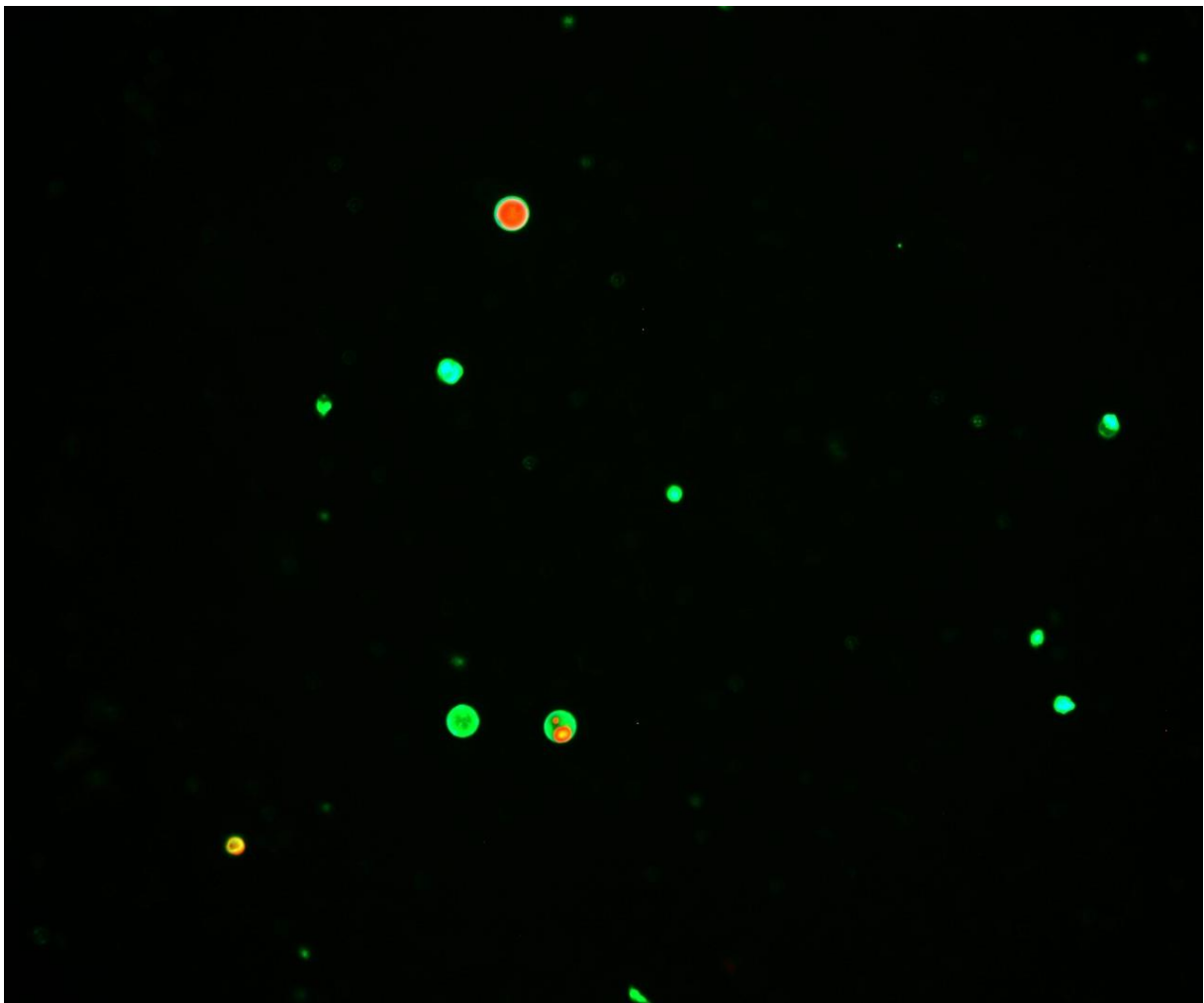
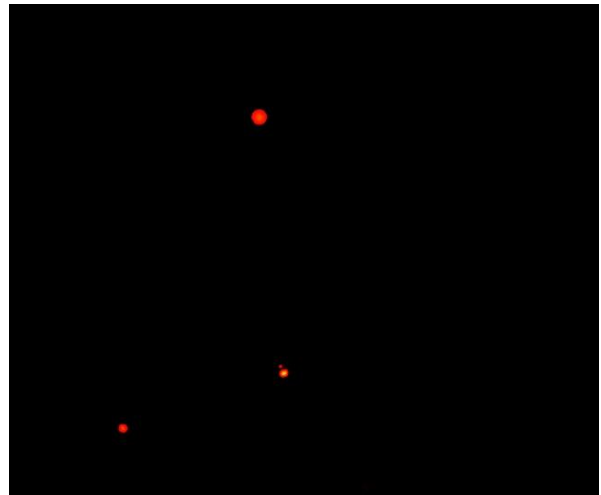
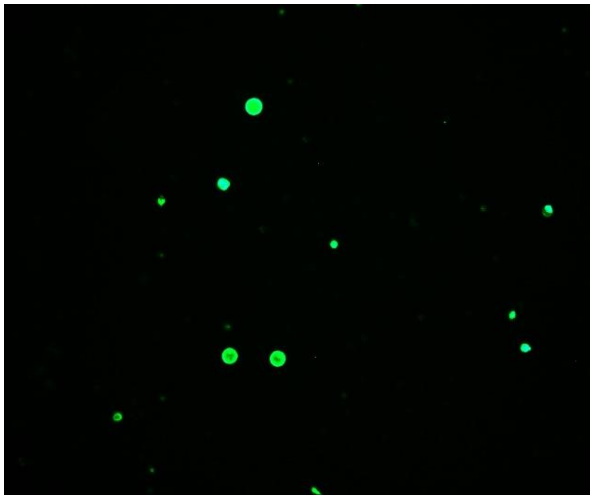
44 nm 1 $\mu\text{g/ml}$

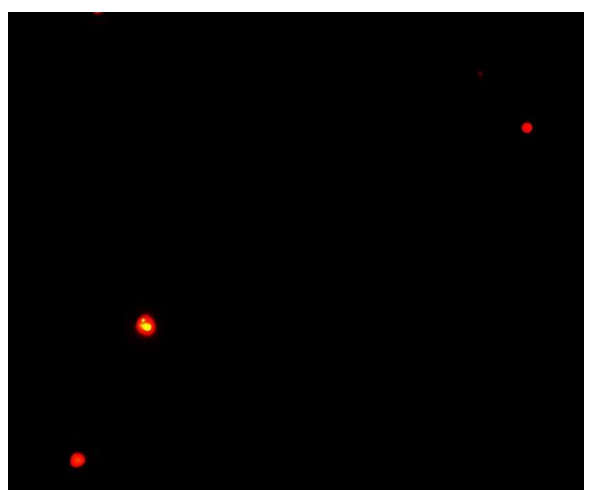
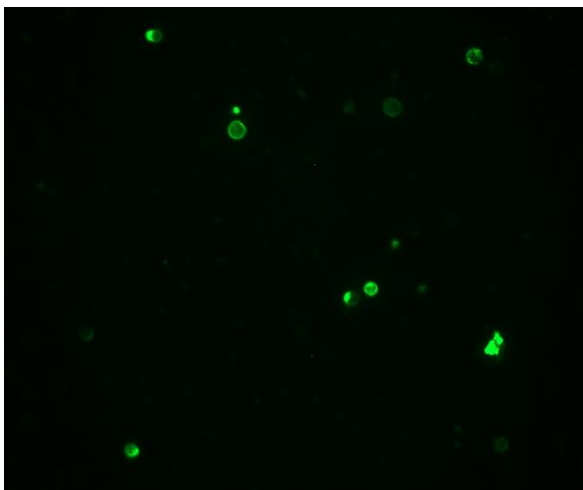
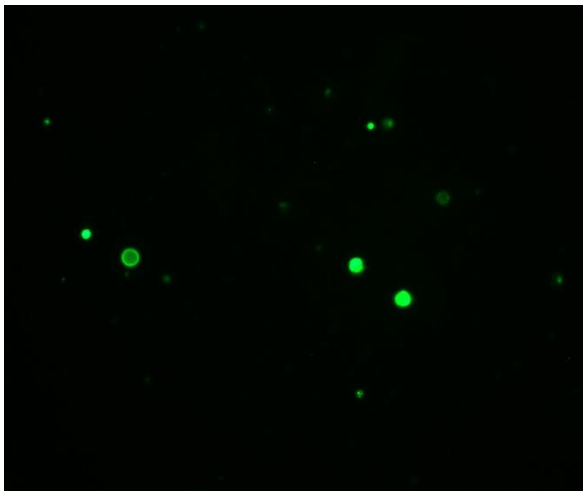
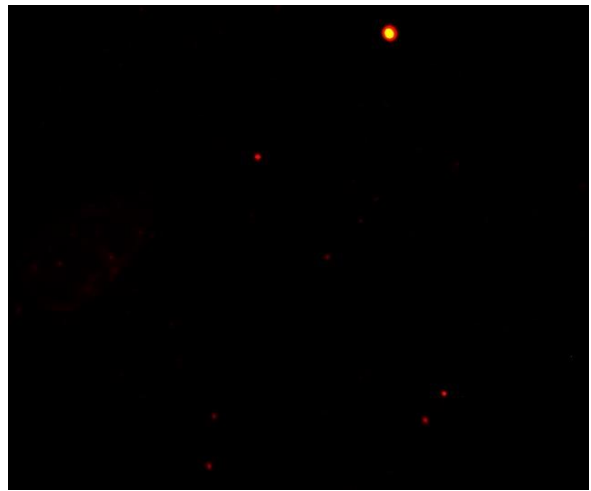
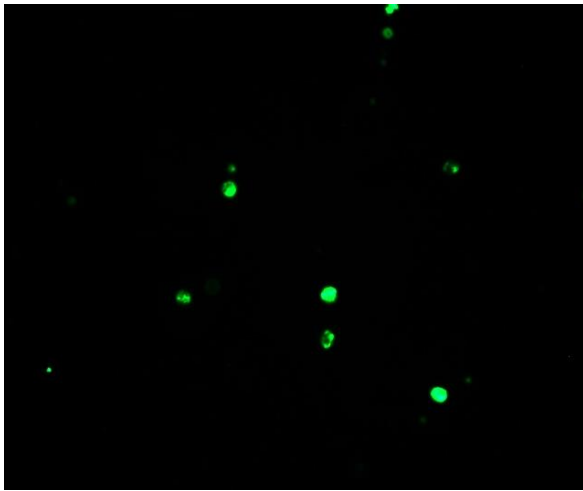




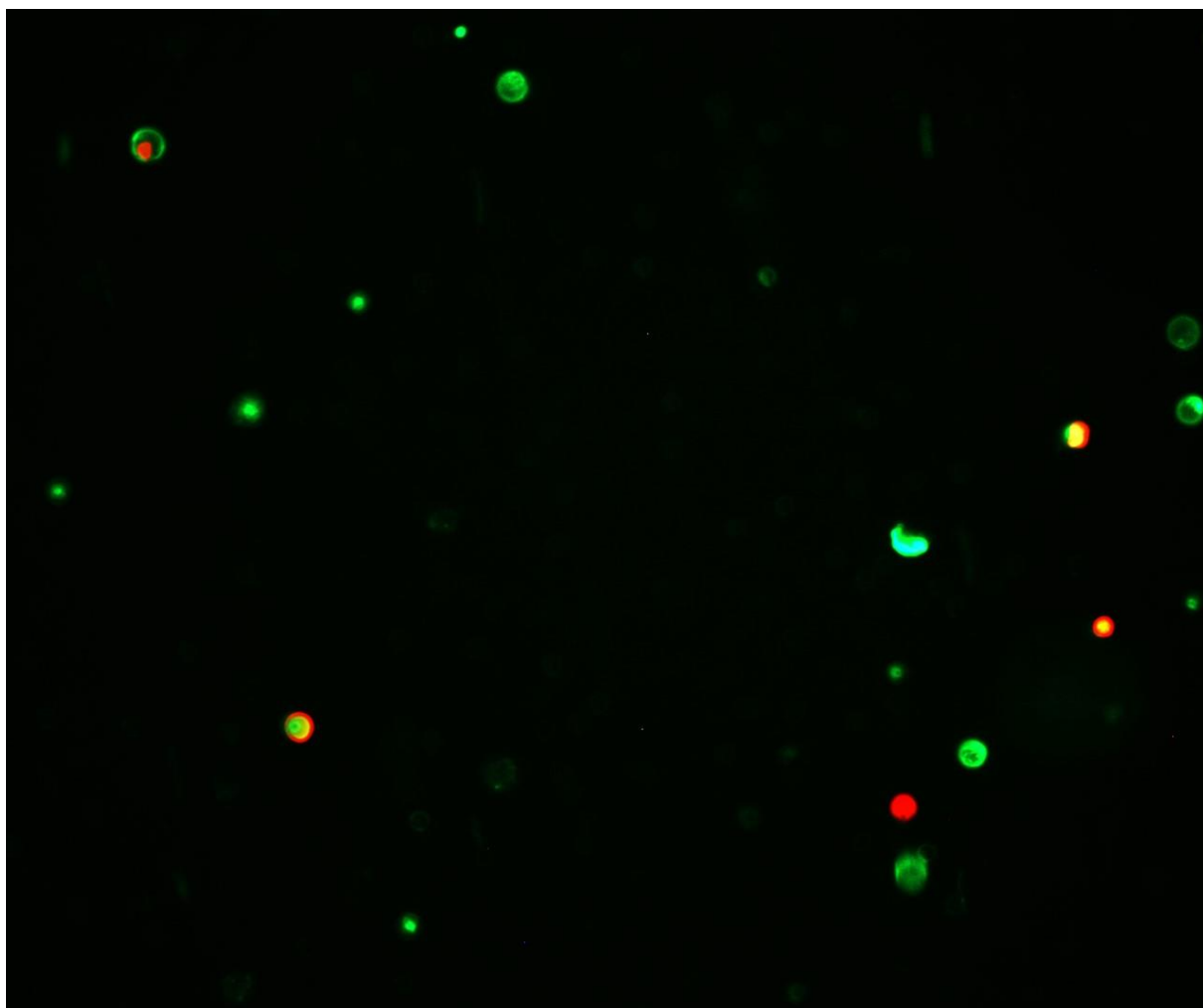
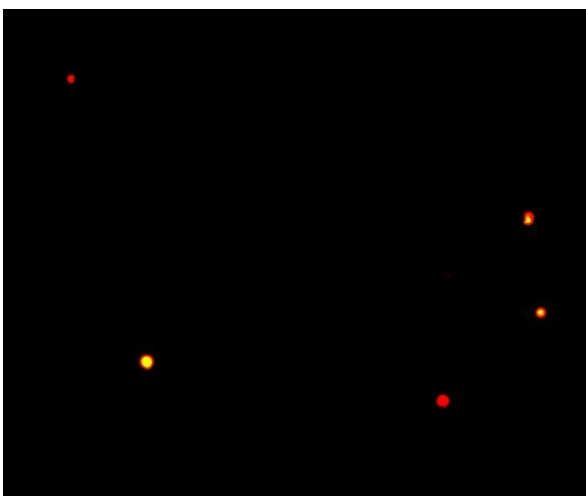
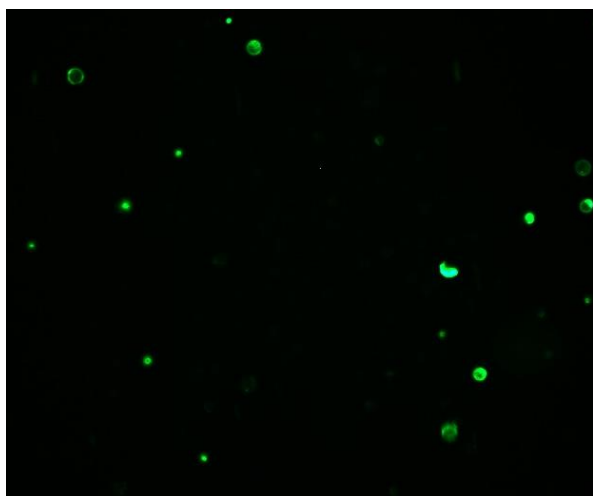


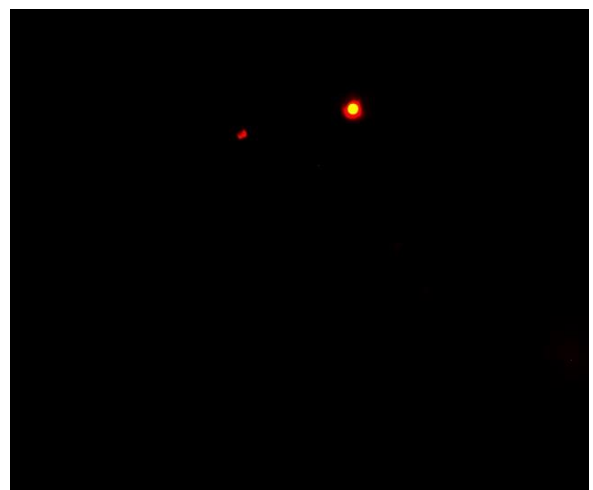
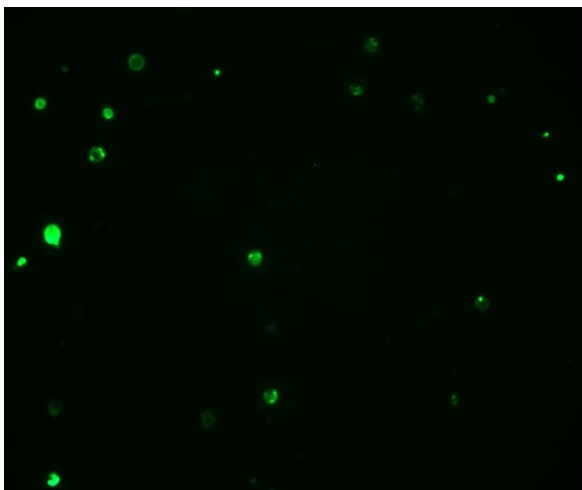
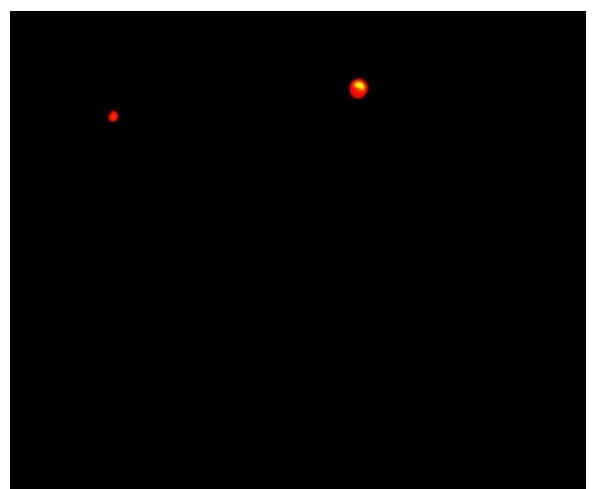
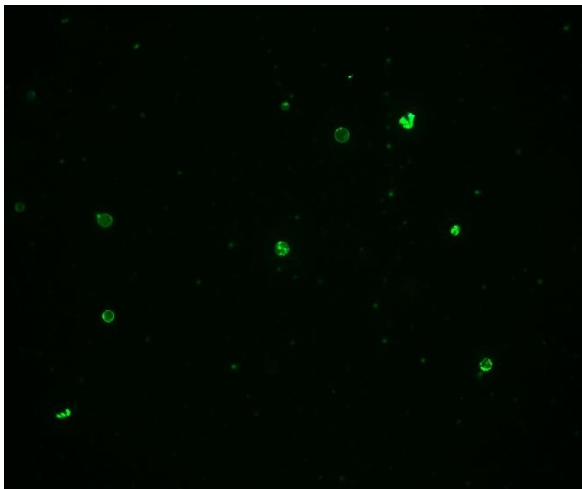
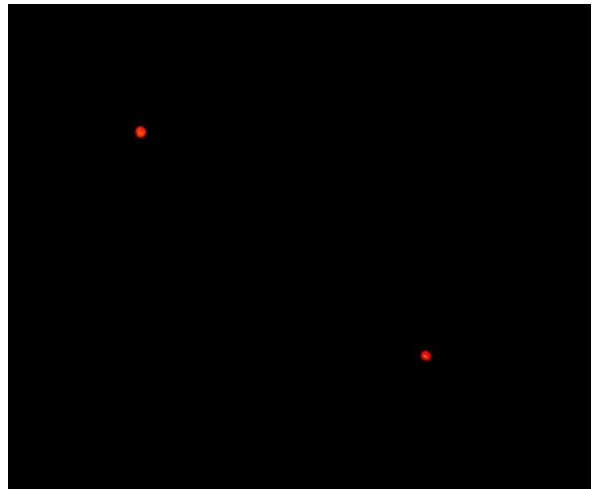
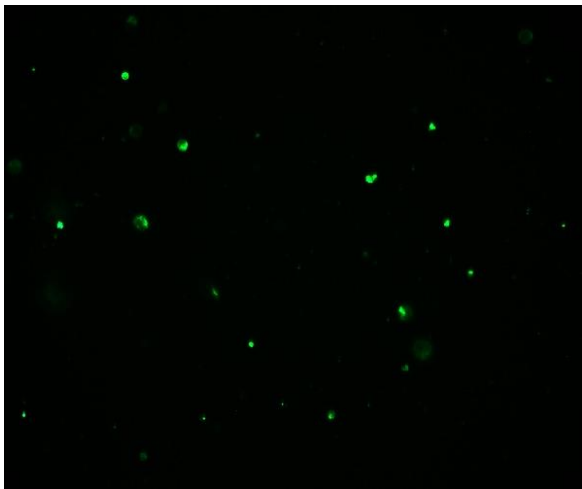
44 nm 10 $\mu\text{g/ml}$

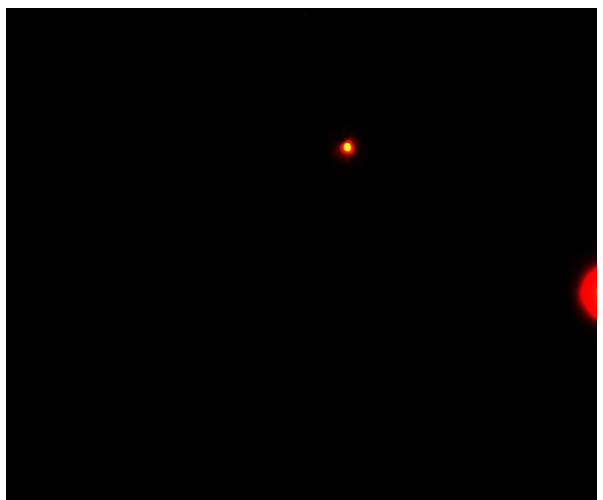
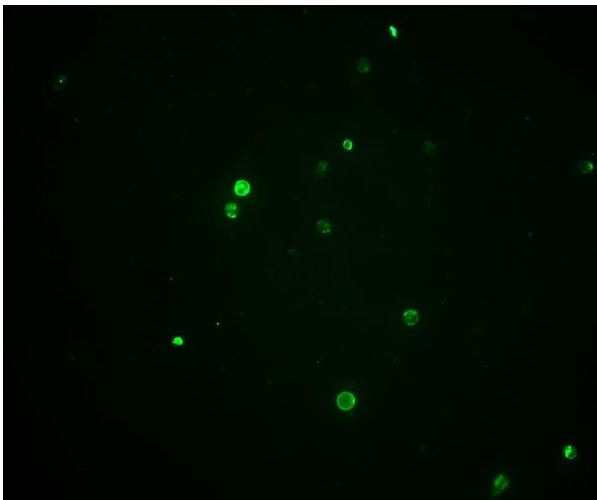
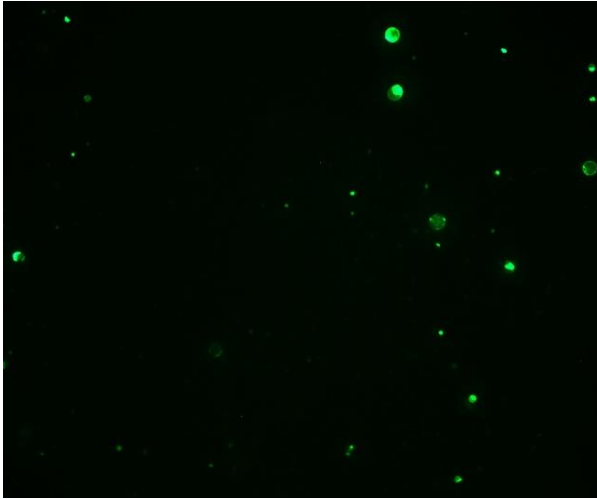




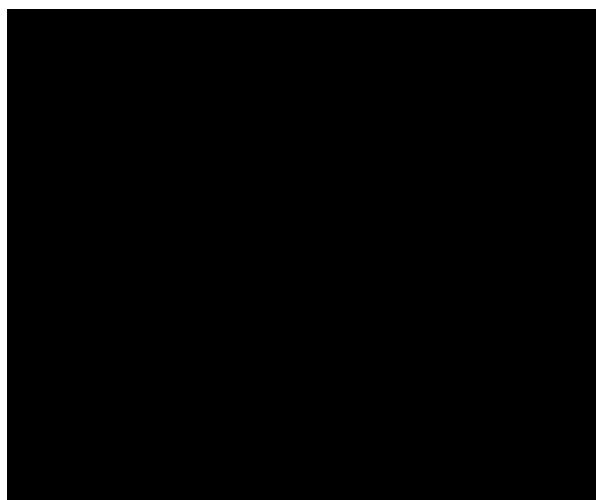
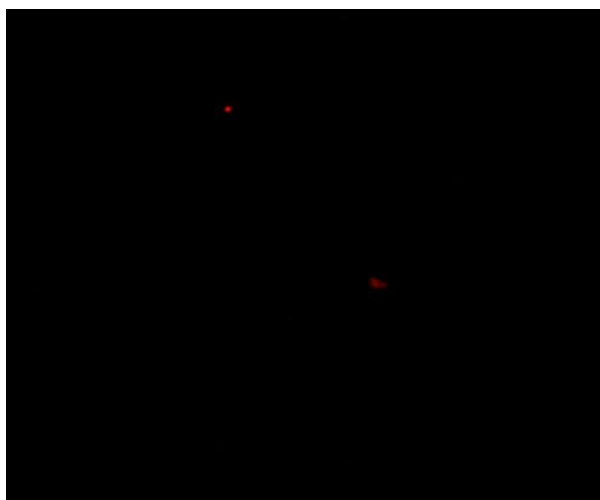
44 nm 100 µg/ml

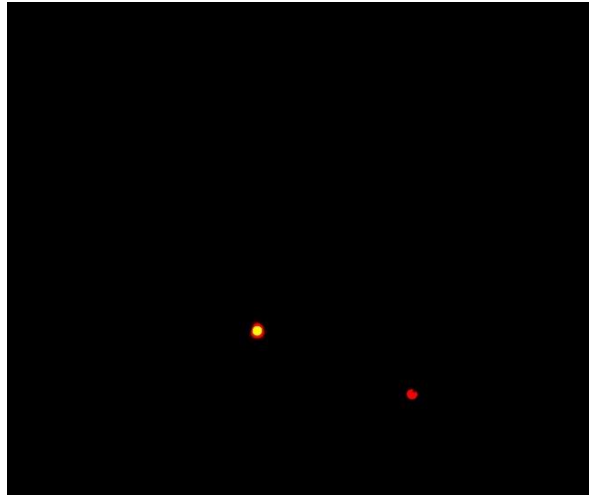
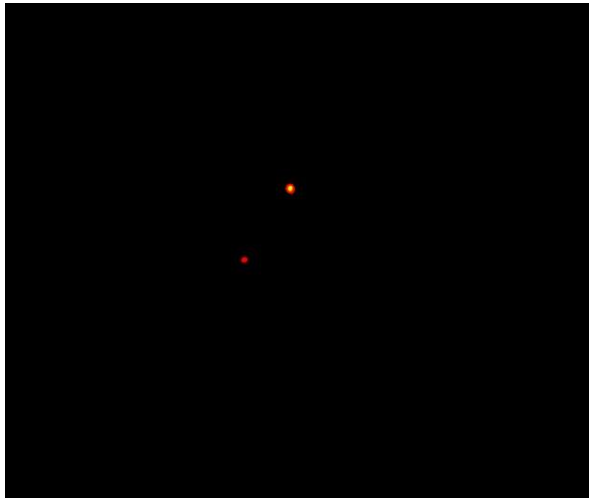
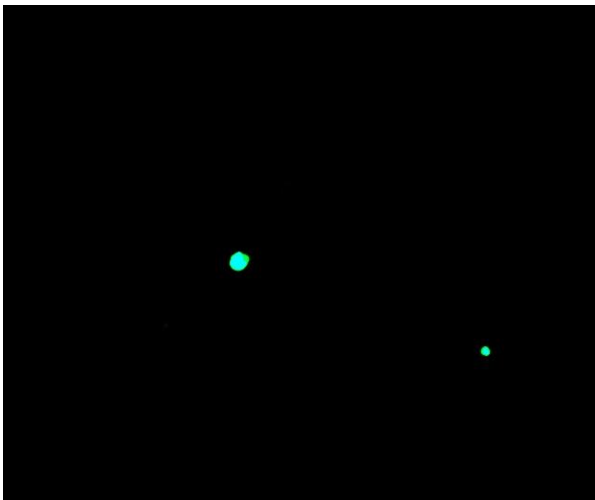
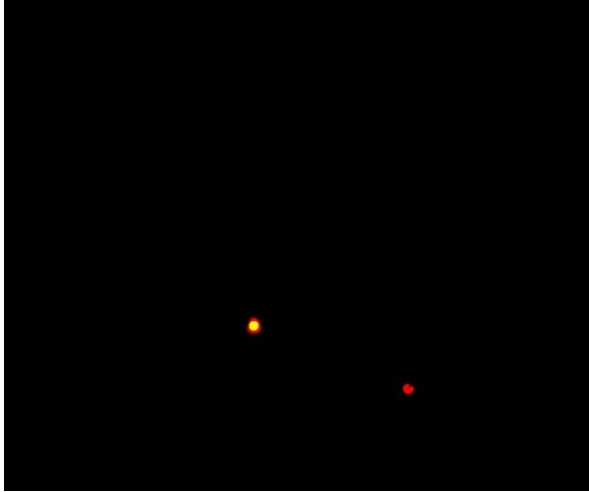


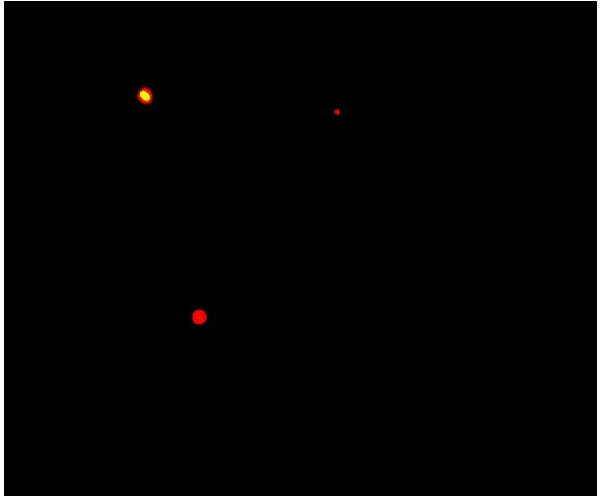
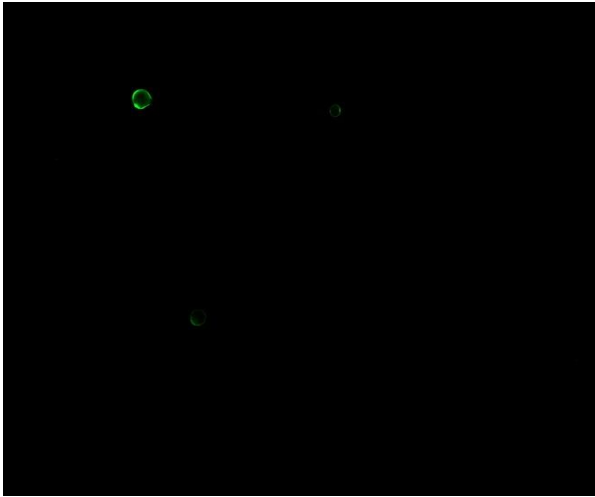




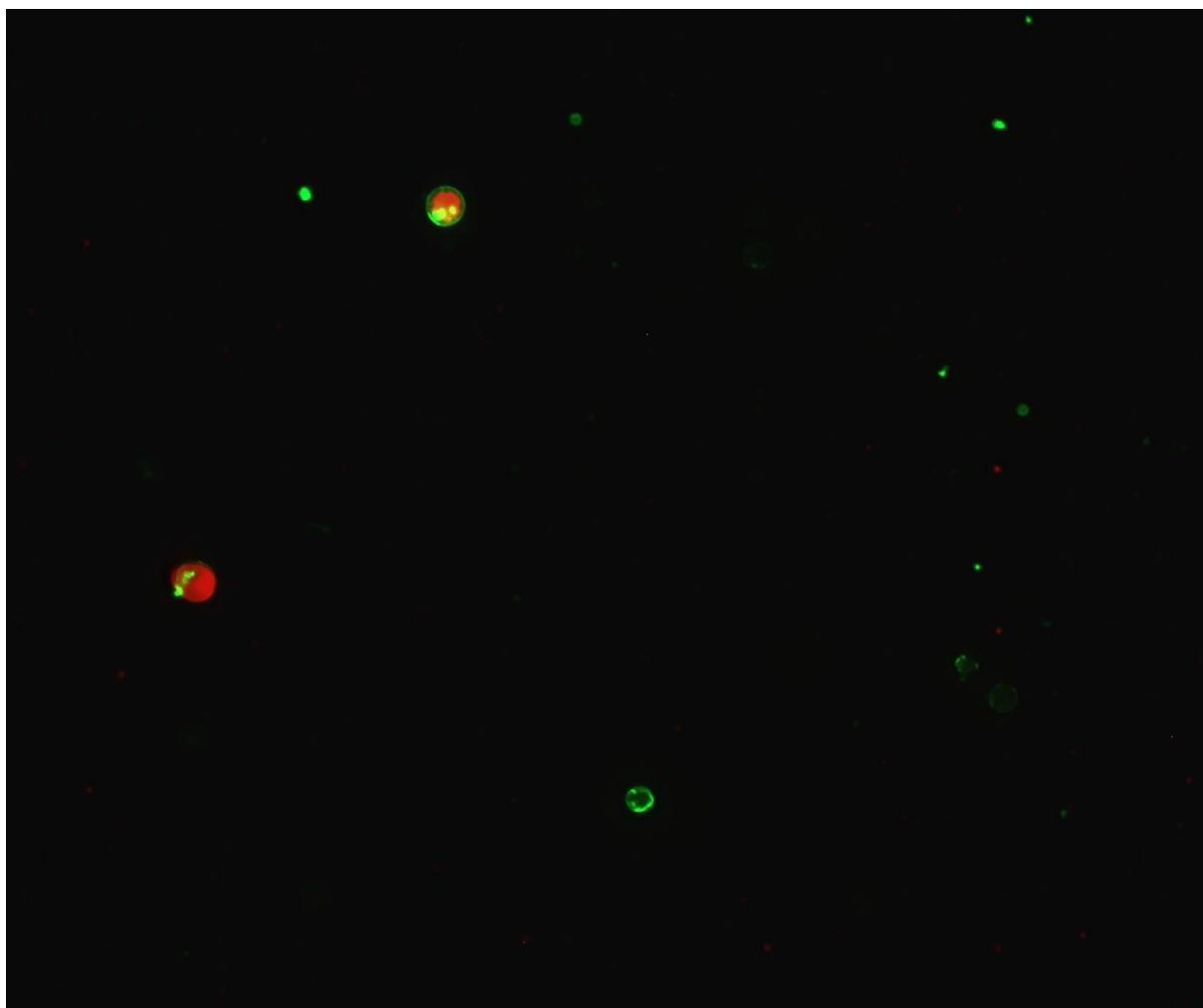
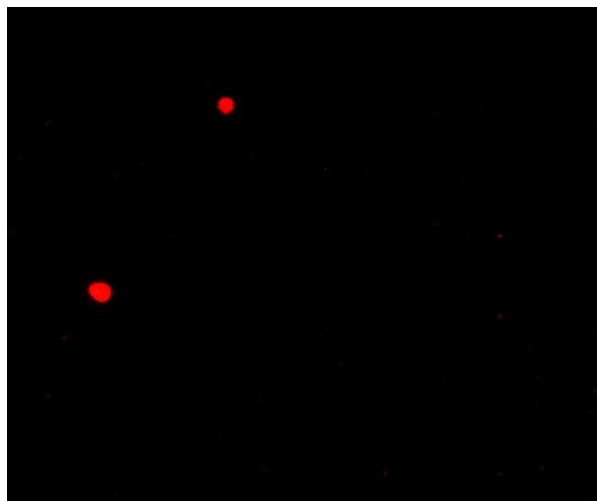
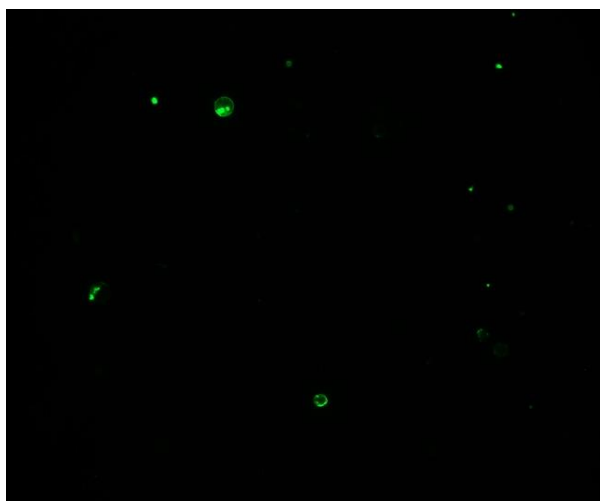
72 nm 1 μ g/ml

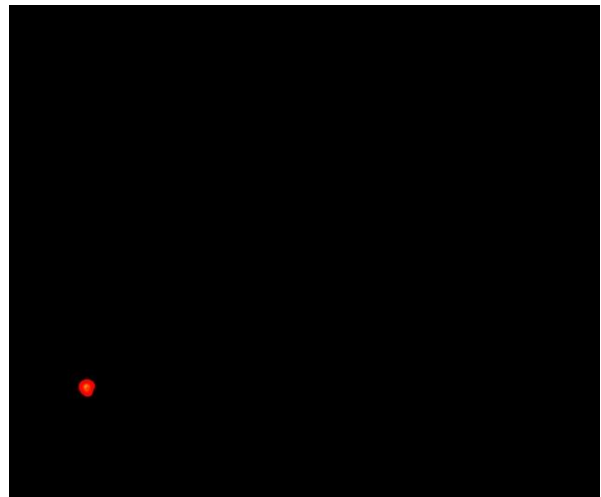
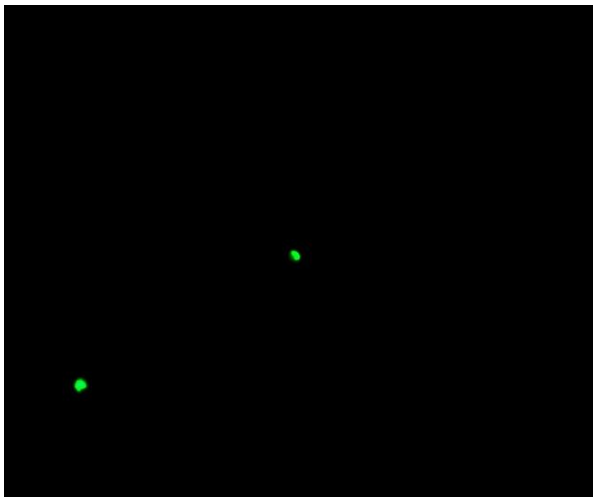
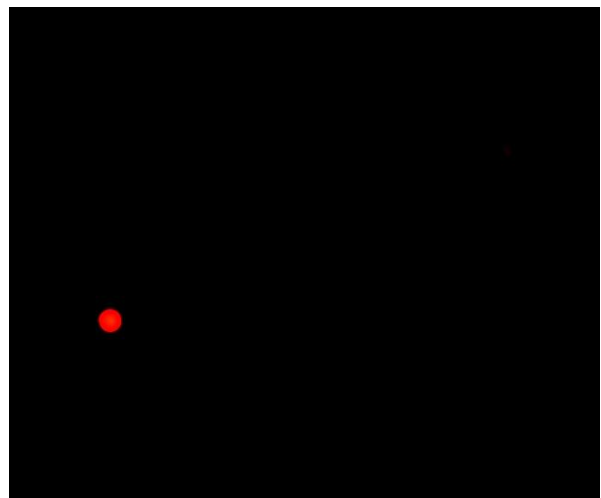
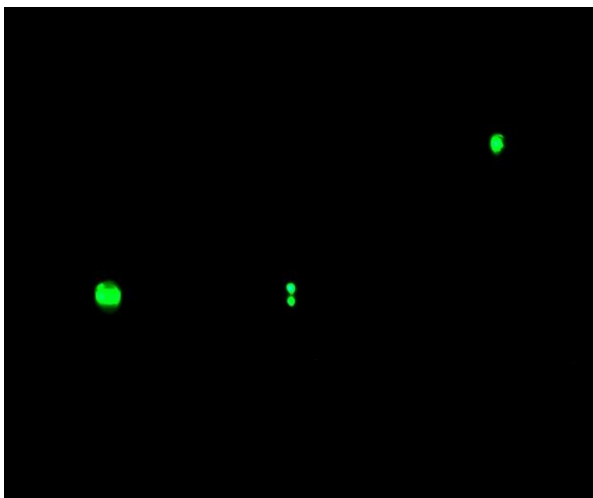
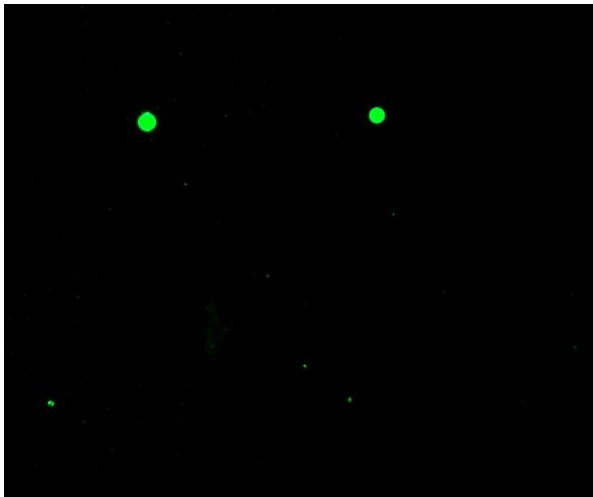


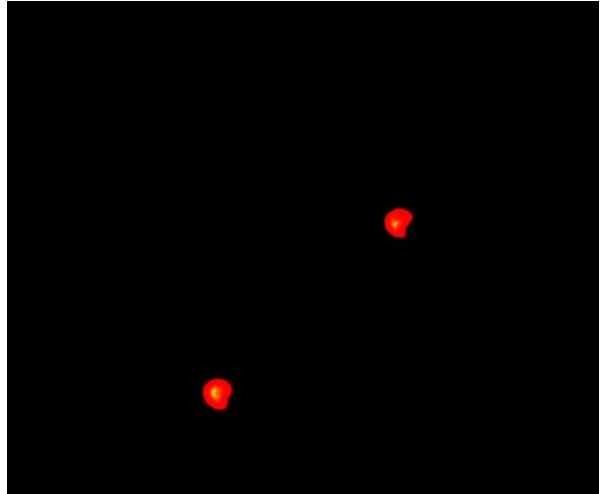
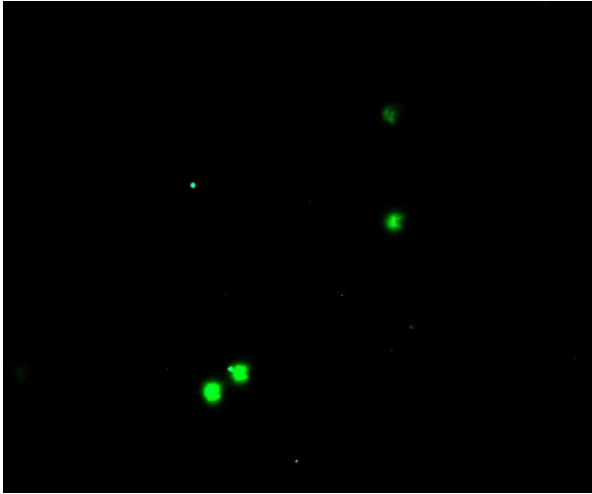




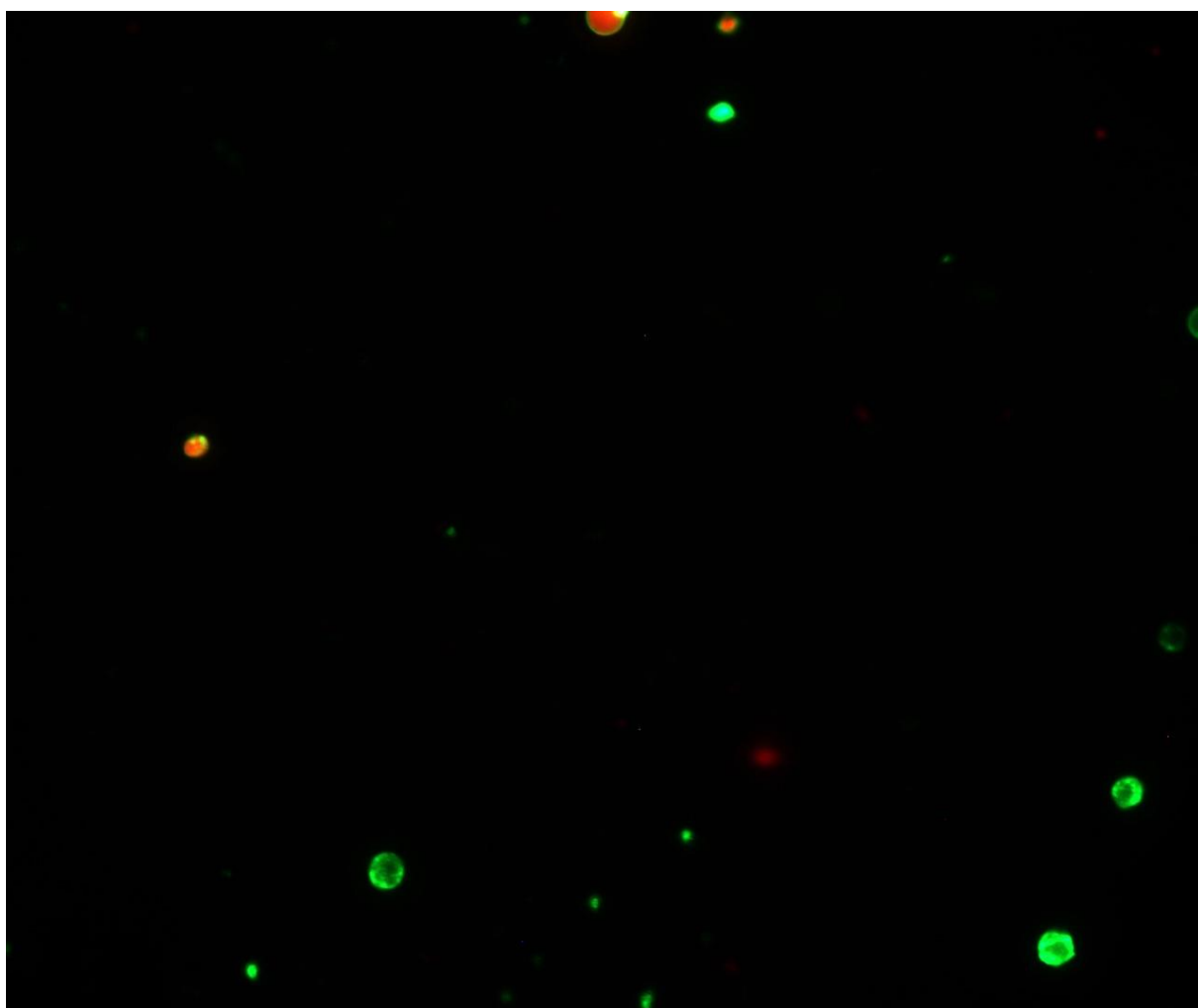
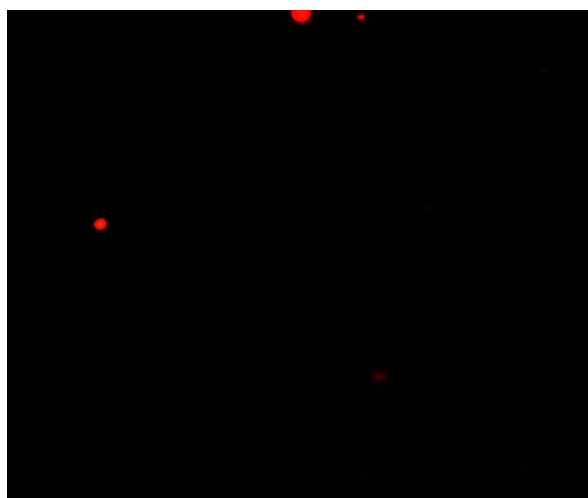
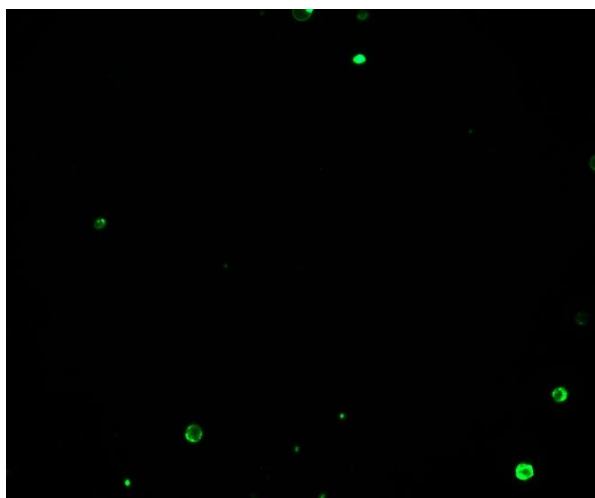
72 nm 10 $\mu\text{g/ml}$

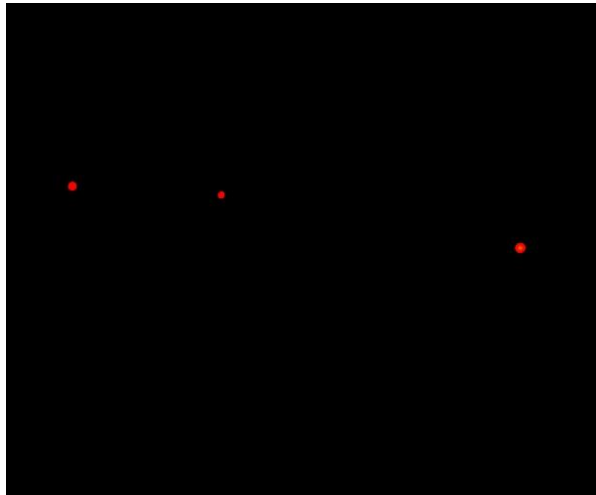
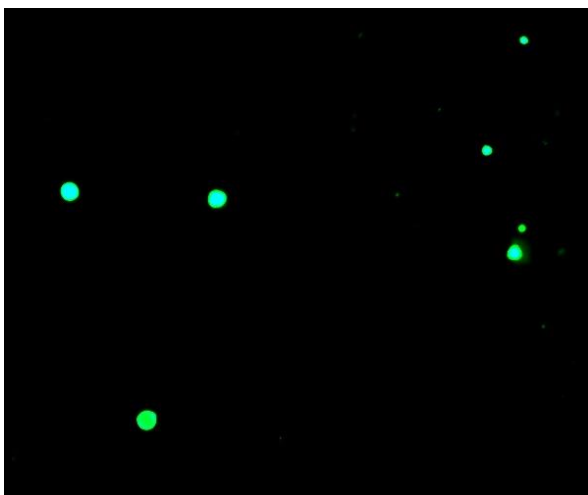
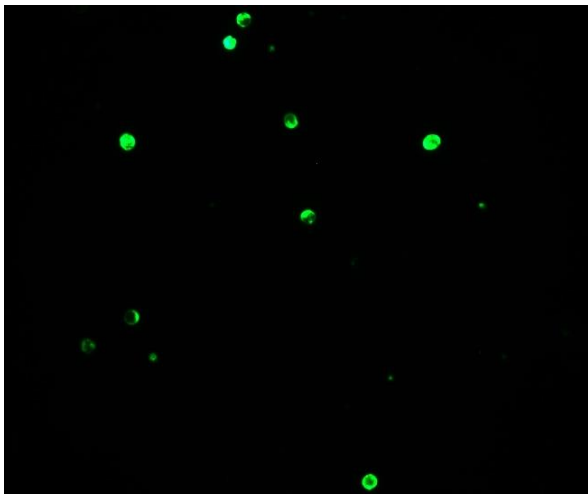
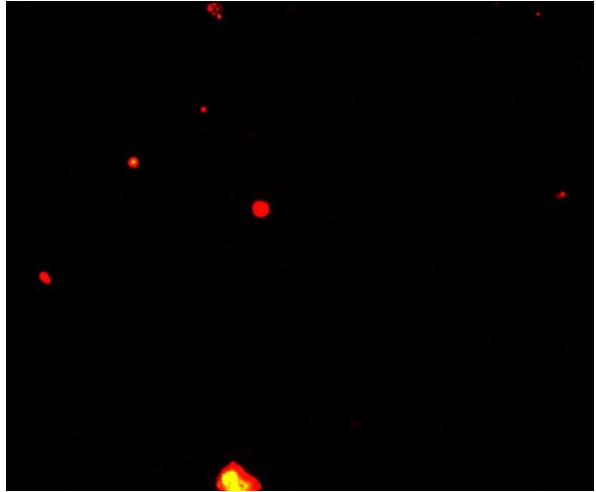
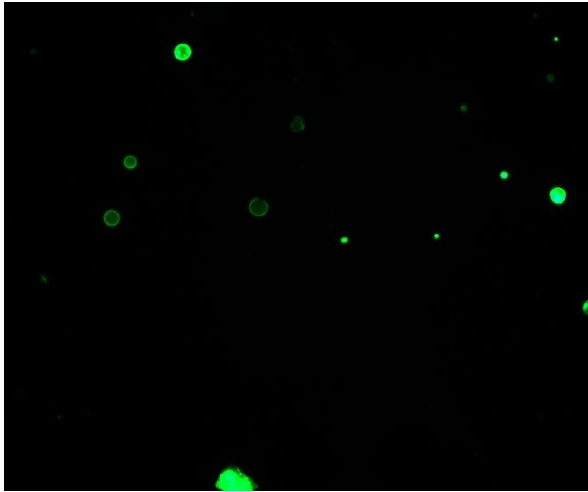


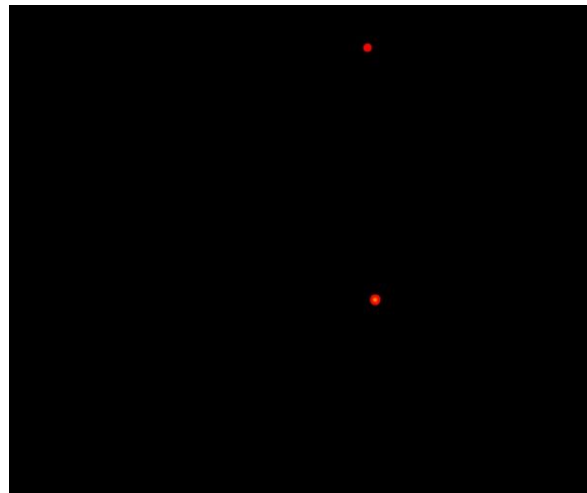
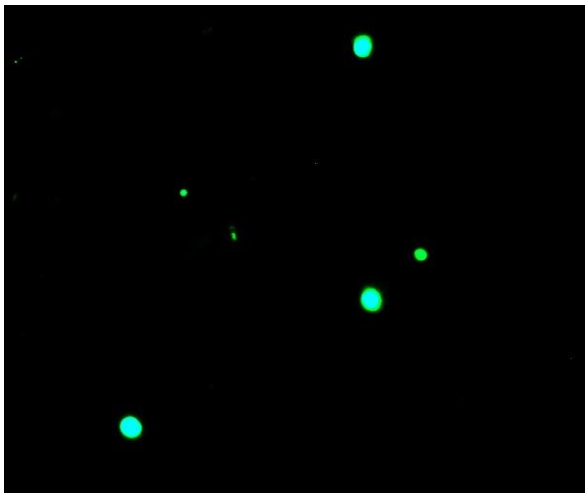
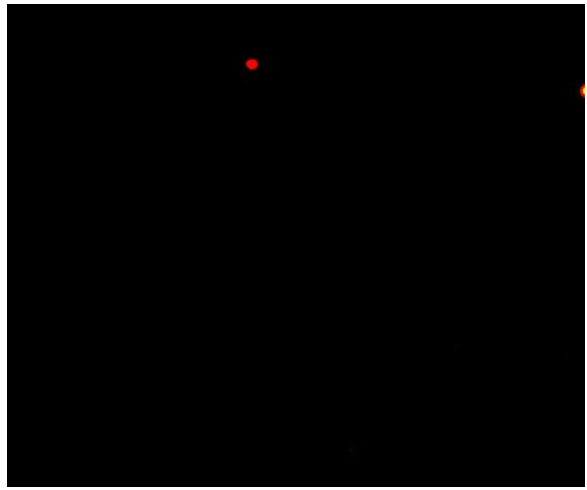
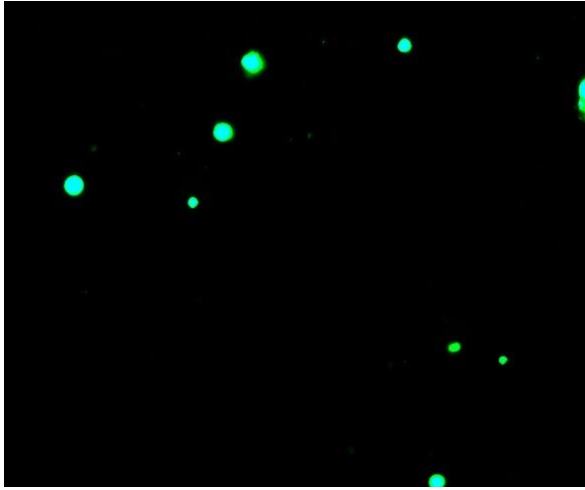




72 nm 100 $\mu\text{g/ml}$







OŚWIADCZENIA WSPÓLAUTORÓW PRAC

Łódź dn.15.05.2023

Mgr Kinga Malinowska (Kik)

Katedra Biofizyki Skazań Środowiska

Uniwersytet Łódzki

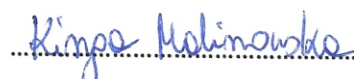
Oświadczenie współautora

Dotyczy publikacji

1. Kik K. (Malinowska), Bukowska B., Sicińska P., (2020). *Polystyrene nanoparticles: Sources, occurrence in the environment, distribution in tissues, accumulation and toxicity to various organisms*. Environmental Pollution 262; 114297. doi.org/10.1016/j.envpol.2020.114297. Punkty MEiN = 100; IF = 8,071.

Oświadczam, że mój udział w publikacji polegał na współudziale w powstaniu koncepcji pracy, zebraniu literatury, napisaniu pracy oraz jej zredagowaniu. Brałam również udział w przygotowaniu ilustracji oraz wykonałam korektę manuskryptu po recenzjach.

Mój udział oceniam na **70%**.



Kinga Malinowska

Łódź dn.15.05.2023

Prof. dr hab. Bożena Bukowska

Katedra Biofizyki Skazań Środowiska

Uniwersytet Łódzki

Oświadczenie współautora

Dotyczy publikacji

1. Kik K. (Malinowska), Bukowska B., Sicińska P., (2020). *Polystyrene nanoparticles: Sources, occurrence in the environment, distribution in tissues, accumulation and toxicity to various organisms.* Environmental Pollution 262; 114297. doi.org/10.1016/j.envpol.2020.114297. Punkty MEiN = 100; IF = 8,071.

Oświadczam, że mój udział w publikacji polegał na współudziale w powstaniu koncepcji pracy oraz korekcie manuskryptu.

Mój udział oceniam na 10%.



Bożena Bukowska

Łódź dn.15.05.2023

Dr Paulina Sicińska

Katedra Biofizyki Skazań Środowiska

Uniwersytet Łódzki

Oświadczenie współautora

Dotyczy publikacji

1. Kik K. (Malinowska), Bukowska B., Sicińska P., (2020). *Polystyrene nanoparticles: Sources, occurrence in the environment, distribution in tissues, accumulation and toxicity to various organisms*. Environmental Pollution 262; 114297. doi.org/10.1016/j.envpol.2020.114297. Punkty MEiN = 100; IF = 8,071.

Oświadczam, że mój udział w publikacji polegał na współudziale w powstaniu koncepcji pracy, ocenie merytorycznej manuskryptu oraz jego korekcie po recenzjach.

Mój udział oceniam na **20%**.



Paulina Sicińska

Łódź dn.15.05.2023

Mgr Kinga Malinowska (Kik)

Katedra Biofizyki Skażeń Środowiska

Uniwersytet Łódzki

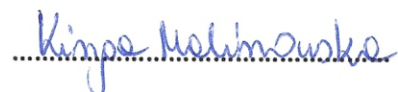
Oświadczenie współautora

Dotyczy publikacji

1. Kik K. (Malinowska), Bukowska B., Krokosz A., Sicińska P., (2020). *Oxidative properties of polystyrene nanoparticles with different diameters in human peripheral blood mononuclear cells (in vitro study)*. *Int. J. Mol. Sci.* 22, 4406, Punkty MEiN = 140; IF = 5.923.

Oświadczam, że mój udział w publikacji polegał na współudziale w powstaniu koncepcji pracy, zaplanowaniu eksperymentów oraz napisaniu powyższego artykułu. Jestem wykonawcą prawie wszystkich eksperymentów. Dokonałam oceny poziomu reaktywnych form tlenu, wysoce reaktywnych form tlenu, peroksydacji lipidów poprzez pomiar fluorescencji kwasu cis parynarowego oraz przeprowadziłam ocenę utleniania białek poprzez pomiar fluorescencji tryptofanu. Ponadto wykonałam badania zmian w eksternalizacji fosfatydyloseryny z wykorzystaniem znaczników fluorescencyjnych Ankesyny V i jodku propidyny. Do metody dynamicznego rozpraszania światła (DLS) przygotowywałam próbki do pomiaru. Dokonałam również interpretacji i analizy statystycznej wyników.

Mój udział oceniam na **65%**.



Kinga Malinowska

Łódź dn.15.05.2023

Prof. dr hab. Bożena Bukowska

Katedra Biofizyki Skażeń Środowiska

Uniwersytet Łódzki

Oświadczenie współautora

Dotyczy publikacji

1. Kik K. (Malinowska), Bukowska B., Krokosz A., Sicińska P., (2020). *Oxidative properties of polystyrene nanoparticles with different diameters in human peripheral blood mononuclear cells (in vitro study)*. *Int. J. Mol. Sci.* 22, 4406, Punkty MEiN = 140; IF = 5.923.

Oświadczam, że mój udział w publikacji polegał na współudziale w powstaniu koncepcji pracy, zaplanowaniu części eksperymentów oraz korekcie merytorycznej napisanej pracy.

Mój udział oceniam na **10%**.



Bożena Bukowska

Łódź dn.15.05.2023

Dr hab. Anita Krokosz, prof. UŁ

Katedra Biofizyki Skazań Środowiska

Uniwersytet Łódzki

Oświadczenie współautora

Dotyczy publikacji

1. Kik K. (Malinowska), Bukowska B., Krokosz A., Sicińska P., (2020). *Oxidative properties of polystyrene nanoparticles with different diameters in human peripheral blood mononuclear cells (in vitro study)*. *Int. J. Mol. Sci.* 22, 4406, Punkty MEiN = 140; IF = 5.923.

Oświadczam, że mój udział w publikacji polegał na wykonaniu eksperymentów dotyczących analizy wielkości nanocząstek za pomocą metody dynamicznego rozpraszania światła (DLS) i interpretacji uzyskanych wyników.

Mój udział oceniam na 5%.



.....
Anita Krokosz

Łódź dn.15.05.2023

Dr Paulina Sicińska

Katedra Biofizyki Skażeń Środowiska

Uniwersytet Łódzki

Oświadczenie współautora

Dotyczy publikacji

1. Kik K. (Malinowska), Bukowska B., Krokosz A., Sicińska P., **(2020)**. *Oxidative properties of polystyrene nanoparticles with different diameters in human peripheral blood mononuclear cells (in vitro study)*. *Int. J. Mol. Sci.* 22, 4406, Punkty MEiN = 140; IF = 5.923.

Oświadczam, że mój udział w publikacji polegał na współudziale w powstaniu koncepcji pracy oraz nadzorze merytorycznym nad prowadzonymi eksperymentami oraz przeprowadzoną przez Doktorantkę analizą statystyczną wyników. Wykonałam również korektę manuskryptu po recenzjach.

Mój udział oceniam na **20%**.



Paulina Sicińska

Łódź dn.15.05.2023

Mgr Kinga Malinowska (Kik)

Katedra Biofizyki Skazań Środowiska

Uniwersytet Łódzki

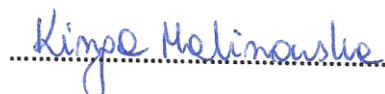
Oświadczenie współautora

Dotyczy publikacji

1. Malinowska, K., Bukowska, B., Piwoński, I., Foksiński, M., Kisielevska, A., Zarakowska, E., Gackowski, D., Sicińska P., (2022). *Polystyrene nanoparticles – the mechanism of their genotoxicity in human peripheral blood mononuclear cells*. *Nanotoxicology* 1-21. <https://doi.org/10.1080/17435390.2022.2149360> Punkty MEiN = 140; IF = 5.923.

Oświadczam, że mój udział w publikacji polegał na współudziale w powstaniu koncepcji pracy, zaplanowaniu eksperymentów oraz napisaniu pracy. Jestem wykonawcą eksperymentów dotyczących aktywności metabolicznej w PBMCs inkubowanych z nanocząstkami (test MTT) oraz genotoksycznego wpływu nanocząstek na pęknięcia jedno i dwuniciowe, oksydacyjnych uszkodzeń puryn i pirymidyn oraz naprawy DNA wykonanych za pomocą wersji alkalicznej i neutralnej testu kometowego i mikroskopii fluorescencyjnej. Dokonałam interpretacji i analizy statystycznej wyników. Ponadto pozyskałam finansowanie z NCN uzyskując projekt PRELUDIUM. Wykonałam również korektę manuskryptu po recenzjach.

Mój udział oceniam na 55%.


Kinga Malinowska

Łódź dn.15.05.2023

Prof. dr hab. Bożena Bukowska

Katedra Biofizyki Skazań Środowiska

Uniwersytet Łódzki

Oświadczenie współautora

Dotyczy publikacji

1. Malinowska, K., Bukowska, B., Piwoński, I., Foksiński, M., Kisielewska, A., Zarakowska, E., Gackowski, D., Sicińska P., (2022). *Polystyrene nanoparticles – the mechanism of their genotoxicity in human peripheral blood mononuclear cells*. *Nanotoxicology* 1-21. <https://doi.org/10.1080/17435390.2022.2149360> Punkty MEiN = 140; IF = 5.923.

Oświadczam, że mój udział w publikacji polegał na współudziale w powstaniu koncepcji pracy, zaplanowaniu doświadczeń, nawiązywaniu współpracy umożliwiającej realizację eksperymentów, interpretacji uzyskanych wyników oraz korekcie napisanej przez Doktorantkę pracy.

Mój udział oceniam na 10%.



Bożena Bukowska

Łódź dn.15.05.2023

dr hab. Ireneusz Piwoński, prof. UŁ
Katedra Technologii i Chemii Materiałów,
Wydział Chemii
Uniwersytet Łódzki

Oświadczenie współautora

Dotyczy publikacji

1. Malinowska, K., Bukowska, B., Piwoński, I., Foksiński, M., Kisielewska, A., Zarakowska, E., Gackowski, D., Sicińska P., (2022). *Polystyrene nanoparticles – the mechanism of their genotoxicity in human peripheral blood mononuclear cells*. *Nanotoxicology* 1-21. <https://doi.org/10.1080/17435390.2022.2149360> Punkty MEiN = 140; IF = 5.923.

Oświadczam, że mój udział w publikacji polegał na wykonaniu części eksperymentów dotyczących analizy mikroskopowej przy użyciu mikroskopii sił atomowych (AFM) oraz skaningowej mikroskopii elektronowej (SEM). Ponadto brałem udział w opisie tych wyników, ich wizualizacji oraz korekcie merytorycznej napisanej pracy.

Mój udział oceniam na 15%.



Ireneusz Piwoński

Łódź dn.15.05.2023

dr hab. Marek Foksiński, prof. UMK

Katedra Biochemii Klinicznej

Uniwersytet Mikołaja Kopernika w Toruniu

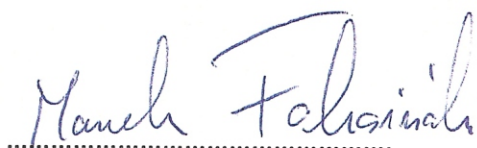
Oświadczenie współautora

Dotyczy publikacji

1. Malinowska, K., Bukowska, B., Piwoński, I., Foksiński, M., Kisielewska, A., Zarakowska, E., Gackowski, D., Sicińska P., (2022). *Polystyrene nanoparticles – the mechanism of their genotoxicity in human peripheral blood mononuclear cells*. *Nanotoxicology* 1-21. <https://doi.org/10.1080/17435390.2022.2149360> Punkty MEiN = 140; IF = 5.923.

Oświadczam, że mój udział w publikacji polegał na nadzorze merytorycznym badań dotyczących poziomu 8-oksodG przy zastosowaniu dwuwymiarowej chromatografii cieczowej i interpretacji uzyskanych wyników.

Mój udział oceniam na 4%.



Marek Foksiński

Łódź dn.15.05.2023

dr Aneta Kisielewska

Katedra Technologii i Chemii Materiałów,

Wydział Chemii

Uniwersytet Łódzki

Oświadczenie współautora

Dotyczy publikacji

1. Malinowska, K., Bukowska, B., Piwoński, I., Foksiński, M., Kisielewska, A., Zarakowska, E., Gackowski, D., Sicińska P., (2022). *Polystyrene nanoparticles – the mechanism of their genotoxicity in human peripheral blood mononuclear cells*. Nanotoxicology 1-21. <https://doi.org/10.1080/17435390.2022.2149360> Punkty MEiN = 140; IF = 5.923.

Oświadczam, że mój udział w publikacji polegał na wykonaniu eksperymentów dotyczących analizy wielkości nanocząstek za pomocą metody dynamicznego rozpraszania światła (DLS) i interpretacji uzyskanych wyników.

Mój udział oceniam na 2%.

Aneta Kisielewska

Aneta Kisielewska

Łódź dn.15.05.2023

dr Ewelina Zarakowska

Katedra Biochemii Klinicznej

Uniwersytet Mikołaja Kopernika w Toruniu

Oświadczenie współautora

Dotyczy publikacji

1. Malinowska, K., Bukowska, B., Piwoński, I., Foksiński, M., Kisielewska, A., Zarakowska, E., Gackowski, D., Sicińska P., (2022). *Polystyrene nanoparticles – the mechanism of their genotoxicity in human peripheral blood mononuclear cells*. *Nanotoxicology* 1-21. <https://doi.org/10.1080/17435390.2022.2149360> Punkty MEiN = 140; IF = 5.923.

Oświadczam, że mój udział w publikacji polegał na wykonaniu części analiz dotyczących oceny poziomu 8-oksodG przy zastosowaniu dwuwymiarowej chromatografii cieczowej.

Mój udział oceniam na 2%.



Ewelina Zarakowska

Łódź dn.15.05.2023

dr hab. Daniel Gackowski, prof. UMK

Katedra Biochemii Klinicznej

Uniwersytet Mikołaja Kopernika w Toruniu

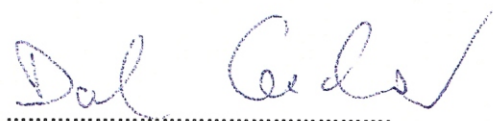
Oświadczenie współautora

Dotyczy publikacji

1. Malinowska, K., Bukowska, B., Piwoński, I., Foksiński, M., Kisielewska, A., Zarakowska, E., Gackowski, D., Sicińska P., (2022). *Polystyrene nanoparticles – the mechanism of their genotoxicity in human peripheral blood mononuclear cells*. *Nanotoxicology* 1-21. <https://doi.org/10.1080/17435390.2022.2149360> Punkty MEiN = 140; IF = 5.923.

Oświadczam, że mój udział w publikacji polegał na wykonaniu części analiz dotyczących oceny poziomu 8-oksodG przy zastosowaniu dwuwymiarowej chromatografii cieczowej.

Mój udział oceniam na 2%.



Daniel Gackowski

Łódź dn.15.05.2023

dr Paulina Sicińska

Katedra Biofizyki Skazań Środowiska

Uniwersytet Łódzki

Oświadczenie współautora

Dotyczy publikacji

1. Malinowska, K., Bukowska, B., Piwoński, I., Foksiński, M., Kisiełewska, A., Zarakowska, E., Gackowski, D., Sicińska P., (2022). *Polystyrene nanoparticles – the mechanism of their genotoxicity in human peripheral blood mononuclear cells*. *Nanotoxicology* 1-21. <https://doi.org/10.1080/17435390.2022.2149360> Punkty MEiN = 140; IF = 5.923.

Oświadczam, że mój udział w publikacji polegał na współudziale w powstaniu koncepcji pracy, nadzorze merytorycznym nad prowadzonymi eksperymentami oraz przeprowadzoną przez Doktorantkę analizą statystyczną wyników.

Mój udział oceniam na 10%.



Paulina Sicińska

Łódź dn.15.05.2023

Mgr Kinga Malinowska (Kik)

Katedra Biofizyki Skazań Środowiska

Uniwersytet Łódzki

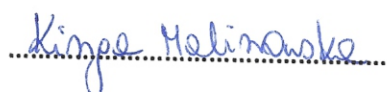
Oświadczenie współautora

Dotyczy publikacji

1. Malinowska K., Sicińska P., Michałowicz J., Bukowska B., (2023). *The effect of non-functionalized polystyrene nanoparticles of different diameters on the induction of apoptosis and mTOR level in human peripheral blood mononuclear cells.*

Oświadczam, że mój udział w publikacji polegał na współudziale w powstaniu koncepcji pracy oraz napisaniu pracy. Jestem wykonawcą wszystkich eksperymentów dotyczących apoptozy tj. analizy mikroskopowej komórek apoptotycznych, poziomu jonów wapnia w cytozolu z wykorzystaniem znacznika Fluo3/AM, oceny mitochondrialnego potencjału transbłonowego za pomocą znacznika fluorescencyjnego MitoTracker Red CMXRos oraz oceny aktywności kaspaz 3, 8 i 9. Ponadto jestem współwykonawcą analizy poziomu mTOR. Dokonałam również interpretacji i analizy statystycznej wyników.

Mój udział oceniam na 55%.



Kinga Malinowska

Łódź dn.15.05.2023

Dr Paulina Sicińska

Katedra Biofizyki Skażeń Środowiska

Uniwersytet Łódzki

Oświadczenie współautora

Dotyczy publikacji

1. Malinowska K., Sicińska P., Michałowicz J., Bukowska B., (2023). *The effect of non-functionalized polystyrene nanoparticles of different diameters on the induction of apoptosis and mTOR level in human peripheral blood mononuclear cells.*

Oświadczam, że mój udział w publikacji polegał na współudziale w powstaniu koncepcji pracy, nadzorze merytorycznym nad prowadzonymi analizami i pomocy przy analizie poziomu mTOR. Wykonałam również schemat podsumowujący wyniki pracy i brałam udział w korekcie manuskryptu.

Mój udział oceniam na **20%**.



Paulina Sicińska

Łódź dn.15.05.2023

Prof. dr hab. Jaromir Michałowicz

Katedra Biofizyki Skazań Środowiska

Uniwersytet Łódzki

Oświadczenie współautora

Dotyczy publikacji

1. Malinowska K., Sicińska P., Michałowicz J., Bukowska B., (2023). *The effect of non-functionalized polystyrene nanoparticles of different diameters on the induction of apoptosis and mTOR level in human peripheral blood mononuclear cells.*

Oświadczam, że mój udział w publikacji polegał na pomocy merytorycznej w napisaniu pracy.
Mój udział oceniam na 5%.



Jaromir Michałowicz

Łódź dn.15.05.2023

Prof. dr hab. Bożena Bukowska

Katedra Biofizyki Skażeń Środowiska

Uniwersytet Łódzki

Oświadczenie współautora

Dotyczy publikacji

1. Malinowska K., Sicińska P., Michałowicz J., Bukowska B., (2023). *The effect of non-functionalized polystyrene nanoparticles of different diameters on the induction of apoptosis and mTOR level in human peripheral blood mononuclear cells.*

Oświadczam, że mój udział w publikacji polegał na współudziale w powstaniu koncepcji pracy, zaplanowaniu doświadczeń, interpretacji uzyskanych wyników oraz korekcie napisanej przez Doktorantkę pracy.

Mój udział oceniam na **20%**.



Bożena Bukowska